Université du Québec
INRS-Institut Armand Frappier

CHARACTERIZATION OF CANINE DISTEMPER VIRUS NEUROINVASION USING A FERRET MODEL OF INFECTION

By
Penny Ann Rudd

A thesis submitted in partial fulfillment of the requirements of the degree of *Philosophiae Doctor* (PhD) in Immunology and Virology

Evaluation Committee

Committee president and Internal examinator	Pierre J. Talbot, INRS-Institut Armand Frappier
External examinators	Samuel David, McGill University.
	Earl G. Brown, Ottawa University
Thesis director	Veronika von Messling, INRS-Institut Armand Frappier

"Man cannot discover new oceans unless he has the courage to lose sight of the shore."

~ André Gide

ABSTRACT

Morbilliviruses cause an acute disease characterized by rash, respiratory and gastrointestinal signs, and severe immunosuppression. In addition, neurological complications can occur and the prevalence varies within the genus. The highest incidence of CNS involvement is associated with canine distemper virus (CDV), with up to 30% of all acute cases resulting in encephalopathies. Only one in a thousand people infected with measles virus experience neurological involvement, whereas neurological disease in ungulate morbilliviruses is exceedingly rare.

To characterize mechanisms of morbillivirus pathogenesis, our laboratory has developed a small animal model, using the ferret, to better understand morbillivirus pathogenesis and immunosuppression. Ferrets are natural hosts for CDV, and develop the typical rash, fever, severe leukopenia, gastrointestinal and respiratory signs of disease. Also, when inoculated with wild type strains, ferrets succumb to the infection within two to five weeks. The goal of my thesis was to characterize the events which lead up to and occur during the acute phase of CDV central nervous system (CNS) infection in ferrets. In order to accomplish this, three specific objectives were defined.

The first research objective was to determine the pathways involved in CDV neuroinvasion and to identify the cell types targeted by the virus. By using histology and confocal microscopy, we showed that CDV not only enters the CNS by the hematogenous route but, as previously suggested in studies with dogs, also uses the olfactory pathway.

In the second objective we investigated the kinetics of CDV neurodissemination and the resulting damage that arises at early disease stages during acute encephalitis. Towards this, a recombinant virus of the highly neurovirulent strain Snyder Hill was constructed and we observed that despite a generalized immunosuppression, infected animals developed a strong local inflammatory response. This response was characterized by the presence of activated microglia, gliosis in highly infected brain regions and the

expression of the pro-inflammatory cytokines interleukin-6, interferon-β and tumor necrosis factor-α.

For the final objective, we wanted to investigate the transneuronal spread of morbilliviruses. An *in vitro* model of infection using a primary culture of ferret neurons was established and we demonstrated that this model mimics many key aspects of CDV infection seen *in vivo*. We observed that CDV spreads non-directionally along communicating neurons and determined that cell-cell contact is required for efficient transneuronal dissemination. Although its development is still very recent, this system will be useful to examine in more detail the mechanisms involved in morbillivirus transneuronal spread.

Taken together my work contributes to a better understanding of the events involved in morbillivirus CNS infection and may lead to new treatment strategies to limit CNS sequelae or even to prevent CNS invasion.

Penny A. Rudd

Veronika von Messling

ACKNOWLEDGEMENTS

First and foremost I would like to express my sincere gratitude to Dr Veronika von Messling, my thesis advisor, who has provided me with the best mentoring I could ever have hoped for. I am sincerely grateful for all of your advice, knowledge and time spent on helping me make the most of my research project. Your pragmatism, enthusiasm, determination and devotion to your work and students are inspiring.

I would also like to acknowledge all the professors that have participated on my thesis committees for taking the time out of your busy schedules to give me many valuable suggestions and constructive advice.

I am also grateful to the Fondation Armand-Frappier for their recognition and financial support provided throughout my doctorate degree. Their studentships are really very valuable to students and encourage fantastic training opportunities and contribute to improving the quality of life of young researchers.

It is a pleasure to thank all of my lab members, past and present. They make coming to work everyday an enjoyable experience. I really want to thank Nick who has been a great colleague for more than seven years. How will I survive a postdoc without your crazy antics to cheer me up? To François for his great coffee moments, lunches at Lugano's and of course happy hours! To Stéphane, I will miss your particular sense of Belgian humor. I only wonder that now our paths are separating who will hate you the least? ☺ To Danielle and Bevan two great people I really enjoy interacting with in and out of the lab. Christophe, thank you for spicing up things. Now, you will have to find someone new to have many "lively" discussions with. I know you will miss me the most ;-)! Louis, Ronan, Isabelle, Alex, Eveline and Xiao you each bring something special to the lab dynamics and I thank you all and wish you the best of luck with the pursuit of your goals. Chantal, thank you for your great organization skills and all the great treats you have brought me.

I also want to thank all of my friends who always have kind words of encouragement. I especially want to acknowledge Sandra and Mélanie past colleagues and great friends, who know all too well what is involved in doing a PhD and understand me so well.

Next, I want to thank everyone in my family, because a good family is the best basis for a good life. Even if you don't always understand what I do at the lab, your love and support have been greatly appreciated. To mom and Dad, I bet you never thought when I was a child that I would love school so much that I would not stop until I got a doctorate. The good news is that I will get a job now ☺. All jokes aside, I know you are very proud and I love you.

And last but not least, I could not have pursued my goal without the unconditional love of my husband Vincent. Thank you for all the times you drove me to the lab at crazy hours and on holidays, not to mention all those countless hours you have spent waiting… You are a remarkable man and you truly are my pillar of strength. Je t'adore…

TABLE OF CONTENTS

LIST OF TABLES AND FIGURES

LIST OF ABREVIATIONS

α	alpha
α-GFAP	anti-glial fibrillary acidic protein
aa	amino acid
ADEM	acute demyelinating encephalomyelitis
ATCC	American Type Culture Collection
β	beta
BDNF	brain-derived neurotrophic factor
BrdU	5-bromo-2'-deoxyuridine
BSA	bovine serum albumin
°C	degree Celsius
CDE	canine distemper encephalitis
cDNA	complementary DNA
CDV	canine distemper virus
CeMV	cetacean morbillivirus
CHO	chinese hamster ovary
CNS	central nervous system
CSF	cerebrospinal fluid
ctr	control
DAB	3, 3'-diaminobenzidine
DAPI	4', 6-diamidino-2-phenylindole
DC	dendritic cell
DMEM	Dulbecco's modified Eagle's medium
DNA	deoxyribonucleic acid
d.p.i.	days post-infection
DTH	delayed type hypersensitivity
EAE	experimental allergic encephalomyelitis
EDTA	ethylenediaminetetraacetic acid
eGFP	enhanced green fluorescent protein
ETB	embryo transportation buffer

F	fusion
FBS	fetal bovine serum
FIP	fusion inhibitory peptide (Z-D-Phe-L-Phe-Gly-OH)
γ	gamma
H	hemagglutinin
h	hour
HBSS	Hank's balanced salt solution
H&E	hematoxylin and eosin
HIV	human immunodeficiency virus
Hsp	heat shock protein
HSV	herpes simplex virus
i.c.	intracranial
ICAM	intercellular adhesion molecule
i.e.	*id est*
IFN	interferon
IFNAR	interferon-α receptor
IL	interleukin
i.n.	intranasal
i.p.	intraperitoneal
IP-10	IFN-γ inducible protein 10
IRF	interferon regulatory factor
i.v.	intravenous
Jak	Janus activated kinase
kb	kilobase
kDa	kilodalton
kg	kilogram
L	large
LCM	laser capture-microdissection
LPMV	La Piedad Michoacan paramyxovirus
MAb	monoclonal antibody
MAP-1	microtubule associated protein 1

MAP-2	microtubule associated protein 2
MBP	myelin basic protein
MDA-5	melanoma differentiation-associated gene-5
MeV	measles virus
mg	milligram
MHC	major histocompatibility complex
MIBE	measles inclusion body encephalitis
Mig	monokine inducible by γ
min	minutes
MIP	macrophage inflammatory protein
mL	milliliter
mM	millimolar
mm	millimeter
m.o.i.	multiplicity of infection
MRI	magnetic resonance imaging
mRNA	messenger RNA
N	nucleocapsid
NGF	nerve-growth factor
NK	natural killer
nm	nanometer
NR	N protein receptor
NSE	neuron specific enolase
NT2	human neural precursor
NT3	neurotrophin 3
ODE	old dog encephalitis
OEC	olfactory ensheathing cell
ORF	open reading frame
P	phosphoprotein
PBMC	peripheral blood mononuclear cell
PBS	phosphate buffered saline
PHA	phytohemagglutinin

p.i.	post-infection
PFA	paraformaldehyde
PPRV	Peste-des-petits-ruminants virus
RANTES	regulated upon activation normal T-cell expressed and secreted
RdRp	rNA-dependent RNA polymerase L
RNA	ribonucleic acid
RPV	Rinderpest virus
RT	room temperature
RT-PCR	reverse transcriptase-polymerase chain reaction
SD	standard deviation
SH	Snyder Hill
SLAM	signaling lymphocytic activation molecule
SSPE	subacute sclerosing encephalitis
STAT	signal transducers and activators of transcription
TCID	tissue culture infectious dose
TGF	transforming growth factor
Th1/Th2	T-helper Type 1 and 2
TNF	tumor necrosis factor
U	unit
µg	microgram
µL	microliter
µM	micromolar
µm	micrometer
UTR	untranslated region
VCAM	vascular-cell adhesion molecule
WBC	white blood cell
w/v	weight per volume
YAC	yeast artificial chromosome

CHAPTER 1

INTRODUCTION

1. Morbilliviruses

1.1 Taxonomy and Morphology

Paramyxoviruses belong to the order *Mononegavirales,* which comprises all single-stranded viruses that have a non-segmented, negative-stranded ribonucleic acid (RNA) genome (Table 1). The order includes four families: *Bornaviridae, Rhabdoviridae, Filoviridae* and *Paramyxoviridae*. The last family is further divided into two subfamilies, the *Paramyxovirinae* and the *Pneumovirinae*. Five genera belong to the first subfamily and include *Avulavirus, Henipavirus, Morbillivirus, Respirovirus* and *Rubulavirus,* while the *Pneumovirus* and the *Metapneumovirus* genera belong to the latter subfamily. Paramyxoviruses are pleomorphic in shape and the virion has a diameter of approximately 150-300 nm (Takimoto and Portner, 2004). The variability in shape and size can be attributed to the lack of stringency during the budding stage of the replication cycle (Fauquet, 2005). All members of the *Paramyxovirus* family have two structural modules: an internal ribonucleoprotein core, or ribonucleoprotein complex (RNP) that contains the single-stranded RNA genome, and an outer module, made of membrane-associated proteins, which form the envelope.

Morbilliviruses are a genus in the *Paramyxovirinae* subfamily, which includes six members: the human pathogen *Measles virus* (MeV, type species), *Canine distemper virus* (CDV), *Rinderpest virus* (RPV), *Peste-des-petits-ruminants virus* (PPRV), *Phocine distemper virus* (PDV) and *Cetacean morbillivirus* (CeMV) (Figure 2). Morbilliviruses are distinguished by three criteria: host range, genetic sequence and antigenetic differences. Sequence similarities range from low to moderate depending on the protein examined. All morbilliviruses have the identical gene order and number of genes. Other distinguishing features of this genus are its lack of neuraminidase activity on the hemagglutinin protein and the ability to produce both intracytoplasmic and intranuclear inclusion bodies containing nucleocapsid-like structures.

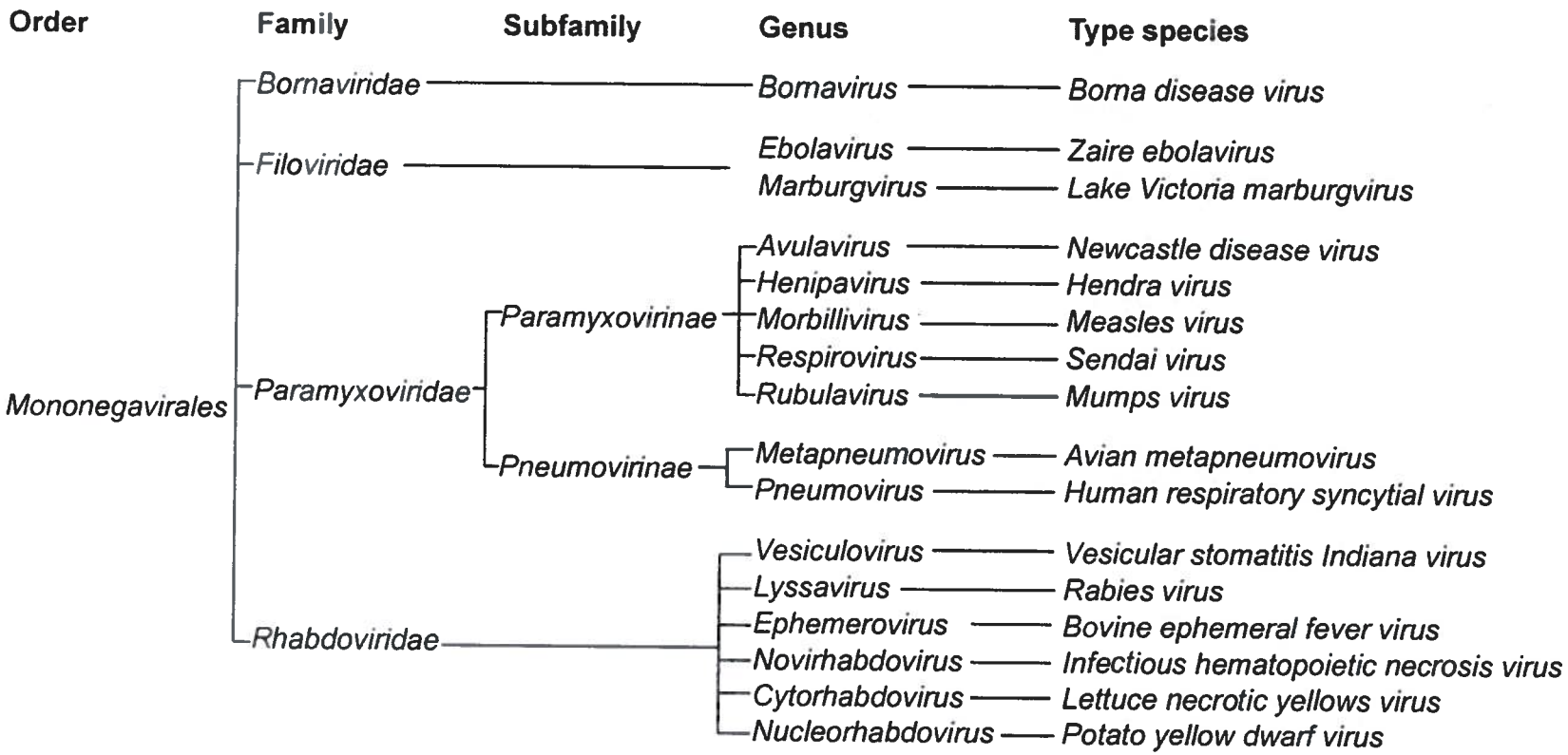

Fig. 1 Taxonomic classification of *Mononegavirales* viruses. Taxonomic classification of *Mononegavirales* viruses according to the International Committee on the Taxonomy of Viruses database (ICTVdb).

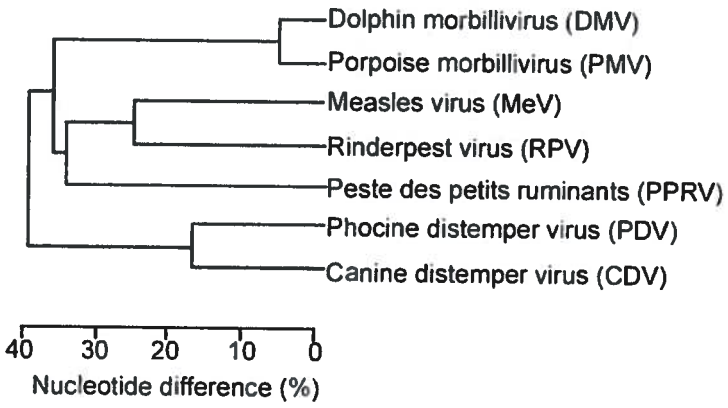

Fig. 2 Phylogenetic relationship between morbilliviruses. Phylogenetic tree showing the relationships between the different morbilliviruses based on sequence analysis of genes encoding the H protein (Modified from Sips et al., 2007).

1.2 Genome Organization, Viral Proteins, Transcription and Replication

Morbillivirus genomes are just under 16 kilobases (kb) in size. Each genome codes for six genes, which results in the production of eight proteins. The gene order is: nucleocapsid (N), phospho- (P), matrix (M), fusion (F), haemagglutinin (H) and large (L) (Figure 3A). All genes are tandemly linked and separated by short untranslated regions (UTR) (Lamb, 1996). These UTRs contain conserved junctional sequences that act as transcriptional start and polyadenylation/stop sites. Gene expression is preceded by polymerase entry at a single 3' end followed by a start/stop transcription mechanism. The junction found between each gene contains three regions: a gene end, an intergenic region and a gene start site. At the end of a viral gene, the polymerase can terminate transcription and release a polyadenylated messenger RNA (mRNA) before initiating transcription of the next gene. In some instances, the polymerase can terminate the transcription without initiating at the next entry site, which explains the gradient of transcription. The abundance of viral mRNAs decreases with distance from the 3' promoter. The next important step is replication of the genome. Replication provides additional templates for transcription and further genome replication. During replication, the RNA-dependent RNA polymerase L (RdRp) initiates at the extreme 5' end of the genome, synthesizes a full-length complementary positive-strand RNA (antigenome). In turn, the antigenome RNA functions as a template for synthesis of full-length progeny negative-strand genomes. This requires that the RNA synthesizing machinery enter an anti-termination mode, whereby the signals at gene boundaries are ignored.

The genomic RNA is encapsidated by the N protein and, together with the RdRp and P proteins, forms a functional unit called the RNP. The P open reading frame (ORF) overlaps the V ORF and access to the latter is achieved by co-transcriptional insertion of non-templated guanine nucleotides at a precise location or "editing site". This produces mRNAs that differ in one or two nucleotides and hence the P and V proteins share an identical amino terminus but have unique carboxyl termini (Cattaneo et al., 1989a; Thomas et al., 1988). All *Paramyxovirinae* members that edit their P mRNA are also governed by the 'rule of six', i.e. their genomes must be of polyhexameric length (6n+0)

to replicate efficiently (Jacques and Kolakofsky, 1991; Murphy and Parks, 1997). Morbilliviruses have a second functional unit, which is the envelope, and it consists of the M, H and F proteins (Figure 3B).

1.3 Viral Protein Functions

1.3.1 The RNP Proteins

1.3.1.1 The Nucleocapsid Protein (N)

Like all nucleocapsids of all the viruses in the *Paramyxoviridae* family, the morbillivirus nucleocapsid (N) has a characteristic herringbone-like appearance (Karlin et al., 2002). The N protein is the major component of the morbillivirus virion. All morbillivirus N proteins have two distinct domains. The first is a well-conserved hydrophobic and globular core domain, which is thought to interact with the genomic RNA and the second is a hypervariable disordered and hydrophilic tail (Bourhis, 2007). In infected cells, N appears either in a monomeric form or as a complex with the P and L proteins forming the RNP. In its monomeric form, N is responsible for the encapsidation of the nascent genomic RNA chain during replication. In addition, interactions with the M protein during viral assembly have been observed (Bourhis et al., 2006).

In vitro, the N protein also has immunosuppressive properties, either due to binding of the Fc gamma receptor type II (CD32) on antigen presenting cells (Marie et al., 2001), or through interactions with an unidentified N protein receptor (NR) expressed on a large variety of cells in humans and mice (Laine et al., 2003). Via its hydrophilic tail, N directly interacts with the NR and arrests T cells in G0/G1 cell cycle phase instead of inducing apoptosis (Bourhis, 2007). However, the importance of these effects for morbillivirus pathogenesis remains to be investigated.

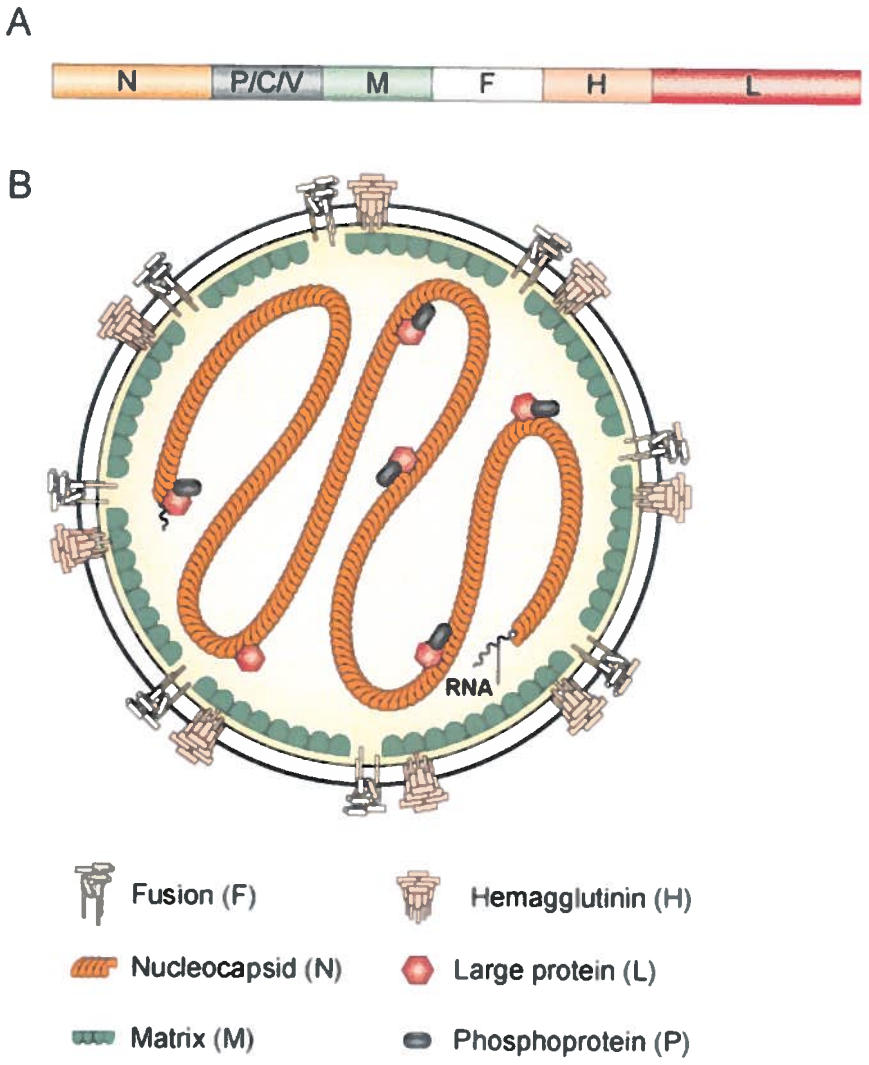

FIG. 3 Morbillivirus genome organization and schematic of the virion. (A) Typical genome map showing the different proteins encoded by morbilliviruses and (B) schematic of the morbillivirus virion (Adapted from Moss and Griffin, 2006).

In the infected cell, the N protein interacts with various cellular proteins such as heat shock protein 72 (Hsp72) and interferon regulatory factor 3 (IRF-3), resulting in the modulation of viral replication and interferon induction (tenOever et al., 2002; Zhang et al., 2002). Hsp proteins have been shown to be involved in the activation of immune responses (Wallin et al., 2002), while IRF-3 plays an essential role in antiviral immune responses by controlling interferon (IFN) induction (Sato et al., 2000).

1.3.1.2 The Phosphoprotein (P)

The P protein plays a vital role in transcription and replication. One of its primary functions is to interact with the N and L proteins, thus tethering the polymerase onto the nucleocapsid template. In addition, the P protein also plays a chaperone role for the N protein. In the absence of viral RNA or any other viral protein, N can self-assemble on cellular RNA thus forming nucleocapsid-like particles (Karlin et al., 2002; Spehner et al., 1991). P is able to bind N in its monomeric form preventing its self-association in the absence of RNA synthesis and retains the soluble form of N to the cytoplasm (Bourhis et al., 2006; Curran et al., 1995). This N-P complex is used by the polymerase to encapsidate newly synthesized genomic RNA. Enzymatic studies showed that the N-terminal domain of P is neither involved in polyadenylation nor capping of viral messenger RNA. However, it was not determined if the C-terminal domain is capable of such activities (Chinchar and Portner, 1981). It has been shown that the C-terminus of P is required for the stability of L. The absence of such P-L complexes leads to the degradation of L (Horikami et al., 1994; Smallwood et al., 1994). In addition, electron microscopy experiments have shown that the P protein is not randomly distributed but rather grouped in well defined clusters, which sometimes contain the L protein (Portner et al., 1988). It is possible that the association between the P and L proteins is necessary for these complexes to stretch over the helical template locally and become active during RNA synthesis.

1.3.1.3 The Large Protein (L)

The poorly characterized L protein is by far the largest of all the morbillivirus proteins and due to the gradient of transcription is the least abundant (Poch et al., 1990). Its coding sequence is around 6500 nucletotides, which is more than one third of the total genome length. All morbillivirus L genes have a single ORF positioned at residue 23 thereby creating 5' UTRs of identical size (McIlhatton et al., 1997). The L protein contains the polymerase activity of the RdRp while P mediates the contact between L and N (Bankamp et al., 1996; Cevik et al., 2004). Genetic and biochemical studies indicate that the L protein mediates viral mRNA capping, methylation and polyadenylation (Abraham et al., 1975; Hercyk et al., 1988; Hunt and Hutchinson, 1993).

The L protein is formed of three distinct domains separated by two highly variable hinge regions. Sequence analysis indicates that the first domain is thought to possess a RNA binding function, the second is thought to have replicative and transcriptive activity, and the third domain may be another nucleotide binding domain or a protein kinase (Poch et al., 1990). Introduction of epitope tags into the hinge regions show that H1 region does not tolerate insertions since this abolishes L function whereas the same insertions in H2 had no affect on L function. This study also demonstrated that the presence of the third domain is essential in maintaining L protein function (Duprex et al., 2002). It has been suggested that the tri-domain structure of the L protein may be functionally similar to the three-protein replication machinery seen in orthomyxoviruses however, this comparison remains to be experimentally proven (McIlhatton et al., 1997).

1.3.2 The Envelope Proteins

1.3.2.1 The Hemagglutinin (H) and Fusion (F) Glycoproteins

The hemagglutinin (H) and fusion (F) proteins are the two morbillivirus envelope glycoproteins. The envelope is formed of a lipid bilayer derived from the cellular plasma membrane of its host cell. The glycoproteins form the viral spikes (Fig. 3B), which can be seen by electron microscopy on the surface of the virus particles. The H protein is a type II glycoprotein without neuraminidase activity, whose head domain was crystallized as a dimer (Colf et al., 2007; Hashiguchi et al., 2007). The full-length H protein first forms a disulfide-linked dimer with another H protein (Plemper et al., 2000) and then with a trimer of the fusion protein F. The main role of the H protein is to mediate attachment to the target cell by binding to the cellular receptors CD46 or signaling lymphocyte activation molecule (SLAM, CD150). The F protein is a type I glycoprotein, which mediates the fusion of the virus envelope with the membrane of the host cell. In order to be biologically active, the F protein must be post-translationally cleaved. This cleavage is mediated by the proprotein convertase furin and yields the F_1 and F_2 subunits (Watanabe et al., 1995).

Morbilliviruses enters their host target cells by pH-independent membrane fusion at the cell surface. Receptor binding results in conformational changes of the H protein dimer that in turn triggers F-protein trimer conformational changes, ultimately resulting in membrane fusion between the envelope and host cell (Navaratnarajah et al., 2009; Yin et al., 2006). Fusion activity of the glycoprotein complex is controlled at different levels, including the strength of association of the F-protein trimer with the H-protein dimers (Plemper et al., 2002). Moreover, the membrane-associated viral matrix protein restricts fusion through its interactions with the cytoplasmic tails of F and H, probably by stabilizing the glycoprotein complex (Cathomen et al., 1998a; Cathomen et al., 1998b; Tahara et al., 2007). Infection of susceptible cells in culture induces widespread cell–cell fusion, producing giant multinucleated cells or syncytia, which is the hallmark cytopathic effect of a morbillivirus infection.

The H/F complex has also been demonstrated to be involved in immunosuppression (Weidmann et al., 2000a; Weidmann et al., 2000b). Infected cells, inactivated virus particles, as well as cells expressing F and H proteins are able to prevent cell proliferation suggesting that surface contact-dependent signaling events are implicated in immunosuppression (Niewiesk et al., 1997). In contrast, recombinant measles viruses expressing a vesicular stomatitis virus G protein in place of F and H cannot inhibit lymphocyte proliferation (Schlender et al., 1996). Moreover, addition of antibodies directed against the MeV glycoproteins restores lymphocyte proliferation (Sanchez-Lanier et al., 1988). The importance of the F/H complex for immunosuppression was also seen in RPV and PPRV (Heaney et al., 2002).

1.3.2.2 The Matrix Protein (M)

The M protein plays crucial roles in virus budding (Cathomen et al., 1998a), structural integrity of the virus (McIlhatton et al., 1997; Mebatsion et al., 1999), transcriptional regulation (Suryanarayana et al., 1994), and infectivity (Garoff et al., 1998). It is located on the inner leaflet of the viral envelope and is initially synthesized in the cytoplasm but rapidly associates with cellular membranes (Bellini et al., 1986; Riedl et al., 2002). More specifically, the M protein is found both in perinuclear inclusions, which are formed by the RNPs and at the inner side of the plasma membrane of infected cells where it interacts with the cytoplasmic domains of the viral surface glycoproteins F and H. M appears to act by concentrating viral envelope proteins and the RNPs to the site of virus assembly (Buechi and Bachi, 1982). It has been shown that M down regulates the glycoprotein-mediated cell-cell fusion and initiates the final virus assembly and budding process at the plasma membrane, since abrogation of the M protein function greatly affects MeV assembly (Cathomen et al., 1998a; Moll et al., 2002).

In contrast to other paramyxoviruses (Sanderson et al., 1994; Schmitt et al., 1999) MeV M is not co-transported with F and H proteins but reaches the cell surface independently (Naim et al., 2000). Furthermore, M co-transports the RNPs to the plasma membrane, after sufficient surface accumulation of M (Runkler et al., 2007). Since it has been demonstrated that actin depolymerization drugs interfere with viral budding, the cytoskeleton is likely involved in the transport of the viral components to the cell surface (Bohn et al., 1986; Stallcup et al., 1983).

Despite its involvement in multiple interactions with cellular and viral proteins (Moyer et al., 1990) and fusion regulatory function, a possible implication of the M protein in sorting and release of the virus was also investigated. In polarized epithelial cells, apical virus budding is M protein dependent, since F and H proteins both have basolateral sorting signals within their cytoplasmic domains (Maisner et al., 1998; Moll et al., 2001; Moll et al., 2004).

In addition, it has been proposed that the M protein may be a contributing factor to the development of persistent brain infection known as subacute sclerosing panencephalitis (SSPE) (Billeter et al., 1994). In fact, most viruses isolated from SSPE patients demonstrate hypermutations throughout the entire M protein (Ayata et al., 1989; Cattaneo et al., 1988; Wong et al., 1989). However, its exact role in the establishment of SSPE remains to be determined.

1.3.3 Non-Structural Proteins V and C

The V and C proteins are involved in immunosuppression and particle assembly (Devaux and Cattaneo, 2004; Kerdiles et al., 2006). The P/V/C locus in paramyxoviruses is associated with host immune evasion by interfering with antiviral cytokines in the IFN family. This interference can be due to either the inhibition of IFN signaling (Didcock et al., 1999), prevention of apoptosis (He et al., 2002; Wansley and Parks, 2002), induction of cell cycle changes (Lin and Lamb, 2000), inhibition of double-stranded RNA signaling, or prevention of IFN synthesis (He et al., 2002; Poole et al., 2002; Wansley and

Parks, 2002). Like other paramyxoviruses the MeV V protein has been shown to inhibit IFN responses by interacting with signal transducer and activator of transcription (STAT)-1 and -2 (Caignard et al., 2007; Palosaari et al., 2003). In response to type I IFN, the MeV V protein can interrupt the Janus activated kinase (JAK)-STAT pathway by blocking the melanoma differentiation-associated gene-5 (MDA-5) mediated induction pathway (Nakatsu et al., 2008), and can either hinder the dimerization of STAT proteins and their nuclear localization (Palosaari et al., 2003) or prevent the phosphorylation of STAT-1 and 2 (Takeuchi et al., 2003). Another report has demonstrated the ability of the MeV C protein to inhibit the production of type I IFN in human cells by disrupting the corresponding signaling pathway (Shaffer et al., 2003). In addition to its role in virulence, a recent study showed that the C protein is actually present in virions and plays a role in the production of infectious MeV particles by enhancing assembly and stabilizing infectivity (Devaux and Cattaneo, 2004). Infection of ferrets *(Mustela putorius furo)* with recombinant CDVs lacking their V or C proteins demonstrated that the V protein is required for the swift invasion of mucosal tissues and lymphoid organs whereas the C protein plays a role in subsequent infectious phases (von Messling et al., 2006). Taken together, these findings suggest that V and C contribute importantly to morbillivirus pathogenesis.

1.4 Host Range and Disease

Morbilliviruses obtained their collective name from the diminutive form of morbus, meaning plague (Rima and Duprex, 2006). Members of the *Morbillivirus* genus are responsible for some of the most contagious and severe human and animal diseases. Cattle, sheep, goats, seals, porpoises and dolphins are also affected by morbillivirus infections. All viruses in this genus cause an acute disease characterized by rash, respiratory and gastrointestinal signs, and severe immunosuppression (Griffin, 2001; Moss et al., 2004; Schneider-Schaulies and Schneider-Schaulies, 2008). The virus is transmitted by aerosols (Appel, 1969), and has a strong lymphotropism due to the presence of its receptor SLAM (CD150) on several types of immune cells (described in

section 1.5.2 SLAM/CD150) (Cocks et al., 1995; Sidorenko and Clark, 2003; Tatsuo et al., 2001).

MeV is the most well known member of this genus and is the only human pathogen. In industrialized countries, MeV infection is not usually life threatening, and it only rarely causes serious long-lasting sequelae. Acute MeV infections are characterized by rash, fever, cough, coryza, conjunctivitis and photophobia. A hallmark feature of MeV infection is the appearance of Koplik's spots on the mucosal surface of the mouth 1-2 days prior to other symptoms (Figure 4). Complications of acute measles usually affect the respiratory and intestinal tracts but can include otitis and encephalitis (Schneider-Schaulies et al., 2002). Despite an effective vaccine, measles is associated with high morbidity and mortality rates ranging from 5-10% in developing countries (Clemens et al., 1988; Diaz et al., 1992).

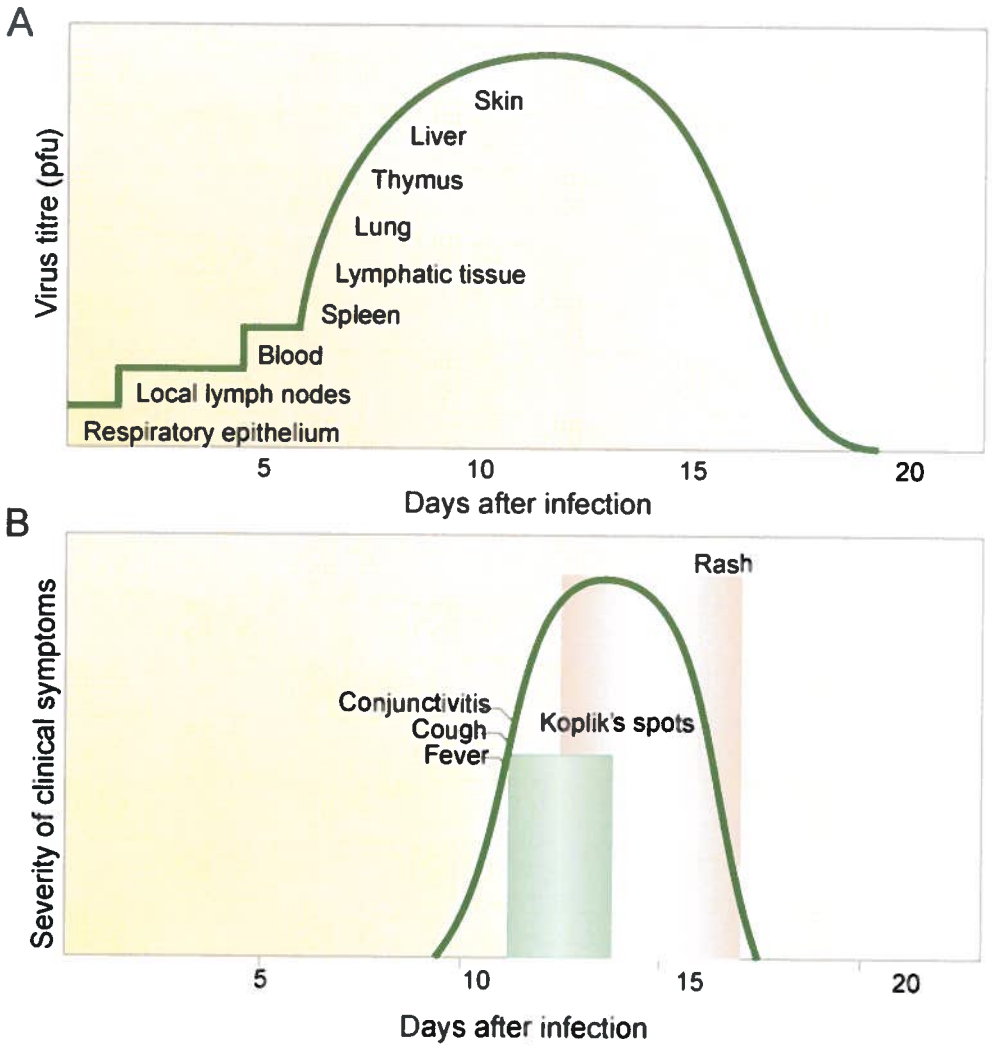

Fig. 4 Pathogenesis of measles virus infection. (A) Spread of the virus through the body from the initial site of infection in respiratory epithelia to the skin. Sites of infection are overlaid with virus titre (plaques forming units). (B) Appearance of clinical symptoms over time, including the appearance of Koplik's spots and rash (Modified from Moss and Griffin, 2006).

CDV was first identified in domestic dogs. Dogs affected by this virus usually lost their normal "good temper" hence the name distemper. In 1905 the French scientist Henri Carré first demonstrated that a CDV infection could be transmitted by a filterable agent thereby proving Koch's postulates (Carré, 1905). CDV not only infects carnivores of the *Canidae* family but also *Mustelidae* (ferrets mink, otter), *Ursidae* (bears), *Mephitidae* (skunks), *Hyaenidae* (hyenas), *Ailuridae* (red panda), *Pinnipedia,* (seals), *Procyonidae* (raccoons), *Viverridae* (civets) and *Felidae* (lions, tigers, cheetahs) (Appel et al., 1994; Cattet et al., 2004; Qin et al., 2007; Roelke-Parker et al., 1996; von Messling et al., 2003; Woolf et al., 1986).

1.5 Receptors

1.5.1 CD46

The first receptor to be identified for MeV was CD46 (Dorig et al., 1993; Naniche et al., 1993). CD46 is a type-1 transmembrane glycoprotein of 57-67 kilodaltons (kDa) that belongs to a family of complement factors involved in protection from self-cell destruction by complement (Liszewski et al., 1991; Sidorenko and Clark, 2003). It is ubiquitously expressed in several isoforms on all nucleated cells (Bartz et al., 1998; Naniche et al., 1993). MeV vaccine strains and some wild-type strains can cause a down-regulation of CD46 resulting in an increased susceptibility of infected cells to complement-mediated lysis (Schneider-Schaulies et al., 1995; Schnorr et al., 1995). Genetic and biochemical analyses have identified several aa in MeV involved in the interaction with CD46, of which aa 481 of the MeV H protein was shown to be the most important (Lecouturier et al., 1996). However, further studies revealed that this receptor is mainly used by MeV vaccine strains and Vero cell-adapted wild-type strains since CD46 specific antibodies did not prevent infection of lymphocytes (Bartz et al., 1998; Hsu et al., 1998).

1.5.2 SLAM/CD150

SLAM or CD150 is expressed on immature thymocytes, activated T and B cells, memory T cells, monocytes and mature dendritic cells (DCs), in both humans and mice (Cocks et al., 1995; Minagawa et al., 2001; Sidorenko and Clark, 2003; Tatsuo et al., 2001). SLAM was first identified as a MeV receptor by functional expression cloning in 2000 (Tatsuo et al., 2000). Furthermore, the use of anti-SLAM antibodies inhibited MeV entry, confirming SLAM's role as cellular receptor (Erlenhoefer et al., 2001). SLAM has subsequently been identified as a general morbillivirus receptor with CDV using canine SLAM and RPV bovine SLAM (Tatsuo et al., 2001). It has also been demonstrated that CDV wild-type strains are readily isolated in Vero cells stably expressing canine SLAM thereby indicating that SLAM is used as the main receptor *in vivo* (Seki et al., 2003). An additional study revealed that a SLAM-blind recombinant virus is unable to cause disease in its natural host emphasizing the importance of this molecule for pathogenesis (von Messling et al., 2006).

1.5.3 Other Receptors

Although the tissue distribution of SLAM explains the morbillivirus lymphotropism, they are also known to infect epithelial, endothelial and neuronal cells *in vivo* (Herndon and Rubinstein, 1968; McChesney et al., 1997; Sakaguchi et al., 1986). Since these cells do not express SLAM and since wild-type viruses do not use CD46 as a receptor, the existence of additional cellular receptors has been postulated (Cocks et al., 1995; Yanagi et al., 2006). Studies with recombinant MeVs expressing the green fluorescent protein demonstrated SLAM- and CD46- independent entry in CHO and EL4 cells providing further evidence for an additional receptor (Hashimoto et al., 2002; Leonard et al., 2008). The same phenomenon is seen in other morbilliviruses; however, it is not known if they all use the same molecule (Bundza et al., 1988; Di Guardo et al., 2005; von Messling et al., 2004; Wohlsein et al., 1993). Very recently, it has been demonstrated *in vitro* that MeV infection occurs via CD147/EMMPRIN (extracellular matrix metalloproteinase inducer) (Watanabe et al., 2010). CD147 is a transmembrane

glycoprotein and is expressed on many different cell types including epithelial and neuronal cells. The authors suggest that CD147 may function as an entry receptor for MeV in SLAM-negative cells, however it remains to be determined whether this molecule actually plays a role for MeV infection *in vivo*.

1.6 Immunosuppression

MeV induces specific immunity and causes a generalized suppression of the immune response that can last up to six months after primary infection (Kerdiles et al., 2006; Schneider-Schaulies and ter Meulen, 2002). This immunosuppression is characterized by lymphopenia of both CD4+ and CD8+ T-cells without significantly altering the CD4/CD8 ratio (Arneborn and Biberfeld, 1983; Okada et al., 2000). An increased expression of Fas (CD95) and annexin V staining on both types of T-cells occurs during the acute phase of measles infection, suggesting that apoptosis plays a part in the observed lymphopenia (Ryon et al., 2002). This is also true for acute CDV infections (Schobesberger et al., 2005). However, a significant amount of uninfected cells present in lymphoid tissues undergo apoptosis (Kumagai et al., 2004; Moro et al., 2003a), indicating that mechanisms other than virus-dependent apoptosis are involved in lymphopenia (Kajita et al., 2006; Moro et al., 2003b; Schobesberger et al., 2005).

MeV infection is also characterized by a cytokine imbalance favouring a prolonged T-helper 2 (Th2) response at late stages. This suppresses cellular immunity to secondary infections (Griffin and Ward, 1993), which are responsible for the majority of measles associated deaths. The initial T-helper 1 (Th1) response mediates viral clearance, while the Th2 response is involved in the development of virus-specific antibodies. Increased levels of interleukin (IL)-10 have been found for weeks in the plasma of children infected with measles (Moss et al., 2002). IL-10 down-regulates the synthesis of numerous cytokines, suppresses macrophage activation, abolishes T-cell proliferation, and promotes the release of cytokine inhibitors (Chernoff et al., 1995; de Waal Malefyt et al., 1991; Sieling et al., 1993). The suppressive nature of IL-10 on CD4+ T-cells and macrophages may play a role in inhibition of delayed-type hypersensitivity (DTH)

responses and further contribute to increased susceptibility to secondary infections (Moss et al., 2004). It has been determined for CDV in dogs that a lack of detectable cytokine expression in peripheral blood mononuclear cells (PBMC) is associated with a high viral load and viremia, indicating that an overwhelming virus infection may suppress cytokine production in lymphoid cells (Grone et al., 1998). This observation was corroborated in the ferret model, where a lack of cytokine expression in peripheral blood leukocytes leads to severe immunosuppression and the lethal outcome. In contrast, surviving ferrets exhibited a robust and sustained cytokine production with an initial Th1- followed by a Th2-biased immune response (Svitek and von Messling, 2007).

Another characteristic of MeV infection is the inhibition of lymphocyte proliferation following mitogenic, allogeneic or recall antigen stimulation *ex vivo* (Borrow and Oldstone, 1995; Hirsch et al., 1984). This effect is not only seen for MeV but for all morbillivirus infections (Heaney et al., 2002). *Ex vivo* studies have demonstrated that IL-2 is sufficient to reverse the proliferation inhibition of PBMCs from MeV-infected patients, suggesting that classical anergy is the cause of lymphocyte unresponsiveness to mitogen stimulation (Griffin et al., 1987). In addition, contact between MeV-infected cells and human PBMCs was sufficient to inhibit lymphocyte proliferation *in vitro* (Sanchez-Lanier et al., 1988), which could be reversed by adding anti-MeV serum or carbobenzoxy-D-Phe-L-Phe-Gly or fusion inhibitory peptide (FIP), a synthetic oligopeptide known to inhibit MeV-induced fusion (Yanagi et al., 1992). This observation indicates the importance of the interactions between the MeV glycoproteins H and F with cell surface receptors for T cell proliferation.

2. Central Nervous System Complications and Morbilliviruses

Members of the *Morbillivirus* genus, CDV, PDV, and the CeMV of dolphins and porpoises exhibit high levels of central nervous system (CNS) infection in their natural hosts (Domingo et al., 1990; Griot et al., 2003; Kennedy, 1998). In contast, CNS complications are rarely observed for MeV and have not been reported for RPV and PPRV infections (Cosby et al., 2002). However, it is possible that all morbilliviruses have the potential to infect the CNS, since RPV and PPRV are neurovirulent in mouse models (Galbraith et al., 2002).

2.1 Complications Associated with MeV

Infection of the CNS during acute measles may be a regular occurrence, since changes in electroencephalograms are observed in approximately half of all patients (Nasr et al., 2000). Most patients rapidly clear the virus and do not suffer from long-term sequelae. However, patients with abnormal responses or immunocompromised individuals can suffer severe neurological consequences. Three different types of CNS complications can arise during or after acute measles infection.

2.1.1 Acute Demyelinating Encephalomyelitis (ADEM)

Acute demyelinating encephalomyelitis (ADEM) occurs in approximately 1/1000 MeV cases, 10-20% of which result in death (Miller, 1964). Clinically, ADEM is characterized by an acute onset of focal neurological signs such as motor weakness or paraplegia and encephalopathy. Patients usually present impaired consciousness, fever and stiffness of the neck, and in some cases seizures. ADEM occurs about 5 to 6 days after the onset of rash and is characterized by minimal amounts or absence of virus in the brain of patients. Furthermore, virus can only be detected with highly sensitive techniques such as *in situ* hybridization. ADEM is associated with widespread perivascular demyelination of neurons that surround small cerebral vessels. Furthermore, there is a loss of myelin basic proteins (MBP) in regions where demyelination occurs, which is

reminiscent of experimental allergic encephalitis (EAE) (Gendelman et al., 1984). Taken together these findings suggest that ADEM results from an autoimmune reaction rather than from the virus itself. However, due to its low prevalence, the characterization of ADEM has been difficult.

2.1.2. Measles Inclusion Body Encephalitis (MIBE)

The second neurological complication associated with MeV is measles inclusion body encephalitis (MIBE). It is seen only in immunocompromised or immunodeficient individuals and may be accompanied by giant cell pneumonia (Kaplan et al., 1992; Mustafa et al., 1993). The mortality rate reaches approximately 75%, and all survivors have significant neurological sequelae (Mustafa et al., 1993). Imaging studies, such as brain MRI and computed tomography, are often normal in MIBE patients so specific diagnosis requires a brain biopsy (Freeman et al., 2004). The median length of time from acute MeV or exposure to MIBE onset is 4 months. There is currently no effective treatment for MIBE. MIBE has been documented to arise following vaccination, in patients with dysgammaglobulinaemia or a pre-existing undiagnosed immune abnormality (Bitnun et al., 1999; Mawhinney et al., 1971). The mechanisms by which the virus reaches the CNS and establishes viral persistence are not well understood. A case study reported that while the patient had an absence of an antibody response to certain vaccines, he did show specific antibodies to other antigens, including MeV, suggesting an abnormality in the humoral response (Bitnun et al., 1999). MIBE is characterized by a progressive neurological deterioration, including seizures and altered mental status. Biopsies have shown that MIBE causes gliosis with the presence of intracytoplasmic and intranuclear inclusions in glial cells and neurons. Very little inflammation is present and in most cases virus can be isolated from the brains of patients (Ohuchi et al., 1987).

2.1.3. Subacute Sclerosing Panencephalitis (SSPE)

The third and most uncommon neurological complication associated with MeV is SSPE. This encephalopathy affects approximately one out of every million cases of MeV infection. However, it has been reported that in some areas, like Papua New Guinea, the prevalence can be as high as one out of every ten to twenty-five thousand cases (Sips et al., 2007; Takasu et al., 2003). On average, patients experience the first symptoms of SSPE about eight years after the acute infection (Connolly et al., 1967; Modlin et al., 1977) and one contributing factor for the risk of developing SSPE is a natural infection before the age of two (Jabbour et al., 1972). The first signs of SSPE include a low attention span and severe motor dysfunction such as ataxia. The disease progresses to a vegetative state, ultimately resulting in death. Upon examination, demyelination and extensive infection of neurons are seen in all cases. In addition, in later stages of the disease, oligodendrocytes, astrocytes and endothelial cells are all infected (Kirk et al., 1991). Immunohistochemical analysis shows an increase in major histocompatibility complex (MHC) classes I and II positive cells in the brains of SSPE patients, which are mostly macrophages/microglia and reactive astrocytes, and occasionally neurons (Gendelman et al., 1984; Hofman et al., 1991).

In SSPE patients humoral and cell-mediated immune functions are normal (Norrby and Kristensson, 1997). Extremely high titers of neutralizing antibodies are found in the cerebrospinal fluid (CSF) and in the serum of patients suffering from SSPE (Hall and Choppin, 1979). Most of these antibodies are directed against the MeV structural proteins N, F and H, while very few antibodies against P and M are found. Viral genomes from autopsied SSPE patients carry many mutations in the M, F and H proteins rendering them non-functional (Ayata et al., 2007; Billeter et al., 1994). In contrast, the RNP proteins were found unaltered. Among the most common modifications seen are point mutations and deletions, hypermutation events, insertion of premature stop codons and even the truncation and or distortion of the cytoplasmic domain of the F protein (Cattaneo et al., 1986; Schmid et al., 1992; Wong et al., 1989). These changes

could explain why the virus is still able to replicate, but unable to effectively form particles (Billeter et al., 1994; Cattaneo et al., 1989b).

2.2. Canine Distemper Encephalitis (CDE)

2.2.1 The Acute Phase

CDV causes a wide range of encephalopathies in dogs, including acute non-inflammatory encephalitis, acute encephalitis associated with lymphocyte infiltration and perivascular cuffing, acute demyelination of white matter, a subacute to chronic form of encephalitis that involves the degeneration and necrosis of various cell populations accompanied by demyelination and last of all old dog encephalitis (Axthelm and Krakowka, 1998). Previous studies have shown that these different CDV induced neuropathologies are strain specific (Summers et al., 1984). Certain strains, such as Cornell A75/17 and Ohio strain R252 induce progressive demyelination, while an infection with Snyder Hill (SH) strain leads to acute disease, seizures and polioencephalitis, which is a hallmark of canine distemper encephalomyelitis (McCullough et al., 1974; Summers et al., 1979, 1984; Vandevelde and Zurbriggen, 2005). CDV enters the CNS by infecting mononuclear cells that cross the blood-brain barrier, but it may also be released into the CSF by infected epithelial cells in the choroid plexus and then fuse with the ependymal cells of the ventricles (Higgins et al., 1982; Vandevelde and Zurbriggen, 2005).

Not all dogs infected with CDV die, and only 50% develop signs of disease. Mortality rates vary depending on the strain and the dog's ability to mount an effective immune response (Appel, 1969; Appel et al., 1982; Krakowka et al., 1975). Based on histopathological studies and examination of CSF from infected dogs, it is thought that CDV always transits through the CNS of infected animals. However, if the animal clears the virus in a timely manner, only minimal damage will be observed. A delayed immune response results in clinical encephalomyelitis of varying degrees of severity (Summers and Appel, 1994).

Encephalitis during the acute phase of disease usually correlates with the presence of virus in the brain, and its development is highly predictable (Vandevelde and Zurbriggen, 2005). The initial myelin lesions develop during the period of severe immunosuppression, and are not accompanied by an inflammatory response since there is no evidence of perivascular cuffing (Vandevelde et al., 1982). One of the first signs of demyelination involves ballooning of the myelin sheets, vacuolation of the white matter, myelin phagocytosis and astrocytic swelling. To explain these findings, many studies have tried to establish a correlation with an infection of oligodendrocytes, although very few contain CDV mRNA (Vandevelde and Zurbriggen, 2005). Morphological changes have been observed without evidence of necrosis or apoptosis (Blakemore et al., 1989; Summers and Appel, 1987). Instead, demyelination appears to correlate with the infection of glia in the white matter (Vandevelde et al., 1985; Zurbriggen et al., 1995). The exact mechanism of demyelination during this early phase is still unknown. It is plausible that oligodendrocytes are affected by neighbouring infected cells. During the acute phase, MHC class II is up-regulated in the white matter, most likely in microglial cells (Alldinger et al., 1996), which may have detrimental effects on the myelin sheets.

2.2.2 The Chronic Phase of Distemper and Inflammatory Demyelination

At six to seven weeks post-infection, which coincides with recovery from immunosuppression, perivascular cuffing by lymphocytes, plasma cells and monocytes are seen in the initially virus-produced brain lesions. This infiltration then leads to additional immune-mediated tissue damage (Vandevelde et al., 1981; Wisniewski et al., 1972). In addition to immune cell infiltration, large amounts of intrathecal antibodies are produced (Vandevelde et al., 1986; Wunschmann et al., 1999). The pro-inflammatory cytokines IL-6, IL-8, IL-12 and tumor necrosis factor (TNF)-α are also up-regulated, whereas levels of anti-inflammatory cytokines such as IL-10 and transforming growth factor (TGF)-β remain stable, and the pro-inflammatory cytokines IL-1, IL-2 and IFN-γ are undetectable (Markus et al., 2002). Studies have shown that antiviral immune complexes against CDV are able to induce oligodendroglial degeneration in mixed brain cell cultures. They also showed that the depletion of macrophages in such cultures

resulted in preventing the oligodendrocyte loss and therefore also preventing demyelination. These results suggest that demyelination may in fact result from a by-stander effect that is caused by antibody dependent cellular toxicity (Botteron et al., 1992; Griot-Wenk et al., 1991). Antibodies against myelin and MBP have also been found in the serum and CSF of clinical and experimental cases of CDV (Krakowka et al., 1973; Vandevelde et al., 1986). However, these immunological events do not correlate with disease progression and the importance of these findings remains to be determined. Viral persistence may also contribute to the chronic phase demyelination (Vandevelde and Zurbriggen, 2005). CDV can persist in the white matter outside demyelinating lesions (Bollo et al., 1986), and may lead to recurrent immune activation (Vandevelde and Zurbriggen, 2005). Since astrocytes are a prime target of CDV, the high level of infection observed in these cells likely contributes to the overall tissue damage in the CNS of infected dogs during the chronic phase of the disease (Nedergaard et al., 2003; Ransom et al., 2003; Seifert et al., 2006).

2.3 Old Dog Encephalitis (ODE)

Old dog encephalitis (ODE) is a rare condition in elderly dogs that have recovered from a CDV infection that occurred many years before. Rarely, it can be vaccine-associated without any evidence of a previous subclinical CDV infection. Progressive cortical neurological signs with multifocal severe perivascular and parenchymal lymphoplasmacytic encephalitis, and cerebral neuronal infection are characteristic for ODE. The cerebrum and brainstem are the main areas of damage. In experimental infections of gnotobiotic dogs, clinical signs of ODE include ataxia, generalized tremors and hyperkinesis. At later times post-infection, dogs may develop grand mal seizures, circling behaviour, blindness, and paresis before succumbing to the disease (Axthelm and Krakowka, 1998).

The similarities between SSPE in humans and ODE in dogs have generated a lot of interest. First, both of these afflictions are extremely rare, and occur years after vaccination or initial infection. They are accompanied by demyelination and the result of viral persistence in the CNS. However, one main difference between these two neurological complications lies at the molecular level. SSPE isolates replicate poorly in MeV susceptible cell lines, indicating that the initial virus became replication deficient. In addition, most mutations appear to be in the M protein, leading to a reduction of M-specific antibodies (Hall and Choppin, 1979; Hall et al., 1979; Stephenson et al., 1981). In contrast, ODE isolates show few mutations in viral proteins (Shapshak et al., 1982). Furthermore, dogs produce antibodies against all viral proteins, including M (Hall et al., 1980).

3. Models for the Study of Morbillivirus Neurovirulence

Since CNS complications are only seen in CDV and MeV infections, researchers must use either natural hosts of CDV, such as the dog or the ferret, or transgenic animal models expressing one of the two known MeV receptors CD46 or SLAM to study neurovirulence. These animal models were initially used to examine pathogenesis or immunosuppression and have subsequently been adapted to study neurovirulence.

3.1 Transgenic Mouse Models

NSE-CD46 transgenic mice express the BC1 isoform of CD46, under the control of the neuron specific enolase (NSE) promoter. This promoter restricts the expression of CD46 to only CNS neurons. However, by restricting the expression of CD46, this model does not replicate the natural ubiquitous distribution of CD46 found in humans. NSE-CD46 mice are usually infected either intranasally (i.n.) or intracranially (i.c.) with vaccine strains of MeV. Only neonatal or immunodeficient adult mice succumb to the disease. Upon infection these animals mount an inflammatory response, including infiltration of CD4+ and CD8+ T cells, an up-regulation of MHC class I and II molecules, gliosis, apoptosis and the expression of chemokines such as regulated upon activation normal T-cell expressed and secreted (RANTES), IFN-γ inducible protein 10 (IP-10), macrophage inflammatory protein 1 α (MIP-1 α) and -1β, and pro-inflammatory cytokines such as IL-1β, IL-6, and TNF-α. Despite this robust immune response, these mice cannot effectively control the infection and eventually die from the disease. In contrast, immunocompetent adult mice are able to mount an efficient immune response and survive the infection. These transgenic mice are also an important source of primary culture of hippocampal neurons expressing CD46. The use of these cells is then used to corroborate *in vivo* findings (Lawrence et al., 1999; Manchester et al., 1999; Manchester and Rall, 2001).

YAC-CD46 mice are another transgenic model, which express a yeast artificial chromosome (YAC) containing the entire human CD46 encoding gene. This allows the expression of CD46 under the control of its natural promoter resulting in widespread expression throughout the animal, which mimics the natural distribution seen in humans (Mrkic et al., 1998; Oldstone et al., 1999). YAC-CD46 mice express all four major isoforms of CD46, and the overall CD46 expression is among the highest of all transgenic mouse models. Intracranial injection of MeV in this model results in an immune response similar to the NSE-CD46 mice (Oldstone et al., 1999). However, MeV replication is restricted to CNS neurons, while normal MeV targets such as astrocytes and microglia remain uninfected. It is possible that the expression of other receptors is needed for efficient infection of these cell types. YAC-CD46 mice can also be infected intraperitoneally (i.p.) or intravenously (i.v.), resulting in low-level replication without viremia or clinical signs (Manchester and Rall, 2001). It is hypothesized that under these conditions, the immunocompetent mice can clear the viral infection before widespread dissemination.

The YAC-CD46 mice were bred with an interferon-α receptor deficient mice ($IFNAR^{-/-}$) (Mrkic et al., 1998). Like the parental strain, these mice widely express all four major isoforms of CD46 at high levels. Intranasal infection with the MeV Edmonston strain, a typical vaccine strain, resulted in limited replication. Infectious virus was only occasionally recovered from lungs and brain and never detected in other regions (Mrkic et al., 1998), and pathological changes in the lungs included inflammation. These findings are comparable to those observed in intranasally infected macaques (Albrecht et al., 1980; McChesney et al., 1997). Intracranial inoculation of MeV in $IFNAR^{-/-}$ CD46 mice resulted in meningitis with inflammatory infiltrates of leukocytes and extensive vacuolization and necrosis of nearby brain parenchyma. Reactive astrocytes were also detected around but not in regions of necrosis. Curiously, a lesser extent of infection was also observed in non-transgenic IFNAR deficient mice demonstrating that factors other than CD46 are important for MeV replication in the CNS.

Thus far there are four different transgenic mouse models that express the other known MeV receptor SLAM. To date, only one has been used to address questions regarding neurovirulence. This model consists of a C57BL/6 genetic background expressing human SLAM linked to the mouse hydroxymethylglutaryl coenzyme A reductase promoter region. SLAM is therefore ubiquitously expressed, but the highest expression levels of SLAM were seen in the brain. When these mice are inoculated intracranially with vaccine or wild-type strains, MeV N specific RNA can be detected up to three months after the infection indicating that MeV can establish persistence in the CNS even if no virus particles were isolated from these brains. In contrast, when suckling mice are infected intracranially, infectious particles could be retrieved from brains and spinal cord as early as 72 h post-infection suggesting active virus replication and dissemination (Sellin et al., 2006). Even though both vaccine and wild-type strains are virulent in this model, the vaccine strains remain less pathogenic.

3.2 Ferret Model of SSPE

The ferret, a natural CDV host, has been used as an SSPE model. Upon intracerebral inoculation of brain tissues from SSPE cases, ferrets developed signs of neurological involvement such as ataxia, hind limb spasticity and a general loss of interest in their environment. Some animals also manifested abnormal electroencephalograms three to five weeks post-infection. Histopathology revealed the presence of perivascular cuffing, neuronophagia, microglia and reactive astrocytes. No signs of demyelination were observed, and the cerebellums of all animals did not show signs of infection and/or damage. Electron microscopy studies did not reveal any virus particles in the brain of these animals nor were antibodies detected in serum samples. These observations demonstrated the feasibility of propagating an infectious agent isolated from the brains of SSPE patients in ferret brains (Katz et al., 1968).

To reproduce all features of SSPE in ferrets, animals were first vaccinated against MeV and followed by infection with an SSPE isolate six weeks later. The D.R. strain used in that study was a cell-associated non-productive lacking the expression of the M protein. With this experimental approach the outcome of infection included encephalitis in 50% of all ferrets (Mehta and Thormar, 1979), resembling the condition seen in SSPE patients. Furthermore, serum antibody titers against MeV increased during the subclinical period and cell-associated SSPE virus was present in the brains for a period of up to eight and a half months post-infection indicating an active immune response in the CNS of infected animals. In addition, when ferrets are first immunized against MeV and then infected with D.R., the histopathology resembles those seen in humans afflicted with SSPE (Brown et al., 1985). These findings confirm that ferrets can be persistently infected with a SSPE virus, and low level production of virus proteins and particles can continuously stimulate an immune response as with human SSPE cases. Overall, this strengthens the validation of the ferret model as a means to investigate certain aspects of SSPE.

3.3 Other Animal Models

It is important to mention that other animal models exist for the study of morbillivirus infections. Macaques have been crucial for the development of measles vaccines (DeSwart, 2009). Unfortunately, these animals are rarely used to examine neuropathogenesis. Only a few investigators have used tissues collected from monkeys to model human CNS disease (Albrecht et al., 1977; Steele et al., 1982), since cost and availability limit the use of primates.

More recently, a cotton rat model (*Sigmodon hispidus*) has been developed for the study of MeV pathogenesis. These animals are inbred and can be infected with a broad range of MeV strains including vaccine, wild-type and even recombinant measles viruses without adaptation. They support MeV replication in the respiratory tract and lymphoid organs and develop the classical immunosuppression that accompanies measles. Because of their small size and availability they are more cost-effective than non-human primate

models. Cotton rats have been proven especially useful to screen antiviral substances and vaccines. Regrettably, it has not been determined if they are a suitable model for the study of morbillivirus neurovirulence (Niewiesk, 1999, 2009; Wyde et al., 1992).

4. Hypothesis and Research Objectives

All animal models used to investigate morbillivirus neurovirulence have advantages and drawbacks. No transgenic mouse model fully reproduces the tissue distribution for both known human measles receptors, CD46 and SLAM. In order to induce clinical signs of CNS dysfunction, neonatal mice or intracranial inoculation must be used. Only primates develop measles-like disease, but neurological complications are rare. Even though CNS involvement is more frequently associated with CDV infections in dogs, the incidence is still too low to make a mechanistic investigation affordable.

Recently, ferrets infected with CDV have been shown to efficiently mimic all aspects of a morbillivirus infection including severe leukopenia and gastrointestinal and respiratory signs, and frequently involve CNS infection. Since tropism and tissue distribution of many, if not all, morbillivirus infections are similar, findings in ferrets can likely be extrapolated to other morbillivirus infections. Our working hypothesis is that the ferret model could also be used to study the events leading to and occurring during the acute phase of CNS infection.

Our group has previously shown that animals infected with the 5804P strain, which kills within two weeks, never manifest neurological signs while those infected with the A75/17 strain survive for three to five weeks and develop CNS disease. The first research objective was to use the A75/17 strain to characterize morbillivirus neuroinvasion. Towards this, we first confirmed the neurovirulent potential of A75/17 in the ferret model. Next, we investigated the timing and sequence of events during the acute phase of morbillivirus CNS invasion by using immunohistochemistry techniques to determine which pathways are used by CDV to access the brain and its target cells.

For most virus infections of the CNS immune-mediated damage, the route of inoculation, and death of infected cells, all contribute to the pathology observed. Our second objective aimed at investigating the role of these factors in early canine distemper neuropathogenesis. Towards this, we infected ferrets with the Snyder Hill strain, which causes CNS disease within two weeks. We first compared the neuroinvasion kinetics upon intranasal and intraperitoneal inoculation to assess whether the point of entry into the periphery can influence viral dissemination into the CNS. Next, we characterized the pathological changes and associated inflammatory response triggered by the infection.

Based on our results obtained in the context of the first objective, which suggest that CDV spreads along the olfactory route across communicating neurons to gain access to the inner regions of the CNS, we hypothesized that CDV disseminates trans-neuronally. To test this hypothesis, an *in vitro* model of primary culture of ferret neurons was established. We first characterized our neuronal culture and then examined if most of the virus produced during a neuronal infection is released in the supernatant or remain cell bound. The primary culture of neurons also allowed us to use a modified Campenot chamber system previously described for the use of studying pseudorabies virus infection (Ch'ng and Enquist, 2006). This system duplicates all of the *in vivo* correlates of trans-neuronal spread and permits us to determine if CDV can disseminate across neurons in an anterograde or retrograde direction.

CHAPTER 2

PUBLICATIONS

Publication no. 1

Journal of Virology, October 2006, p. 9361-9370, Volume 80, No. 19.

Canine Distemper Virus Uses both the Anterograde and the Hematogenous Pathway for Neuroinvasion

Penny A. Rudd,[1] Roberto Cattaneo,[2] and Veronika von Messling[1]*

INRS-Institut Armand-Frappier, University of Quebec, Laval, Quebec, Canada,[1] Virology and Gene Therapy Graduate Track, Mayo Clinic College of Medicine, Rochester, Minnesota[2]

* Corresponding author.

Mailing address: INRS-Institut Armand-Frappier, University of Quebec,
531, Boul. des Prairies,
Laval, Quebec H7V 1B7,
Canada. Phone: (450) 687-5010. Fax: (450) 686-5305.
E-mail: veronika.vonmessling@iaf.inrs.ca

Abstract

Canine distemper virus (CDV), a member of the Morbillivirus genus that also includes measles virus, frequently causes neurologic complications, but the routes and timing of CDV invasion of the central nervous system (CNS) are poorly understood. To characterize these events, we cloned and sequenced the genome of a neurovirulent CDV (strain A75/17) and produced an infectious cDNA that expresses the green fluorescent protein. This virus fully retained its virulence in ferrets: the course and signs of disease were equivalent to those of the parental isolate. We observed CNS invasion through two distinct pathways: anterogradely via the olfactory nerve and hematogenously through the choroid plexus and cerebral blood vessels. CNS invasion only occurred after massive infection of the lymphatic system and spread to the epithelial cells throughout the body. While at early time points, mostly immune and endothelial cells were infected, the virus later spread to glial cells and neurons. Together, the results suggest similarities in the timing, target cells, and CNS invasion routes of CDV, members of the Morbillivirus genus, and even other neurovirulent paramyxoviruses like Nipah and mumps viruses.

Introduction

Canine distemper virus (CDV) and the closely related viruses that infect marine mammals have the highest incidence of central nervous system (CNS) complications among viruses of the genus Morbillivirus. Up to 30% of dogs exhibit signs of neurologic involvement during or after CDV infection, and most wild carnivores that succumb to CDV have some evidence of CNS infection (8, 18, 20, 38, 51). With 1 in 1,000 cases, the neurovirulent potential of measles virus (MeV) is comparatively lower, but CNS complications remain one of the main problems associated with MeV infections in countries with an established health care system (32). Because of its relatively high degree of neurovirulence and the availability of a sensitive small animal model, CDV is an ideal candidate to characterize the events involved in morbillivirus neuroinvasion.

All morbilliviruses display a strong lymphotropism, which correlates with the presence of their principal receptor, the signaling lymphocytic activation molecule (SLAM, CD150), on a variety of immune cells (6, 36, 40). In ferrets infected with a virulent CDV strain, more than 50% of circulating peripheral blood mononuclear cells (PBMC) contain infectious virus, and up to 10% of PBMC in MeV-infected monkeys are virus positive (46, 53). Because of these findings and the fact that morbilliviruses are highly cell associated, it is thought that the contact between virus and CNS occurs through infected PBMC. Previous studies of typical wild-type isolates like strain A75/17 in dogs further support this theory (38).

At the onset of the symptomatic disease around 14 days after intranasal inoculation, infected cells are predominantly detected in the perivascular spaces of the CNS, the choroid plexus, and the ependyma (19, 39). Around 3 weeks after infection, CDV-positive glial cells and neurons are found in the white matter, and the beginning of demyelination is observed in these regions (41). The CNS infection peaks 4 to 5 weeks after inoculation, when virus is detected in neurons and glial cells throughout white and gray matter in a focal fashion (23, 45, 52). Around 10% of dogs die at this time from acute encephalitis developing while their immune system fails to control the infection.

In animals that mount an effective cellular and humoral immune response, perivascular cuffing and lymphocyte infiltration of the infected areas occur at the same time as the rash and other signs of disease recede, and CDV-specific neutralizing antibodies are detected in the serum and cerebrospinal fluid (CSF) (39, 41, 52). This immune response results in virus clearance from the CNS, but can be accompanied by continued demyelination, which is ultimately responsible for the development of neurological signs in a subset of animals several weeks after recovery from the acute infection (38, 44).

Despite this body of knowledge, the timing and sequence of events during the acute phase of morbillivirus CNS invasion remain unclear, principally because only a fraction of experimentally infected dogs develop acute encephalitis (38, 51) and the available rodent models require injection of the virus into the brain to cause infection (10, 22). We have previously established a morbillivirus pathogenesis model based on the study of CDV in ferrets, one of its natural hosts (46, 47). CDV-infected ferrets develop an acute disease that is usually lethal within 2 to 5 weeks, and there is little variation between animals infected with the same strain (37, 47).

To expand our ferret model to the characterization of morbillivirus neuroinvasion, we first confirmed the neurovirulent potential of A75/17 in ferrets. This strain is a typical representative of canine street isolates that has been extensively characterized in dogs (38). We generated an infectious cDNA clone of this strain, which corresponded exactly to the sequence deposited in GenBank (accession no. AF164967), and introduced the reporter gene coding for enhanced green fluorescent protein (eGFP) in this cDNA. The resulting virus facilitated monitoring the CNS invasion routes. We show that CNS invasion occurs only after extensive spread to epithelia. We demonstrate anterograde invasion via the olfactory bulb in addition to the previously characterized hematogenous spread through the choroid plexus and cerebral blood vessels (19). This work directly visualizes, for the first time, different stages of morbillivirus neuroinvasion during the acute disease phase, providing new insights into the disease progression and cellular targets.

Materials and Methods

Cells and viruses

VerodogSLAMtag cells (47) and 293 cells (ATCC CRL-1573) were maintained in Dulbecco's modified Eagle's medium (Invitrogen, Burlington, Ontario, Canada) with 5% fetal calf serum (Invitrogen, Burlington, Ontario, Canada). Zeocin (Invitrogen, Burlington, Ontario, Canada) was added (1 mg/ml) to the VerodogSLAMtag cells to maintain the constitutive expression of canine SLAM. All viruses were propagated in VerodogSLAMtag cells. A lymph node homogenate of a dog experimentally infected with CDV strain A75/17 was a kind gift of Max Appel.

Construction and recovery of recombinant viruses

To generate an infectious cDNA clone of the neurovirulent CDV strain A75/17, RNA was isolated directly from the lymph node homogenate. The cloning strategy was the same as those used previously for other CDV vaccine and wild-type strains (47). Briefly, the RNA was reverse transcribed using Superscript II (Invitrogen, Burlington, Ontario, Canada), and the entire genome was amplified in 10 fragments using high-fidelity polymerase (Roche Diagnostics, Laval, Quebec, Canada) and subcloned into pCR-TOPO (Invitrogen, Burlington, Ontario, Canada). At least four clones of each fragment were sequenced to establish a consensus sequence. The viral cDNA clone was then assembled from fragments corresponding to the consensus sequence using naturally occurring unique restriction sites, yielding pA75/17. An eGFP-expressing derivative containing the eGFP open reading frame in an additional transcription unit between the H and L genes (pA75/17eH) was obtained following the cloning strategy for 5804PeH (46). The corresponding recombinant viruses were recovered as described previously, using an MVA-T7-based system (48).

Animal infection, grading of clinical signs, and imaging

The animal experiments were carried out as described previously (47). Briefly, unvaccinated male ferrets (Mustela putorius furo) 16 weeks and older (Marshall Farms, North Rose, NY) were then infected intranasally with 10^4 50% tissue culture infectious doses ($TCID_{50}$) of the respective virus under general anesthesia (10 mg/kg ketamine, 1 mg/kg midazolam; CDMV, St. Hyacinthe, Quebec, Canada). Following the infection, animals were monitored daily for signs of disease, and blood was collected at various time points from the jugular vein under general anesthesia.

A grading system was established to evaluate the severity of clinical signs and to determine end points for the removal of animals from the study. Animals that failed to eat for more than 48 h, experienced weight loss of 15 to 20%, became severely dehydrated, developed CNS signs (circling behavior, paralysis, or focal or generalized seizures), displayed any other important reduction in functional status (severe pneumonia and/or diarrhea), or became moribund before the end of the protocol were euthanized with an overdose of pentobarbital (Nembutal; CDMV, St. Hyacinthe, Quebec, Canada). The Macro-Illumination imaging system (Lightools, Encinitas, CA) was used to monitor eGFP expression in organs (46). All animal experiments were approved by the Institutional Animal Care and Use Committee of the Experimental Biology Centre of the INRS-Institut Armand-Frappier.

Lymphocyte proliferation assay and quantification of cell-associated viremia

A small amount of heparinized whole blood was used directly for a white blood cell (WBC) count (Unopette; BD Biosciences, Mississauga, Ontario, Canada), and plasma and PBMC were isolated using Ficoll (GE Healthcare, Baie d'Urfé, Quebec, Canada) gradient centrifugation. The proliferation activity was determined using the 5-bromo2'-deoxyuridine (BrdU) cell proliferation assay (Roche Diagnostics, Laval, Quebec, Canada) according to the manufacturer's instructions. Briefly, the PBMC isolated from each animal were split into two duplicates and either stimulated with 100 μg/ml

phytohemagglutinin (PHA; Sigma, Oakville, Ontario, Canada) or left untreated. The next day, BrdU was added to a final concentration of 10 μM, and cells were incubated for another 24 h before they were transferred into black 96-well plates, washed, and fixed at 65 °C for 1 h. BrdU incorporation was detected using a peroxidase-linked anti-BrdU antibody and revealed with a chemiluminescent substrate. The signal was detected using a microplate luminescence counter (Luminoskan Ascent, Thermo Electron Corp., Calgary, Alberta, Canada). The proliferation activity was expressed as a ratio between stimulated and nonstimulated cells, allowing for comparison of samples that differ in absolute cell numbers due to the virus-induced leukopenia.

The erythrocytes in EDTA-treated blood were lysed in ACK lysis buffer (150 mM NH_4Cl, 10 mM $KHCO_3$, 0.01 mM EDTA, pH 7.2 to 7.4), and the isolated PBMC were washed once with phosphate-buffered saline (PBS) solution (Invitrogen, Burlington, Ontario, Canada) and counted. To quantify the cell-associated viremia, quadruplicates of a 10-fold serial dilution of the isolated PBMC were transferred onto VerodogSLAMtag cells seeded in 96-well plates and cultivated for 4 days. The cell-associated virus titer was expressed as $TCID_{50}$ per 10^6 cells.

Antibodies and staining reagents

Infected T cells were identified immunohistochemically using a mouse anti-CD3 antibody, infected endothelial cells using a mouse anti-von Willebrand factor, and infected glial cells using a rabbit anti-glial fibrillary acidic protein antiserum (all DAKO Cytomation, Mississauga, Ontario, Canada). These antibodies recognize a conserved epitope and have been reported to cross-react with the respective ferret cell type. Neurons were detected using NeuroTrace 530/615 (Invitrogen, Burlington, Ontario, Canada), a red fluorescent variant of the Nissl stain. To visualize all cells present in the field of view, either the nuclear stain 4',6-diamidino-2-phenylindole (DAPI) or the actin stain Alexa Fluor 568-phalloidin was used (both Invitrogen, Burlington, Ontario, Canada).

Staining of tissue sections and microscopic analysis

Animals were euthanized with an overdose of pentobarbital (CDMV, St. Hyacinthe, Quebec, Canada) intraperitoneally. Once a deep plane of anesthesia was reached, each animal was perfused first with 160 ml PBS, followed by 80 ml of 4% paraformaldehyde (PFA). Tissues were harvested, fixed in 4% PFA for at least 24 h at 4 °C, and stored in PBS. Prior to sectioning, samples were placed in 30% sucrose in PBS overnight at 4 °C, immersed in tissue embedding compound (Triangle Biomedical Sciences, Durham, NC), and frozen on dry ice for at least 1 h. Serial 10- to 15-μm sections were cut using a cryostat (Kryostat 1720 digital; Leitz, Midland, Ontario, Canada) and mounted on Superfrost Plus slides (Fisher Scientific, Whitby, Ontario, Canada), air dried, and stored at –20 °C.

For immunostaining, sections were thawed for 15 min, blocked for 30 min using normal horse serum (Invitrogen, Burlington, Ontario, Canada) diluted to 1/100 in PBS, and incubated with the respective primary antibody for 60 to 90 min at room temperature. After a 1-h incubation with the appropriate Alexa Fluor 568-conjugated secondary antibody (Invitrogen, Burlington, Ontario, Canada), coverslips were mounted in Prolong Gold antifade reagent (Invitrogen, Burlington, Ontario, Canada) and left to harden overnight at 4 °C. Fluorescent images were captured using either a standard fluorescent microscope or the confocal laser microscope (MRC 1000; Bio-Rad, Mississauga, Ontario, Canada).

For hematoxylin and eosin staining, slides were fixed in 100% MeOH and rehydrated prior to staining for 5 min in Harris' hematoxylin solution (EMD Industries, Gibbstown, NJ). Sections were rinsed in double-distilled H2O, dipped in an ammonia solution, and counterstained with acidified eosin Y (Sigma-Aldrich, Oakville, Ontario, Canada). Slides were dehydrated, mounted in Entellan mounting medium (EMD Industries, Gibbstown, NJ), and air-dried overnight.

Results

A75/17 and its eGFP-expressing derivative A75eH are highly neurovirulent in ferrets

To characterize the mechanism underlying morbillivirus neurovirulence, we chose CDV strain A75/17. This virus has been primarily characterized in dogs, where it causes acute disease including neurological signs in 10% of infected animals (38). In the more sensitive ferret model, rash signifying the onset of the symptomatic disease phase started around 10 days postinoculation (d.p.i.) with the nonrecombinant virus (Fig. 1B, A75/17). All animals subsequently developed severe generalized rash, increasing signs of gastrointestinal and respiratory involvement, and ultimately circling behavior and seizures suggestive of CNS involvement, leading to their sacrifice for humane reasons within 3 to 5 weeks after infection (Fig. 1B, A75/17).

To produce an infectious cDNA of this strain and eventually insert a reporter gene for easy monitoring of the infection, we cloned and sequenced the viral genome. We confirmed the consensus sequence deposited in GenBank with the accession no. AF164967. We then assembled an infectious clone based on this consensus sequence and introduced eGFP in an additional transcription unit between the H and L genes (Fig. 1A), to directly visualize infected cells and document viral spread as described previously (46). The corresponding recombinant virus, named A75eH, elicited equivalent courses of disease (Fig. 1B, A75eH, right side), indicating that eGFP gene addition had no attenuating effect. Animals infected with either virus experienced a 90% loss of WBC in the peripheral blood within the first week after infection (Fig. 1C) and were unable to mount a neutralizing antibody response (data not shown). However, after an initial dramatic drop, the remaining lymphocytes recovered some of their ability to proliferate in response to nonspecific PHA stimulation (Fig. 1D), correlating with the prolonged survival compared to animals infected with the previously used CDV strain 5804P, which succumb to the disease after 14 days (47).

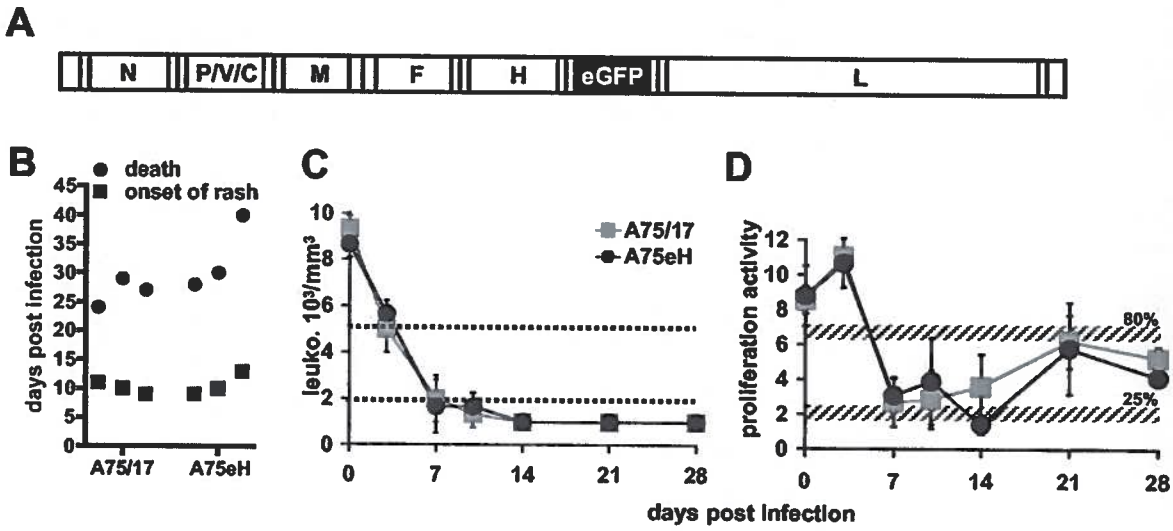

Fig. 1 Comparison of the pathogenicity of the parental CDV strain A75/17 and its eGFP expression recombinant derivative A75eH. (A) Scheme of the A75eH genome with the eGFP open reading frame introduced as an additional transcription unit between the hemagglutinin (H) and polymerase (L) genes. The genome is shown as a white elongated box. The genes are indicated by the letters N (nucleocapsid), P (phosphoprotein), M (matrix), F (fusion), H, and L. The additional eGFP-containing transcription unit is represented by a black box and is marked "eGFP." (B) Time course of infection of groups of three animals. Each pair of symbols represents one animal. Squares indicate the onset of rash, and circles indicate the time of euthanasia for humane reasons. (C) Leukocyte number and (D) in vitro proliferation activity of lymphocytes from these animals. The group (n = 3) infected with A75/17 is represented by gray squares, and the group (n = 3) infected with A75eH is represented by black circles. Days post-infection are indicated on the x axis, and leukocyte number (leuko.) or proliferation activity is indicated on the y axis. Dotted lines or broad hatched gray lines indicate threshold levels used for the classification as moderate or severe immunosuppression, respectively.

A75eH causes CNS infection

To determine how the observed neurological signs were related to infection, we measured virus titer in WBC, urine, and CSF. Cell-associated virus titers in WBC peaked at 7 d.p.i., followed by a slight drop towards the end of the infection (Fig. 2A). Cell-free virus was detected in the urine 7 d.p.i., reaching values similar to those found in the WBC 14 d.p.i., which correlated with the extensive spread to epithelia throughout the body during the second week of the infection (Fig. 2A). In the CSF, cell-free virus was first detected at 21 d.p.i. and increased steadily until the death of the animal, indicating a substantial infection in CNS areas with contact with the CSF (Fig. 2A).

Macroscopic examination of a brain at the time of euthanasia revealed multiple eGFP-expressing foci in the brain stem (Fig. 2B and C) and the surface of the frontal lobes adjacent to the olfactory bulb (Fig. 2D and E). The median section revealed strong eGFP expression throughout the olfactory bulb and within the frontal lobes (Fig. 2F and G), while the more caudal parts of the cerebrum and the cerebellum were negative (Fig. 2E and G). This pattern was observed in all animals sacrificed at the end stage of the disease. However, the extent of the spread correlated with the duration of the infection in the respective animal; with those surviving for 35 to 40 days displaying the most widespread eGFP expression, while positive foci were mainly found in the olfactory bulb and adjacent cerebrum in those that had to be sacrificed earlier.

Infection of the CNS occurs after spread to epithelia

We have previously shown that lymphatic organs are the primary targets during the early stages of CDV spread followed by a widespread infection of epithelia throughout the body that coincides with the onset of rash, fever, and gastrointestinal and respiratory signs (46). To determine the timing of CNS invasion, we sacrificed two to three animals at weekly intervals and visualized the extent of infection in Peyer's patches as representative of the lymphatic organs, lung for epithelial tissues, and olfactory bulb as a possible point of CNS entry.

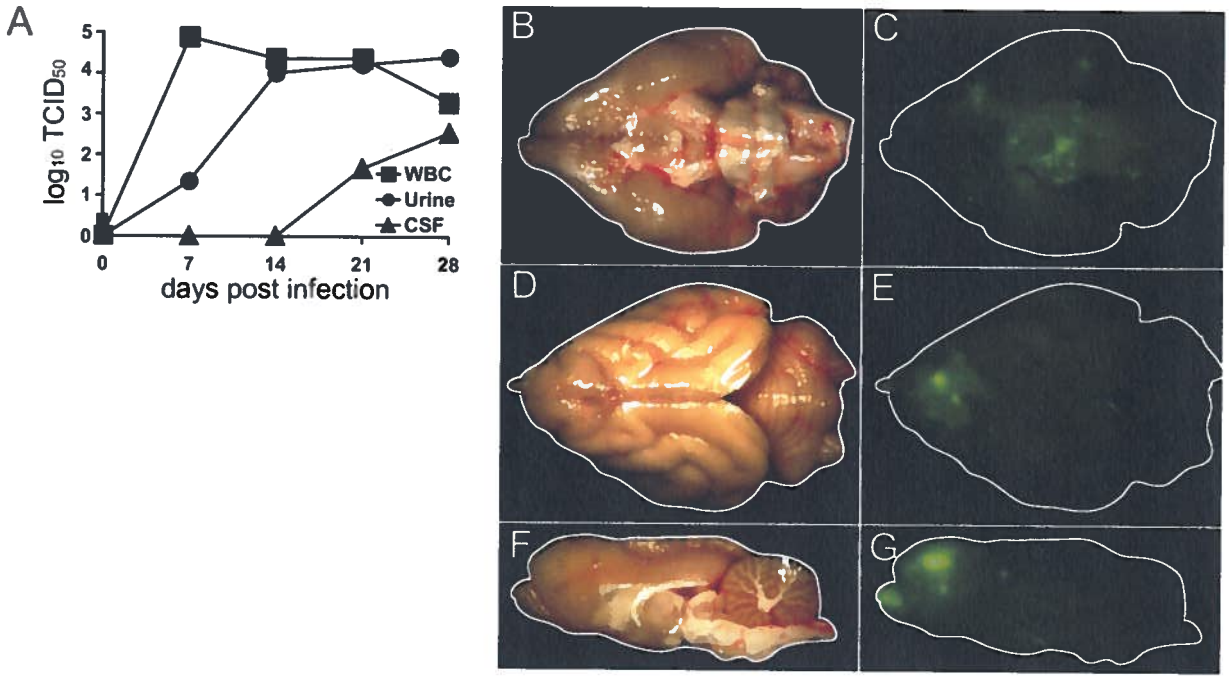

Fig. 2 Replication of CDV in different body fluids and the brain. (A) Number of CDV-infected cells or infectious units in PBMC, urine, and CSF. The cell associated virus titer in the PBMC is expressed as $TCID_{50}$ per million cells, and the cell-free virus titer in urine and CSF is expressed as $TCID_{50}$ per ml. (B to G) Visualization of infection in the brain at the end stage of the disease. (B and C) Ventral view of the brain by (B) normal light or (C) eGFP fluorescence excitation. Contours are outlined with a white line. (D and E) Dorsal views of the same sample. (F and G) Saggital cut separating the left and right hemispheres.

The intensity of eGFP expression in Peyer's patches reached its maximum after 1 week (data not shown) and maintained this level throughout the course of the infection (Fig. 3I to L). Again in accordance with our previous findings, we detected eGFP expression in the lung 1 week after inoculation, which was initially limited to the larger bronchi (Fig. 3E and F) and subsequently became increasingly generalized (Fig. 3G and H). The earliest green foci in the olfactory bulb were revealed 21 d.p.i. (Fig. 3A to C). At that time, no eGFP signal was found in other regions of the brain, further suggesting that the olfactory bulb is an important port of entry. A consecutive increase in eGFP expression in the olfactory bulb and spread to adjacent parts of the CNS were observed in animals sacrificed at or after 28 d.p.i. (Fig. 3D).

CDV accesses the brain through different pathways

While our macroscopic analysis highlighted the importance of the olfactory bulb, previous studies with CDV and MeV have identified the choroid plexus and cerebral blood vessels as likely origins of morbillivirus neuroinvasion (11, 39). To analyze the involvement of these structures during different disease stages, we examined saggital cryosections of the CNS for sites of eGFP expression. Consistent with our macroscopic findings, only single green cells with the round morphology typical of circulating lymphocytes were seen sporadically in the choroid plexus and in the lumen of capillaries at the onset of clinical signs around 7 d.p.i. (data not shown). However, the overall fluorescence did not exceed background levels seen in non-infected controls (Fig. 4A, E, and I), indicating that the intranasal inoculation did not lead to a direct infection of olfactory neurons. After 2 weeks, coinciding with a high-titer cell-associated viremia (Fig. 2A) and the spread to epithelia (Fig. 3F), infected cells were found in the choroid plexus (Fig. 4B) and the vicinity of cerebral blood vessels (Fig. 4F). The first eGFP-positive olfactory nerve fibers were also detected at this time (Fig. 4J), concomitantly with a massive infection of the respiratory mucosa (Fig. 3F). These findings suggest that the infection of the brain requires prolonged exposure to infected cells, regardless of the point of entry. At 21 d.p.i., when the first macroscopic signal was detected in the

olfactory bulb (Fig. 3C), a majority of olfactory nerve fibers were infected and spread into the olfactory glomeruli was observed (Fig. 4K).

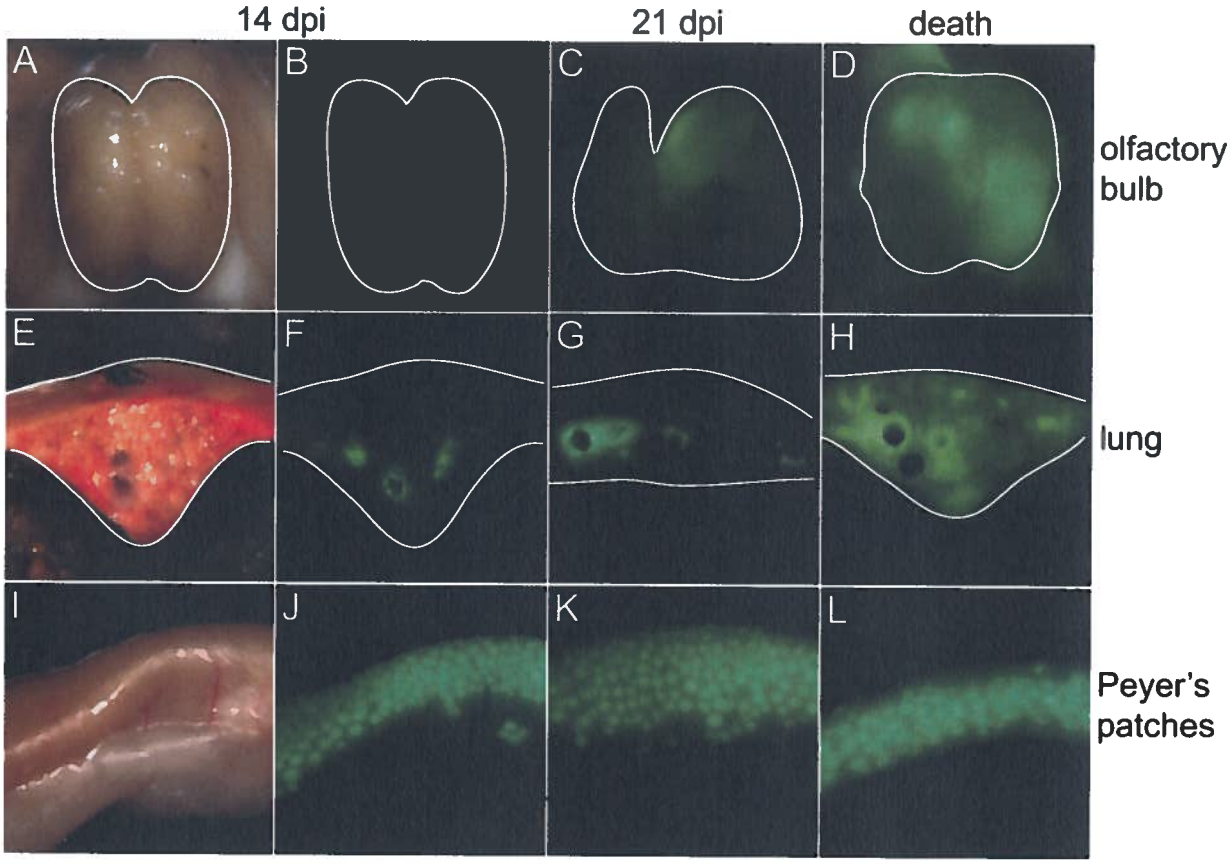

Fig. 3 Time course of CDV dissemination in different tissues. Shown are a macroscopic visualization of infection in the olfactory bulb (A to D), a transverse section of a lung lobe (E to H), and Peyer's patches (panels I to L). The contours of the organs are outlined by a white line. (A, E, and I) Normal light photographs of the different tissues from an animal sacrificed at 14 d.p.i. (B, F, and J) Same organs and time point as above but photographed after eGFP fluorescence excitation. Also shown are the same organs as above from an animal sacrificed at 21 d.p.i. (C, G, and K) and at the time of euthanasia (D, H, and L), photographed after eGFP fluorescence excitation.

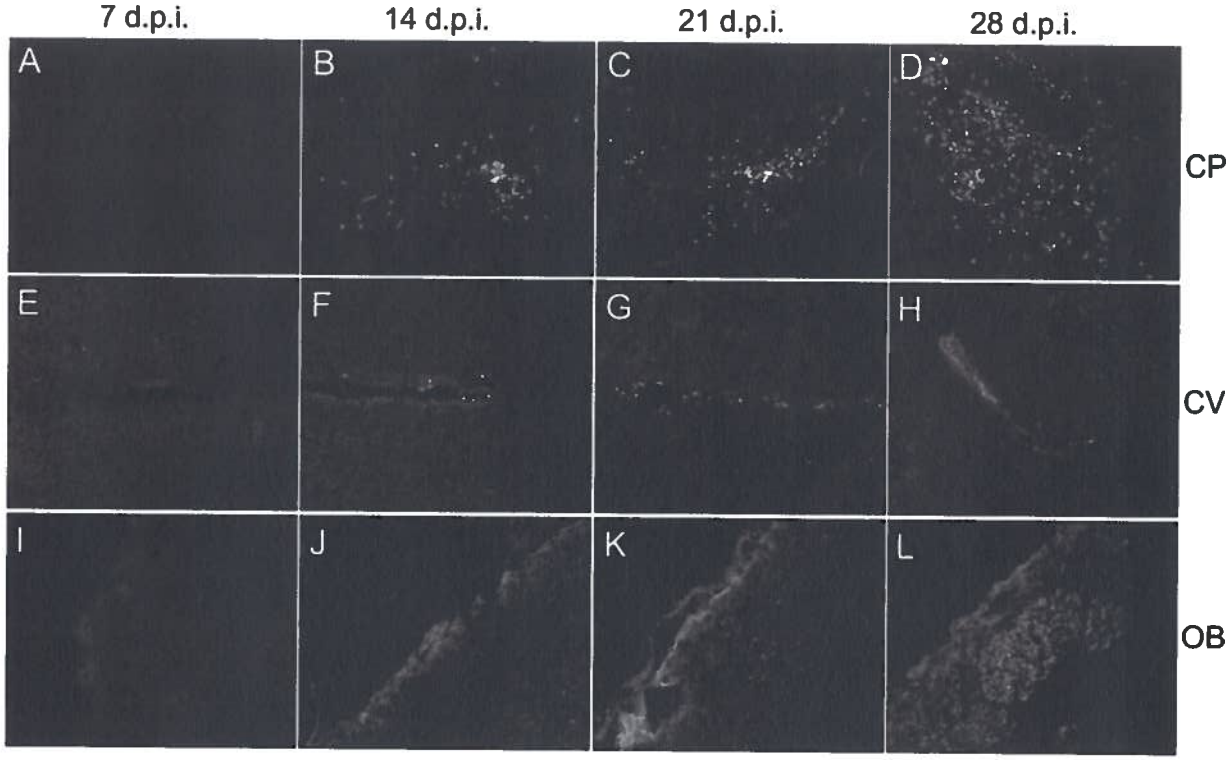

Fig. 4 Time course of CDV dissemination in the CNS. After macroscopic imaging, PFA-perfused brains were fixed in 4% PFA at 4 °C for an additional 48 h and transferred into 30% sucrose in PBS at 4 °C overnight. Four- to 7-mm-thick saggital sections were then immersed in tissue embedding compound and frozen on dry ice. Ten- to 15-μm cryosections were subsequently analyzed for eGFP expression at a 200-fold magnification. Positive cells were mainly detected in the choroid plexus (CP; panels A to D), along cerebral blood vessels (CV; panels E to H), and in the olfactory bulb (OB; panels I to L). Representative regions from animals sacrificed at 7 d.p.i (A, E, and I), 14 d.p.i. (B, F, and J), 21 d.p.i. (C, G, and K), and 28 d.p.i. (D, H, and L) are shown.

The simultaneous increase of eGFP-expressing cells associated with the choroid plexus and blood vessels (Fig. 4C and G) coincided with the detection of free virus in the CSF (Fig. 2A). Within the subsequent weeks, the number of infected cells at the different entry points increased continuously (Fig. 4D, H, and L). In addition, there was evidence of virus spread to the lining of the ventricles, the pia mater, and the underlying molecular layer of the cerebral and cerebellar cortex via the CSF (Fig. 5A and B), invasion of the brain parenchyma surrounding blood vessels indicative of direct hematogenous dissemination (Fig. 5C), and migration from the olfactory glomeruli to mitral cells and further towards the olfactory cortex (Fig. 5D). The only histopathological change consistently observed in all animals, was a lymphocyte infiltration in the choroid plexus starting at 14 d.p.i. and persisting until the time of death (Fig. 5E). The brain parenchyma (Fig. 5F) and olfactory bulb (not shown) rarely showed signs of inflammation, most likely due to the severe leukopenia and immunosuppression at this time.

Extensive hematogenous infection of glial cells and neurons is a late event

To identify the target cells over the course of the infection, we stained consecutive saggital sections with markers specific for the different cell types present in the brain. Up to 21 d.p.i., the eGFP-expressing cells detected in the choroid plexus and those with a round morphology found in the vicinity of blood vessels were mostly T cells (Fig. 6A, E, and I). Occasionally, infected monocytes or B cells were also found in these locations (data not shown), consistent with the high-level viremia (Fig. 2A, squares). Capillary endothelial cells were the only infected nonimmune cells associated with hematogenous spread consistently detected between 14 and 21 d.p.i. (Fig. 6B, F, and J). Once the virus had gained access to the ventricles and pia mater via the CSF around 28 d.p.i., glial cells were the dominating infected cell type (Fig. 6C, G, and K). At this time, the first eGFP-positive neurons were also observed: mostly in close proximity to infected glial cells (Fig. 6D, H, and L). Consistent with CSF-mediated dissemination, infected epithelial cells were detected in the dura mater and the choroid plexus (data not shown).

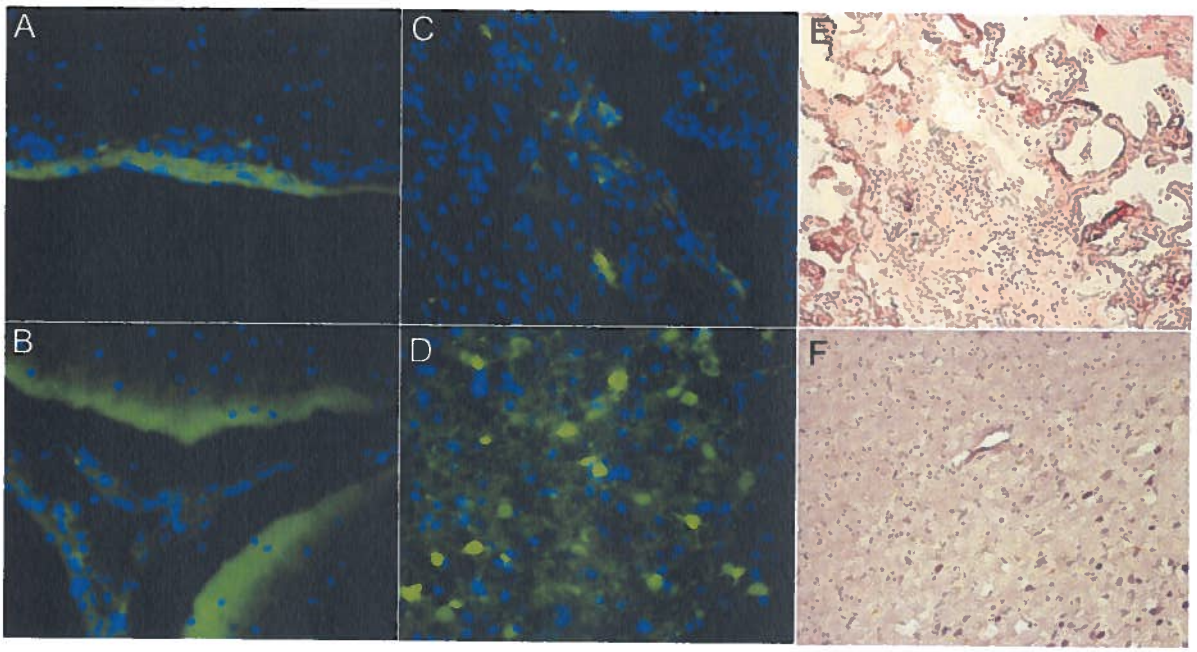

Fig. 5 CDV spread and histopathological changes in the CNS at advanced disease stages. Shown is microscopic analysis of cryosections stained blue with DAPI to visualize cell nuclei at a 400-fold magnification (A to D) or stained with hematoxylin and eosin at a 200-fold magnification (E and F). (A) Pia mater, (B) parenchyma bordering a blood vessel in the cerebellum, (C) ependyma bordering a ventricle, and (D) olfactory bulb. (E) Choroid plexus and (F) parenchyma of the frontal lobe from an animal sacrificed at 28 d.p.i.

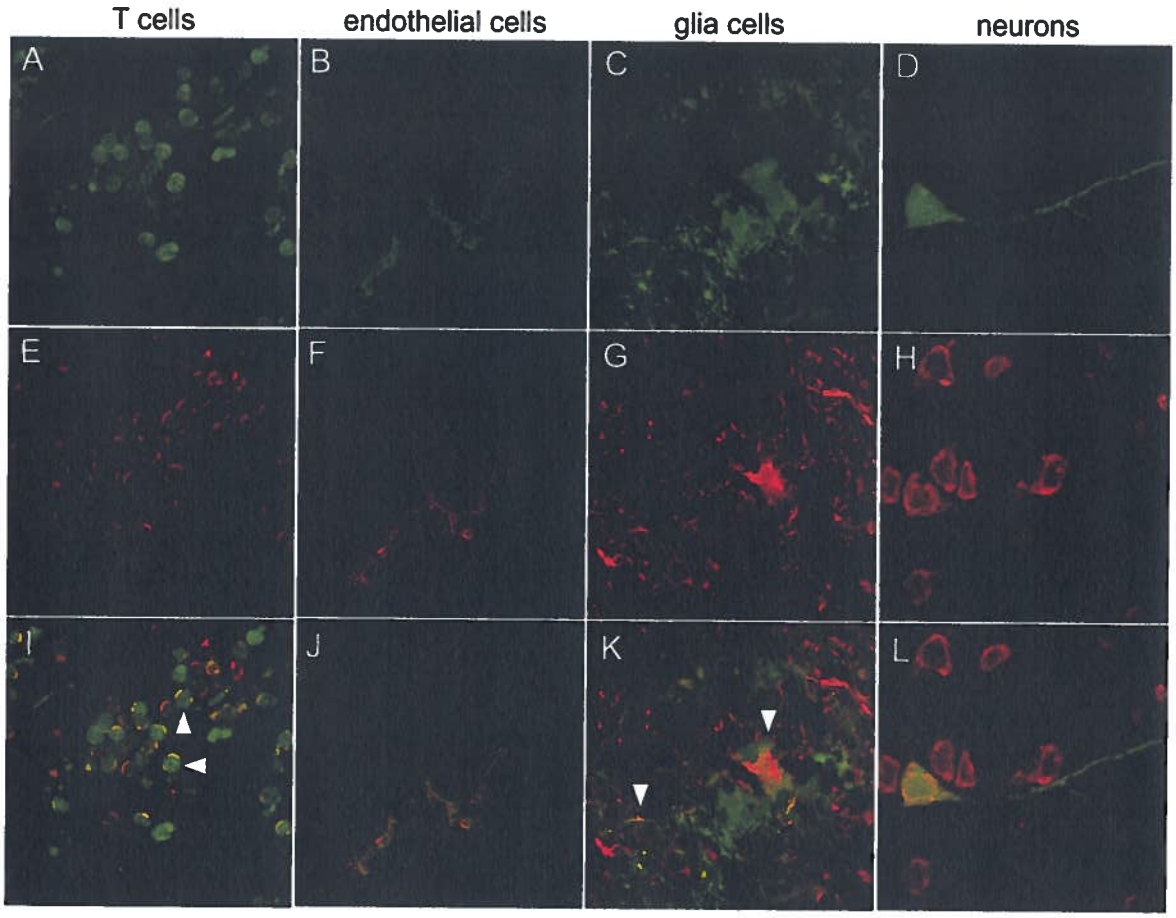

Fig. 6 Identification of cells infected through hematogenous spread. Shown is confocal microscopic analysis of cryosections stained with antibodies against different cellular markers at a 1,000-fold magnification. (A to D) CDV-infected cells; (E to H) respective cellular markers, visualized with an Alexa Fluor 568-labeled secondary antibody; and (I to L) composite image of the two colors. (A, E, and I) Infected T cells in the choroid plexus and (B, F, and J) endothelial cells in a cerebral capillary at 14 d.p.i. identified with a mouse anti-CD3 or anti-von Willebrand factor antibody, respectively. (C, G, and K) Infected glial cells and (D, H, and L) neurons at 28 d.p.i. visualized with a rabbit anti-glial fibrillary acidic protein polyclonal antiserum or the 530/615 NeuroTrace Nissl stain, respectively. Examples of double-positive cells are indicated by white triangles. The partial overlap of red and green signals seen in some cases is due to the fact that most of the antibodies recognize proteins located in the cell membrane while eGFP is expressed in the cytoplasm.

The olfactory bulb is a main point of CDV CNS entry

In contrast to many other respiratory viruses with neurovirulent potential (2, 4), direct CNS entry via the olfactory bulb was not considered a major infection route for morbilliviruses. However, in our study, olfactory nerves were infected as early as 14 d.p.i. (Fig. 4J), and the olfactory bulb was the first location of macroscopic eGFP expression (Fig. 3C). We were able to follow this CNS invasion pathway microscopically from the neurons located in the olfactory mucosa, along the olfactory nerve filaments passing through the cribriform plate, and into the olfactory glomeruli, which constitute the synapse between olfactory nerve fibers and mitral cells.

At 14 d.p.i., infected cells were detected throughout the olfactory mucosa in cryosections stained with the neuronal cell body-specific Nissl stain (Fig. 7A, yellow cells), indicating that these cells were infected at the same time as the surrounding mucosal epithelial cells. The green staining seen at the rostral margin of the olfactory bulb at this time (Fig. 4J) represents multiple individual olfactory nerve filaments (Fig. 7B, counterstained with an actin marker). The detection of infected mitral cells as early as 21 d.p.i. (Fig. 7C, green cell, counterstained with an actin marker) indicates that the virus is transmitted across neuronal synapses and thus has the potential to spread anterogradely to deeper CNS structures.

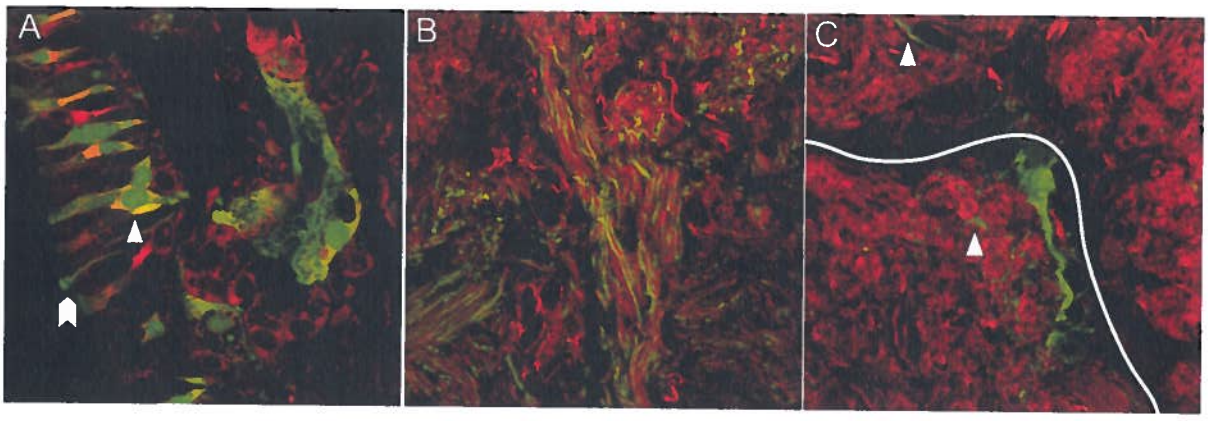

Fig. 7 Visualization of CNS invasion via the olfactory route. Shown is confocal microscopic analysis of cryosections at 1,000-fold magnification. (A) Merged image of the olfactory mucosa at 14 d.p.i. stained with the 530/615 NeuroTrace Nissl stain to visualize neuronal cell bodies. The triangle indicates an infected olfactory receptor neuron, and the arrowhead marks a sensory cilia protruding into the mucus layer. (B and C) Merged images of (B) the olfactory nerve filaments at 14 d.p.i. and (C) the olfactory glomeruli at 21 d.p.i. stained with Alexa Fluor 568-phalloidin to visualize actin in the surrounding structures. An individual olfactory glomerulum is located in the lower left corner of panel C, indicated by a white line. Examples of individual nerve fibers are highlighted by white triangles.

Discussion

Neurovirulent distemper in ferrets and dogs

Ferrets are exquisitely sensitive to CDV and usually succumb to the infection without ever developing an effective immune response (47). Taking advantage of eGFP-expressing 5804P-derived viruses, we previously demonstrated massive infection of lymphatic organs and the resulting dramatic depletion of circulating lymphocytes during the initial disease phases.

At 7 d.p.i., most of the remaining circulating lymphocytes are infected, setting the stage for the invasion of epithelial tissues, including the upper and lower respiratory tract (46). Here we operated with the neurovirulent strain A75eH, which does not kill infected animals within 2 weeks and therefore allows us to monitor subsequent disease phases, including neuroinvasion. We report the detection of first positive cells in the CNS around 2 weeks p.i., coinciding with widespread epithelial infection. This timing indicates that CNS invasion occurs only after extensive spread through lymphatic and epithelial tissues rather than directly as a consequence of the intranasal route of infection as has been reported for primary neurotropic viruses (28). The localization of infected cells in the olfactory nerves, the choroid plexus, and the vicinity of blood vessels furthermore reflects two distinct routes of invasion: anterogradely via the olfactory nerves and hematogenously through infected circulating lymphocytes.

The course of CDV in dogs initially follows the same pattern, including the infection of cells in locations consistent with hematogenous invasion (31). However, neutralizing antibodies are detected in up to 90% of the animals 2 to 3 weeks p.i., indicating the onset of an effective antiviral immune response that controls and then eliminates the infection and coincides with resolution of the disease signs (31, 39, 41). In the CNS, an inflammatory process characterized by lymphocyte invasion is observed, which results in a chronic demyelinating disease in 10 to 30% of the animals (52). In ferrets and the subset of dogs that fail to mount an immune response, the virus continues

its spread through the brain, ultimately establishing a widespread infection of different CNS cell types (39, 45). In ferrets, we observed that this spread occurs, depending on the port of entry, either from the outer layers into the parenchyma or anterogradely from the olfactory nerve through the mitral cells further along the olfactory signaling route. Given the other similarities in the course of disease in ferrets and dogs, entry through the olfactory bulb may occur in dogs as well.

CDV neurovirulence in ferrets as morbillivirus neuroinvasion model

The incidence of CNS invasion associated with morbillivirus infection varies among the different family members. CDV and the viruses that infect marine mammals frequently cause CNS complications, while rinderpest and peste des petits ruminants viruses generally do not affect the brain (7). Measles virus holds an intermediate position, as it causes several distinct but relatively rare CNS diseases. Among those, postinfectious encephalomyelitis occurs in 1 in 1,000 cases within weeks of acute measles, but the extent of viral replication seems minor and the pathology is immune mediated (14, 32). On the other hand, extensive viral replication was documented in the context of a rare fatal course of the acute disease (24, 30), and two chronic manifestations, measles inclusion body encephalitis and subacute sclerosing panencephalitis (SSPE) (5). The former occurs between 2 and 6 months after acute infection and is limited to individuals with an innate immune defect resulting in an inability to clear the virus during acute infection and subsequent persistence in the CNS (16, 32). A similar disease form, known as old dog encephalitis, is also observed for CDV, where it occurs more frequently (3). All chronic manifestations of morbillivirus CNS infections are inevitably fatal and characterized by massive and widespread infection of neurons (25).

While the significance of our observations for the pathogenic mechanisms underlying SSPE and old dog encephalitis remains to be explored, hematogenous invasion has been deduced from histological analysis of brain sections of measles patients who died from acute encephalitis and the histopathological analyses of marine mammals that succumbed to morbillivirus infections (9, 11, 21, 30). In addition, the dissemination

pattern documented in the later infection stages in ferrets strongly resembles that of fatal measles in individuals that are unable to combat the infection (13, 24). This link between the extent of spread and the ability of the host's immune response to control the infection is also apparent in studies in immunocompetent and immunosuppressed mice (26, 42). In summary, our findings suggest that CDV neuroinvasion in ferrets reflects the events occurring in the context of other morbillivirus infections.

Mechanisms of CNS entry by Paramyxoviridae

This study shows remarkable parallels between CDV entry into the CNS of ferrets and the mechanisms of brain invasion by other Paramyxoviridae. Several paramyxoviruses with neurovirulent potential, including morbilliviruses, mumps virus, and Newcastle disease virus, efficiently infect circulating lymphocytes, resulting in a cell-associated viremia that lasts throughout the symptomatic disease phase (32, 34, 50). This provides ample opportunity for infected lymphocytes to traffic through the blood-brain and blood-choroid plexus barrier and locally release virus, starting infection of resident epithelial and endothelial cells (12, 15). Consistent with this hematogenous route of CNS invasion, infected cells are usually first detected in the choroid plexus and in close association with cerebral blood vessels (34, 39). Once inside the CSF, the viruses may invade the different membranes surrounding the CNS, the ependyma, and the superficial lining of the cerebral cortex (34, 49), followed by infection of neurons and glia cells in close proximity and subsequent spread into deeper layers (19, 26, 29). Taken together, these observations suggest that paramyxoviruses use classical hematogenous CNS invasion pathways described for several other neurotropic viruses (17, 33).

In addition to hematogenous CNS invasion, entry via the olfactory bulb has been demonstrated for Sendai, La Piedad Michoacan, and, more recently, Nipah viruses, all of which also cause massive respiratory epithelial infection (1, 27, 49). In the olfactory mucosa, which lines the roof of the nasal cavity, the dendrites of mature olfactory receptor neurons and these respiratory epithelial cells reside in close proximity, and easy virus transition between the different cell types is conceivable. Since the axons of the

bipolar olfactory receptor neurons enter the olfactory bulb by passing through the cribriform plate, these neurons, once infected, provide direct access to the CNS. The axons synapse in the olfactory glomeruli with the dendrites of mitral cells, the corresponding second order neurons, which in turn project further to the deeper olfactory and limbic systems, thus providing a rapid way of accessing these regions for v· uses capable of crossing the synaptic space (35). This pathway is used by various neurotropic viruses (28), and the capacity to move transcellularly across either dendrodendritic or axonal synapses has been identified as an important neurovirulence determinant (43). Our findings add to the mounting evidence that entry via the olfactory bulb and spread along the olfactory signaling route are common among paramyxoviruses and should be considered alongside the classical hematogenous entry pathway.

Acknowledgements

We thank Marcel Desrosiers for excellent support with the confocal microscopy and Brian Ward and Christoph Springfeld for comments on the manuscript. We are thankful to all laboratory members for support and lively discussions.

This work was supported by a grant from the CIHR (MOP-66989) to V.V.M. and a scholarship from the Fondation Armand-Frappier to P.A.R.

References

1. Allan, G. M., F. McNeilly, I. Walker, T. Linne, J. Moreno-Lopez, P. Hernandez, S. Kennedy, B. P. Carroll, B. Herron, J. C. Foster, and B. Adair. 1996. A sequential study of experimental porcine paramyxovirus (LPMV) infection of pigs: immunostaining of cryostat sections and virus isolation. J. Vet. Diagn. Investig. 8:405-413.

2. Aronsson, F., B. Robertson, H. G. Ljunggren, and K. Kristensson. 2003. Invasion and persistence of the neuroadapted influenza virus A/WSN/33 in the mouse olfactory system. Viral Immunol. 16:415-423.

3. Axthelm, M. K., and S. Krakowka. 1998. Experimental old dog encephalitis (ODE) in a gnotobiotic dog. Vet. Pathol. 35:527-534.

4. Barnett, E. M., M. D. Cassell, and S. Perlman. 1993. Two neurotropic viruses, herpes simplex virus type 1 and mouse hepatitis virus, spread along different neural pathways from the main olfactory bulb. Neuroscience 57:1007-1025.

5. Cattaneo, R., A. Schmid, D. Eschle, K. Baczko, V. ter Meulen, and M. A. Billeter. 1988. Biased hypermutation and other genetic changes in defective measles viruses in human brain infections. Cell 55:255-265.

6. Cocks, B. G., C. C. Chang, J. M. Carballido, H. Yssel, J. E. de Vries, and G. Aversa. 1995. A novel receptor involved in T-cell activation. Nature 376:260-263.

7. Cosby, S. L., W. P. Duprex, L. A. Hamill, M. Ludlow, and S. McQuaid. 2002. Approaches in the understanding of morbillivirus neurovirulence. J. Neurovirol. 8(Suppl. 2):85-90.

8. Domingo, M., L. Ferrer, M. Pumarola, A. Marco, J. Plana, S. Kennedy, M. McAliskey, and B. K. Rima. 1990. Morbillivirus in dolphins. Nature 348:21.

9. Domingo, M., J. Visa, M. Pumarola, A. J. Marco, L. Ferrer, R. Rabanal, and S. Kennedy. 1992. Pathologic and immunocytochemical studies of morbillivirus infection in striped dolphins (Stenella coeruleoalba). Vet. Pathol. 29:1-10.

10. Duprex, W. P., I. Duffy, S. McQuaid, L. Hamill, S. L. Cosby, M. A. Billeter, J. Schneider-Schaulies, V. ter Meulen, and B. K. Rima. 1999. The H gene of rodent brain-adapted measles virus confers neurovirulence to the Edmonston vaccine strain. J. Virol. 73:6916-6922.

11. Esolen, L. M., K. Takahashi, R. T. Johnson, A. Vaisberg, T. R. Moench, S. L. Wesselingh, and D. E. Griffin. 1995. Brain endothelial cell infection in children with acute fatal measles. J. Clin. Investig. 96:2478-2481.

12. Frisk, A. L., M. König, A. Moritz, and W. Baumgärtner. 1999. Detection of canine distemper virus nucleoprotein RNA by reverse transcription-PCR using serum, whole blood, and cerebrospinal fluid from dogs with distemper. J. Clin. Microbiol. 37:3634-3643.

13. Gazzola, P., L. Cocito, E. Capello, L. Roccatagliata, M. Canepa, and G. L. Mancardi. 1999. Subacute measles encephalitis in a young man immunosuppressed for ankylosing spondylitis. Neurology 52:1074-1077.

14. Gendelman, H. E., J. S. Wolinsky, R. T. Johnson, N. J. Pressman, G. H. Pezeshkpour, and G. F. Boisset. 1984. Measles encephalomyelitis: lack of evidence of viral invasion of the central nervous system and quantitative study of the nature of demyelination. Ann. Neurol. 15:353-360.

15. Goh, K. J., C. T. Tan, N. K. Chew, P. S. Tan, A. Kamarulzaman, S. A. Sarji, K. T. Wong, B. J. Abdullah, K. B. Chua, and S. K. Lam. 2000. Clinical features of Nipah virus encephalitis among pig farmers in Malaysia. N. Engl. J. Med. 342:1229-1235.

16. Griffin, D. E. 2001. Measles virus, p. 1401-1441. In D. M. Knipe and P. M. Howley (ed.), Fields virology, 4th ed., vol. 1. Lippincott Williams & Wilkins, Philadelphia, Pa.

17. Griffin, D. E., A. P. Byrnes, and S. H. Cook. 2004. Emergence and virulence of encephalitogenic arboviruses. Arch. Virol. Suppl. 2004:21-33.

18. Griot, C., M. Vandevelde, M. Schobesberger, and A. Zurbriggen. 2003. Canine distemper, a re-emerging morbillivirus with complex neuropathogenic mechanisms. Anim. Health Res. Rev. 4:1-10.

19. Higgins, R. J., S. G. Krakowka, A. E. Metzler, and A. Koestner. 1982. Primary demyelination in experimental canine distemper virus induced encephalomyelitis in gnotobiotic dogs. Sequential immunologic and morphologic findings. Acta Neuropathol. (Berlin) 58:1-8.

20. Kennedy, S. 1998. Morbillivirus infections in aquatic mammals. J. Comp. Pathol. 119:201-225.

21. Kennedy, S., J. A. Smyth, P. F. Cush, P. Duignan, M. Platten, S. J. McCullough, and G. M. Allan. 1989. Histopathologic and immunocytochemical studies of distemper in seals. Vet. Pathol. 26:97-103.

22. Liebert, U. G., and V. ter Meulen. 1987. Virological aspects of measles virus-induced encephalomyelitis in Lewis and BN rats. J. Gen. Virol. 68:1715-1722.

23. Lisiak, J. A., and M. Vandevelde. 1979. Polioencephalomalacia associated with canine distemper virus infection. Vet. Pathol. 16:650-660.

24. McQuaid, S., S. L. Cosby, K. Koffi, M. Honde, J. Kirk, and S. B. Lucas. 1998. Distribution of measles virus in the central nervous system of HIV-seropositive children. Acta Neuropathol. (Berlin) 96:637-642.

25. McQuaid, S., J. Kirk, A. L. Zhou, and I. V. Allen. 1993. Measles virus infection of cells in perivascular infiltrates in the brain in subacute sclerosing panencephalitis: confirmation by non-radioactive in situ hybridization, immunocytochemistry and electron microscopy. Acta Neuropathol. (Berlin) 85:154-158.

26. Miyamae, T. 2005. Differential invasion by Sendai virus of abdominal parenchymal organs and brain tissues in cortisone- and cyclophosphamide-based immunosuppressed mice. J. Vet. Med. Sci. 67:369-377.

27. Mori, I., T. Komatsu, K. Takeuchi, K. Nakakuki, M. Sudo, and Y. Kimura. 1995. Parainfluenza virus type 1 infects olfactory neurons and establishes long-term persistence in the nerve tissue. J. Gen. Virol. 76:1251-1254.

28. Mori, I., Y. Nishiyama, T. Yokochi, and Y. Kimura. 2005. Olfactory transmission of neurotropic viruses. J. Neurovirol. 11:129-137.

29. Parede, L., and P. L. Young. 1990. The pathogenesis of velogenic Newcastle disease virus infection of chickens of different ages and different levels of immunity. Avian Dis. 34:803-808.

30. Plaza, J. A., and G. J. Nuovo. 2005. Histologic and molecular correlates of fatal measles infection in children. Diagn. Mol. Pathol. 14:97-102.

31. Rima, B. K., N. Duffy, W. J. Mitchell, B. A. Summers, and M. J. Appel. 1991. Correlation between humoral immune responses and presence of virus in the CNS in dogs experimentally infected with canine distemper virus. Arch. Virol. 121:1-8.

32. Rima, B. K., and W. P. Duprex. 2006. Morbilliviruses and human disease. J. Pathol. 208:199-214.

33. Ryan, G., T. Grimes, B. Brankin, M. J. Mabruk, M. J. Hosie, O. Jarrett, and J. J. Callanan. 2005. Neuropathology associated with feline immunodeficiency virus infection highlights prominent lymphocyte trafficking through both the blood-brain and blood-choroid plexus barriers. J. Neurovirol. 11:337-345.

34. Saika, S., M. Kidokoro, T. Ohkawa, A. Aoki, and K. Suzuki. 2002. Pathogenicity of mumps virus in the marmoset. J. Med. Virol. 66:115-122.

35. Shepherd, G., and C. A. Greer. 1990. Olfactory bulb, p. 133-169. In G. M. Shepherd (ed.), Synaptic organization of the brain. Oxford University Press, Oxford, United Kingdom.

36. Sidorenko, S. P., and E. A. Clark. 2003. The dual-function CD150 receptor subfamily: the viral attraction. Nat. Immunol. 4:19-24.

37. Stephensen, C. B., J. Welter, S. R. Thaker, J. Taylor, J. Tartaglia, and E. Paoletti. 1997. Canine distemper virus (CDV) infection of ferrets as a model for testing Morbillivirus vaccine strategies: NYVAC- and ALVAC-based CDV recombinants protect against symptomatic infection. J. Virol. 71:1506-1513.

38. Summers, B. A., H. A. Greisen, and M. J. Appel. 1984. Canine distemper encephalomyelitis: variation with virus strain. J. Comp. Pathol. 94:65-75.

39. Summers, B. A., H. A. Greisen, and M. J. Appel. 1979. Early events in canine distemper demyelinating encephalomyelitis. Acta Neuropathol. (Berlin) 46:1-10.

40. Tatsuo, H., N. Ono, and Y. Yanagi. 2001. Morbilliviruses use signaling lymphocyte activation molecules (CD150) as cellular receptors. J. Virol. 75:5842-5850.

41. Tipold, A., P. Moore, A. Zurbriggen, I. Burgener, G. Barben, and M. Vandevelde. 1999. Early T cell response in the central nervous system in canine distemper virus infection. Acta Neuropathol. (Berlin) 97:45-56.

42. Urbanska, E. M., B. J. Chambers, H. G. Ljunggren, E. Norrby, and K. Kristensson. 1997. Spread of measles virus through axonal pathways into limbic structures in the brain of TAP1 –/– mice. J. Med. Virol. 52:362-369.

43. van den Pol, A. N., K. P. Dalton, and J. K. Rose. 2002. Relative neurotropism of a recombinant rhabdovirus expressing a green fluorescent envelope glycoprotein. J. Virol. 76:1309-1327.

44. Vandevelde, M., and A. Zurbriggen. 2005. Demyelination in canine distemper virus infection: a review. Acta Neuropathol. (Berlin) 109:56-68.

45. Vandevelde, M., A. Zurbriggen, R. J. Higgins, and D. Palmer. 1985. Spread and distribution of viral antigen in nervous canine distemper. Acta Neuropathol. (Berlin) 67:211-218.

46. von Messling, V., D. Milosevic, and R. Cattaneo. 2004. Tropism illuminated: lymphocyte-based pathways blazed by lethal morbillivirus through the host immune system. Proc. Natl. Acad. Sci. USA 101:14216-14221.

47. von Messling, V., C. Springfeld, P. Devaux, and R. Cattaneo. 2003. A ferret model of canine distemper virus virulence and immunosuppression. J. Virol. 77:12579-12591.

48. von Messling, V., G. Zimmer, G. Herrler, L. Haas, and R. Cattaneo. 2001. The hemagglutinin of canine distemper virus determines tropism and cytopathogenicity. J. Virol. 75:6418-6427.

49. Weingartl, H., S. Czub, J. Copps, Y. Berhane, D. Middleton, P. Marszal, J. Gren, G. Smith, S. Ganske, L. Manning, and M. Czub. 2005. Invasion of the central nervous system in a porcine host by Nipah virus. J. Virol. 79:7528-7534.

50. Wilczynski, S. P., M. L. Cook, and J. G. Stevens. 1977. Newcastle disease as a model for paramyxovirus-induced neurologic syndromes. II. Detailed characterization of the encephalitis. Am. J. Pathol. 89:649-666.

51. Winters, K. A., L. E. Mathes, S. Krakowka, and R. G. Olsen. 1983. Immunoglobulin class response to canine distemper virus in gnotobiotic dogs. Vet. Immunol. Immunopathol. 5:209-215.

52. Wunschmann, A., S. Alldinger, E. Kremmer, and W. Baumgartner. 1999. Identification of CD4+ and CD8+ T cell subsets and B cells in the brain of dogs with spontaneous acute, subacute-, and chronic-demyelinating distemper encephalitis. Vet. Immunol. Immunopathol. 67:101-116.

53. Zhu, Y. D., J. Heath, J. Collins, T. Greene, L. Antipa, P. Rota, W. Bellini, and M. McChesney. 1997. Experimental measles. II. Infection and immunity in the rhesus macaque. Virology 233:85-92.

Publication no. 2

Journal of General Virology, April 2010, p. 980-989, Volume 91 (Pt 4).

Epub Ahead of print Dec 16th 2009.

Acute Canine Distemper Encephalitis is Associated with Rapid Neuronal Loss and Local Immune Activation

Penny A. Rudd, Louis-Étienne Bastien-Hamel and Veronika von Messling*

INRS-Institut Armand-Frappier, University of Quebec, Laval, Canada

* Corresponding author.

Mailing address: INRS-Institut Armand-Frappier, University of Quebec,

531, Boul. des Prairies,

Laval, Quebec H7V 1B7,

Canada. Phone: (450) 687-5010. Fax: (450) 686-5305.

E-mail: veronika.vonmessling@iaf.inrs.ca

Abstract

For most virus infections of the central nervous system (CNS) immune-mediated damage, the route of inoculation, and death of infected cells, all contribute to the pathology observed. To investigate the role of these factors in early canine distemper neuropathogenesis, we infected ferrets either intranasally or intraperitoneally with the neurovirulent strain Snyder Hill. Regardless of the route of inoculation, the virus primarily targeted the olfactory bulb, brainstem, hippocampus and cerebellum, whereas only occasional foci were detected in the cortex. The infection led to widespread neuronal loss, which correlated with the clinical signs observed. Increased numbers of activated microglia, reactive gliosis, and different pro-inflammatory cytokines, were detected in the infected areas, suggesting that the presence and ultimate death of infected cells at early times after infection trigger strong local immune activation despite the observed systemic immunosuppression.

Introduction

Morbilliviruses cause an acute disease characterized by generalized immunosuppression, rash, respiratory and gastrointestinal signs, and occasional but devastating neurologic complications (Griffin, 2001; Moss *et al.*, 2004; Schneider-Schaulies & Schneider-Schaulies, 2008). Within the genus *Morbillivirus*, carnivore viruses are associated with the highest incidence of neuroinvasion, with up to 30% of dogs and almost all wild carnivores experiencing central nervous system (CNS) infection (Appel & Summers, 1995; Confer *et al.*, 1975; Summers *et al.*, 1984; van Moll *et al.*, 1995). Therefore, the study of canine distemper virus (CDV) in one of its natural hosts is frequently used to characterize mechanisms of morbillivirus neuropathogenesis (Appel *et al.*, 1982; Headley *et al.*, 2001; Rima *et al.*, 1991; Summers *et al.*, 1984).

Of the different CDV strains available, Snyder Hill causes the most reproducible course of disease including consistent neuroinvasion. In dogs infected intranasally with Snyder Hill, first clinical signs are seen after 4 days, and around 50% of animals ultimately succumb to the disease (Appel, 1969; Summers *et al.*, 1984). In those animals, virus is found in the CNS as early as 9 days after infection. At this stage, Snyder Hill displays a high affinity for cells in the grey matter throughout the brain (Appel, 1969). The resulting polioencephalitis reproduces key aspects of measles inclusion body encephalitis, which occurs in immunodeficient patients (Chadwick *et al.*, 1982). Neurological signs, including tremors and circling behaviour, first develop after 12 days and progress rapidly to seizures or paralysis, leading to death within 2-3 weeks after infection (Appel, 1969; Summers *et al.*, 1984). In ferrets, the virus is lethal with all animals developing the above-mentioned neurological manifestations (Stephensen *et al.*, 1997).

Due to the severe leukopenia and generalized immunosuppression associated with CDV infections, little inflammation has been observed in the CNS of dogs during the acute phase of disease. Local immune responses are limited to mild microglial activation and proliferation, and occasional perivascular cuffing, consisting mainly of T cells (Tipold *et al.*, 1999; Wunschmann *et al.*, 1999). The neurological signs and pathological changes observed are thus considered to be a direct result of the infection (Vandevelde & Zurbriggen, 2005; Vandevelde *et al.*, 1985; Zurbriggen *et al.*, 1998). However, the detection of different cytokine and chemokine mRNAs in the cerebrospinal fluid (CSF) of animals with chronic CDV-induced CNS lesions suggests that an aberrant local immune response may contribute importantly to disease progression (Frisk *et al.*, 1999).

To investigate the kinetics of CDV neurodissemination and the resulting local immune response at early disease stages in more detail, we produced an enhanced green fluorescent protein (eGFP)-expressing infectious clone of the Snyder Hill strain and characterized its neuropathogenesis in ferrets. The importance of the route of inoculation and blood-brain barrier integrity were examined, and the principal target regions and cell types in the CNS at different times after infection were identified. To determine the presence and extent of the local immune response, tissue sections were stained for different markers of immune activation with newly produced antisera against pro-inflammatory ferret cytokines.

Results

An eGFP-expressing derivative of the CDV Snyder Hill strain retains parental growth characteristics and virulence

To characterize the virus-host interactions involved in morbillivirus neuropathogenesis, we generated an infectious cDNA clone of the CDV Snyder Hill strain that carried the eGFP open reading frame in an additional transcription unit between the hemagglutinin (H) and polymerase (L) genes (Fig. 1A). Towards this, the parental Snyder Hill strain (ATCC VR-526) was plaque purified on VerodogSLAMtag cells and subsequently passaged twice in ferrets, where the second ferret was inoculated with blood-free CSF collected from the first. The infectious cDNA clone represents the consensus sequence of virus isolated from the CSF of the second animal and corresponds to the sequence of the parental ATCC strain. The growth kinetics of the eGFP-expressing recombinant SHeH in VerodogSLAMtag cells were similar to the non-recombinant parental strain (Fig. 1B), and it produced a comparable cytopathic effect (data not shown).

To determine if SHeH had retained the overall virulence and neurotropism of the parental strain, a group of four ferrets was infected intranasally with 10^5 50% tissue culture infectious doses ($TCID_{50}$) of either SH or SHeH. Onset and severity of clinical signs were similar in both groups (Fig. 1C), and all animals developed neurological signs. At least half of the animals displayed nausea and vomiting, suggestive of meningitis, starting as early as 6 days after infection. Facial spasms or disordered movement indicative of cerebellar involvement was observed in the majority of animals at later disease stages. All SH- or SHeH-infected animals succumbed to the disease within 12-16 days after infection, thereby reproducing the clinical course and disease duration seen in animals infected with the original ATCC virus (data not shown). Macroscopic examination of the brains at the time of death revealed strong infection of the olfactory bulb (Fig. 1D), and widespread eGFP expression in olfactory nerves and mitral cells was observed microscopically (Fig 1E). Taken together, these analyses indicate that the recombinant eGFP-expressing virus reproduces the parental disease phenotype.

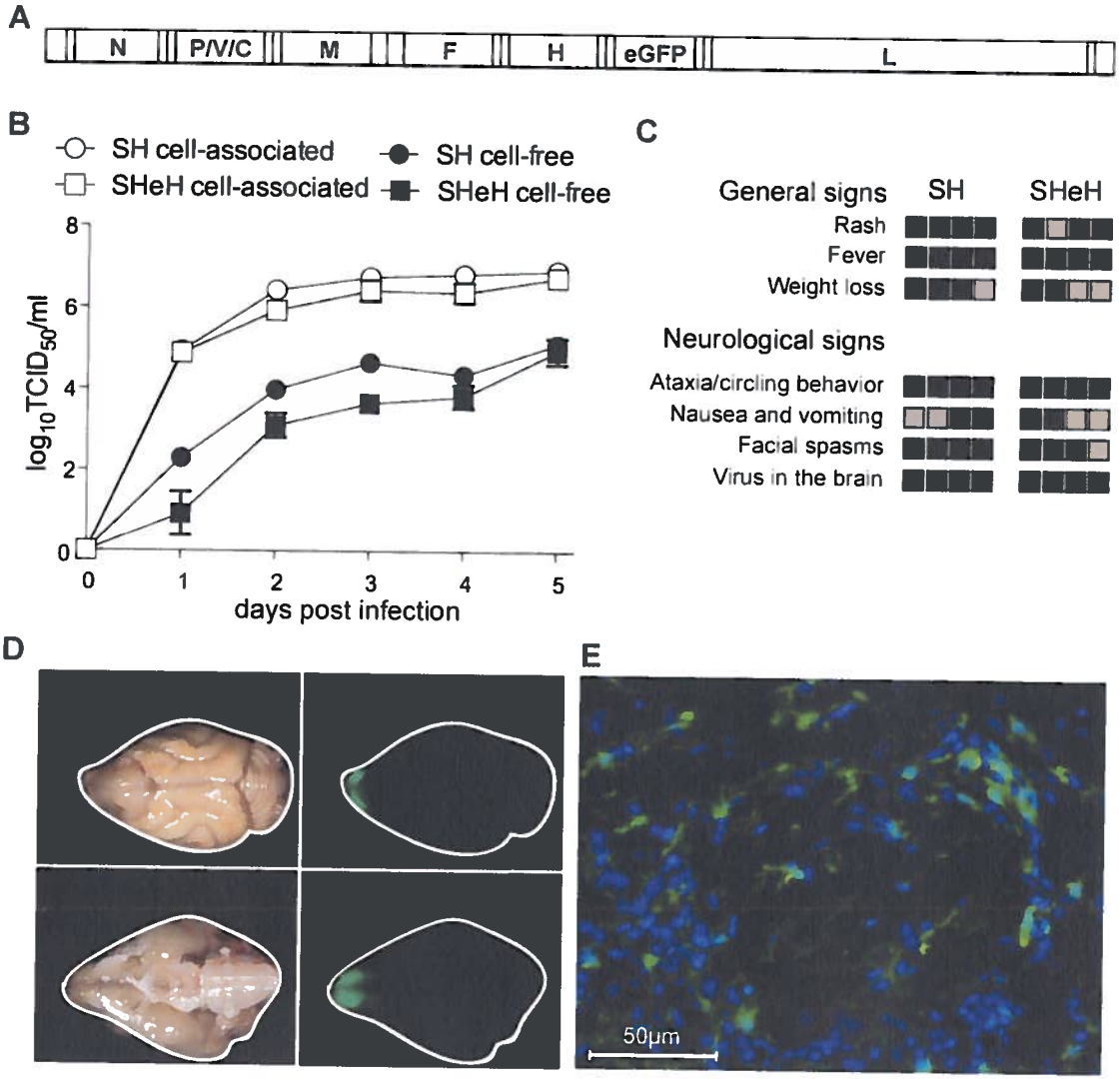
A
N
P/V/C
M
F
H
eGFP
L
B
SH cell-associated
SH cell-free
SHeH cell-associated
SHeH cell-free
log10TCID50/ml
days post infection
C
General signs
SH
SHeH
Rash
Fever
Weight loss
Neurological signs
Ataxia/circling behavior
Nausea and vomiting
Facial spasms
Virus in the brain
D
E
50µm

Fig. 1 Production and characterization of recombinant SH viruses. (A) Schematic diagram of the SH genome with the eGFP open reading frame introduced as an additional transcription unit between the hemagglutinin (H) and polymerase (L) genes. (B) Growth kinetics of the SH parental virus (circles) and its eGFP-expressing derivative SHeH (squares). VerodogSLAMtag cells were infected with a m.o.i. of 0.01 and samples were harvested for 5 days. Error bars indicate standard deviations. (C) Clinical scores observed in ferrets infected with SH or SHeH. Each square represents one animal and the colour indicates the severity of the respective criteria with black representing the most severe manifestation, grey a moderate severity, and white no change. (D) Macroscopic distribution of eGFP expression in the CNS at the time of death, 15 days after infection. Brain contours are outlined with a white line. (E) Microscopic analysis of eGFP expression in the olfactory bulb. Nuclei are stained with DAPI. Pictures of cryosections are taken at a 400x magnification; bar, 50 μm.

CDV neuroinvasion is independent of the inoculation route and does not require blood-brain barrier damage

Using different eGFP-expressing CDV strains, we have shown previously that the virus first targets lymphatic tissues and organs and then spreads to epithelia and the CNS (Rudd *et al.*, 2006; von Messling *et al.*, 2004). However, the anatomical proximity of the olfactory bulb to the nasal cavities raises the possibility that intranasal inoculation may lead to direct infection of olfactory neurons, thereby facilitating neuroinvasion. To investigate the importance of the route of inoculation for CDV neuroinvasion, we compared disease progression and dissemination in animals infected intraperitoneally or intranasally with 10^5 $TCID_{50}$ of SHeH. All animals showed first signs of rash and fever around 6 days after infection and had to be euthanized around day 14 (Fig. 2A). Starting at 7 days after infection, severe leukopenia and inhibition of PBMC proliferation activity following phytohemagglutinin (PHA) stimulation was observed in both groups (Fig. 2B and C), and the kinetics of the cell-associated viremia were similar (Fig. 2D). No differences were noted with respect to overall virus distribution in the brain (data not shown), and eGFP expression in the olfactory bulbs was first detected macroscopically at day 14 in the final disease stage (Fig. 2E), regardless of the route of inoculation.

Since it had also been suggested that infection-induced damage of the blood-brain barrier contributes to neuroinvasion (Axthelm & Krakowka, 1987), we assessed blood-brain barrier integrity over the course of the infection. Towards this, animals received an intracardiac injection of Evans blue, which is unable to cross an intact blood-brain barrier due to its large molecular mass, 45 min before sacrifice at different times after infection. Diffuse staining of the brain was only observed at the day 14 time point (Fig. 3), when CNS infection was already macroscopically detectable (Fig. 1D and 2E), and the animals were showing neurological signs, indicating that CDV neuroinvasion occurs without severely damaging the blood-brain barrier.

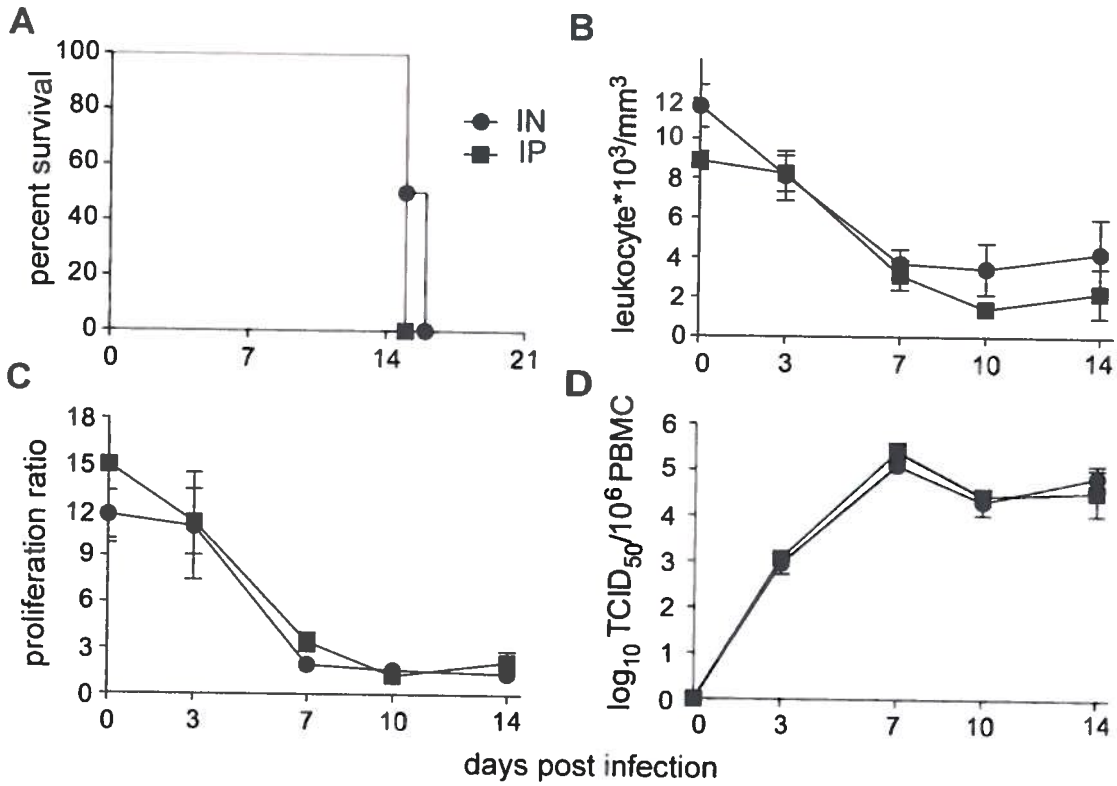
A
percent survival
100
80
60
40
20
0
0
7
14
21
IN
IP
B
leukocyte*10^3/mm^3
12
10
8
6
4
2
0
0
3
7
10
14
C
proliferation ratio
18
15
12
9
6
3
0
0
3
7
10
14
D
log10 TCID50/10^6 PBMC
6
5
4
3
2
1
0
0
3
7
10
14
days post infection

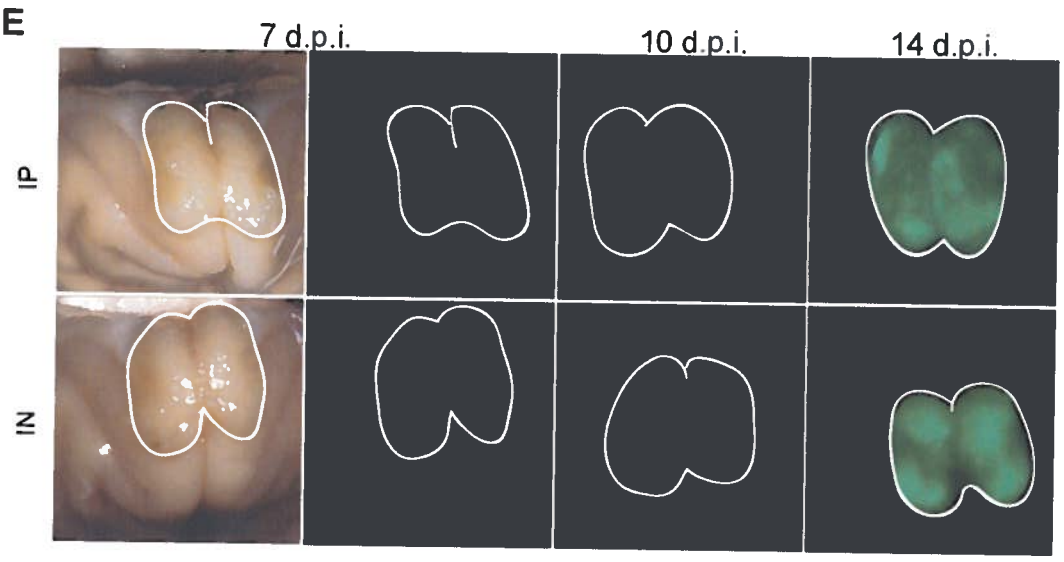
E
7 d.p.i.
10 d.p.i.
14 d.p.i.
IP
IN

Fig. 2 Comparison of intranasal and intraperitoneal inoculation. (A) Survival curve of groups of 4 ferrets infected with 10^5 $TCID_{50}$ of SHeH either intranasally (IN) or intraperitoneally (IP). Animals that reached experimental end points were euthanized. The time of death is represented by a step down in the graph. (B-D) Leukocyte numbers (B), *in vitro* proliferation activity (C), and cell-associated viremia (D) are depicted for both groups of animals. Time post-infection is indicated on the x-axis, and leukocyte numbers, proliferation activity, or number of CDV-infected cells per million PBMCs are indicated on the y-axis. (E) Visualization of olfactory bulb infection. Macroscopic eGFP expression is first detected 14 days after infection regardless of the route of inoculation. Olfactory bulb contours are outlined by a white line.

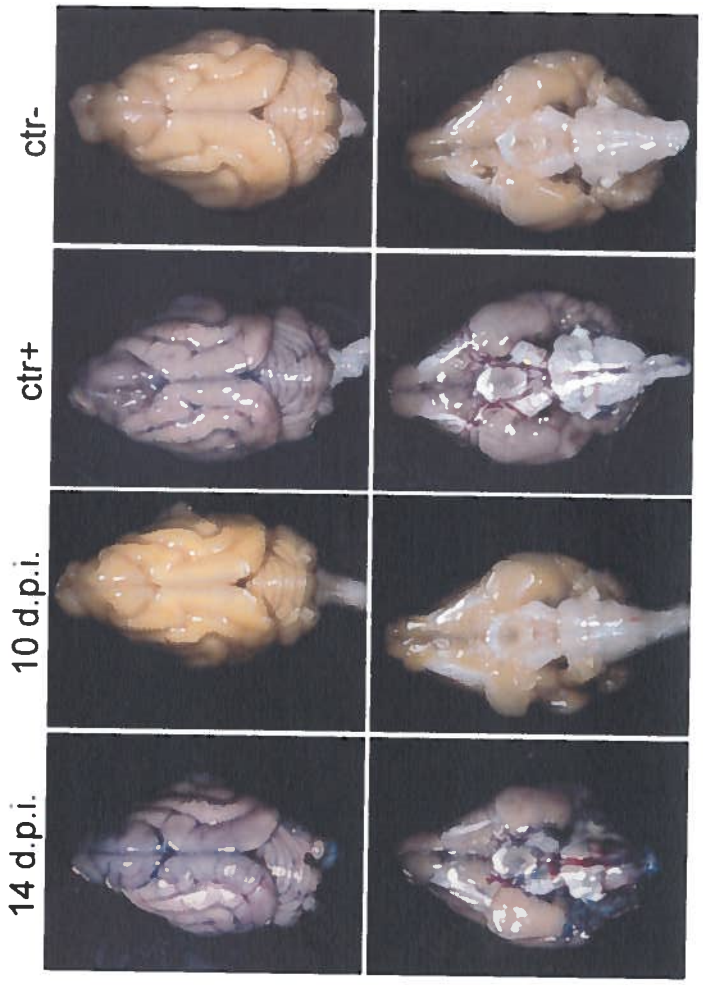

Fig. 3 Assessment of blood-brain barrier integrity over the course of CDV infection. Animals received a 5 ml intracardiac injection of a 2% (w/v) solution of Evans blue dye dissolved in 0.9% NaCl 45 min prior to sacrifice and were subsequently perfused with PBS at various times post infection. As positive control, a non-infected animal was injected with 10 ml of a 20% mannitol solution intracardially prior to the Evans blue dye. A non-infected animal that also received the Evans blue injection is shown as negative control. Ventral and dorsal photographs of the brains are shown.

SHeH infection results in substantial neuronal damage and gliosis

To assess the kinetics of neuroinvasion and identify target areas, two or three animals were sacrificed at days 7, 10, and 14 after infection and sagittal brain sections were stained for the presence of CDV-infected cells. The first infected cells were detected in the cerebellum and the olfactory bulb after 7 days, and a continuous increase was observed as the disease progressed (Fig. 4A). Similar infection kinetics were also observed in the choroid plexus, hippocampus, and brainstem, while only occasional foci were seen in the cerebrum (data not shown). Within these regions, neurons in general, but particularly Purkinje and granular cells, were targeted preferentially. Evaluation of the onset and extent of histopathological changes revealed little infiltration of mononuclear cells, indicative of an inflammatory response over the course of the infection. Even at the time of death, only occasional foci were found, mostly in close proximity to highly infected areas (Fig. 4B). Instead, many infected neurons underwent morphological changes indicative of severe neuronal injury including acute neuronal necrosis (Fig. 4C), atrophy (data not shown), and ballooning resembling karyolysis (Fig. 4D). Neuronophagia was also occasionally observed (data not shown).

To determine whether these infection-induced morphological changes ultimately resulted in cell death, we focused on the cerebellum, where the first infected Purkinje cells were found on day 7 (Fig. 4A, top row). A progressive increase of infection and loss of Purkinje cells were observed, resulting in a 35% reduction and a threefold increase in distance between neighbouring cells at the time of death (Fig. 4A, top row, and Fig. 5A and B). TUNEL staining revealed no increase in apoptosis in the different brain areas over the course of the infection (Fig. 5C), suggesting that the virus-induced cell death occurs via an alternative mechanism.

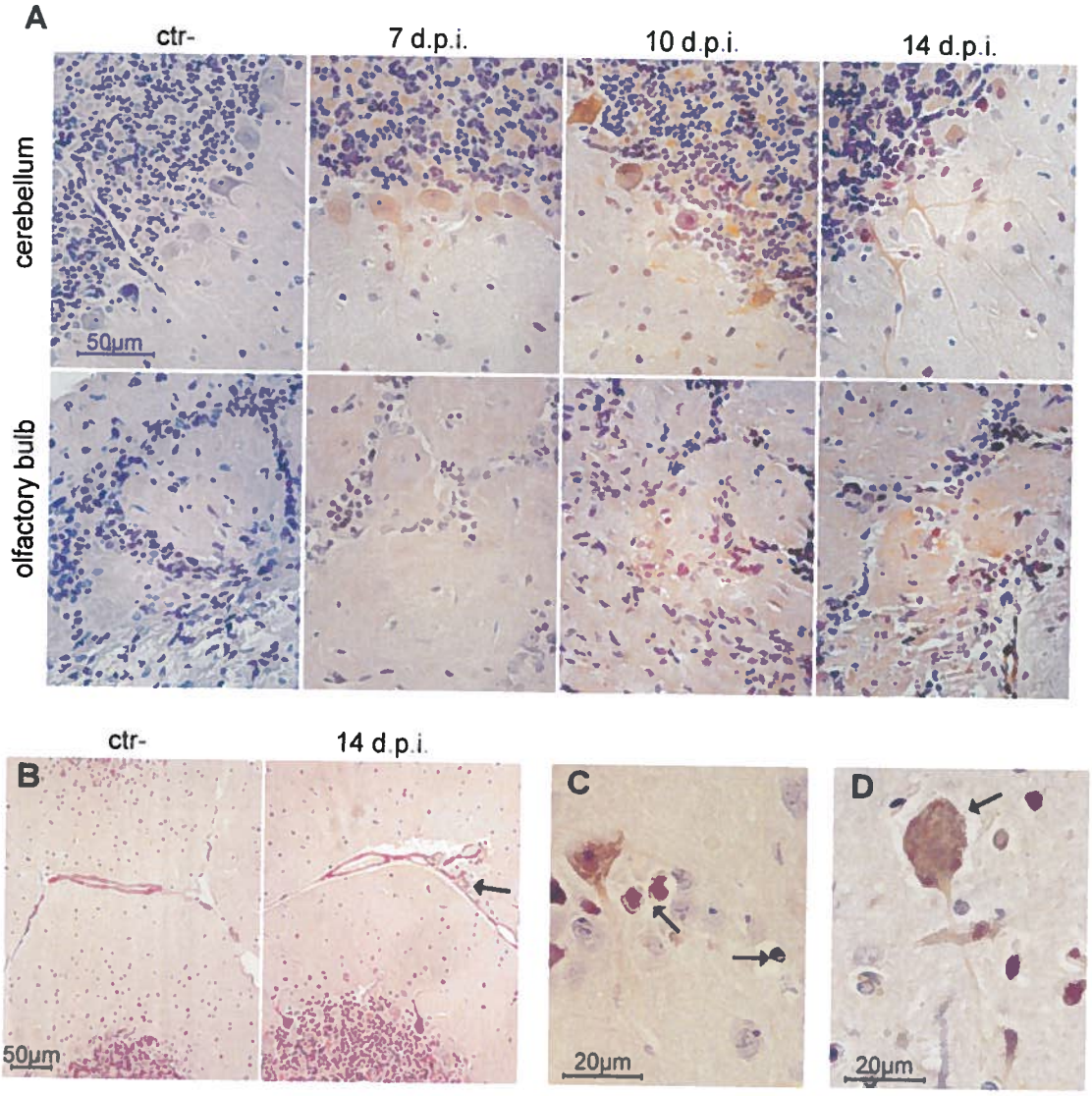
A
ctr-
7 d.p.i.
10 d.p.i.
14 d.p.i.
cerebellum
olfactory bulb
50µm
ctr-
14 d.p.i.
B
C
D
50µm
20µm
20µm

Fig. 4 Immunohistochemical detection of infection levels in cerebellum and olfactory bulb at different times after infection and associated morphological changes. (A) Two or three animals were sacrificed on days 7, 10, and 14 after infection and sagittal brain sections were stained with an N protein-specific mononclonal antibody and counterstained with hematoxylin. Pictures are taken at 400x magnification; bar, 50 μm (B) Hematoxylin/eosin-stained sections from either a non-infected animal (left panel) or an animal sacrificed on day 14 post-infection (right panel). Arrow indicates infiltration of immune cells around cerebral vessels in the cerebellum. Pictures are taken at 20x magnification. (C and D) Sagittal sections of paraffin-embedded brain tissue were stained for the presence of CDV nucleoprotein and counterstained with hematoxylin. Pictures are taken at 1000x magnification; bars, 20 μm. Black arrows indicate either (C) necrotic neurons or (D) a ballooning neuron reminiscent of karyolysis.

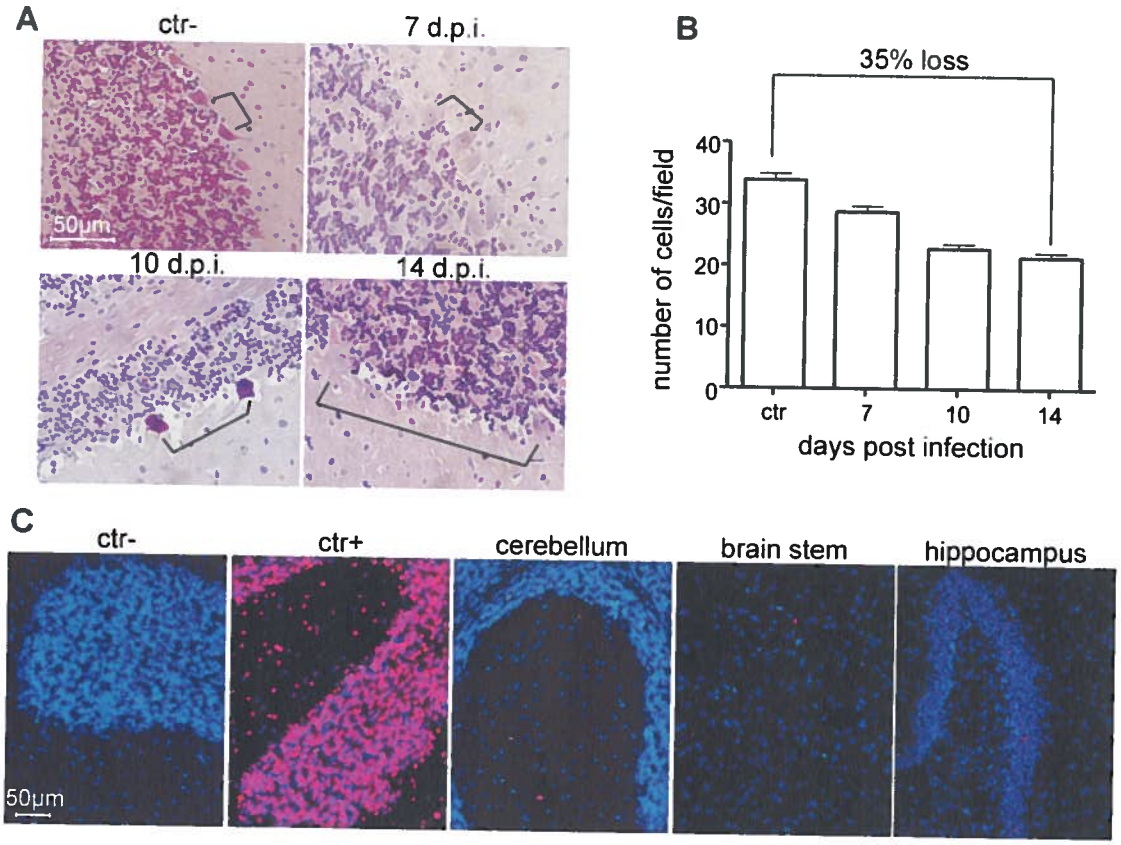

Fig. 5 Infection-associated cell death. (A) Loss of Purkinje cells over the course of the infection. Paraffin-embedded cerebellum sections from ferrets that were either mock infected or sacrificed at days 7, 10, and 14 after infection. Slides were stained with hematoxylin and eosin and photographed at 400x magnification; bar, 50 µm. (B) Quantification of Purkinje cell loss. Ten independent fields of view from at least two different animals euthanized at the respective time point. The control column represents a non-infected ferret. (C) TUNEL staining of sagittal sections of cerebellum, brainstem, and hippocampus of an animal sacrificed 14 days after infection. TUNEL-positive cells are indicated by red fluorescence, and cell nuclei are counterstained with DAPI. Pictures are taken at 200x magnification; bar, 50 µm.

Pro-inflammatory cytokines are present in the CNS

CDV causes severe leukopenia, and T and B lymphocytes are one of its main targets with infection levels over 70% within the first week (von Messling *et al.*, 2004). It is thus not surprising that few signs of an inflammatory response, such as lymphocyte infiltration and perivascular cuffing, are seen. To investigate whether the infection results in local immune activation, we evaluated the extent of gliosis, an indicator of neuroinflammation, and the presence of activated microglial cells, and of cells expressing interferon (IFN)-β and pro-inflammatory cytokines. Reactive gliosis, as indicated by an increase in glial fibrillary acidic protein (GFAP)-positive cells, was detected in areas surrounding infected cells within the first week and continued as the infection progressed (Fig.6A). A limited number of activated microglia were found at early infection stages, but their presence diminished as the infection progressed (Fig. 6B). Similar kinetics were observed for interleukin-6 (IL-6), whilst a gradual increase of Beta interferon (IFN-β) and tumor necrosis factor (TNF)-α expressing cells was seen (Fig. 7), many of which were infected (Fig. 8, and data not shown). This local TNF-α expression may contribute to the breakdown of the blood-brain barrier observed at late infection stages (Fig. 3).

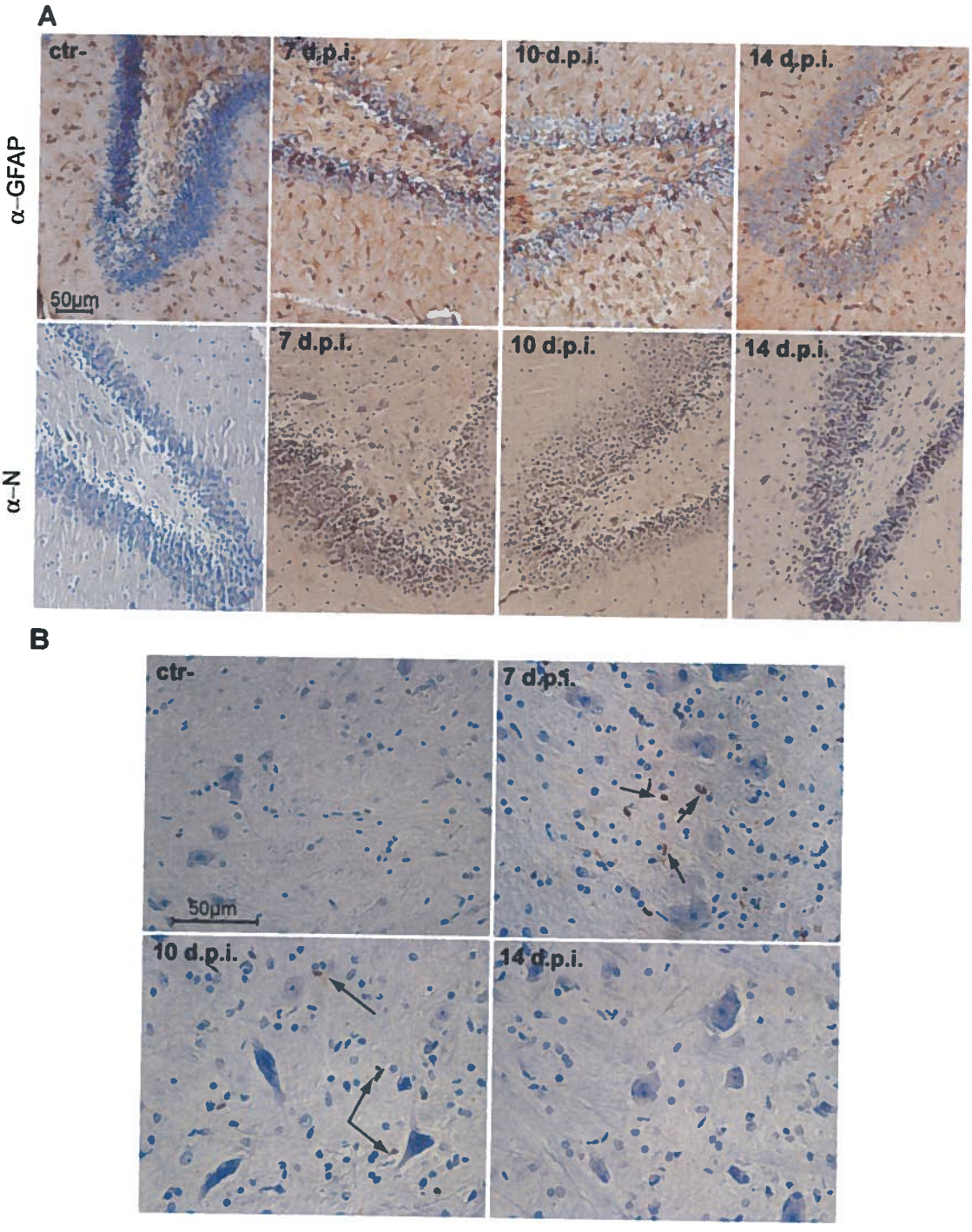
A
ctr-
7 d.p.i.
10 d.p.i.
14 d.p.i.
α–GFAP
50μm
7 d.p.i.
10 d.p.i.
14 d.p.i.
α–N
B
ctr-
7 d.p.i.
50μm
10 d.p.i.
14 d.p.i.

Fig. 6 Inflammatory response in the hippocampus and brainstem. (A) Extent of gliosis and infection in the hippocampus over the course of the infection. Astrocytes were stained using a rabbit antiserum against GFAP, and infected cells were detected using a N protein-specific monoclonal antibody. All slides were counterstained with hematoxylin. Pictures are taken at 200x magnification; bar, 50 μm (B) Presence of activated microglia/macrophages in the brainstem was detected with monoclonal antibody detecting rat Mac-2. Arrows indicate positive cells. Pictures are taken at 400x magnification; bar, 50 μm.

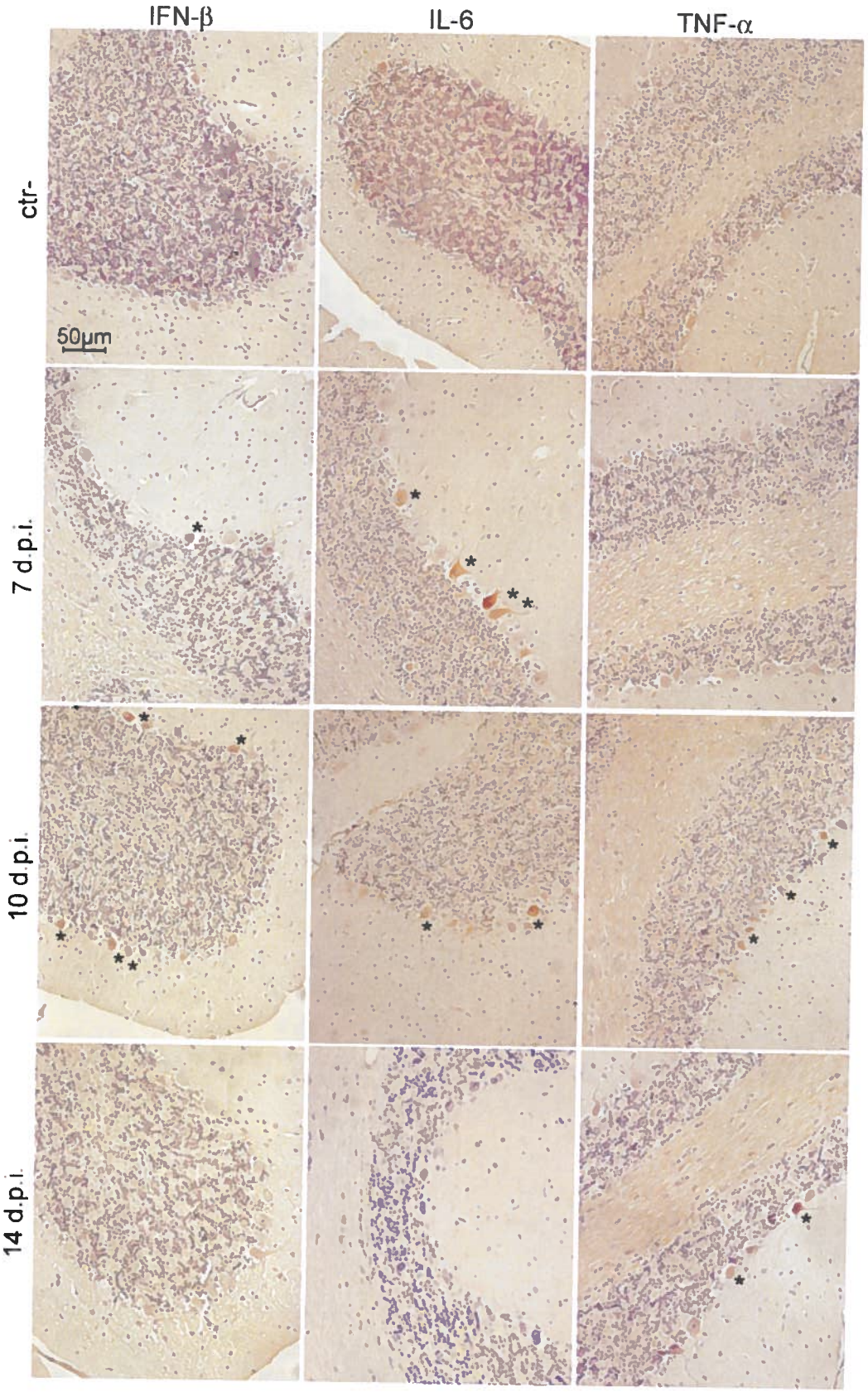
IFN-β
IL-6
TNF-α
ctr-
7 d.p.i.
10 d.p.i.
14 d.p.i.
50μm

Fig. 7 Presence of pro-inflammatory cytokines in the cerebellum. IFN-β (left column), IL-6 (middle column), and TNF-α (right column) were detected in paraffin sections of the cerebellum using polyclonal antibodies raised in chicken directed against the respective ferret cytokine. All slides were counterstained with hematoxylin. Stars highlight positive cells. Pictures are taken at 400x magnification; bar, 50 μm.

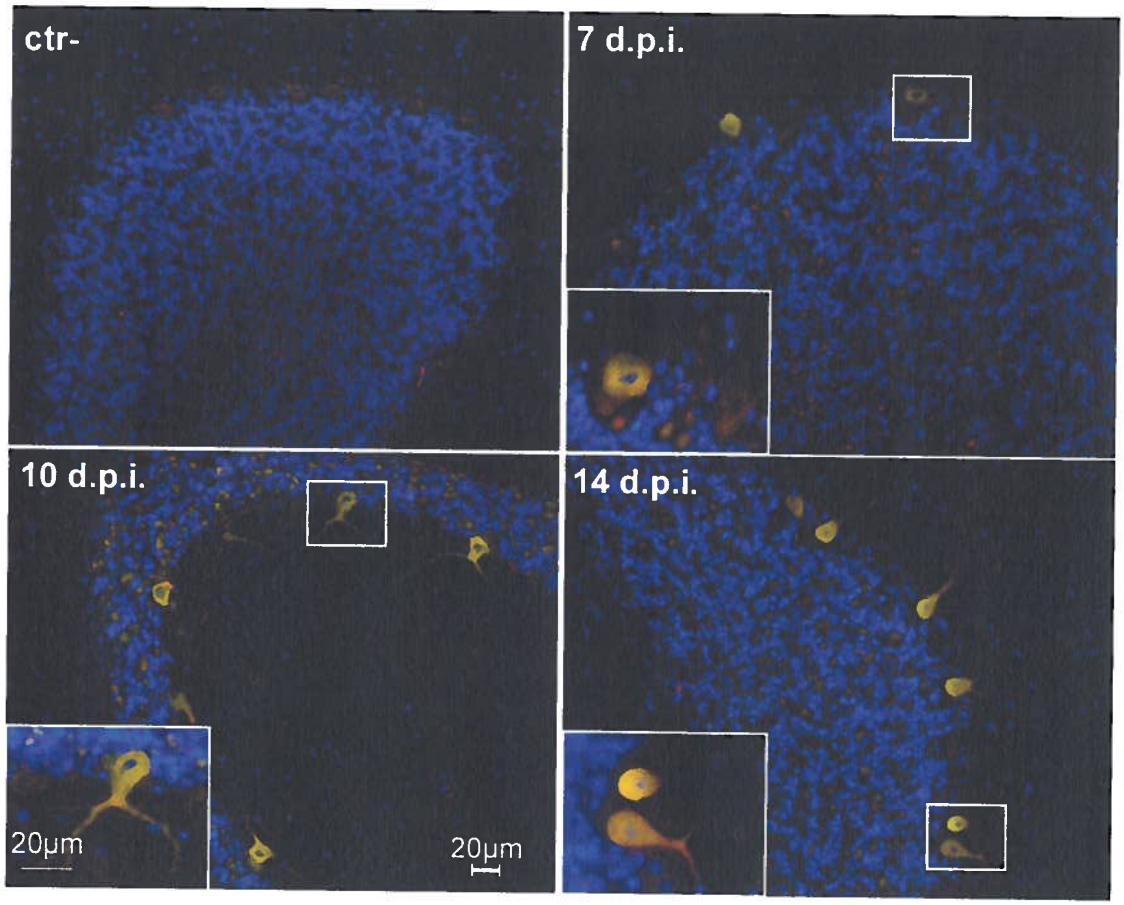

Fig. 8 Co-localization of CDV and IFN-β in the cerebellum. Paraffin sections were incubated with an antiserum directed against IFN-β raised in rabbits and visualized by using an Alexa Fluor 568- labeled secondary antibody (red). Infected cells were stained with a monoclonal antibody recognizing CDV N followed by a Alexa Fluor 488- labeled secondary antibody (green). Merge images are shown of representative sections from a non-infected control animal (upper left), and of animals sacrificed on days 7 (upper right), 10 (lower left) and 14 (lower right) post-infection. Images were taken at 400x magnifications. Inlets show a 1000x magnification of areas defined by rectangles. Nuclei were stained using 4',6-diamidino-2 phenylindole (DAPI); bars, 20 µm.

Discussion

In addition to the CNS diseases caused by primarily neurotropic viruses, neurological complications are associated with a number of viral infections (Acharya & Pacheco, 2008; Gnann, 2002; Letendre *et al.*, 2009; Whitley & Gnann, 2002). Once these viruses succeed in invading the CNS, damage caused by the death of infected cells is often amplified by the local immune response. This immune activation may persist long after the viral infection has been resolved and may lead to continued neuronal injury and loss (Stoica *et al.*, 2000), or contribute to neurodegeneration by affecting other CNS cell populations. As some morbillivirus neurological complications occur in the context of genetic or acquired immunodeficiencies, whilst others are associated with an excessive inflammatory response, we investigated the contribution of infection and immune response to CDV neuropathogenesis during the early infection phase. We show that the virus targets cells in the olfactory bulb, brainstem, hippocampus, and cerebellum, regardless of the route of inoculation. Development of neurological signs, especially motor deficits, correlates with the progressive loss of infected neurons in these areas. Only a mild transitory inflammatory response is detected at early stages, despite of the presence of pro-inflammatory cytokines. Even though insufficient in the context of lethal systemic disease, this local cytokine expression in combination with inflammatory mediators released upon non-apoptotic death of the infected neurons, may trigger the aberrant inflammatory response observed in chronic neurological complications associated with morbillivirus infections.

The inoculation route does not influence morbillivirus dissemination

For many neurotropic viruses, the point of entry in the periphery determines the time course of neuroinvasion and even the CNS area affected (Anderson & Field, 1983; Kuss *et al.*, 2008; Sinchaisri *et al.*, 1992). Previous studies have shown that upon intranasal inoculation, immune cells are the initial morbillivirus targets, followed by spread to epithelia and the CNS (de Swart *et al.*, 2007; von Messling *et al.*, 2004). In addition to the well-characterized hematogenous route (Higgins *et al.*, 1982), we

demonstrated that the olfactory bulb is a main point of morbillivirus CNS entry (Rudd *et al.*, 2006). The similar CDV neuroinvasion kinetics observed upon intranasal and intraperitoneal inoculation indicate that this sequential dissemination constitutes an integral part of morbillivirus pathogenesis. The most likely explanation for this phenomenon is that immune cells expressing the morbillivirus high-affinity receptor, the signaling lymphocyte activation molecule (SLAM, CD150) (Cocks *et al.*, 1995; Sidorenko & Clark, 2003; Tatsuo *et al.*, 2001), are equally available in the upper respiratory tract and the peritoneal cavity. The importance of this initial infection of immune cells has been illustrated by the complete attenuation of SLAM-blind viruses *in vivo* (von Messling *et al.*, 2006). Once the infection is established in the immune system, subsequent spread to epithelia and the CNS is independent of the original site of inoculation.

Morbilliviruses are unable to prevent local immune activation in the CNS

The immunosuppressive effects of morbilliviruses on immune cells have been extensively studied *in vitro* and *in vivo*. Contact with the viral glycoproteins inhibits lymphocyte proliferation (Sanchez-Lanier *et al.*, 1988; Schlender *et al.*, 1996), and the V protein efficiently prevents innate immune activation and induction of an antiviral state (Caignard *et al.*, 2007; Ohno *et al.*, 2004; Palosaari *et al.*, 2003; Takeuchi *et al.*, 2003). Lethal disease is characterized by severe leukopenia and a complete lack of cytokine induction and loss of proliferation capacity in PBMCs (Svitek & von Messling, 2007). Here we observed an immune activation in resident CNS cells that increased as the infection progressed, suggesting that the virus is unable to block an innate tissue response. A similar tissue response in epithelia may explain the apparent dichotomy of an efficient cellular and humoral antiviral response in the presence of generalized immunosuppression observed in uncomplicated measles virus MeV and other non-fatal morbillivirus infections.

Distemper encephalomyelitis – an unwanted consequence of early CNS immune activation?

In the context of viral infections, pro-inflammatory cytokines and chemokines released upon non-physiological death of infected cells usually result in recruitment of circulating immune cells that ultimately clear the infection. However, due to the severe leukopenia associated with morbillivirus infections, only very few immune cells are available for recruitment to the sites of injury during the acute disease phase, explaining the general lack of infiltration. Time-course studies and retrospective analyses of natural cases in dogs indicate that CDV demyelinating leukoencephalomyelitis, which occurs weeks to years after recovery from the acute disease, involves a two-step process: the initial damage during the acute disease phase is directly caused by the virus, whereas plaque progression after the recovery of the immune system is thought to be primarily immune-mediated (Alldinger *et al.*, 1996; Baumgartner *et al.*, 1989; Summers & Appel, 1994). Our observation of widespread death of infected neurons coinciding with sustained local immune activation in the context of a fatal disease supports this model, but suggests that the aberrant inflammatory response seen after virus clearance may be triggered by this early immune activation.

Materials and Methods

Cells and viruses

VerodogSLAMtag cells and 293 cells (ATCC CRL-1573) were maintained in Dulbecco's modified Eagle's medium (DMEM, Invitrogen) with 5% fetal bovine serum (FBS, Invitrogen). The CDV Snyder Hill strain (ATCC VR-526) and all recombinant viruses produced were propagated in VerodogSLAMtag cells. For plaque purification, the ATCC inoculum was serially diluted in tenfold steps and added to VerodogSLAMtag cells seeded in six-well plates. After thirty minutes at 37°C, medium was replaced with a 2% agar overlay, and the plates were incubated for three days. Individual syncytia were picked, and virus stocks were produced.

Construction and recovery of recombinant viruses

To generate an infectious cDNA clone of the Snyder Hill strain, RNA was isolated from VerodogSLAMtag cells infected with CSF obtained from the last infected ferret (see detailed description in the following paragraph) using the RNeasy mini kit (QIAGEN). The cloning strategy used followed that described previously for other CDV strains (von Messling *et al.*, 2003). Briefly, the RNA was reverse transcribed using Superscript II (Invitrogen), and the complete genome was amplified in ten separate fragments using high-fidelity polymerase (Roche) and subcloned into pCR2.1-TOPO (Invitrogen). At least four clones of each fragment were sequenced to establish the consensus sequence. The viral genomic cDNA clone was assembled from fragments corresponding to the consensus sequence using naturally occurring unique restriction sites, yielding pSH (GenBank Acc. No. GU138403). The eGFP open reading frame was then introduced as an additional transcription unit between the H and L genes following the same approach as for 5804PeH (von Messling *et al.*, 2004), yielding pSHeH.

Recombinant viruses were recovered using a vaccinia-free system (Anderson & von Messling, 2008; Martin *et al.*, 2006). Towards this, semi-confluent 293 cells seeded in six-well plates were transfected with 4 μg of plasmid carrying the full-length genome, 0.5 μg of measles virus (MeV) nucleoprotein (N), 0.1 μg of MeV phosphoprotein (P), 0.5 μg of MeV L and 0.7 μg of T7 polymerase expression plasmids using Lipofectamine 2000 (Invitrogen). Two days post transfection, 293 cells were overlayed onto 10 cm culture dishes containing a confluent monolayer of VerodogSLAMtag cells. The resulting co-cultures were maintained in DMEM containing 5% FBS until syncytia were observed. Virus stocks were then produced by transferring individual syncytia onto fresh VerodogSLAMtag cells. Multi-step growth curves were performed by infecting VerodogSLAMtag cells with m.o.i. of 0.01 of the respective strain and incubating them at 32°C. Cells and supernatant were harvested for five days, and the virus titers were determined by limited dilution method and expressed as $TCID_{50}$.

Animal infection, virulence assessment, and imaging

The animal experiments were carried out as described previously (von Messling *et al.*, 2003) and were approved by the INRS-Institut Armand-Frappier Institutional Animal Care and Use Committee. Male ferrets (*Mustela putorius furo*, Marshall Farms) without antibodies against CDV were used for all experiments.

For the *in vivo* passages, one ferret was infected intranasally under general anesthesia (10 mg/kg ketamine, 1 mg/kg midazolam, CDMV) with $3x10^4$ $TCID_{50}$ of plaque-purified ATCC Snyder Hill virus. At the onset of severe neurologic signs, 16 days after infection, the animal was euthanized, and blood-free CSF was harvested. Five hundred μl CSF corresponding to $5x10^3$ $TCID_{50}$ was used to intranasally inoculate a second ferret. This animal succumbed to the infection 12 days after the intranasal inoculation. The viral RNA isolated from the cerebrospinal fluid of this animal was used to generate the recombinant Snyder Hill virus.

For pathogenesis assessment, animals were infected intranasally with 10^5 $TCID_{50}$ of the respective viruses and monitored daily for signs of disease, temperature, and body weight loss. Blood was collected at various time points from the jugular vein under general anesthesia. A grading system was established to evaluate the severity of clinical signs. Animals that failed to eat for more than 48 h, experienced weight loss of more than 15%, became severely dehydrated, developed CNS signs, including circling behavior, paralysis, or focal or generalized seizures, displayed any other important reduction in functional status such as severe pneumonia and/or diarrhea, or became moribund before the end of the protocol were euthanized with an overdose of pentobarbital (CDMV). The Macro-Illumination imaging system (Lightools) was used to observe eGFP expression in organs (von Messling *et al.*, 2004).

Assessment of immunosuppressive activity

For the total white blood cell count, 10 μl of heparinized blood was added to 990 μl of a 3% solution of acetic acid, and nucleated cells were counted. The proliferation activity was determined using the 5-bromo-2'-deoxyuridine (BrdU) cell proliferation assay (Roche) according to the manufacturer's instructions. Briefly, the PBMCs from each animal isolated by Ficoll (GE Healthcare) gradient centrifugation were split into two duplicates and either stimulated with 2 μg/ml phytohemagglutinin (PHA, Sigma) or left untreated. After 24 h incubation, BrdU was added to a final concentration of 10 μM, and cells were incubated for another 24 h. Cells were then transferred into a black 96-well plate, washed, and fixed at 65 °C for 1 h. BrdU incorporation was detected using a peroxidase-coupled anti-BrdU antibody and a chemiluminescent substrate. The proliferation activity was expressed as a ratio between stimulated and non-stimulated cells, allowing for comparison of samples that differ in absolute cell numbers due to the virus-induced leukopenia. Cell-associated viremia was quantified in PBMCs isolated by lysing erythrocytes in EDTA-treated blood in ACK lysis buffer (150 mM NH_4Cl, 10 mM $KHCO_3$, 0.01 mM EDTA, pH 7.2 to 7.4), and co-cultivated with VerodogSLAMtag cells in quadruplicates of 10-fold serial dilutions. Wells were evaluated for cytopathic effect after 3 days, and titers were expressed as 50% $TCID_{50}$ per 10^6 cells.

Assessment of blood-brain barrier integrity

Animals were anesthetized and injected intracardially with 5 ml of a 2% (w/v) Evans blue (Sigma) solution diluted in 0.9% NaCl. Forty-five min later, animals were euthanized and perfused with phosphate-buffered saline (PBS, Invitrogen) until the drainage was colorless. For the positive control, the animal was first injected intracardially with 10 ml of a 20% mannitol solution, followed by the Evans blue injection. Ventral and dorsal views of the brains were imaged under normal light using the Macro-Illumination imaging system (Lightools, Encinitas, CA).

Preparation of antigens and production of polyclonal antibodies

To produce purified proteins, ferret cytokines were amplified as described previously (Svitek & von Messling, 2007). PCR products were cloned into the pET32a vector (Novagen), confirmed by sequencing, and transformed into *Escherichia coli* BL21 (DE3) competent cells (Novagen) for expression. Proteins were then purified by electropheresis and extracted using 0.1% SDS. Antigenic sequences were chosen by the Jameson-Wolf index, yielding the following peptides: IFN-β, CLKDRMNFKIPEEIQKSQK; IL-6, CGDSKDDATSNRPPLTSAD; and TNF-α, CVKSSSRTPSDKPV. Rabbit and chicken antisera were raised against either purified bacterial proteins or synthetic peptides, respectively, following the standard protocol (Cocalico Biologicals).

Cryosections and immunohistochemistry

Animals were euthanized with an overdose of intraperitoneal pentobarbital (CDMV). Each animal was perfused first with 160 ml PBS (Invitrogen), followed by 80 ml of 4% paraformaldehyde (PFA, Electron Microscopy Sciences). Tissues were harvested, fixed in 4% PFA for at least 24 h at 4°C, and stored in PBS. Prior to sectioning, samples were placed in 30% sucrose in PBS overnight at 4°C, immersed in tissue embedding compound (Triangle Biomedical Sciences), and frozen on dry ice for at

least 1 h. Serial 5- to 10-μm sections were cut using a cryostat (Kryostat 1720 digital; Leitz) and mounted on Superfrost Plus slides (Fisher Scientific), air dried, and stored at –20°C. Nuclei were stained with 4',6-diamidino-2-phenylindole (DAPI), and coverslips were mounted with Prolong Gold antifade reagent (Invitrogen) and left to harden overnight at 4°C.

For immunohistochemistry staining, paraffin sections were deparaffinized and rehydrated following standard immunohistochemistry protocols. Endogenous peroxidase was quenched with 0.3% H_2O_2 in PBS for 12 min. For GFAP staining, the slides were incubated in 10 mM sodium citrate (pH 6) solution (Fisher Scientific) and microwaved for 15 min before being transferred into PBS. After blocking with a 1/50 dilution of horse serum in PBS, the respective primary antibody, rabbit-anti GFAP (DAKO), mouse ascitic fluid against rat Mac-2 (kind gift from Dr. Pierre Talbot, INRS-Institut Armand-Frappier), mouse monoclonal antibody against the CDV N protein (VMRD), or the chicken hyperimmune serum against the respective ferret cytokine, was added for 1 h at room temperature, followed by incubation with an appropriate biotinylated secondary antibody, and subsequently peroxidase-labeled streptavidin (Vector laboratories), each for 45 min at room temperature. Positive cells were visualized using 3,3'-diaminobenzidine (DAB) substrate (Sigma), and slides were counterstained in hematoxylin. For hematoxylin/eosin staining, paraffin-embedded sections were incubated for 30 min in xylene and then rehydrated prior to staining for 5 min in Harris' hematoxylin solution (EMD Industries, Gibbstown, NJ). Sections were rinsed in double-distilled H_2O, dipped in a 0.3% ammonia solution, and counterstained with acidified eosin Y (Sigma). Slides were dehydrated, mounted in Entellan mounting medium (EMD Industries) and air-dried overnight.

For double-staining, slides were first incubated with the rabbit hyperimmune serum against the respective cytokine, followed by an Alexa Fluor 568-labeled secondary antibody (Invitrogen), and then stained for CDV using the N protein-specific monoclonal antibody, followed by a biotinylated secondary antibody and Alexa Fluor 488-labeled

streptavidin. Nuclei were counterstained with DAPI, and coverslips were mounted with Prolong Gold antifade reagent (Invitrogen) and left to harden overnight at 4°C.

TUNEL assay

The extent of apoptosis in the tissue was determined by TUNEL assay, using the *In situ* cell death detection kit, POD (Roche) according to manufacturer's instructions. Briefly, 5 µm thick paraffin embedded sections were deparaffinized and rehydrated following standard immunohistochemistry protocols. Slides were then permeabilized using 0.1% sodium citrate and 0.1% Triton X-100 dissolved in water for 8 min at room temperature, rinsed twice in PBS, and incubated with the TUNEL reaction mixture for 1 h at 37°C. Slides were washed twice with PBS and counterstained with DAPI. The positive control was obtained by treating slides with 0.5 U deoxyribonuclease I (Fermentas) for 10 min at room temperature before adding the TUNEL reaction mixture. All slides were analyzed by fluorescence microscopy.

Acknowledgements

We thank Dr. Hélène Jacomy for critical reading of the manuscript. We are also thankful to all laboratory members for continuing support and valuable discussions, and to Chantal Thibault for technical assistance. This work was supported by the Canadian Institutes of Health Research (grant MOP-66989) and the Canadian Foundation for Innovation (grant 9488) to V.v.M., and scholarships from the Armand-Frappier Foundation to P.A.R. and L-E.B.-H.

References

1. Acharya, J. N. & Pacheco, V. H. (2008). Neurologic complications of hepatitis C. *Neurologist* 14, 151-156.

2. Alldinger, S., Wunschmann, A., Baumgartner, W., Voss, C. & Kremmer, E. (1996). Up-regulation of major histocompatibility complex class II antigen expression in the central nervous system of dogs with spontaneous canine distemper virus encephalitis. *Acta Neuropathol* 92, 273-280.

3. Anderson, D. E. & von Messling, V. (2008). Region between the canine distemper virus M and F genes modulates virulence by controlling fusion protein expression. *J Virol* 82, 10510-10518.

4. Anderson, J. R. & Field, H. J. (1983). The distribution of herpes simplex type 1 antigen in mouse central nervous system after different routes of inoculation. *J Neurol Sci* 60, 181-195.

5. Appel, M. J. (1969). Pathogenesis of canine distemper. *Am J Vet Res* 30, 1167-1182.

6. Appel, M. J., Shek, W. R. & Summers, B. A. (1982). Lymphocyte-mediated immune cytotoxicity in dogs infected with virulent canine distemper virus. *Infect Immun* 37, 592-600.

7. Appel, M. J. & Summers, B. A. (1995). Pathogenicity of morbilliviruses for terrestrial carnivores. *Vet Microbiol* 44, 187-191.

8. Axthelm, M. K. & Krakowka, S. (1987). Canine distemper virus: the early blood-brain barrier lesion. *Acta Neuropathol* 75, 27-33.

9. Baumgartner, W., Orvell, C. & Reinacher, M. (1989). Naturally occurring canine distemper virus encephalitis: distribution and expression of viral polypeptides in nervous tissues. *Acta Neuropathol* 78, 504-512.

10. Caignard, G., Guerbois, M., Labernardiere, J. L., Jacob, Y., Jones, L. M., Wild, F., Tangy, F. & Vidalain, P. O. (2007). Measles virus V protein blocks Jak1-mediated phosphorylation of STAT1 to escape IFN-alpha/beta signaling. *Virology* 368, 351-362.

11. Chadwick, D. W., Martin, S., Buxton, P. H. & Tomlinson, A. H. (1982). Measles virus and subacute neurological disease: an unusual presentation of measles inclusion body encephalitis. *J Neurol Neurosurg Psychiatry* 45, 680-684.

12. Cocks, B. G., Chang, C. C., Carballido, J. M., Yssel, H., de Vries, J. E. & Aversa, G. (1995). A novel receptor involved in T-cell activation. *Nature* 376, 260-263.

13. Confer, A. W., Kahn, D. E., Koestner, A. & Krakowka, S. (1975). Biological properties of a canine distemper virus isolate associated with demyelinating encephalomyelitis. *Infect Immun* 11, 835-844.

14. de Swart, R. L., Ludlow, M., de Witte, L., Yanagi, Y., van Amerongen, G., McQuaid, S., Yuksel, S., Geijtenbeek, T. B., Duprex, W. P. & Osterhaus, A. D. (2007). Predominant infection of CD150+ lymphocytes and dendritic cells during measles virus infection of macaques. *PLoS Pathog* 3, e178.

15. Frisk, A. L., Baumgartner, W. & Grone, A. (1999). Dominating interleukin-10 mRNA expression induction in cerebrospinal fluid cells of dogs with natural canine distemper virus induced demyelinating and non-demyelinating CNS lesions. *J Neuroimmunol* 97, 102-109.

16. Gnann, J. W., Jr. (2002). Varicella-zoster virus: atypical presentations and unusual complications. *J Infect Dis* 186 Suppl 1, S91-98.

17. Griffin, D. E. (2001). Measles virus. In *Fields Virology*, fourth edn, pp. 1401-1441 Edited by D. M. Knipe, Howley, P.M. Philidelphia: Lippincott Williams and Wilkins.

18. Headley, S. A., Soares, I. C. & Graca, D. L. (2001). Glial fibrillary acidic protein (GFAP)-immunoreactive astrocytes in dogs infected with canine distemper virus. *J Comp Pathol* 125, 90-97.

19. Higgins, R. J., Krakowka, S. G., Metzler, A. E. & Koestner, A. (1982). Primary demyelination in experimental canine distemper virus induced encephalomyelitis in gnotobiotic dogs. Sequential immunologic and morphologic findings. *Acta Neuropathol* 58, 1-8.

20. Kuss, S. K., Etheredge, C. A. & Pfeiffer, J. K. (2008). Multiple host barriers restrict poliovirus trafficking in mice. *PLoS Pathog* 4, e1000082.

21. Letendre, S. L., Ellis, R. J., Everall, I., Ances, B., Bharti, A. & McCutchan, J. A. (2009). Neurologic complications of HIV disease and their treatment. *Top HIV Med* 17, 46-56.

22. Martin, A., Staeheli, P. & Schneider, U. (2006). RNA polymerase II-controlled expression of antigenomic RNA enhances the rescue efficacies of two different members of the Mononegavirales independently of the site of viral genome replication. *J Virol* 80, 5708-5715.

23. Moss, W. J., Ota, M. O. & Griffin, D. E. (2004). Measles: immune suppression and immune responses. *Int J Biochem Cell Biol* 36, 1380-1385.

24. Ohno, S., Ono, N., Takeda, M., Takeuchi, K. & Yanagi, Y. (2004). Dissection of measles virus V protein in relation to its ability to block alpha/beta interferon signal transduction. *J Gen Virol* 85, 2991-2999.

25. Palosaari, H., Parisien, J. P., Rodriguez, J. J., Ulane, C. M. & Horvath, C. M. (2003). STAT protein interference and suppression of cytokine signal transduction by measles virus V protein. *J Virol* 77, 7635-7644.

26. Rima, B. K., Duffy, N., Mitchell, W. J., Summers, B. A. & Appel, M. J. (1991). Correlation between humoral immune responses and presence of virus in the CNS in dogs experimentally infected with canine distemper virus. *Arch Virol* 121, 1-8.

27. Rudd, P. A., Cattaneo, R. & von Messling, V. (2006). Canine distemper virus uses both the anterograde and the hematogenous pathway for neuroinvasion. *J Virol* 80, 9361-9370.

28. Sanchez-Lanier, M., Guerin, P., McLaren, L. C. & Bankhurst, A. D. (1988). Measles virus-induced suppression of lymphocyte proliferation. *Cell Immunol* 116, 367-381.

29. Schlender, J., Schnorr, J. J., Spielhoffer, P., Cathomen, T., Cattaneo, R., Billeter, M. A., ter Meulen, V. & Schneider-Schaulies, S. (1996). Interaction of measles virus glycoproteins with the surface of uninfected peripheral blood lymphocytes induces immunosuppression in vitro. *Proc Natl Acad Sci U S A* 93, 13194-13199.

30. Schneider-Schaulies, J. & Schneider-Schaulies, S. (2008). Receptor interactions, tropism, and mechanisms involved in morbillivirus-induced immunomodulation. *Adv Virus Res* 71, 173-205.

31. Sidorenko, S. P. & Clark, E. A. (2003). The dual-function CD150 receptor subfamily: the viral attraction. *Nat Immunol* 4, 19-24.

32. Sinchaisri, T. A., Nagata, T., Yoshikawa, Y., Kai, C. & Yamanouchi, K. (1992). Immunohistochemical and histopathological study of experimental rabies infection in mice. *J Vet Med Sci* 54, 409-416.

33. Stephensen, C. B., Welter, J., Thaker, S. R., Taylor, J., Tartaglia, J. & Paoletti, E. (1997). Canine distemper virus (CDV) infection of ferrets as a model for testing Morbillivirus vaccine strategies: NYVAC- and ALVAC-based CDV recombinants protect against symptomatic infection. *J Virol* 71, 1506-1513.

34. Stoica, G., Tasca, S. I. & Wong, P. K. (2000). Motor neuronal loss and neurofilament-ubiquitin alteration in MoMuLV-ts1 encephalopathy. *Acta Neuropathol* 99, 238-244.

35. Summers, B. A. & Appel, M. J. (1994). Aspects of canine distemper virus and measles virus encephalomyelitis. *Neuropathol Appl Neurobiol* 20, 525-534.

36. Summers, B. A., Greisen, H. A. & Appel, M. J. (1984). Canine distemper encephalomyelitis: variation with virus strain. *J Comp Pathol* 94, 65-75.

37. Svitek, N. & von Messling, V. (2007). Early cytokine mRNA expression profiles predict Morbillivirus disease outcome in ferrets. *Virology* 362, 404-410.

38. Takeuchi, K., Kadota, S. I., Takeda, M., Miyajima, N. & Nagata, K. (2003). Measles virus V protein blocks interferon (IFN)-alpha/beta but not IFN-gamma signaling by inhibiting STAT1 and STAT2 phosphorylation. *FEBS Lett* 545, 177-182.

39. Tatsuo, H., Ono, N. & Yanagi, Y. (2001). Morbilliviruses use signaling lymphocyte activation molecules (CD150) as cellular receptors. *J Virol* 75, 5842-5850.

40. Tipold, A., Moore, P., Zurbriggen, A., Burgener, I., Barben, G. & Vandevelde, M. (1999). Early T cell response in the central nervous system in canine distemper virus infection. *Acta Neuropathol* 97, 45-56.

41. van Moll, P., Alldinger, S., Baumgartner, W. & Adami, M. (1995). Distemper in wild carnivores: an epidemiological, histological and immunocytochemical study. *Vet Microbiol* 44, 193-199.

42. Vandevelde, M. & Zurbriggen, A. (2005). Demyelination in canine distemper virus infection: a review. *Acta Neuropathol* 109, 56-68.

43. Vandevelde, M., Zurbriggen, A., Higgins, R. J. & Palmer, D. (1985). Spread and distribution of viral antigen in nervous canine distemper. *Acta Neuropathol* 67, 211-218.

44. von Messling, V., Milosevic, D. & Cattaneo, R. (2004). Tropism illuminated: lymphocyte-based pathways blazed by lethal morbillivirus through the host immune system. *Proc Natl Acad Sci U S A* 101, 14216-14221.

45. von Messling, V., Springfeld, C., Devaux, P. & Cattaneo, R. (2003). A ferret model of canine distemper virus virulence and immunosuppression. *J Virol* 77, 12579-12591.

46. von Messling, V., Svitek, N. & Cattaneo, R. (2006). Receptor (SLAM [CD150]) recognition and the V protein sustain swift lymphocyte-based invasion of mucosal tissue and lymphatic organs by a morbillivirus. *J Virol* 80, 6084-6092.

47. Whitley, R. J. & Gnann, J. W. (2002). Viral encephalitis: familiar infections and emerging pathogens. *Lancet* 359, 507-513.

48. Wunschmann, A., Alldinger, S., Kremmer, E. & Baumgartner, W. (1999). Identification of CD4+ and CD8+ T cell subsets and B cells in the brain of dogs with spontaneous acute, subacute-, and chronic-demyelinating distemper encephalitis. *Vet Immunol Immunopathol* 67, 101-116.

49. Zurbriggen, A., Schmid, I., Graber, H. U. & Vandevelde, M. (1998). Oligodendroglial pathology in canine distemper. *Acta Neuropathol* 95, 71-77.

Publication no. 3

In preparation.

Canine Distemper Disseminates Along Communicating Neurons

Penny A. Rudd and Veronika von Messling*

INRS-Institut Armand-Frappier, University of Quebec, Laval, Canada

* Corresponding author.

Mailing address: INRS-Institut Armand-Frappier, University of Quebec,

531, Boul. des Prairies,

Laval, Quebec H7V 1B7,

Canada. Phone: (450) 687-5010. Fax: (450) 686-5305.

E-mail: veronika.vonmessling@iaf.inrs.ca

Abstract

Canine distemper virus (CDV), though not a primary neurotropic virus, frequently causes central nervous system (CNS) complications. CDV enters the CNS at late disease stages by hematogenous and olfactory routes, and preferentially targets neurons and glial cells. To investigate the mechanisms involved in transneuronal spread within the CNS we established and characterized primary cultures of ferret neurons. Within the first week of seeding, over 90% of cells were neurons, and we observed that the culture was fully permissive to CDV infection. Replication and dissemination was however slower than in SLAM expressing cells, thereby mimicking *in vivo* dissemination pattern. CDV spread in these cultures required cell-to-cell contact, suggesting that CDV propagates transneuronally. Analysis in a multi-chamber system revealed that CDV disseminated both retro- and anterogradely along communicating neurons, which may play an important role in CDV neuropathogenesis. Taken together, this new *in vitro* model will be useful for further studying mechanisms involved in transneuronal spread.

Introduction

Dissemination along communicating neurons represents an important propagation mechanism for viruses in the central nervous system (CNS), thereby contributing to pathogenesis. This form of spread has been extensively characterized for a wide variety of neurotropic viruses (Card et al., 1993; Finke and Conzelmann, 2005; Mettenleiter, 2003), as well as for viruses that are not predominantly neurotropic but frequently enter the CNS as a consequence of a primary infection (Diamond, 2009; Grose, 2004; Ivey et al., 2009; Samuel et al., 2007). Members of the *Paramyxoviridae* family only occasionally infect the CNS, and the role of transneuronal dissemination in neuropathogenesis remains unkown (Johnson, 1987; Summers and Appel, 1994; Weingartl et al., 2005).

Within the *Morbillivirus* genus, canine distemper virus (CDV) causes the highest incidence of CNS involvement with up to 30% of all acute cases resulting in various types of encephalopathies (Appel and Summers, 1995; Summers et al., 1984). Most morbillivirus-associated CNS complications occur at later disease stages after widespread infection of lymphatic and epithelial tissues (Bonami et al., 2007; Rudd et al., 2006; Schneider-Schaulies et al., 2003). In ferrets, CDV gains access to the CNS by disseminating along the olfactory signaling route (Rudd et al., 2006) suggesting that CDV spreads along communicating neurons. Furthermore, *in vitro* studies in primary cultures of neurons revealed that measles virus (MeV) dissemination in the CNS depends on cell contact. Viral nucleocapsids are found in axons and at presynaptic membranes, indicative of cell-to-cell transmission (Lawrence et al., 2000). This has been confirmed using rat organotypic hippocampal slices as well as other *in vitro* models, where neuron-to-neuron spread was directly observed (Ehrengruber et al., 2002; Ludlow et al., 2005; McQuaid et al., 1998; Weingartl et al., 2005).

To investigate the mechanisms of morbillivirus transneuronal spread in more detail, we established an *in vitro* model based on the infection of primary cultures of ferret neurons with a neurovirulent CDV strain. We first determined the proportion of neurons and overall viability of our cultures. Next, we examined the replication efficiency of CDV in neurons, and examined whether CDV dissemination is cell-contact dependent. Finally, directional dissemination of CDV was investigated using a modified Campenot chamber system.

Results

Characterization of primary cultures of ferret neurons

To investigate CDV neuronal transport, we established primary culture of ferret neuron. Towards this, we harvested fetuses from pregnant jills at a gestational age of 39 days. Fetal brains were collected and meninges, cerebella and brain stems were discarded, while cortices and olfactory bulbs were physically and chemically dissociated to yield a single-cell suspension. Following Percoll gradient purification, cells were seeded in tissue culture dishes previously coated with poly-DL-ornithine and natural mouse laminin. Neuronal processes start to develop as early as 24 hours post-plating, and clear neurite outgrowth and the formation of neural connections were observed after three days (Fig. 1A, left panel). These connections increased over time and resulted in the formation of complex neuronal networks by day 7 post-plating (Fig. 1A, right panel).

To assess the overall viability, the cultures were incubated with an ethidium bromide/acridine orange solution at various times post-seeding. Ethidium bromide stains DNA orange but is excluded from live cells, whereas acridine orange is cell-permeable and stains live cells green. To calculate the percentage of viable cells, six fields of view were counted for each time point. Three days after seeding, more than 87% of all cells were alive (Fig. 1B and C), and the viability remained stable for at least 7 days (Fig. 1B and C). Even after 28 days in culture, a large proportion of cells were still viable (Fig. 1B). Among the viable cells, 95% stained positive for the neuronal marker Nissl on days 3 and 7 post-seeding, and the remaining cells were identified as glial cells (Fig. 2A and B). After 14 days, the proportion of glial cells began to increase due to their ability to proliferate (data not shown).

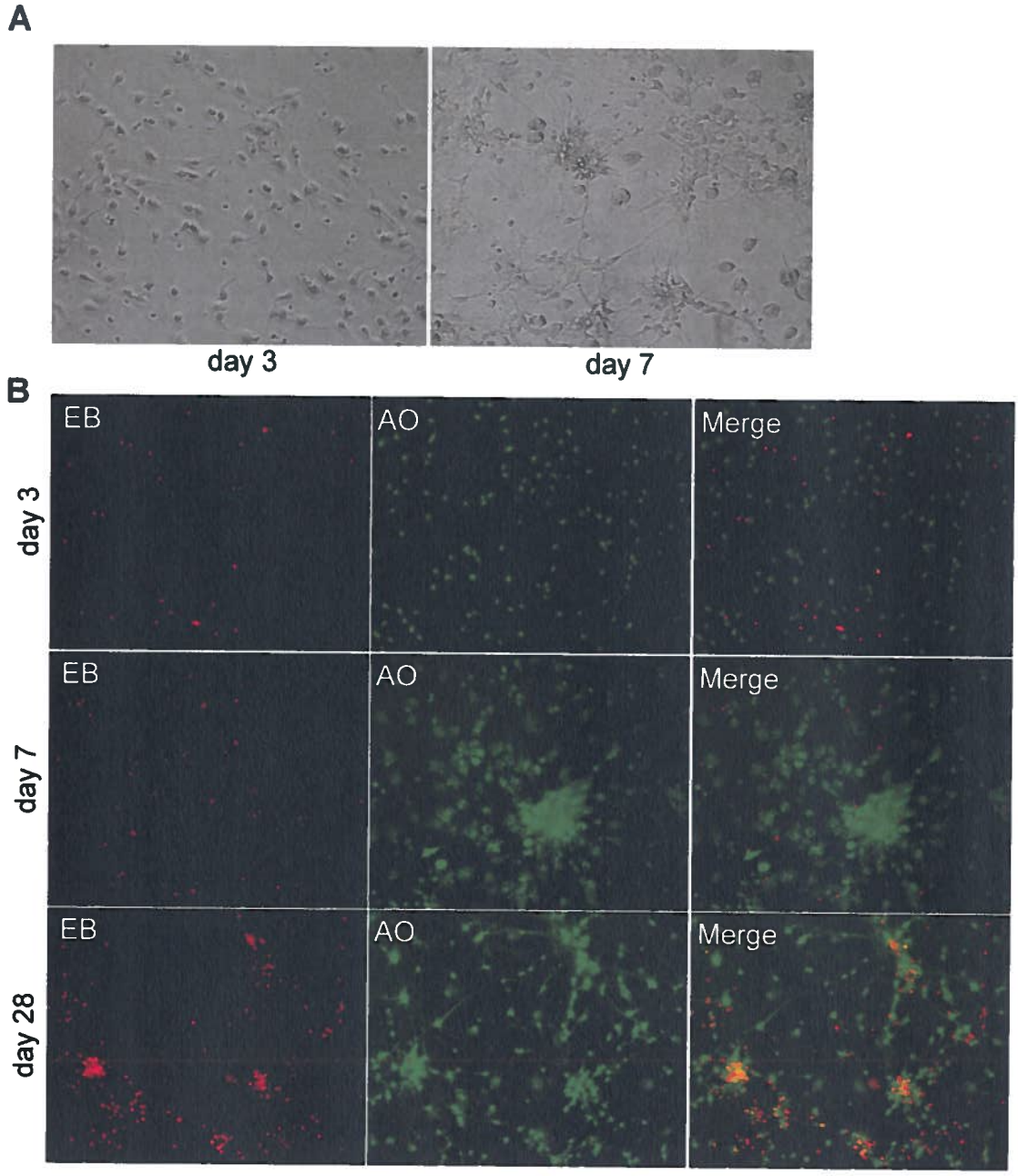
A
day 3
day 7
B
EB
AO
Merge
day 3
day 7
day 28
C
% viability
100
80
60
40
20
0
3
7
days post plating

Fig. 1 Isolation and primary culture of ferret neurons. (A) Phase contrast images of primary cultures of neurons on day 3 (left panel) or 7 (right panel) post-plating. (B) Viability of the cell culture was assessed on day 3 (first row) and 7 (second row) using an ethidium bromide/acridine orange solution. Dead cells are seen in the first column, live cells are seen in the second column and merge images are shown in the last column. All pictures were taken at 200x magnification. (C) Percent viability was quantified by counting ethidium bromide and acridine orange positive cells in six independent fields of view per time point. Error bars represent the standard deviation (SD).

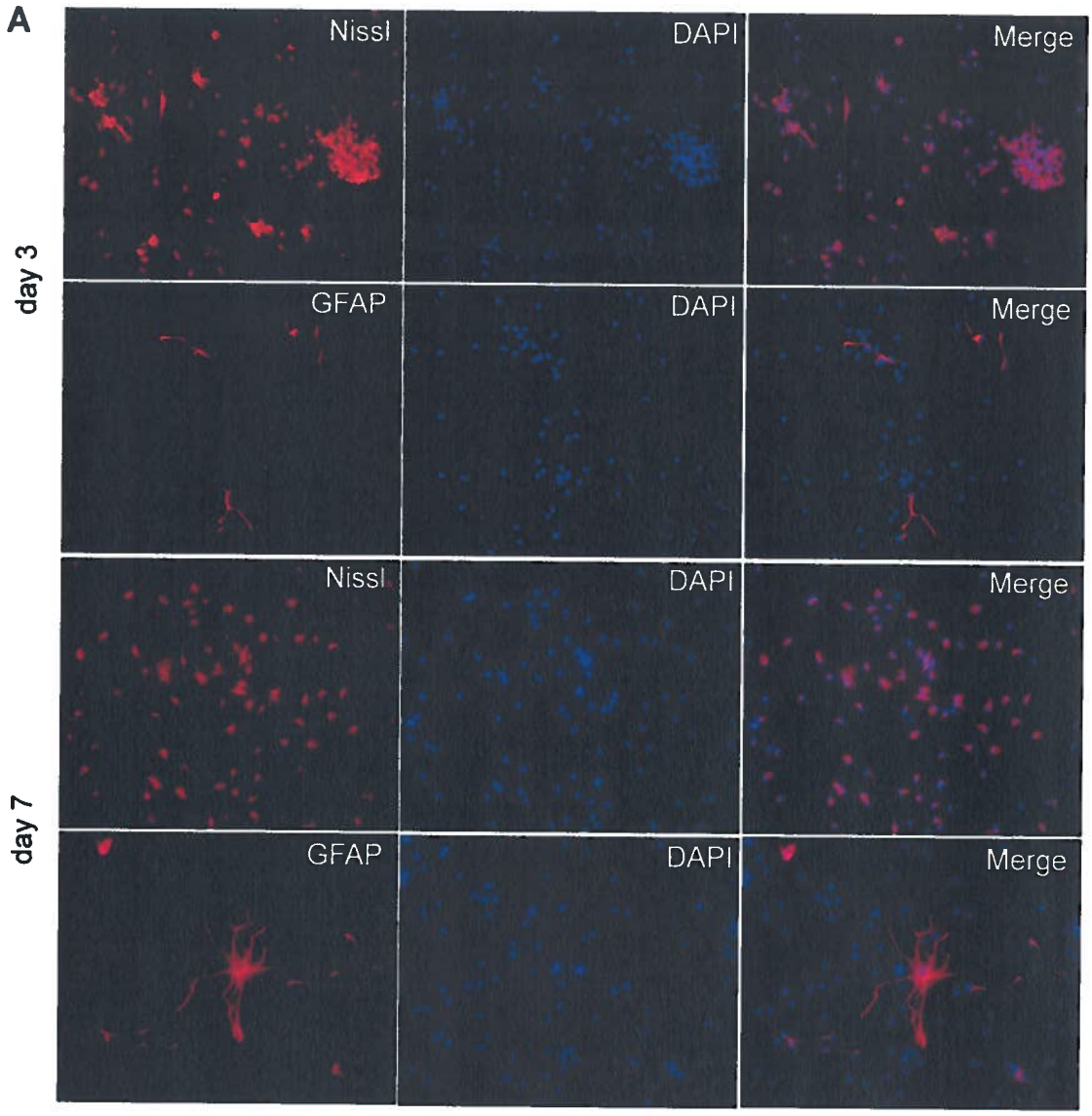
A
Nissl
DAPI
Merge
day 3
GFAP
DAPI
Merge
Nissl
DAPI
Merge
day 7
GFAP
DAPI
Merge

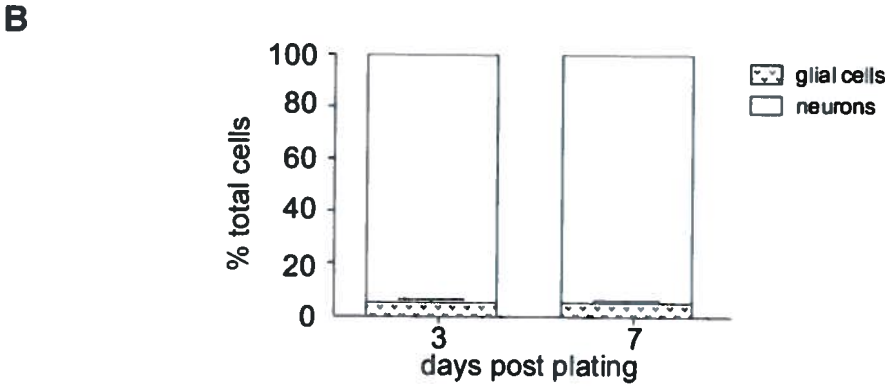
B
100
80
60
40
20
0
% total cells
3
7
days post plating
glial cells
neurons

Fig. 2 Characterization of a primary culture of mixed brain cells. (A) Identification of cell types present in the cultures. Brain cells were grown in Lab-Tek II chamber slides and on days 3 (first two rows) and 7 (bottom two rows) post-plating, cells were fixed with 4% paraformaldehyde (PFA) and stained with of NeuroTrace Fluorescent Nissl 530/615 or with a polyclonal glial fibrillary acidic protein (GFAP) antibody (first column). Cells were counterstained using 4', 6-diamidino-2-phenylindole (DAPI) (second column), washed and mounted using ProLong Gold antifade reagent. Merge images are shown (last column). Pictures were taken at 200x magnification. (B) Quantification of the proportion of the two main cell types present in the primary culture. Nissl- and GFAP-positive cells were counted in six independent fields of view per time point. Error bars represent SD.

CDV causes a productive infection in neuron cultures

To determine the optimal experimental conditions, cultures were infected with the eGFP-expressing CDV strain Snyder Hill (SHeH) with multiplicities of infection (m.o.i.) ranging between 0.1 and 5 at various times post-seeding. Efficient infection was observed as soon as neuronal processes form, starting 24 h after isolation of the cells (data not shown). Cells were infected between 3 and 7 days after isolation for all further studies. Small infected foci were first detected after 2 days (data not shown), and overall infection levels gradually increased until after around 10 days post-infection, when most of the cells were infected (Fig. 3B). Even after 18 days of infection, cell cultures were largely morphologically unaffected (Fig. 3A).

To investigate the efficiency of CDV replication in neurons, kinetics of released and cell-associated virus production were performed. Cell-associated titers in neuron cultures were consistently hundred-fold higher than those of released particles (Fig. 3B), similar to VerodogSLAMtag cells, which express the high affinity receptor SLAM. Even though the growth kinetic in neuron cultures were two times slower than in VerodogSLAMtag cells, similar particle release ratios were observed, demonstrating that the neuron cultures support efficient CDV replication (Fig. 3C).

CDV dissemination is dependent on cell contact

To determine if CDV dissemination in neurons is dependent upon cell-cell contact, images of the same area were taken on days 3, 4 and 8 post-infection and the distribution of eGFP expression was assessed. Spread of eGFP to cells in close proximity to the original focus was observed, indicating that CDV propagates along neuronal processes (Fig. 4A). Analysis of the same region at higher magnification revealed that the only cells that are infected are in direct contact with each other or are part of a neural cell cluster (Fig. 4B).

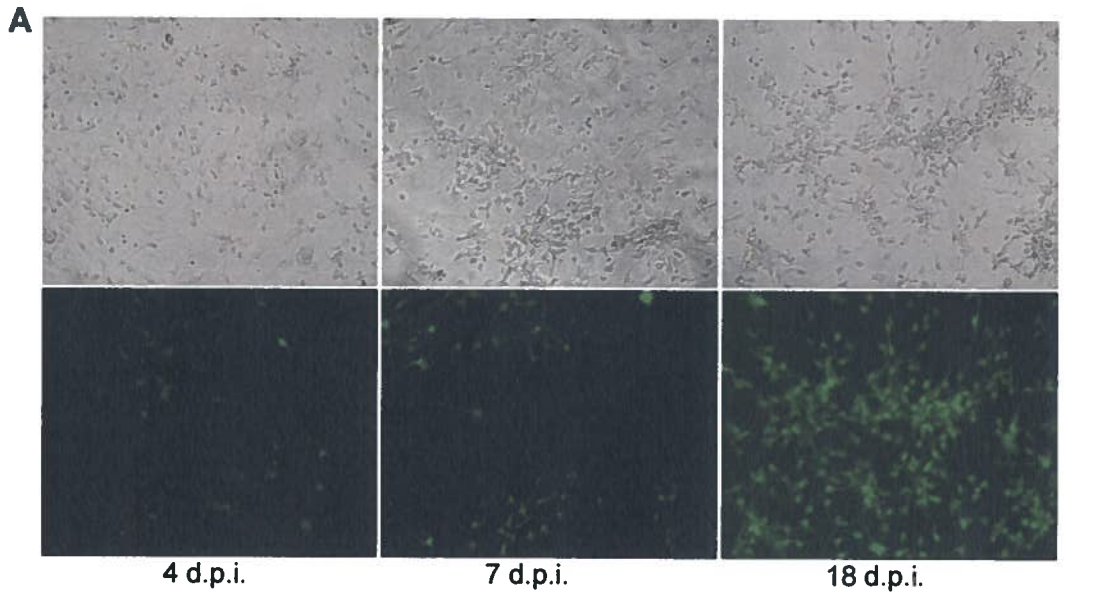
A
4 d.p.i.
7 d.p.i.
18 d.p.i.

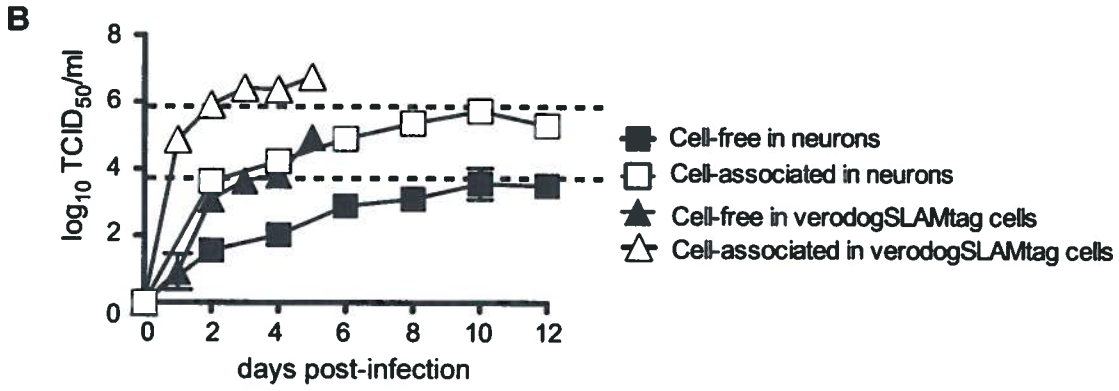
B
log10 TCID50/ml
days post-infection
Cell-free in neurons
Cell-associated in neurons
Cell-free in verodogSLAMtag cells
Cell-associated in verodogSLAMtag cells

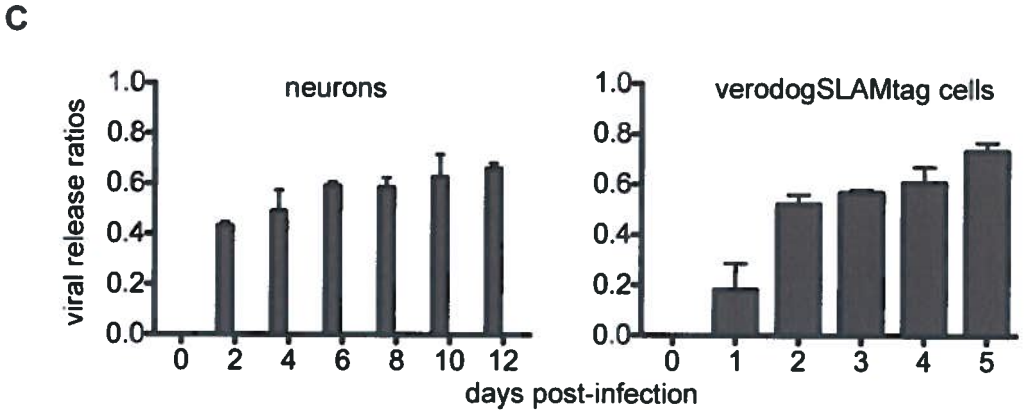
C
neurons
verodogSLAMtag cells
viral release ratios
days post-infection

Fig. 3 Infection efficiency of primary brain cell cultures over the course of CDV infection. (A) Cell cultures were infected at 3 days post-plating with a multiplicity of infection (m.o.i.) of 0.1 of the eGFP-expressing CDV Snyder Hill strain (SHeH). Phase contrast images were taken of a representative field of view (top row) and eGFP expression levels are shown (bottom row) on days 4, 7 and 18 post-infection. Photos were taken at 200x magnification. (B) Multi-step growth curves were performed by infecting cells with SHeH at a m.o.i. of 0.1. Cells and supernatant were harvested every second day for 12 days for neurons, and every day for five days in VerodogSLAMtag cells. Virus titers were determined by limited dilution method and expressed as $TCID_{50}$. Dashed lines represent maximal viral titers obtained in neurons and error bars indicate SD. (C) The ratio of released to cell-associated infectivity was calculated by dividing the titers of cell-free virus found in the supernatant by the titers of cell-associated virus. All titers were determined by limited dilution method after viral kinetics. Each time point represents triplicates and error bars indicate standard deviation. Days post-infection are indicated on the x-axis and ratios of viral release are indicated on the y-axis.

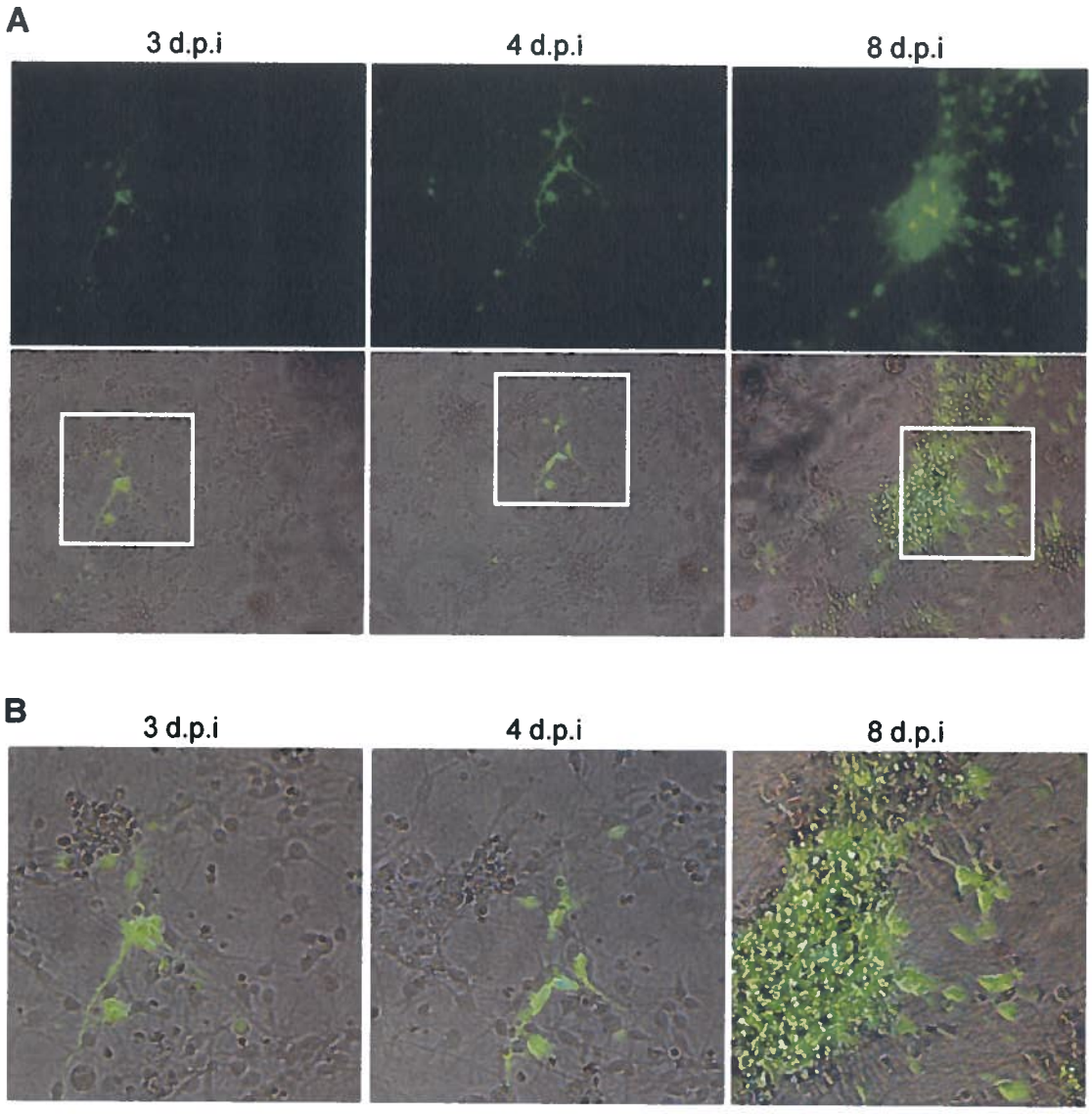

Fig. 4 CDV dissemination is cell-contact dependent. (A) Fluorescent images and fluorescent and phase contrast merged images are shown of the same region of SHeH infected neuron cultures on either day 3 (left), 4 (middle) or 8 (right) post-infection. Newly expressing eGFP neurons are only found within close proximity to previously infected cells or within a neural cluster. Images are shown at 200x magnifications. (B) Magnification of images eGFP expressing regions for days 3, 4 and 8 post-infection.

CDV spreads along neuronal processes in anterograde and retrograde directions

To investigate if CDV disseminates directionally along neuronal processes, a compartmentalized neuronal culture system, similar to the one used to characterize the spread of pseudorabies virus (Ch'ng and Enquist, 2005) was used (Fig. 5). Briefly, tissue culture dishes are etched with a pin rake and coated with poly-DL-ornithine and natural mouse laminin, and a Teflon ring is attached to the dish using silicone grease (Dow Corning). Immediately after assembly, chambers are tested for leakiness, and infected and non-infected VerodogSLAMtag cells were seeded in neighbouring chambers to assure that virus could not transfer between compartments (data not shown).

To determine if CDV can spread retrogradely from VerodogSLAMtag cells to a neuronal cell body via neurites, primary cultures of ferret neurons were seeded in the right compartment. Once neurites were sufficiently developed and had crossed over to the left chamber, infected VerodogSLAMtag cells were added to that chamber and overlaid with methylcellulose. Infected neurons were detected as early as three days later (Fig. 6A). We next examined if CDV can also disseminate anterogradely from infected neurons towards VerodogSLAMtag cells, neurons were seeded in the left compartment and infected once neurites had fully developed and crossed over to the right chamber. VerodogSLAMtag cells were added to the B chamber and overlaid with methylcellulose. Infected VerodogSLAMtag cells were observed 3 days later after widespread infection of neurons (Fig. 6B).

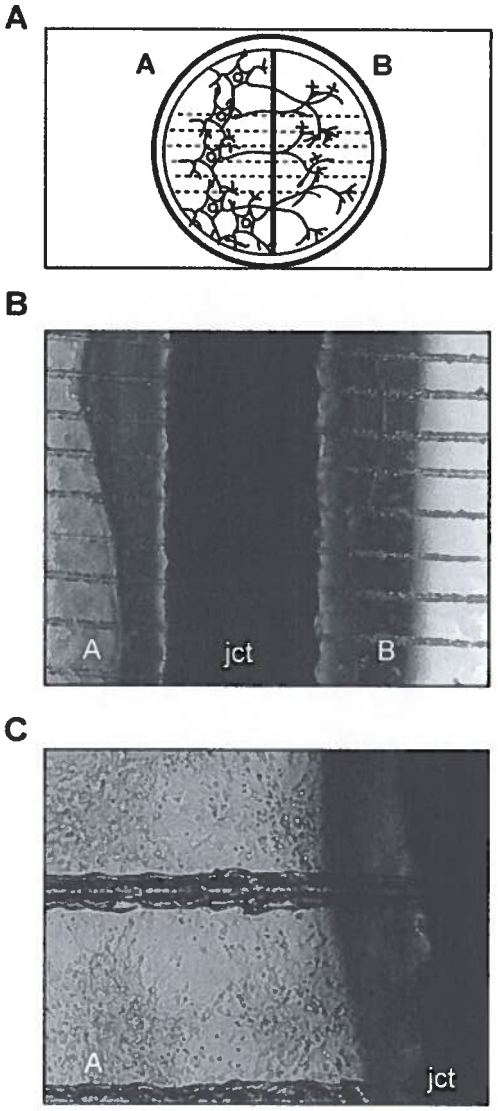

Fig. 5 Modified Campenot chamber system. (A) Diagram representing the chamber system including the etched grooves, Teflon ring, neurons and directional neurite outgrowth towards the adjacent chamber. (B) Phase contrast images of the multi-chamber set-up consisting of the A chamber (left) and the B chamber (right). In the middle area is the junction in the Teflon ring that physically separates the two chambers as well as the silicon grease used to hold the ring to the dish and add an extra barrier. The image shown is at 40x magnification. (C) Photo of the A chamber after primary cultures have been seeded for 12 days and extensive neuronal networks have developed. Picture was taken at a 200x magnification.

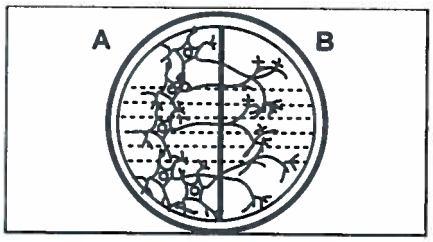
A
B

A


A
B
verodogSLAMtag cell
retrograde

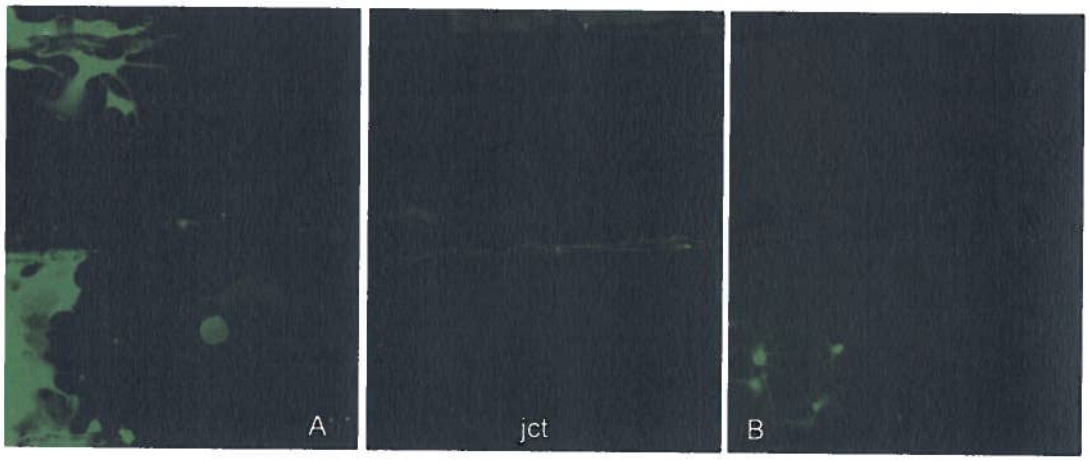
A
jct
B

B


A
B
anterograde
verodogSLAMtag cell

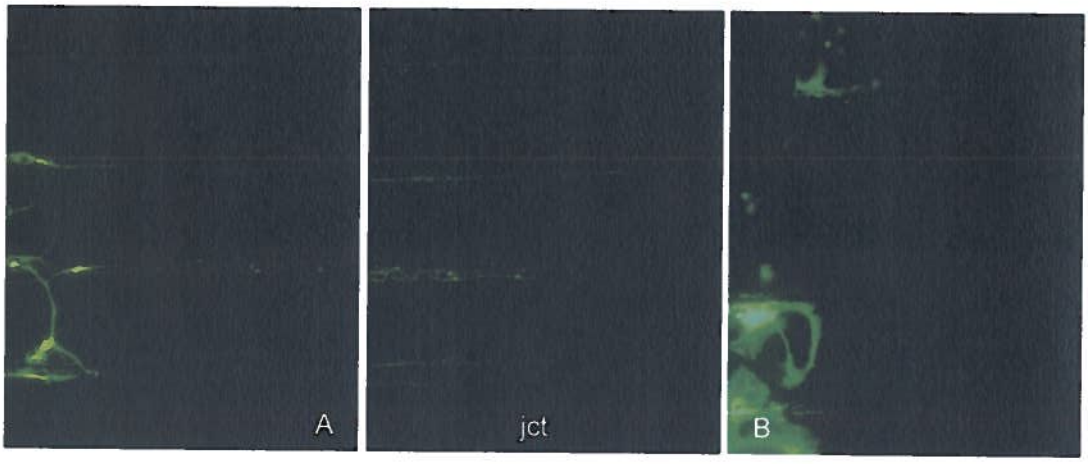
A
jct
B

Fig. 6 Bi-directional spread of CDV in neurons. (A) Chambers were prepared as described in material and methods and retrograde CDV trafficking from SLAM-positive cells to a neuronal cell bodies via neurites was examined. Towards this, primary cultures of ferret neurons were seeded in the B compartment, and once neurites were sufficiently developed and crossed over to the adjacent chamber, around 10 days, VerodogSLAMtag cells were infected with SHeH at an m.o.i. of 1 and seeded in the A chamber. VerodogSLAMtag cells were overlaid with media containing 1% methylcellulose. (B) Anterograde CDV transport was examined by plating neurons in the left compartment. Once neurites had fully developed, cultures were infected with an m.o.i. of 1. VerodogSLAMtag cells were added to the right chamber and overlaid with media containing 1% methylcellulose. Pictures were taken 3 days after seeding of the VerodogSLAMtag cells, and 200x magnifications are shown.

Discussion

Although morbilliviruses are not primarily neurotropic, CNS complications are not uncommon (Appel, 1969; Schneider-Schaulies et al., 2003; Summers et al., 1984). However, the mechanisms involved in morbillivirus dissemination to and within the CNS remain poorly understood. Neuron cultures have long been used to gain insight in molecular and cellular mechanisms involved in CNS diseases. Primary cultures of brain cells are usually produced from embryonic or juvenile animals and are often isolated from cortex, olfactory bulb or spinal cord (Barnett and Roskams, 2008; Hilgenberg and Smith, 2007; Wiese et al.). In a previous study, we reported that CDV CNS invasion occurs via the olfactory signaling route, suggesting that neurons may be responsible for transporting the virus into and within the CNS (Rudd et al., 2006). To investigate if the virus disseminates along neuronal pathways, we established primary cultures of ferret neurons and characterized their susceptibility to infection and viral spread.

Ferret neurons fully support CDV replication

The permissiveness of primary CNS cell cultures to morbillivirus infection is controversial. In MeV-infected neuron cultures from transgenic mice, no virus release was observed (Lawrence et al., 2000; Rall et al., 1997). In contrast, canine astrocyte and microglia cultures supported a productive CDV infection (Vandevelde and Zurbriggen, 2005; Vandevelde et al., 1985), and here we show that CDV replicates efficiently in ferret primary neuron cultures. The observed discrepancy may be due to the fact that mice and rats are not susceptible to morbillivirus infections, and that rodent cell lines generally do not support morbillivirus replication (Niewiesk et al., 1997). The detection of maximum viral titers at a slower kinetic than in a SLAM-expressing cell line, reproduces the dissemination kinetics seen *in vivo*, where SLAM-expressing lymphocytes are infected initially, followed by spread to epithelial cells and subsequently neurons (de Swart et al., 2007; Rudd et al., 2006; von Messling et al., 2004).

CDV Disseminates along neuronal signaling pathways

Consistent with other studies of morbillivirus infection of CNS cells, we found that cell contact is required to allow dissemination within the culture (Ehrengruber et al., 2002; Lawrence et al., 2000; Zurbriggen et al., 1995). In fact, viral spread was limited to cells that appeared to be in direct contact via their processes, and investigations are ongoing to determine whether CDV dissemination involves passage through synapses like it has been suggested for MeV (Allen et al., 1996; Makhortova et al., 2007). In infected neurons, we found that CDV disseminated retro- and anterogradely. This is in agreement with studies of herpes and West Nile virus, which also disseminate efficiently across communicating neurons (Samuel et al., 2007; Smith et al., 2001) and likely applies to most neurotropic viruses. Our findings thus support the morbillivirus macroscopic and histologic observations of morbillivirus dissemination along neuronal signaling pathways (Ehrengruber et al., 2002; Urbanska et al., 1997).

Materials and methods

Cells and virus strains

VerodogSLAMtag cells were maintained in Dulbecco's modified Eagle's medium (DMEM, Invitrogen) with 5% fetal bovine serum (FBS, Invitrogen). The recombinant e-GFP expressing CDV Snyder Hill strain used was (Rudd et al., 2010) propagated in VerodogSLAMtag cells.

Preparation of culture dishes

Culture dishes were coated with 500 µg/mL poly-DL-ornithine (Sigma Aldrich) solution diluted in 0.1 M borate buffer (boric acid, pH 8.3) one day before the experiment. Four to five hours prior to the harvest of the brain, dishes were washed three times with tissue culture grade water (Invitrogen) and 10 µg/mL of natural mouse laminin (Invitrogen) diluted in CMF Saline G buffer (6.1 mM glucose, 5.3 mM KCl, 136.9 mM NaCl, 1.1 mM K_2HPO4, 1.08 mM Na_2PO_4, pH 7.4) was added. Before plating, all dishes were washed twice with CMF Saline G buffer and air-dried.

Primary brain cell cultures

Primary neuron cultures were established from ferret fetuses harvested on gestational day 39. Briefly, c-sections were performed on healthy jills and embryos were collected, rinsed thoroughly in embryo transportation buffer (ETB) (Hank's Buffered Salt Solution (HBSS), 2.5 mM HEPES (Invitrogen), 35 mM glucose (Sigma), 4 mM $NaHCO_3$) and decapitated. Meninges, brain stems, cerebella were discarded and remaining cortices and olfactory bulbs were washed three times with HBSS (Invitrogen). After the final wash, all but 1 mL of buffer was removed. Brains were then cut into very fine pieces and then gently passed through a 40 µm cell strainer (BD Falcon) with a syringe plunger (Falcon). Extra buffer was added to allow remaining cells to be passed through. After one wash with HBSS, cells were digested using digestion solution (HBSS

without Mg2+ or Ca2+ (Invitrogen), 1 mM sodium pyruvate (Invitrogen), 10 mM HEPES, 3% BSA, 1.2 mM $MgSO_4$, 40 µg/mL deoxyribonuclease I (Sigma), 250 µg/mL TPCK-trypsin (Sigma) about 15 min at 37°C in a water bath with continuous shaking. Then neutralization buffer was added (HBSS without Mg2+ or Ca2+, 1 mM sodium pyruvate, 10 mM HEPES, 3% BSA, 0.2 mM $MgSO_4$, 6,8 µg/mL deoxyribonuclease I, 1 mg/mL trypsin inhibitor (Invitrogen)) to stop the reaction by gently inverting the tube for 3 min at room temperature before centrifuging for 5 min at 800 g. Remaining non-digested material was resuspended in 1 mL of HBSS and gently triturated using three different sizes of fire-polished Pasteur pipettes, starting with the larger size. Cells were washed twice, resuspended in 3 mL of HBSS + 0.3% BSA, and underlayed below a Percoll (GE Healthcare) gradient consisting of 100%, 60% and 35% Percoll in HBSS. After centrifugation at 1850 g for 30 min., cells were collected, resuspended in neuron culture medium (neurobasal medium (Invitrogen), 2% B27 supplement (Invitrogen), 0.5 mM Glutamax (Invitrogen), 25 uM glutamic acid (Invitrogen) and plated as needed. The neuron culture medium was replaced every 2 to 3 days. To prevent contamination, all buffers contained 1% penicillin/streptomycin. All experimental protocols related to animal use were approved by the INRS-Institut Armand-Frappier Institutional Animal Care and Use Committee. All pictures of cell cultures were taken using an Eclipse TE2000-U model compound microscope with a DXM1200F digital camera (Nikon).

Cell viability assay

Cell viability was determined by using a solution of 25.36 µM ethidium bromide and 11.3 µM acridine in PBS. Cells were visualized immediately using an Eclipse TE2000-U model compound microscope with a DXM1200F digital camera (Nikon).

Nissl and Glial Fibrillary Acidic Protein (GFAP) staining

Cells were grown in Lab-Tek II chamber slides (Nalge Nunc International). On days 3, 7, 10, 14 and 28 post-plating, cells were washed twice with PBS and fixed with 4% paraformaldehyde for 10 min at room temperature, and permeabilized with 0.1%

Triton X-100 (diluted in PBS) for 10 min on ice. For Nissl staining, protocol followed manufacturer's instructions. Briefly, a 1/300 dilution of NeuroTrace Fluorescent Nissl 530/615 stain (Invitrogen) was added to appropriate chambers and incubated for 1 h. Cells were washed twice with PBS plus 0.1% Triton X-100, twice with PBS and a final 2 h wash. Cells were counterstained with 4', 6-diamidino-2-phenylindole (DAPI), and mounted using ProLong Gold antifade reagent (Invitrogen). For GFAP staining, non-specific background was eliminated by blocking slides for 60 min using normal horse serum (Invitrogen). Next, a α-GFAPrabbit antiserum (DAKO) was added and incubated for 1 h at RT, followed by 1 h incubation with the appropriate Alexa Fluor 568-conjugated secondary antibody (Invitrogen). Cells were counterstained with DAPI and mounted using ProLong Gold antifade reagent.

Viral kinetics

Multi-step growth curves were performed by infecting either VerodogSLAMtag cells or primary cultures of mixed brain cells with a m.o.i. of 0.1 of SHeH and incubating them at 32°C. Cells and supernatant were harvested daily for five days or every second day for 12 days, and the virus titers were determined by limited dilution method and expressed as 50% tissue culture infection doses ($TCID_{50}$).

Chamber culture system

The chamber system was adapted from (Ch'ng and Enquist, 2005). Briefly, all Teflon rings were purchased from Tyler Research (Alberta, Canada) and were sterilized prior to use. 35 mm tissue culture dishes were coated as described above. We used a silicone grease (Dow Corning) loaded syringe attached to a p200 truncated tip to apply a thin, continuous strip of silicone grease over the entire bottom surface of the Teflon ring. A 50 μl drop of neuron medium (neurobasal medium, 2% B27 supplement, 0.5 mM Glutamax, and 1% penicillin/streptomycin, containing 1% methylcellulose (serum free) was placed in the center of each tissue culture dish covering the etched grooves. This step prevented the seal from being entirely devoid of moisture, which is needed for axon

penetration. Finally, the silicone grease-coated ring was gently seated on the tissue culture dish such that the etched grooves spanned all compartments, forming a watertight seal between each side. Neuron medium was then placed in both compartments immediately after chambers were assembled and tested for leakiness.

Acknowledgements

We are thankful to all laboratory members for continuing support and valuable discussions, and to Chantal Thibault for technical assistance. This work was supported by the Canadian Institutes of Health Research (grant MOP-66989) and the Canadian Foundation for Innovation (grant 9488) to V.v.M., and a studentship from the Armand-Frappier Foundation to P.A.R.

References

1. Allen, I.V., McQuaid, S., McMahon, J., Kirk, J., and McConnell, R. (1996). The significance of measles virus antigen and genome distribution in the CNS in SSPE for mechanisms of viral spread and demyelination. J Neuropathol Exp Neurol *55*, 471-480.

2. Appel, M.J. (1969). Pathogenesis of canine distemper. Am J Vet Res *30*, 1167-1182.

3. Appel, M.J., and Summers, B.A. (1995). Pathogenicity of morbilliviruses for terrestrial carnivores. Vet Microbiol *44*, 187-191.

4. Barnett, S.C., and Roskams, A.J. (2008). Olfactory ensheathing cells: isolation and culture from the neonatal olfactory bulb. Methods Mol Biol *438*, 85-94.

5. Bonami, F., Rudd, P.A., and von Messling, V. (2007). Disease duration determines canine distemper virus neurovirulence. J Virol *81*, 12066-12070.

6. Card, J.P., Rinaman, L., Lynn, R.B., Lee, B.H., Meade, R.P., Miselis, R.R., and Enquist, L.W. (1993). Pseudorabies virus infection of the rat central nervous system: ultrastructural characterization of viral replication, transport, and pathogenesis. J Neurosci *13*, 2515-2539.

7. Ch'ng, T.H., and Enquist, L.W. (2005). Neuron-to-cell spread of pseudorabies virus in a compartmented neuronal culture system. J Virol *79*, 10875-10889.

8. de Swart, R.L., Ludlow, M., de Witte, L., Yanagi, Y., van Amerongen, G., McQuaid, S., Yuksel, S., Geijtenbeek, T.B., Duprex, W.P., and Osterhaus, A.D. (2007). Predominant infection of CD150+ lymphocytes and dendritic cells during measles virus infection of macaques. PLoS Pathog *3*, e178.

9. Diamond, M.S. (2009). Virus and host determinants of West Nile virus pathogenesis. PLoS Pathog *5*, e1000452.

10. Ehrengruber, M.U., Ehler, E., Billeter, M.A., and Naim, H.Y. (2002). Measles virus spreads in rat hippocampal neurons by cell-to-cell contact and in a polarized fashion. J Virol *76*, 5720-5728.

11. Finke, S., and Conzelmann, K.K. (2005). Replication strategies of rabies virus. Virus Res *111*, 120-131.

12. Grose, C. (2004). The puzzling picture of acute necrotizing encephalopathy after influenza A and B virus infection in young children. Pediatr Infect Dis J *23*, 253-254.

13. Hilgenberg, L.G., and Smith, M.A. (2007). Preparation of dissociated mouse cortical neuron cultures. J Vis Exp, 562.

14. Ivey, N.S., MacLean, A.G., and Lackner, A.A. (2009). Acquired immunodeficiency syndrome and the blood-brain barrier. J Neurovirol *15*, 111-122.

15. Johnson, R.T. (1987). The pathogenesis of acute viral encephalitis and postinfectious encephalomyelitis. J Infect Dis *155*, 359-364.

16. Lawrence, D.M., Patterson, C.E., Gales, T.L., D'Orazio, J.L., Vaughn, M.M., and Rall, G.F. (2000). Measles virus spread between neurons requires cell contact but not CD46 expression, syncytium formation, or extracellular virus production. J Virol *74*, 1908-1918.

17. Ludlow, M., McQuaid, S., Cosby, S.L., Cattaneo, R., Rima, B.K., and Duprex, W.P. (2005). Measles virus superinfection immunity and receptor redistribution in persistently infected NT2 cells. J Gen Virol *86*, 2291-2303.

18. Makhortova, N.R., Askovich, P., Patterson, C.E., Gechman, L.A., Gerard, N.P., and Rall, G.F. (2007). Neurokinin-1 enables measles virus trans-synaptic spread in neurons. Virology *362*, 235-244.

19. McQuaid, S., Campbell, S., Wallace, I.J., Kirk, J., and Cosby, S.L. (1998). Measles virus infection and replication in undifferentiated and differentiated human neuronal cells in culture. J Virol *72*, 5245-5250.

20. Mettenleiter, T.C. (2003). Pathogenesis of neurotropic herpesviruses: role of viral glycoproteins in neuroinvasion and transneuronal spread. Virus Res *92*, 197-206.

21. Niewiesk, S., Schneider-Schaulies, J., Ohnimus, H., Jassoy, C., Schneider-Schaulies, S., Diamond, L., Logan, J.S., and ter Meulen, V. (1997). CD46 expression does not overcome the intracellular block of measles virus replication in transgenic rats. J Virol *71*, 7969-7973.

22. Rall, G.F., Manchester, M., Daniels, L.R., Callahan, E.M., Belman, A.R., and Oldstone, M.B. (1997). A transgenic mouse model for measles virus infection of the brain. Proc Natl Acad Sci U S A *94*, 4659-4663.

23. Rudd, P.A., Bastien-Hamel, L.E., and von Messling, V. (2010). Acute canine distemper encephalitis is associated with rapid neuronal loss and local immune activation. J Gen Virol *91*, 980-989.

24. Rudd, P.A., Cattaneo, R., and von Messling, V. (2006). Canine distemper virus uses both the anterograde and the hematogenous pathway for neuroinvasion. J Virol *80*, 9361-9370.

25. Samuel, M.A., Wang, H., Siddharthan, V., Morrey, J.D., and Diamond, M.S. (2007). Axonal transport mediates West Nile virus entry into the central nervous system and induces acute flaccid paralysis. Proc Natl Acad Sci U S A *104*, 17140-17145.

26. Schneider-Schaulies, J., Meulen, V., and Schneider-Schaulies, S. (2003). Measles infection of the central nervous system. J Neurovirol *9*, 247-252.

27. Smith, G.A., Gross, S.P., and Enquist, L.W. (2001). Herpesviruses use bidirectional fast-axonal transport to spread in sensory neurons. Proc Natl Acad Sci U S A *98*, 3466-3470.

28. Summers, B.A., and Appel, M.J. (1994). Aspects of canine distemper virus and measles virus encephalomyelitis. Neuropathol Appl Neurobiol *20*, 525-534.

29. Summers, B.A., Greisen, H.A., and Appel, M.J. (1984). Canine distemper encephalomyelitis: variation with virus strain. J Comp Pathol *94*, 65-75.

30. Urbanska, E.M., Chambers, B.J., Ljunggren, H.G., Norrby, E., and Kristensson, K. (1997). Spread of measles virus through axonal pathways into limbic structures in the brain of TAP1 -/- mice. J Med Virol *52*, 362-369.

31. Vandevelde, M., and Zurbriggen, A. (2005). Demyelination in canine distemper virus infection: a review. Acta Neuropathol *109*, 56-68.

32. Vandevelde, M., Zurbriggen, A., Dumas, M., and Palmer, D. (1985). Canine distemper virus does not infect oligodendrocytes in vitro. J Neurol Sci *69*, 133-137.

33. von Messling, V., Milosevic, D., and Cattaneo, R. (2004). Tropism illuminated: lymphocyte-based pathways blazed by lethal morbillivirus through the host immune system. Proc Natl Acad Sci U S A *101*, 14216-14221.

34. Weingartl, H., Czub, S., Copps, J., Berhane, Y., Middleton, D., Marszal, P., Gren, J., Smith, G., Ganske, S., Manning, L., *et al.* (2005). Invasion of the central nervous system in a porcine host by nipah virus. J Virol *79*, 7528-7534.

35. Wiese, S., Herrmann, T., Drepper, C., Jablonka, S., Funk, N., Klausmeyer, A., Rogers, M.L., Rush, R., and Sendtner, M. Isolation and enrichment of embryonic mouse motoneurons from the lumbar spinal cord of individual mouse embryos. Nat Protoc *5*, 31-38.

36. Zurbriggen, A., Graber, H.U., Wagner, A., and Vandevelde, M. (1995). Canine distemper virus persistence in the nervous system is associated with noncytolytic selective virus spread. J Virol *69*, 1678-1686.

CHAPTER 3

DISCUSSION

1. Overview

The work accomplished during my thesis has contributed to the general understanding of morbillivirus CNS invasion and pathogenesis. Using canine distemper virus in ferrets as a model system, I demonstrated that morbilliviruses and perhaps also other neurotropic paramyxoviruses can enter the CNS by two separate pathways: the hematogenous and the olfactory route. I also showed, in collaboration with François Bonami, that disease duration is an important factor for neurovirulence. We demonstrated that prolonged infection is required for CDV to reach and damage the CNS regardless of the route of inoculation. I then showed that in the context of acute encephalitis, CNS damage is mediated by a two-step process: first, CDV directly infects neurons and causes substantial neuronal loss, which in turn activates local immune responses such as gliosis, microglia activation and production of pro-inflammatory cytokines. If the infected individual does not succumb to the disease during the acute phase, this local immune activation may contribute to the cell death and demyelination observed in late onset CNS complications. My findings thus support the hypothesis that there is a dynamic interplay between viral infection and host response. The neurotropic potential of all morbilliviruses is likely similar, however the overall host response will determine not only the final disease outcome but also the onset and extent of encephalopathy. My most recent work provides strong evidence that once the virus has reached the CNS it travels efficiently along communicating neurons in a bi-directional manner. This ability is common among neurotropic viruses and allows a swift and efficient dissemination throughout the CNS, thereby contributing to pathogenesis while possibly evading the immune system.

2. CNS Entry: Lessons Learned from CDV

Olfactory neurons are the only type of neurons able to regenerate from basal cells after being damaged. Each cell can serve as a receptor and acts as a first-order neuron since their axon projects directly from the nasal cavity into the brain without an intervening synapse (Kocsis et al., 2009). Olfactory neurons have direct exposure to the external environment, and many neurotropic viruses have been shown to access the brain via the olfactory route (Table 1). It is not surprising that many viruses associated with dissemination along the olfactory pathway also cause respiratory infections. In fact, viral upper respiratory infections are one of the most common causes for hyposmia or anosmia (Doty, 2009). The nasal cavity thus represents a natural portal of entry for these viruses, and prolonged contact and on-site replication likely facilitate olfactory neuron infection.

We found that CDV uses two routes of entry into the CNS: the previously described hematogenous route (Rima et al., 1991) and the olfactory route via olfactory nerves (Rudd et al., 2006). Since CDV infection in ferrets reproduces the key aspects of morbillivirus infections in other hosts, we speculate that our finding may apply to all morbilliviruses and could perhaps even represent a general paramyxovirus neuroinvasion mechanism.

Following our publication reporting CDV CNS entry via the olfactory signaling pathway, Techangamsuwan *et al.* investigated the ability of CDV to infect olfactory ensheathing cells (OECs) and determined their response to infection. OECs surround bundles of olfactory nerves and are found between olfactory mucosa and bulb, and are important for axonal guidance and may have immunoregulatory or antigen-presenting roles (Doucette, 1990; Wewetzer et al., 2005). They observed that primary cultures of canine OECs and Schwann cells were susceptible to CDV infection, and that the extent of infection was strain-dependent (Techangamsuwan et al., 2009). These data thus support our finding that the olfactory pathway plays an important role in CDV neuroinvasion.

Furthermore, Nipah virus, a member of the paramyxovirus family, causes a primarily respiratory illness and widespread infection of the respiratory tract in pigs (Middleton et al., 2002). Consequently, virus is found within the nasal cavity where it replicates following natural infection. Intranasal inoculation of Nipah virus in pigs resulted in the detection of viral antigen in several cranial nerves, particularly the olfactory nerve and in the olfactory bulb shortly after exposure, demonstrating once again the importance of the olfactory pathway for CNS infection (Weingartl et al., 2005). In addition, entry via the olfactory bulb has also been demonstrated for Sendai and La Piedad Michoacan virus, which are also members of the *Paramyxoviridae* family that cause massive respiratory epithelial infection (Allan et al., 1996; Mori et al., 1995). In the case of other neurotropic paramyxoviruses such as phocine distemper virus, dolphin and porpoise morbillivirus, and Newcastle disease virus, the route of CNS invasion has not been investigated in detail (Brown et al., 1999; Griot et al., 2003), but our findings suggest that the possibility of entry via the olfactory bulb should be considered in future studies.

Virus	Species	Method of Application	Receptor Cell Incorporation	Transneuronal Transport
Adeno (recombinant)	Rat	Intranasal	Yes	Yes
Aujeszky's disease (peudorabies)	Pig	Intranasal	Yes	Yes
Borna disease	Rat	Intranasal	Yes	Yes
Bovine herpes	Goat	Intranasal	Yes	Unknown
Canine distemper	Ferret	Intranasal	Yes	Yes
Ectromelia	Mouse	Intranasal	Yes	Yes
Equine herpes	Pig	Intranasal	Yes	Yes
Hepatitis	Mouse	Intranasal	Yes	Yes
Herpes simplex	Rat	Intranasal	Yes	Yes
	Mouse	Corneal	Yes	Yes
	Mouse	Facial skin	Yes	Limited
Influenza A	Mouse	Intranasal	Yes	Yes
Poliomyelitis	Primate	Intranasal	Yes	Yes
Rabies	Mouse	Intranasal	Yes	Yes
St. Louis encephalitis	Hamster	Intraperitoneal	Yes	Yes
Sendai	Mouse	Intranasal	Yes	Limited
Semliki forest	Mouse	Intranasal	Yes	Age dependent
Venezuelan equine encephalitis virus	Mouse	Subcutaneous	Yes	Yes
Vesicular stomatitis virus	Mouse	Intranasal	Yes	Yes

Table 1. Viruses capable of infecting the olfactory pathway. Examples of viruses known to infect olfactory receptor cells from the nasal cavity and, in some cases, to transmit transneuronally to other brain regions (Modified from Doty, 2008).

3. Importance of Virus-Host Interactions

3.1 Acute and Chronic Encephalitis

The uninfected CNS lacks immunological activity. Endothelial cells express low levels of adhesion molecules, which promote interaction with circulating leukocytes, and microglia cells are maintained in a quiescent state through interactions with healthy neurons. Furthermore, the presence of neurotrophins reduces MHC II expression on microglia cells (Neumann et al., 1998). The production of TGF-β by neurons and astrocytes also contributes to maintaining an immunologically inert environment by suppressing the activation of endothelial and other cells (Johnson et al., 1992). Once the CNS becomes infected, swift changes occur to protect resident cells. Among the first events observed is the induction of type I interferon, which is important for host survival. It has been shown that mice lacking the IFN α/β receptor are more likely to succumb to CNS disease when infected with neurotropic viruses like Sindbis or Theiler's murine encephalomyelitis virus (Byrnes et al., 2000; Ryman et al., 2000). In contrast, rapid production of type I interferons after CNS infection is associated with reduction in virus spread and replication before activating the adaptive immune response (Griffin, 2003).

In response to damage or stress, neurons secrete multiple factors, which have not all been identified but include IFN-β, IFN-γ, IL-6, fractalkine (CX3CL1) and secondary lymphoid tissue chemokine (CCL21) (Harrison et al., 1998; Neumann et al., 1997; Rappert et al., 2002). Macrophages and glial cells express the CX3CL1 receptor and thus become activated very early during neuronal infection. They in turn produce a number of proinflammatory cytokines and chemokines including IL-1, IL-6, IL-12, TNF-α, MIP-1β, monocyte chemoattractant protein 1 (MCP1), MCP3, RANTES and IP-10 (Griffin, 2003). The production of these factors generally leads to an up-regulation of MHC molecules, which affects local homeostasis (Fig. 5).

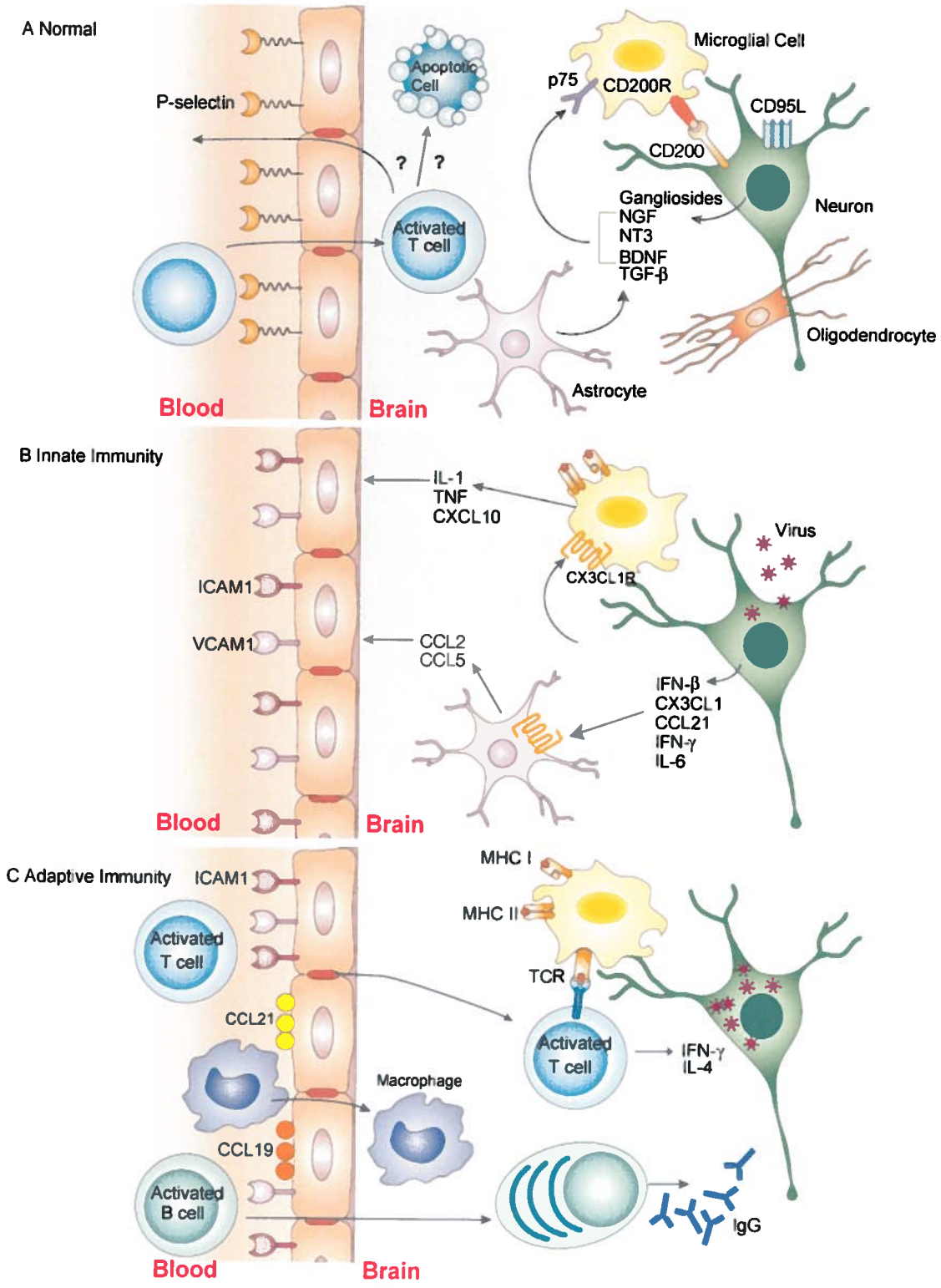
A Normal
P-selectin
Apoptotic Cell
?
?
Activated T cell
Blood
Brain
Microglial Cell
p75
CD200R
CD95L
CD200
Gangliosides
NGF
NT3
BDNF
TGF-β
Neuron
Oligodendrocyte
Astrocyte
B Innate Immunity
IL-1
TNF
CXCL10
ICAM1
VCAM1
CCL2
CCL5
CX3CL1R
Virus
IFN-β
CX3CL1
CCL21
IFN-γ
IL-6
Blood
Brain
C Adaptive Immunity
ICAM1
MHC I
MHC II
TCR
Activated T cell
CCL21
Macrophage
IFN-γ
IL-4
CCL19
Activated B cell
IgG
Blood
Brain

Fig. 5 Immune Responses in the CNS. (A) In the uninfected CNS, endothelial cells express few adhesion molecules. Neurons maintain microglia in a quiescent state through CD200–CD200 receptor (CD200R) interactions and astrocytes produce neurotrophins, such as brain-derived neurotrophic factor (BDNF), nerve-growth factor (NGF) and neurotrophin 3 (NT3), that interact with p75, a low-affinity neurotrophin receptor. Gangliosides are abundant and TGF-β is constitutively produced by neurons and astrocytes. Activated T cells enter the CNS routinely through interaction with low levels of P-selectin expressed by endothelial cells, but leave or die soon thereafter. (B) Virus infection of neurons initiates the early production of IFN-β chemokines and pro-inflammatory cytokines, which results in further activation of microglia and increased expression of adhesion molecules, such as vascular-cell adhesion molecule 1 (VCAM1) and intercellular adhesion molecule 1 (ICAM1), by endothelial cells. (C) By three to four days after infection, inflammatory cells — such as natural killer (NK) cells, macrophages and lymphocytes — that are activated in secondary lymphoid tissue begin to enter the CNS at regions where virus replication is occurring and chemokines, such as CCL19 and CCL21, are expressed by endothelial cells. T cells produce additional cytokines, such as IL-4 and IFN-γ, and the B cells produce antibody, which initiates clearance of virus from infected cells (Adapted from Griffin, 2003).

In my second objective and publication, we further investigated the kinetics of CDV neuroinvasion and determined the presence and extent of local immune activation during the acute stage of infection. Very little is known about CNS immune responses during acute CDV encephalitis and it is not clear whether during early disease stages, lesions are directly caused by the virus and therefore degenerative in nature, or if they are immune-mediated. Some reports demonstrate cell damage and loss due to viral infection while others observed up-regulation of MHC II, activation of microglial cells, and induction of pro-inflammatory cytokines and chemokines, suggesting a role for immune-mediated damage in acute CDV encephalitis (Alldinger et al., 1996; Krakowka et al., 1980; Tipold et al., 1999; Zurbriggen et al., 1998).

Our results showed that despite a systemic immunosuppression, local immune activation in resident CNS cells was triggered (Rudd et al., 2010). Furthermore, we determined that CNS damage occurs as a two-step process. First, CDV infects many regions throughout the CNS including the olfactory bulb, brain stem, hippocampus and cerebellum, leading to direct damage of neurons and subsequent neuronal loss, which correlated with the clinical signs observed. We then detected activation of microglial cells, induction of gliosis and production of cytokines IL-6, IFN-β and TNF-α in response to the infection. These pro-inflammatory cytokines are able to instigate immune-mediated damage, however, likely because of the systemic immunosuppression, we did not observe infiltration of circulating T and B cells. We hypothesize that in a sub-lethal scenario, where the ferrets do not die from the acute infection, the observed activation of the local immune response sets the stage for immune-induced pathology associated with chronic CDV encephalopathies (Alldinger et al., 1996; Beineke et al., 2009; Grone et al., 1998).

All chronic or late-onset morbillivirus CNS complications are attributed to immunopathological complications. In MIBE, glial cell proliferation and varying degrees of perivascular inflammation are seen. In SSPE cases, brain biopsies or postmortem histopathological analysis show the presence of astrogliosis, neuronal loss, degeneration of dendrites, demyelination and infiltration of inflammatory cells (Garg, 2002). Also, SSPE patients have high antibody titers in both serum and CSF. These antibodies

recognize structural proteins like F, H and N, and are almost ten times higher in SSPE patients than in those recovering from the acute stage (Norrby and Kristensson, 1997; Sips et al., 2007) suggesting that the immune response contributes to the pathology observed. Furthermore, demyelination, which occurs after the acute stage, is frequently associated with increased expression of pro-inflammatory cytokines in the blood and CSF of dogs with natural CDV infection (Frisk et al., 1999; Grone et al., 1998), and in chronic distemper encephalitis strong MHC II up-regulation is observed in regions of demyelination that are devoid of CDV antigen strengthening the idea that pathological changes at this time are immune-mediated (Alldinger et al., 1996).

We also observed that disease duration plays an important role in the development and extent of CNS disease (Bonami et al., 2007). By using chimeric viruses, we evaluated the contribution of the H protein in neurological manifestation and disease duration. Towards this, we used two strains of CDV: 5804P, which is lethal within 2 weeks due to sepsis and multi-organ failure without neurological signs of disease (von Messling et al., 2004) and A75/17, which is lethal between 3 and 5 weeks, and causes classical distemper-associated neurological signs, including chewing gum seizures and head pressing (Rudd et al., 2006; Summers et al., 1984). Our results demonstrated that even though 5804P does not cause neurological signs, the virus retains neuroinvasive potential, suggesting that time is a key factor for CNS pathogenesis. Another important factor is the presence of residual immune response. We observed that inhibition of lymphocyte proliferation upon PHA stimulation was less pronounced in animals that survived for longer periods of time (Bonami et al., 2007; Rudd et al., 2006). This residual immune response could be responsible for maintaining a delicate balance between the virus and the host response, thereby delaying death and enabling neuroinvasion.

3.2 CNS Invasion is a Consequence of a Virus-Host Response Imbalance

Taken together, our findings strengthened the idea that morbillivirus CNS disease occurs due to an imbalance of virus-host response interactions, and that both virus and local immune responses are important for its pathogenesis. It is thus highly probable that the timing and quality of the host immune response dictates whether or not morbilliviruses will induce extensive CNS disease. For MeV, it is well established that individuals with impaired immunity are more likely to develop giant cell pneumonia or MIBE and have a greater risk of succumbing to the infection (Markowitz et al., 1988; Mustafa et al., 1993; Rand et al., 1976; Siegel et al., 1977). It was also shown that natural MeV infection in human immunodeficiency virus (HIV)-infected children leads to a prolonged illness and virus detection in PBMCs, nasopharyngeal swabs and in urine as compared to non-HIV- infected children (Permar et al., 2001), suggesting that the impaired immune response results in slower clearance, and can increase the chances of developing CNS complications.

For CDV, strain variations and kinetics of antiviral immune responses have been shown to be associated to disease outcome (Summers et al., 1984). In experimental infections, dogs that have the most prompt and specific antiviral humoral and immune responses recovered completely, while widespread infection and neuroinvasion was observed in animals that could not mount an effective immune response (Tsai et al., 1982). Consistent with this, we do not observe CNS involvement in ferrets inoculated with non-lethal viruses, while all lethal strains are detected in the brain at the end stages of infection. In summary, our results suggest a limited number of possible outcomes following morbillivirus infections: in the absence of an efficient immune response, the host develops a severe disease that leads death before the onset of CNS complications (Bonami et al., 2007). In the presence of a residual but insufficient immune response, the duration of the disease is prolonged, and neurological complications are observed before the animal succumbs to the acute disease (Rudd et al., 2006). We speculate that CNS persistence occurs if the host's immune response is sufficient to control the infection in the periphery after the virus has gained access to the CNS. As long as an equilibrium

between the immune system and the virus is maintained, the immune-mediated pathology is postponed. However, if this balance is disrupted, the host will develop progressive neurologic disease, ultimately leading to death. Finally, the rapid control and elimination of the systemic infection before neuroinvasion as seen in most MeV infections (Moss and Griffin, 2006) effectively prevents neurologic involvement.

4. CDV Transneuronal Spread: A Strategy to Evade Immune Response?

Previously, we demonstrated that CDV can enter the CNS by using the olfactory signaling route (Rudd et al., 2006). However, the mechanisms involved in transneuronal spread within the CNS are still poorly understood. My third manuscript, which is still in preparation aimed at further investigating how CDV disseminates along communicating neurons. Towards this, I established an *in vitro* model of infection using primary cultures of ferret neurons. Our model reproduced many aspects of a neurotropic *in vivo* infection including a general permissiveness of neurons to CDV infection, but slower replication compared to SLAM-expressing cells. We also observed that cell-cell contact is necessary for CDV dissemination. This is consistent with other studies reporting that cell contact is required for morbillivirus dissemination in neurons (Ehrengruber et al., 2002; Lawrence et al., 2000; Zurbriggen et al., 1995). In addition, we observed that infection of neuronal cells *in vitro* does not lead to immediate cell death. Even 18 days post-infection with a wild-type strain, neuron cultures do not appear morphologically affected. Based on a recent report that CDV-infected immune cells are protected from apoptosis (Pillet and von Messling, 2009), the prolonged survival of infected neurons may be due to similar mechanisms. It is possible that after an acute infection, equilibrium is attained between the persistent infection and the local immune response. This persistence could allow the time needed for viruses to accumulate mutations seen in SSPE and MIBE (Cattaneo et al., 1988), and would also explain why chronic infections like SSPE and MIBE appear years after the primary infection. At that time, the equilibrium may be disrupted and onset of immune-mediated damage is initiated, ultimately resulting in death.

5. Perspectives and Future Direction

5.1 Understanding the Contribution of the Olfactory Pathway to CNS Infection

Several viruses such as herpes virus, rabies virus and mouse hepatitis virus, are capable of entering the CNS via the olfactory pathway and spread transneuronally to other regions of the brain. In our first publication, we showed that in addition to the well characterized hematogenous spread, CDV is also able to disseminate along the olfactory pathway to the olfactory glomeruli, where the virus then spreads further into the CNS via the synapses that form between the olfactory neurons and the mitral cells. Although our findings are very interesting, it would be compelling to evaluated the exact contribution of the olfactory pathway to CNS infection and neuropathology. Towards this, we could perform an ablation of the olfactory bulb on ferrets prior to intranasal inoculation. This technique has been successfully used on mice in order to evaluate the relative importance of the olfactory nerve for mouse hepatitis virus infection (Barnett and Perlman, 1993). Furthermore, successful removal of the vomeronasal organ or olfactory bulbs have also been performed on rats, Siberian hamsters *(Phodopus sungorus)*, opossoms *(Monodelphis domestica)* and even ferrets (Kiyokawa et al., 2007; Prendergast et al., 2009; Woodley et al., 2004; Zuri and Halpern, 2005).

5.2 Other Potential Portals into the CNS

When we inoculated groups of ferrets either intranasally or intraperitoneally we observed that the course of the disease and timing of CNS neuroinvasion were identical in both groups (Rudd et al., 2010). As stated in our publication, SLAM-expressing cells are likely equally available in the upper respiratory tract and the peritoneal cavity. Once the infection has been established, it is also possible that the virus has similar ability to infect different cranial nerves. CDV could thus reach the CNS not only through the olfactory nerve (cranial nerve 1) but also via the vagus nerve (cranial nerve 10). Infection of the vagus nerve would explain the nausea and vomiting observed in most animals, since it is responsible for the gag reflex. The direct infection of cranial nerves has been primarily studied in herpes simplex virus (HSV). HSV was detected in vagal sensory ganglia of mice after oral and esophageal inoculation (Gesser et al., 1994). The authors suggested that the virus directly entered nerve endings during the mucosal infection stage and then traveled by axonal transport to the proximal ganglia. In addition, CNS invasion was observed in mice intranasally infected with a mouse-adapted influenza strain via the vagus nerve (Matsuda et al., 2004). Considering the timing of neuroinvasion observed in our study, a similar mechanism could apply to CDV. We know from previous work that infection of neurons occurs after infection of lymphocytes and epithelial cells (Rudd et al., 2006; von Messling et al., 2004). However, further experiments are necessary to validate this hypothesis. One such experiment could be to histologically examine these nerves as well as dorsal root ganglia for the presence of virus using cryo- or paraffin sections of animals that succumbed to CDV infection.

5.3 Deciphering Innate and Adaptive Immune Responses

It will also be interesting to determine which cells in the CNS are producing the cytokines involved in the innate and adaptive immune responses to morbillivirus infections. This would provide additional information about the interactions and roles of resident CNS cells and how they contribute to immune-mediated pathogenesis. Laser

capture-microdissection (LCM) followed by single-cell RT-PCR or immunocytochemical staining (immuno-LCM) on tissues obtained from CDV infected ferrets may be the most appropriate approach. Laser capture microdissection provides precise extraction of cell groups down to the single cell level from tissue sections and single-cell RT-PCR is the most sensitive technique for the determination of gene expression. Combined, these techniques become a powerful tool to investigate complex disease processes. Moreover, this technique has already used to investigate gene expression in neurons, astrocytes and oligodendrocytes (Baskin and Bastian; Ordway et al., 2009; Wang et al., 2004), as well as for the study of intrathecal disease-relevant antibodies in plasma cells from SSPE brains (Burgoon et al., 2005).

5.4 Microtubules: The Superhighways for CDV Dissemination?

Interaction with microtubules and microtubule motor proteins may be used by morbilliviruses to disseminate within the CNS. Microtubules run along the length of the axon and provide the main cytoskeletal tracks for transportation (Fig. 6). The motor proteins myosin, kinesin and dynein are responsible for relocating all cellular components within neurons (Kardon and Vale, 2009). Myosins are a superfamily of motor proteins that move along actin filaments while kinesin and dynein move proteins in the anterograde and retrograde directions along microtubules (Hirokawa et al., 2009; Karki and Holzbaur, 1999). Viruses that associate with microtubules and anterograde motors such as kinesin-1 during viral egress include vaccinia virus and African swine fever virus (Jouvenet et al., 2004; Rietdorf et al., 2001). Furthermore, cytoskeletal proteins have been shown to be important for MeV replication. Actin is packaged in MeV virions, and it is thought that MeV nucleocapsids are transported along actin filaments to reach the cell surface where MeV budding takes place (Bohn et al., 1986). Microtubules have also been shown to play a role in the production of infectious virus since maturation of virions was inhibited upon microtubule disruption (Berghall et al., 2004).

Despite our finding that CDV spreads promiscuously along neurons, the specific mode of virion transport in the neuronal cell body remains unclear. It is conceivable that CDV uses the microtubule network for bi-directional spread, however, further studies are required to confirm this hypothesis. Towards this, the localization of microtubules and CDV in primary ferret neuron cultures could be examined, using an eGFP-expressing virus and an anti-α-tubulin antibody or a monoclonal antibody against microtubule associated protein-1 (MAP-1) shown to be efficient in several cell types including porcine brain cells, HeLa, PtK2, mouse melanoma cell and chinese hamster ovary cells (Sato et al., 1983). We could also disrupt polymerization of microtubules using pharmacological agents such as colchicine or nocodazole and determine their effect on CDV dissemination along neurons.

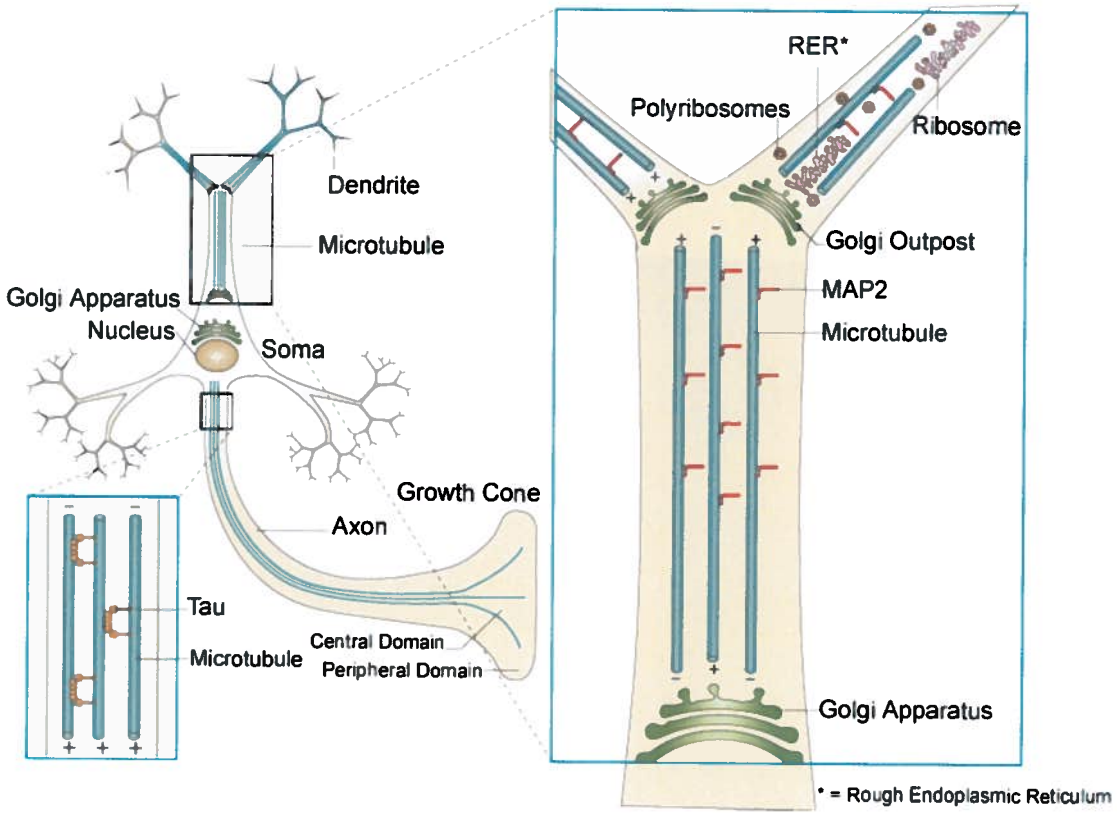

Fig. 6 Microtubule organization in neurons. Axons have tau-bound microtubules of uniform orientation, whereas dendrites have MAP2-bound microtubules of mixed orientation. Dendrites also contain organelles that are not found in axons, such as rough endoplasmic reticulum, polyribosomes and Golgi outposts (Modified from Conde and Caceres, 2009).

6. CONCLUSION

The work accomplished during my doctorate studies validates the ferret as a model to study morbillivirus neurovirulence. My work also contributes to the overall understanding of the timing of events, local immune response, and viral transneuronal spread that occurs during acute encephalitis. I demonstrate that CDV-induced CNS disease in ferrets is a phenomenon that occurs at late disease stages after the virus has spread to lymphatic and epithelial tissues. I also show that disease duration plays an important role in viral and immune-mediated pathogenesis: when the immune system is able to rapidly control virus spread, CNS involvement is not observed; however, when an animal is unable to overcome the virus-induced immunosuppression, CDV enters the CNS and infects a broad range of CNS cells including neurons and astrocytes. This causes substantial neuronal loss in highly infected areas, and induces local immune responses such as gliosis and the secretion of pro-inflammatory cytokines. The extreme sensitivity of ferrets to CDV infection impedes immune mediated damage, since the animals succumb too quickly to the infection. However, the observed activation of local immune responses during the acute stage could explain how aberrant inflammatory responses seen in chronic CNS encephalopathies are triggered. Finally, I established an *in vitro* model of infection using primary cultures of ferret neurons. Using this model, we show that CDV spreads non-directionally along communicating neurons and confirm that cell-cell contact is required for efficient transneuronal dissemination. Although its development is still very recent, this system will be useful to examine the mechanisms involved in morbillivirus transneuronal spread in more detail. Taken together my work leads to a better understanding of the events involved in morbillivirus CNS infection and may eventually contribute to new treatment strategies to limit CNS sequelae or even to prevent CNS invasion.

REFERENCES

Abraham, G., Rhodes, D.P., and Banerjee, A.K. (1975). The 5' terminal structure of the methylated mRNA synthesized in vitro by vesicular stomatitis virus. Cell *5*, 51-58.

Albrecht, P., Burnstein, T., Klutch, M.J., Hicks, H.T., and Ennis, F.A. (1977). Subacute sclerosing panencephalitis: experimental infection in primates. Science *195*, 64-66.

Albrecht, P., Lorenz, D., Klutch, M.J., Vickers, J.H., and Ennis, F.A. (1980). Fatal measles infection in marmosets pathogenesis and prophylaxis. Infect Immun *27*, 969-978.

Allan, G.M., McNeilly, F., Walker, I., Linne, T., Moreno-Lopez, J., Hernandez, P., Kennedy, S., Carroll, B.P., Herron, B., Foster, J.C., *et al.* (1996). A sequential study of experimental porcine paramyxovirus (LPMV) infection of pigs: immunostaining of cryostat sections and virus isolation. J Vet Diagn Invest *8*, 405-413.

Alldinger, S., Wunschmann, A., Baumgartner, W., Voss, C., and Kremmer, E. (1996). Up-regulation of major histocompatibility complex class II antigen expression in the central nervous system of dogs with spontaneous canine distemper virus encephalitis. Acta Neuropathol *92*, 273-280.

Appel, M.J. (1969). Pathogenesis of canine distemper. Am J Vet Res *30*, 1167-1182.

Appel, M.J., Shek, W.R., and Summers, B.A. (1982). Lymphocyte-mediated immune cytotoxicity in dogs infected with virulent canine distemper virus. Infect Immun *37*, 592-600.

Appel, M.J., Yates, R.A., Foley, G.L., Bernstein, J.J., Santinelli, S., Spelman, L.H., Miller, L.D., Arp, L.H., Anderson, M., Barr, M., *et al.* (1994). Canine distemper epizootic in lions, tigers, and leopards in North America. J Vet Diagn Invest *6*, 277-288.

Arneborn, P., and Biberfeld, G. (1983). T-lymphocyte subpopulations in relation to immunosuppression in measles and varicella. Infect Immun *39*, 29-37.

Axthelm, M.K., and Krakowka, S. (1998). Experimental old dog encephalitis (ODE) in a gnotobiotic dog. Vet Pathol *35*, 527-534.

Ayata, M., Hirano, A., and Wong, T.C. (1989). Structural defect linked to nonrandom mutations in the matrix gene of biken strain subacute sclerosing panencephalitis virus defined by cDNA cloning and expression of chimeric genes. J Virol *63*, 1162-1173.

Ayata, M., Shingai, M., Ning, X., Matsumoto, M., Seya, T., Otani, S., Seto, T., Ohgimoto, S., and Ogura, H. (2007). Effect of the alterations in the fusion protein of measles virus isolated from brains of patients with subacute sclerosing panencephalitis on syncytium formation. Virus Res *130*, 260-268.

Bankamp, B., Horikami, S.M., Thompson, P.D., Huber, M., Billeter, M., and Moyer, S.A. (1996). Domains of the measles virus N protein required for binding to P protein and self-assembly. Virology *216*, 272-277.

Barnett, E.M., and Perlman, S. (1993). The olfactory nerve and not the trigeminal nerve is the major site of CNS entry for mouse hepatitis virus, strain JHM. Virology *194*, 185-191.

Bartz, R., Firsching, R., Rima, B., ter Meulen, V., and Schneider-Schaulies, J. (1998). Differential receptor usage by measles virus strains. J Gen Virol *79 (Pt 5)*, 1015-1025.

Baskin, D.G., and Bastian, L.S. Immuno-laser capture microdissection of rat brain neurons for real time quantitative PCR. Methods Mol Biol *588*, 219-230.

Beineke, A., Puff, C., Seehusen, F., and Baumgartner, W. (2009). Pathogenesis and immunopathology of systemic and nervous canine distemper. Vet Immunol Immunopathol *127*, 1-18.

Baumgartner, W., Orvell, C., and Reinacher, M. (1989). Naturally occurring canine distemper virus encephalitis: distribution and expression of viral polypeptides in nervous tissues. Acta Neuropathol *78*, 504-512.

Bellini, W.J., Englund, G., Richardson, C.D., Rozenblatt, S., and Lazzarini, R.A. (1986). Matrix genes of measles virus and canine distemper virus: cloning, nucleotide sequences, and deduced amino acid sequences. J Virol *58*, 408-416.

Berghall, H., Wallen, C., Hyypia, T., and Vainionpaa, R. (2004). Role of cytoskeleton components in measles virus replication. Arch Virol *149*, 891-901.

Billeter, M.A., Cattaneo, R., Spielhofer, P., Kaelin, K., Huber, M., Schmid, A., Baczko, K., and ter Meulen, V. (1994). Generation and properties of measles virus mutations typically associated with subacute sclerosing panencephalitis. Ann N Y Acad Sci *724*, 367-377.

Bitnun, A., Shannon, P., Durward, A., Rota, P.A., Bellini, W.J., Graham, C., Wang, E., Ford-Jones, E.L., Cox, P., Becker, L., *et al.* (1999). Measles inclusion-body encephalitis caused by the vaccine strain of measles virus. Clin Infect Dis *29*, 855-861.

Blakemore, W.F., Summers, B.A., and Appel, M.G. (1989). Evidence of oligodendrocyte infection and degeneration in canine distemper encephalomyelitis. Acta Neuropathol *77*, 550-553.

Bohn, W., Rutter, G., Hohenberg, H., Mannweiler, K., and Nobis, P. (1986). Involvement of actin filaments in budding of measles virus: studies on cytoskeletons of infected cells. Virology *149*, 91-106.

Bollo, E., Zurbriggen, A., Vandevelde, M., and Fankhauser, R. (1986). Canine distemper virus clearance in chronic inflammatory demyelination. Acta Neuropathol *72*, 69-73.

Bonami, F., Rudd, P.A., and von Messling, V. (2007). Disease duration determines canine distemper virus neurovirulence. J Virol *81*, 12066-12070.

Borrow, P., and Oldstone, M.B. (1995). Measles virus-mononuclear cell interactions. Curr Top Microbiol Immunol *191*, 85-100.

Botteron, C., Zurbriggen, A., Griot, C., and Vandevelde, M. (1992). Canine distemper virus-immune complexes induce bystander degeneration of oligodendrocytes. Acta Neuropathol *83*, 402-407.

Bourhis, J.M., Canard, B., and Longhi, S. (2006). Structural disorder within the replicative complex of measles virus: functional implications. Virology *344*, 94-110.

Bourhis, J.M. and Longhi, S. (2007). Measles virus Nucleoprotein (Hauppauge, NY, Nova science publishers), 163p.

Brown, C., King, D.J., and Seal, B.S. (1999). Pathogenesis of Newcastle disease in chickens experimentally infected with viruses of different virulence. Vet Pathol *36*, 125-132.

Brown, H.R., Thormar, H., Barshatzky, M., and Wisniewski, H.M. (1985). Localization of measles virus antigens in subacute sclerosing panencephalitis in ferrets. Lab Anim Sci *35*, 233-237.

Buechi, M., and Bachi, T. (1982). Microscopy of internal structures of Sendai virus associated with the cytoplasmic surface of host membranes. Virology *120*, 349-359.

Bundza, A., Afshar, A., Dukes, T.W., Myers, D.J., Dulac, G.C., and Becker, S.A. (1988). Experimental peste des petits ruminants (goat plague) in goats and sheep. Can J Vet Res *52*, 46-52.

Burgoon, M.P., Keays, K.M., Owens, G.P., Ritchie, A.M., Rai, P.R., Cool, C.D., and Gilden, D.H. (2005). Laser-capture microdissection of plasma cells from subacute sclerosing panencephalitis brain reveals intrathecal disease-relevant antibodies. Proc Natl Acad Sci U S A *102*, 7245-7250.

Burnet, F.M. (1968). Measles as an index of immunological function. Lancet *2*, 610-613.

Byrnes, A.P., Durbin, J.E., and Griffin, D.E. (2000). Control of Sindbis virus infection by antibody in interferon-deficient mice. J Virol *74*, 3905-3908.

Caignard, G., Guerbois, M., Labernardiere, J.L., Jacob, Y., Jones, L.M., Wild, F., Tangy, F., and Vidalain, P.O. (2007). Measles virus V protein blocks Jak1-mediated phosphorylation of STAT1 to escape IFN-alpha/beta signaling. Virology *368*, 351-362.

Carré, H. (1905). Sur la maladie des jeunes chiens. Comptes rendus hebdomadaires des séances de l'Académie des sciences *140*, 2.

Cathomen, T., Mrkic, B., Spehner, D., Drillien, R., Naef, R., Pavlovic, J., Aguzzi, A., Billeter, M.A., and Cattaneo, R. (1998a). A matrix-less measles virus is infectious and elicits extensive cell fusion: consequences for propagation in the brain. EMBO J *17*, 3899-3908.

Cathomen, T., Naim, H.Y., and Cattaneo, R. (1998b). Measles viruses with altered envelope protein cytoplasmic tails gain cell fusion competence. J Virol *72*, 1224-1234.

Cattaneo, R., Kaelin, K., Baczko, K., and Billeter, M.A. (1989a). Measles virus editing provides an additional cysteine-rich protein. Cell *56*, 759-764.

Cattaneo, R., Schmid, A., Eschle, D., Baczko, K., ter Meulen, V., and Billeter, M.A. (1988). Biased hypermutation and other genetic changes in defective measles viruses in human brain infections. Cell *55*, 255-265.

Cattaneo, R., Schmid, A., Rebmann, G., Baczko, K., Ter Meulen, V., Bellini, W.J., Rozenblatt, S., and Billeter, M.A. (1986). Accumulated measles virus mutations in a case of subacute sclerosing panencephalitis: interrupted matrix protein reading frame and transcription alteration. Virology *154*, 97-107.

Cattaneo, R., Schmid, A., Spielhofer, P., Kaelin, K., Baczko, K., ter Meulen, V., Pardowitz, J., Flanagan, S., Rima, B.K., Udem, S.A., *et al.* (1989b). Mutated and hypermutated genes of persistent measles viruses which caused lethal human brain diseases. Virology *173*, 415-425.

Cattet, M.R., Duignan, P.J., House, C.A., and Aubin, D.J. (2004). Antibodies to canine distemper and phocine distemper viruses in polar bears from the Canadian arctic. J Wildl Dis *40*, 338-342.

Cevik, B., Holmes, D.E., Vrotsos, E., Feller, J.A., Smallwood, S., and Moyer, S.A. (2004). The phosphoprotein (P) and L binding sites reside in the N-terminus of the L subunit of the measles virus RNA polymerase. Virology *327*, 297-306.

Ch'ng, T.H., and Enquist, L.W. (2006). An in vitro system to study trans-neuronal spread of pseudorabies virus infection. Vet Microbiol *113*, 193-197.

Chernoff, A.E., Granowitz, E.V., Shapiro, L., Vannier, E., Lonnemann, G., Angel, J.B., Kennedy, J.S., Rabson, A.R., Wolff, S.M., and Dinarello, C.A. (1995). A randomized, controlled trial of IL-10 in humans. Inhibition of inflammatory cytokine production and immune responses. J Immunol *154*, 5492-5499.

Chinchar, V.G., and Portner, A. (1981). Functions of Sendai virus nucleocapsid polypeptides: enzymatic activities in nucleocapsids following cleavage of polypeptide P by Staphylococcus aureus protease V8. Virology *109*, 59-71.

Clemens, J.D., Stanton, B.F., Chakraborty, J., Chowdhury, S., Rao, M.R., Ali, M., Zimicki, S., and Wojtyniak, B. (1988). Measles vaccination and childhood mortality in rural Bangladesh. Am J Epidemiol *128*, 1330-1339.

Cocks, B.G., Chang, C.C., Carballido, J.M., Yssel, H., de Vries, J.E., and Aversa, G. (1995). A novel receptor involved in T-cell activation. Nature *376*, 260-263.

Colf, L.A., Juo, Z.S., and Garcia, K.C. (2007). Structure of the measles virus hemagglutinin. Nat Struct Mol Biol *14*, 1227-1228.

Conde, C., and Caceres, A. (2009). Microtubule assembly, organization and dynamics in axons and dendrites. Nat Rev Neurosci *10*, 319-332.

Connolly, J.H., Allen, I.V., Hurwitz, L.J., and Millar, J.H. (1967). Measles-virus antibody and antigen in subacute sclerosing panencephalitis. Lancet *1*, 542-544.

Cosby, S.L., Duprex, W.P., Hamill, L.A., Ludlow, M., and McQuaid, S. (2002). Approaches in the understanding of morbillivirus neurovirulence. J Neurovirol *8 Suppl 2*, 85-90.

Curran, J., Marq, J.B., and Kolakofsky, D. (1995). An N-terminal domain of the Sendai paramyxovirus P protein acts as a chaperone for the NP protein during the nascent chain assembly step of genome replication. J Virol *69*, 849-855.

de Waal Malefyt, R., Abrams, J., Bennett, B., Figdor, C.G., and de Vries, J.E. (1991). Interleukin 10(IL-10) inhibits cytokine synthesis by human monocytes: an autoregulatory role of IL-10 produced by monocytes. J Exp Med *174*, 1209-1220.

DeSwart, R.L. (2009). Measles studies in the macaque model. Curr Top Microbiol Immunol *330*, 55-72.

Devaux, P., and Cattaneo, R. (2004). Measles virus phosphoprotein gene products: conformational flexibility of the P/V protein amino-terminal domain and C protein infectivity factor function. J Virol *78*, 11632-11640.

Di Guardo, G., Marruchella, G., Agrimi, U., and Kennedy, S. (2005). Morbillivirus infections in aquatic mammals: a brief overview. J Vet Med A Physiol Pathol Clin Med *52*, 88-93.

Diaz, T., Nunez, J.C., Rullan, J.V., Markowitz, L.E., Barker, N.D., and Horan, J. (1992). Risk factors associated with severe measles in Puerto Rico. Pediatr Infect Dis J *11*, 836-840.

Didcock, L., Young, D.F., Goodbourn, S., and Randall, R.E. (1999). Sendai virus and simian virus 5 block activation of interferon-responsive genes: importance for virus pathogenesis. J Virol *73*, 3125-3133.

Domingo, M., Ferrer, L., Pumarola, M., Marco, A., Plana, J., Kennedy, S., McAliskey, M., and Rima, B.K. (1990). Morbillivirus in dolphins. Nature *348*, 21.

Dorig, R.E., Marcil, A., Chopra, A., and Richardson, C.D. (1993). The human CD46 molecule is a receptor for measles virus (Edmonston strain). Cell *75*, 295-305.

Doty, R.L. (2008). The olfactory vector hypothesis of neurodegenerative disease: is it viable? Ann Neurol *63*, 7-15.

Doty, R.L. (2009). The olfactory system and its disorders. Semin Neurol *29*, 74-81.

Doucette, R. (1990). Glial influences on axonal growth in the primary olfactory system. Glia *3*, 433-449.

Duprex, W.P., Collins, F.M., and Rima, B.K. (2002). Modulating the function of the measles virus RNA-dependent RNA polymerase by insertion of green fluorescent protein into the open reading frame. J Virol *76*, 7322-7328.

Ehrengruber, M.U., Ehler, E., Billeter, M.A., and Naim, H.Y. (2002). Measles virus spreads in rat hippocampal neurons by cell-to-cell contact and in a polarized fashion. J Virol *76*, 5720-5728.

Erlenhoefer, C., Wurzer, W.J., Loffler, S., Schneider-Schaulies, S., ter Meulen, V., and Schneider-Schaulies, J. (2001). CD150 (SLAM) is a receptor for measles virus but is not involved in viral contact-mediated proliferation inhibition. J Virol *75*, 4499-4505.

Fauquet, C. (2005). Virus taxonomy: classification and nomenclature of viruses : eighth report, 2nd edn (London, Elsevier/Academic Press).

Freeman, A.F., Jacobsohn, D.A., Shulman, S.T., Bellini, W.J., Jaggi, P., de Leon, G., Keating, G.F., Kim, F., Pachman, L.M., Kletzel, M., *et al.* (2004). A new complication of stem cell transplantation: measles inclusion body encephalitis. Pediatrics *114*, e657-660.

Frisk, A.L., Baumgartner, W., and Grone, A. (1999). Dominating interleukin-10 mRNA expression induction in cerebrospinal fluid cells of dogs with natural canine distemper virus induced demyelinating and non-demyelinating CNS lesions. J Neuroimmunol *97*, 102-109.

Galbraith, S.E., McQuaid, S., Hamill, L., Pullen, L., Barrett, T., and Cosby, S.L. (2002). Rinderpest and peste des petits ruminants viruses exhibit neurovirulence in mice. J Neurovirol *8*, 45-52.

Garg, R.K. (2002). Subacute sclerosing panencephalitis. Postgrad Med J *78*, 63-70.

Garoff, H., Hewson, R., and Opstelten, D.J. (1998). Virus maturation by budding. Microbiol Mol Biol Rev *62*, 1171-1190.

Gendelman, H.E., Wolinsky, J.S., Johnson, R.T., Pressman, N.J., Pezeshkpour, G.H., and Boisset, G.F. (1984). Measles encephalomyelitis: lack of evidence of viral invasion of the central nervous system and quantitative study of the nature of demyelination. Ann Neurol *15*, 353-360.

Gesser, R.M., Valyi-Nagy, T., Altschuler, S.M., and Fraser, N.W. (1994). Oral-oesophageal inoculation of mice with herpes simplex virus type 1 causes latent infection of the vagal sensory ganglia (nodose ganglia). J Gen Virol *75 (Pt 9)*, 2379-2386.

Gopas, J., Itzhaky, D., Segev, Y., Salzberg, S., Trink, B., Isakov, N., and Rager-Zisman, B. (1992). Persistent measles virus infection enhances major histocompatibility complex class I expression and immunogenicity of murine neuroblastoma cells. Cancer Immunol Immunother *34*, 313-320.

Greber, U.F., and Way, M. (2006). A superhighway to virus infection. Cell *124*, 741-754.

Griffin, D.E. (2001a). Measles virus. In Fields Virology, D.M. Knipe, Howley, P.M., ed. (Philidelphia, Lippincott Williams and Wilkins), pp. 1401-1441.

Griffin, D.E. (2001b). Measles virus. In Fields Virology, H. D. M. Knipe, P.M., ed. (Philidelphia, Lippincott Williams and Wilkins), pp. 1401-1441.

Griffin, D.E. (2003). Immune responses to RNA-virus infections of the CNS. Nat Rev Immunol *3*, 493-502.

Griffin, D.E., Johnson, R.T., Tamashiro, V.G., Moench, T.R., Jauregui, E., Lindo de Soriano, I., and Vaisberg, A. (1987). In vitro studies of the role of monocytes in the immunosuppression associated with natural measles virus infections. Clin Immunol Immunopathol *45*, 375-383.

Griffin, D.E., and Ward, B.J. (1993). Differential CD4 T cell activation in measles. J Infect Dis *168*, 275-281.

Griot, C., Vandevelde, M., Schobesberger, M., and Zurbriggen, A. (2003). Canine distemper, a re-emerging morbillivirus with complex neuropathogenic mechanisms. Anim Health Res Rev *4*, 1-10.

Griot-Wenk, M., Griot, C., Pfister, H., and Vandevelde, M. (1991). Antibody-dependent cellular cytotoxicity in antimyelin antibody-induced oligodendrocyte damage in vitro. J Neuroimmunol *33*, 145-155.

Grone, A., Frisk, A.L., and Baumgartner, W. (1998). Cytokine mRNA expression in whole blood samples from dogs with natural canine distemper virus infection. Vet Immunol Immunopathol *65*, 11-27.

Hall, W.W., and Choppin, P.W. (1979). Evidence for lack of synthesis of the M polypeptide of measles virus in brain cells in subacute sclerosing panencephalitis. Virology *99*, 443-447.

Hall, W.W., Lamb, R.A., and Choppin, P.W. (1979). Measles and subacute sclerosing panencephalitis virus proteins: lack of antibodies to the M protein in patients with subacute sclerosing panencephalitis. Proc Natl Acad Sci U S A *76*, 2047-2051.

Hall, W.W., Lamb, R.A., and Choppin, P.W. (1980). The polypeptides of canine distemper virus: synthesis in infected cells and relatedness to the polypeptides of other morbilliviruses. Virology *100*, 433-449.

Harrison, J.K., Jiang, Y., Chen, S., Xia, Y., Maciejewski, D., McNamara, R.K., Streit, W.J., Salafranca, M.N., Adhikari, S., Thompson, D.A., *et al.* (1998). Role for neuronally derived fractalkine in mediating interactions between neurons and CX3CR1-expressing microglia. Proc Natl Acad Sci U S A *95*, 10896-10901.

Hashiguchi, T., Kajikawa, M., Maita, N., Takeda, M., Kuroki, K., Sasaki, K., Kohda, D., Yanagi, Y., and Maenaka, K. (2007). Crystal structure of measles virus hemagglutinin provides insight into effective vaccines. Proc Natl Acad Sci U S A *104*, 19535-19540.

Hashimoto, K., Ono, N., Tatsuo, H., Minagawa, H., Takeda, M., Takeuchi, K., and Yanagi, Y. (2002). SLAM (CD150)-independent measles virus entry as revealed by recombinant virus expressing green fluorescent protein. J Virol *76*, 6743-6749.

He, B., Paterson, R.G., Stock, N., Durbin, J.E., Durbin, R.K., Goodbourn, S., Randall, R.E., and Lamb, R.A. (2002). Recovery of paramyxovirus simian virus 5 with a V protein lacking the conserved cysteine-rich domain: the multifunctional V protein blocks both interferon-beta induction and interferon signaling. Virology *303*, 15-32.

Heaney, J., Barrett, T., and Cosby, S.L. (2002). Inhibition of in vitro leukocyte proliferation by morbilliviruses. J Virol *76*, 3579-3584.

Hercyk, N., Horikami, S.M., and Moyer, S.A. (1988). The vesicular stomatitis virus L protein possesses the mRNA methyltransferase activities. Virology *163*, 222-225.

Herndon, R.M., and Rubinstein, L.J. (1968). Light and electron microscopy observations on the development of viral particles in the inclusions of Dawson's encephalitis (subacute sclerosing panencephalitis). Neurology *18*, 8-20.

Higgins, R.J., Krakowka, S.G., Metzler, A.E., and Koestner, A. (1982). Experimental canine distemper encephalomyelitis in neonatal gnotobiotic dogs. A sequential ultrastructural study. Acta Neuropathol *57*, 287-295.

Hirokawa, N., Noda, Y., Tanaka, Y., and Niwa, S. (2009). Kinesin superfamily motor proteins and intracellular transport. Nat Rev Mol Cell Biol *10*, 682-696.

Hirsch, R.L., Griffin, D.E., Johnson, R.T., Cooper, S.J., Lindo de Soriano, I., Roedenbeck, S., and Vaisberg, A. (1984). Cellular immune responses during complicated and uncomplicated measles virus infections of man. Clin Immunol Immunopathol *31*, 1-12.

Hofman, F.M., Hinton, D.R., Baemayr, J., Weil, M., and Merrill, J.E. (1991). Lymphokines and immunoregulatory molecules in subacute sclerosing panencephalitis. Clin Immunol Immunopathol *58*, 331-342.

Horikami, S.M., Smallwood, S., Bankamp, B., and Moyer, S.A. (1994). An amino-proximal domain of the L protein binds to the P protein in the measles virus RNA polymerase complex. Virology *205*, 540-545.

Hsu, E.C., Sarangi, F., Iorio, C., Sidhu, M.S., Udem, S.A., Dillehay, D.L., Xu, W., Rota, P.A., Bellini, W.J., and Richardson, C.D. (1998). A single amino acid change in the hemagglutinin protein of measles virus determines its ability to bind CD46 and reveals another receptor on marmoset B cells. J Virol *72*, 2905-2916.

Hunt, D.M., and Hutchinson, K.L. (1993). Amino acid changes in the L polymerase protein of vesicular stomatitis virus which confer aberrant polyadenylation and temperature-sensitive phenotypes. Virology *193*, 786-793.

Jabbour, J.T., Duenas, D.A., Sever, J.L., Krebs, H.M., and Horta-Barbosa, L. (1972). Epidemiology of subacute sclerosing panencephalitis (SSPE). A report of the SSPE registry. JAMA *220*, 959-962.

Jacques, J.P., and Kolakofsky, D. (1991). Pseudo-templated transcription in prokaryotic and eukaryotic organisms. Genes Dev *5*, 707-713.

Johnson, M.D., Gold, L.I., and Moses, H.L. (1992). Evidence for transforming growth factor-beta expression in human leptomeningeal cells and transforming growth factor-beta-like activity in human cerebrospinal fluid. Lab Invest *67*, 360-368.

Jouvenet, N., Monaghan, P., Way, M., and Wileman, T. (2004). Transport of African swine fever virus from assembly sites to the plasma membrane is dependent on microtubules and conventional kinesin. J Virol *78*, 7990-8001.

Kajita, M., Katayama, H., Murata, T., Kai, C., Hori, M., and Ozaki, H. (2006). Canine distemper virus induces apoptosis through caspase-3 and -8 activation in vero cells. J Vet Med B Infect Dis Vet Public Health *53*, 273-277.

Kaplan, L.J., Daum, R.S., Smaron, M., and McCarthy, C.A. (1992). Severe measles in immunocompromised patients. JAMA *267*, 1237-1241.

Kardon, J.R., and Vale, R.D. (2009). Regulators of the cytoplasmic dynein motor. Nat Rev Mol Cell Biol *10*, 854-865.

Karki, S., and Holzbaur, E.L. (1999). Cytoplasmic dynein and dynactin in cell division and intracellular transport. Curr Opin Cell Biol *11*, 45-53.

Karlin, D., Longhi, S., and Canard, B. (2002). Substitution of two residues in the measles virus nucleoprotein results in an impaired self-association. Virology *302*, 420-432.

Katz, M., Rorke, L.B., Masland, W.S., Koprowski, H., and Tucker, S.H. (1968). Transmission of an encephalitogenic agent from brains of patients with subacute sclerosing panencephalitis to ferrets. Preliminary report. N Engl J Med *279*, 793-798.

Kennedy, S. (1998). Morbillivirus infections in aquatic mammals. J Comp Pathol *119*, 201-225.
Kerdiles, Y.M., Sellin, C.I., Druelle, J., and Horvat, B. (2006). Immunosuppression caused by measles virus: role of viral proteins. Rev Med Virol *16*, 49-63.

Kerdiles, Y.M., Sellin, C.I., Druelle, J., and Horvat, B. (2006). Immunosuppression caused by measles virus: role of viral proteins. Rev Med Virol *16*, 49-63.

Kirk, J., Zhou, A.L., McQuaid, S., Cosby, S.L., and Allen, I.V. (1991). Cerebral endothelial cell infection by measles virus in subacute sclerosing panencephalitis: ultrastructural and in situ hybridization evidence. Neuropathol Appl Neurobiol *17*, 289-297.

Kiyokawa, Y., Kikusui, T., Takeuchi, Y., and Mori, Y. (2007). Removal of the vomeronasal organ blocks the stress-induced hyperthermia response to alarm pheromone in male rats. Chem Senses *32*, 57-64.

Kocsis, J.D., Lankford, K.L., Sasaki, M., and Radtke, C. (2009). Unique in vivo properties of olfactory ensheathing cells that may contribute to neural repair and protection following spinal cord injury. Neurosci Lett *456*, 137-142.

Krakowka, S., Higgins, R.J., and Koestner, A. (1980). Canine distemper virus: review of structural and functional modulations in lymphoid tissues. Am J Vet Res *41*, 284-292.

Krakowka, S., McCullough, B., Koestner, A., and Olsen, R. (1973). Myelin-specific autoantibodies associated with central nervous system demyelination in canine distemper virus infection. Infect Immun *8*, 819-827.

Krakowka, S., Olsen, R., Confer, A., Koestner, A., and McCullough, B. (1975b). Serologic response to canine distemper viral antigens in gnotobiotic dogs infected with canine distemper virus. J Infect Dis *132*, 384-392.

Kumagai, K., Yamaguchi, R., Uchida, K., and Tateyama, S. (2004). Lymphoid apoptosis in acute canine distemper. J Vet Med Sci *66*, 175-181.

Laine, D., Trescol-Biemont, M.C., Longhi, S., Libeau, G., Marie, J.C., Vidalain, P.O., Azocar, O., Diallo, A., Canard, B., Rabourdin-Combe, C., *et al.* (2003). Measles virus (MV) nucleoprotein binds to a novel cell surface receptor distinct from FcgammaRII via its C-terminal domain: role in MV-induced immunosuppression. J Virol *77*, 11332-11346.

Lamb, R.A. and Knipe., D. (1996). Paramyxoviridae: the viruses and their replication. In Field's Virology, B.N. Fields, Knipe, D. M. , Howley, P.M., Chanock, R.M., Monath, T.P., Melnick, J.L., Roizman, B. and Straus, S.E., ed. (Philidelphia, PA, Lippincott-Raven), pp. 1177-1204.

Lawrence, D.M., Patterson, C.E., Gales, T.L., D'Orazio, J.L., Vaughn, M.M., and Rall, G.F. (2000). Measles virus spread between neurons requires cell contact but not CD46 expression, syncytium formation, or extracellular virus production. J Virol *74*, 1908-1918.

Lawrence, D.M., Vaughn, M.M., Belman, A.R., Cole, J.S., and Rall, G.F. (1999). Immune response-mediated protection of adult but not neonatal mice from neuron-restricted measles virus infection and central nervous system disease. J Virol *73*, 1795-1801.

Lecouturier, V., Fayolle, J., Caballero, M., Carabana, J., Celma, M.L., Fernandez-Munoz, R., Wild, T.F., and Buckland, R. (1996). Identification of two amino acids in the hemagglutinin glycoprotein of measles virus (MV) that govern hemadsorption, HeLa cell fusion, and CD46 downregulation: phenotypic markers that differentiate vaccine and wild-type MV strains. J Virol *70*, 4200-4204.

Leonard, V.H., Sinn, P.L., Hodge, G., Miest, T., Devaux, P., Oezguen, N., Braun, W., McCray, P.B., Jr., McChesney, M.B., and Cattaneo, R. (2008). Measles virus blind to its epithelial cell receptor remains virulent in rhesus monkeys but cannot cross the airway epithelium and is not shed. J Clin Invest *118*, 2448-2458.

Lin, G.Y., and Lamb, R.A. (2000). The paramyxovirus simian virus 5 V p otein slows progression of the cell cycle. J Virol *74*, 9152-9166.

Liszewski, M.K., Post, T.W., and Atkinson, J.P. (1991). Membrane cofactor protein (MCP or CD46): newest member of the regulators of complement activation gene cluster. Annu Rev Immunol *9*, 431-455.

Maisner, A., Klenk, H., and Herrler, G. (1998). Polarized budding of measles virus is not determined by viral surface glycoproteins. J Virol *72*, 5276-5278.

Manchester, M., Eto, D.S., and Oldstone, M.B. (1999). Characterization of the inflammatory response during acute measles encephalitis in NSE-CD46 transgenic mice. J Neuroimmunol *96*, 207-217.

Manchester, M., and Rall, G.F. (2001). Model Systems: transgenic mouse models for measles pathogenesis. Trends Microbiol *9*, 19-23.

Marie, J.C., Kehren, J., Trescol-Biemont, M.C., Evlashev, A., Valentin, H., Walzer, T., Tedone, R., Loveland, B., Nicolas, J.F., Rabourdin-Combe, C., *et al.* (2001). Mechanism of measles virus-induced suppression of inflammatory immune responses. Immunity *14*, 69-79.

Markowitz, L.E., Chandler, F.W., Roldan, E.O., Saldana, M.J., Roach, K.C., Hutchins, S.S., Preblud, S.R., Mitchell, C.D., and Scott, G.B. (1988). Fatal measles pneumonia without rash in a child with AIDS. J Infect Dis *158*, 480-483.

Markus, S., Failing, K., and Baumgartner, W. (2002). Increased expression of pro-inflammatory cytokines and lack of up-regulation of anti-inflammatory cytokines in early distemper CNS lesions. J Neuroimmunol *125*, 30-41.

Matsuda, K., Park, C.H., Sunden, Y., Kimura, T., Ochiai, K., Kida, H., and Umemura, T. (2004). The vagus nerve is one route of transneural invasion for intranasally inoculated influenza a virus in mice. Vet Pathol *41*, 101-107.

Mawhinney, H., Allen, I.V., Beare, J.M., Bridges, J.M., Connolly, J.H., Haire, M., Nevin, N.C., Neill, D.W., and Hobbs, J.R. (1971). Dysgammaglobulinaemia complicated by disseminated measles. Br Med J *2*, 380-381.

McChesney, M.B., Miller, C.J., Rota, P.A., Zhu, Y.D., Antipa, L., Lerche, N.W., Ahmed, R., and Bellini, W.J. (1997). Experimental measles. I. Pathogenesis in the normal and the immunized host. Virology *233*, 74-84.

McCullough, B., Krakowka, S., and Koestner, A. (1974). Experimental canine distemper virus-induced demyelination. Lab Invest *31*, 216-222.

McIlhatton, M.A., Curran, M.D., and Rima, B.K. (1997). Nucleotide sequence analysis of the large (L) genes of phocine distemper virus and canine distemper virus (corrected sequence). J Gen Virol *78 (Pt 3)*, 571-576.

Mebatsion, T., Weiland, F., and Conzelmann, K.K. (1999). Matrix protein of rabies virus is responsible for the assembly and budding of bullet-shaped particles and interacts with the transmembrane spike glycoprotein G. J Virol *73*, 242-250.

Mehta, P.D., and Thormar, H. (1979). Immunological studies of subacute measles encephalitis in ferrets: similarities to human subacute sclerosing panencephalitis. J Clin Microbiol *9*, 601-604.

Middleton, D.J., Westbury, H.A., Morrissy, C.J., van der Heide, B.M., Russell, G.M., Braun, M.A., and Hyatt, A.D. (2002). Experimental Nipah virus infection in pigs and cats. J Comp Pathol *126*, 124-136.

Miller, D.L. (1964). Frequency of Complications of Measles, 1963. Report on a National Inquiry by the Public Health Laboratory Service in Collaboration with the Society of Medical Officers of Health. Br Med J *2*, 75-78.

Minagawa, H., Tanaka, K., Ono, N., Tatsuo, H., and Yanagi, Y. (2001). Induction of the measles virus receptor SLAM (CD150) on monocytes. J Gen Virol *82*, 2913-2917.

Modlin, J.F., Jabbour, J.T., Witte, J.J., and Halsey, N.A. (1977). Epidemiologic studies of measles, measles vaccine, and subacute sclerosing panencephalitis. Pediatrics *59*, 505-512.

Moll, M., Klenk, H.D., Herrler, G., and Maisner, A. (2001). A single amino acid change in the cytoplasmic domains of measles virus glycoproteins H and F alters targeting, endocytosis, and cell fusion in polarized Madin-Darby canine kidney cells. J Biol Chem *276*, 17887-17894.

Moll, M., Klenk, H.D., and Maisner, A. (2002). Importance of the cytoplasmic tails of the measles virus glycoproteins for fusogenic activity and the generation of recombinant measles viruses. J Virol *76*, 7174-7186.

Moll, M., Pfeuffer, J., Klenk, H.D., Niewiesk, S., and Maisner, A. (2004). Polarized glycoprotein targeting affects the spread of measles virus in vitro and in vivo. J Gen Virol *85*, 1019-1027.

Mori, I., Komatsu, T., Takeuchi, K., Nakakuki, K., Sudo, M., and Kimura, Y. (1995). Parainfluenza virus type 1 infects olfactory neurons and establishes long-term persistence in the nerve tissue. J Gen Virol *76 (Pt 5)*, 1251-1254.

Moro, L., de Sousa Martins, A., de Moraes Alves, C., de Araujo Santos, F.G., dos Santos Nunes, J.E., Carneiro, R.A., Carvalho, R., and Vasconcelos, A.C. (2003a). Apoptosis in canine distemper. Arch Virol *148*, 153-164.

Moro, L., Martins, A.S., Alves, C.M., Santos, F.G., Del Puerto, H.L., and Vasconcelos, A.C. (2003b). Apoptosis in the cerebellum of dogs with distemper. J Vet Med B Infect Dis Vet Public Health *50*, 221-225.

Moss, W.J., and Griffin, D.E. (2006). Global measles elimination. Nat Rev Microbiol *4*, 900-908.

Moss, W.J., Ota, M.O., and Griffin, D.E. (2004). Measles: immune suppression and immune responses. Int J Biochem Cell Biol *36*, 1380-1385.

Moss, W.J., Ryon, J.J., Monze, M., and Griffin, D.E. (2002). Differential regulation of interleukin (IL)-4, IL-5, and IL-10 during measles in Zambian children. J Infect Dis *186*, 879-887.

Moyer, S.A., Baker, S.C., and Horikami, S.M. (1990). Host cell proteins required for measles virus reproduction. J Gen Virol *71 (Pt 4)*, 775-783.

Mrkic, B., Pavlovic, J., Rulicke, T., Volpe, P., Buchholz, C.J., Hourcade, D., Atkinson, J.P., Aguzzi, A., and Cattaneo, R. (1998). Measles virus spread and pathogenesis in genetically modified mice. J Virol *72*, 7420-7427.

Murphy, S.K., and Parks, G.D. (1997). Genome nucleotide lengths that are divisible by six are not essential but enhance replication of defective interfering RNAs of the paramyxovirus simian virus 5. Virology *232*, 145-157.

Mustafa, M.M., Weitman, S.D., Winick, N.J., Bellini, W.J., Timmons, C.F., and Siegel, J.D. (1993). Subacute measles encephalitis in the young immunocompromised host: report of two cases diagnosed by polymerase chain reaction and treated with ribavirin and review of the literature. Clin Infect Dis *16*, 654-660.

Naim, H.Y., Ehler, E., and Billeter, M.A. (2000). Measles virus matrix protein specifies apical virus release and glycoprotein sorting in epithelial cells. EMBO J *19*, 3576-3585.

Nakatsu, Y., Takeda, M., Ohno, S., Shirogane, Y., Iwasaki, M., and Yanagi, Y. (2008). Measles virus circumvents the host interferon response by different actions of the C and V proteins. J Virol *82*, 8296-8306.

Naniche, D., Varior-Krishnan, G., Cervoni, F., Wild, T.F., Rossi, B., Rabourdin-Combe, C., and Gerlier, D. (1993). Human membrane cofactor protein (CD46) acts as a cellular receptor for measles virus. J Virol *67*, 6025-6032.

Nasr, J.T., Andriola, M.R., and Coyle, P.K. (2000). ADEM: literature review and case report of acute psychosis presentation. Pediatr Neurol *22*, 8-18.

Navaratnarajah, C.K., Leonard, V.H., and Cattaneo, R. (2009). Measles virus glycoprotein complex assembly, receptor attachment, and cell entry. Curr Top Microbiol Immunol *329*, 59-76.

Nedergaard, M., Ransom, B., and Goldman, S.A. (2003). New roles for astrocytes: redefining the functional architecture of the brain. Trends Neurosci *26*, 523-530.

Neumann, H., Misgeld, T., Matsumuro, K., and Wekerle, H. (1998). Neurotrophins inhibit major histocompatibility class II inducibility of microglia: involvement of the p75 neurotrophin receptor. Proc Natl Acad Sci U S A *95*, 5779-5784.

Neumann, H., Schmidt, H., Cavalie, A., Jenne, D., and Wekerle, H. (1997). Major histocompatibility complex (MHC) class I gene expression in single neurons of the central nervous system: differential regulation by interferon (IFN)-gamma and tumor necrosis factor (TNF)-alpha. J Exp Med *185*, 305-316.

Niewiesk, S. (1999). Cotton rats (Sigmodon hispidus): an animal model to study the pathogenesis of measles virus infection. Immunol Lett *65*, 47-50.

Niewiesk, S. (2009). Current animal models: cotton rat animal model. Curr Top Microbiol Immunol *330*, 89-110.

Niewiesk, S., Eisenhuth, I., Fooks, A., Clegg, J.C., Schnorr, J.J., Schneider-Schaulies, S., and ter Meulen, V. (1997). Measles virus-induced immune suppression in the cotton rat (Sigmodon hispidus) model depends on viral glycoproteins. J Virol *71*, 7214-7219.

Norrby, E., and Kristensson, K. (1997). Measles virus in the brain. Brain Res Bull *44*, 213-220.

Ohuchi, M., Ohuchi, R., Mifune, K., Ishihara, T., and Ogawa, T. (1987). Characterization of the measles virus isolated from the brain of a patient with immunosuppressive measles encephalitis. J Infect Dis *156*, 436-441.

Okada, H., Kobune, F., Sato, T.A., Kohama, T., Takeuchi, Y., Abe, T., Takayama, N., Tsuchiya, T., and Tashiro, M. (2000). Extensive lymphopenia due to apoptosis of uninfected lymphocytes in acute measles patients. Arch Virol *145*, 905-920.

Oldstone, M.B., Lewicki, H., Thomas, D., Tishon, A., Dales, S., Patterson, J., Manchester, M., Homann, D., Naniche, D., and Holz, A. (1999). Measles virus infection in a transgenic model: virus-induced immunosuppression and central nervous system disease. Cell *98*, 629-640.

Ordway, G.A., Szebeni, A., Duffourc, M.M., Dessus-Babus, S., and Szebeni, K. (2009). Gene expression analyses of neurons, astrocytes, and oligodendrocytes isolated by laser capture microdissection from human brain: detrimental effects of laboratory humidity. J Neurosci Res *87*, 2430-2438.

Palosaari, H., Parisien, J.P., Rodriguez, J.J., Ulane, C.M., and Horvath, C.M. (2003). STAT protein interference and suppression of cytokine signal transduction by measles virus V protein. J Virol *77*, 7635-7644.

Permar, S.R., Moss, W.J., Ryon, J.J., Monze, M., Cutts, F., Quinn, T.C., and Griffin, D.E. (2001). Prolonged measles virus shedding in human immunodeficiency virus-infected children, detected by reverse transcriptase-polymerase chain reaction. J Infect Dis *183*, 532-538.

Pillet, S., and von Messling, V. (2009). Canine distemper virus selectively inhibits apoptosis progression in infected immune cells. J Virol *83*, 6279-6287.

Plemper, R.K., Hammond, A.L., and Cattaneo, R. (2000). Characterization of a region of the measles virus hemagglutinin sufficient for its dimerization. J Virol *74*, 6485-6493.

Plemper, R.K., Hammond, A.L., Gerlier, D., Fielding, A.K., and Cattaneo, R. (2002). Strength of envelope protein interaction modulates cytopathicity of measles virus. J Virol *76*, 5051-5061.

Poch, O., Blumberg, B.M., Bougueleret, L., and Tordo, N. (1990). Sequence comparison of five polymerases (L proteins) of unsegmented negative-strand RNA viruses: theoretical assignment of functional domains. J Gen Virol *71 (Pt 5)*, 1153-1162.

Poole, E., He, B., Lamb, R.A., Randall, R.E., and Goodbourn, S. (2002). The V proteins of simian virus 5 and other paramyxoviruses inhibit induction of interferon-beta. Virology *303*, 33-46.

Portner, A., Murti, K.G., Morgan, E.M., and Kingsbury, D.W. (1988). Antibodies against Sendai virus L protein: distribution of the protein in nucleocapsids revealed by immunoelectron microscopy. Virology *163*, 236-239.

Prendergast, B.J., Pyter, L.M., Galang, J., and Kay, L.M. (2009). Reproductive responses to photoperiod persist in olfactory bulbectomized Siberian hamsters (Phodopus sungorus). Behav Brain Res *198*, 159-164.

Qin, Q., Wei, F., Li, M., Dubovi, E.J., and Loeffler, I.K. (2007). Serosurvey of infectious disease agents of carnivores in captive red pandas (Ailurus fulgens) in China. J Zoo Wildl Med *38*, 42-50.

Radtke, K., Dohner, K., and Sodeik, B. (2006). Viral interactions with the cytoskeleton: a hitchhiker's guide to the cell. Cell Microbiol *8*, 387-400.

Rand, K.H., Emmons, R.W., and Merigan, T.C. (1976). Measles in adults. An unforeseen consequence of immunization? JAMA *236*, 1028-1031.

Ransom, B., Behar, T., and Nedergaard, M. (2003). New roles for astrocytes (stars at last). Trends Neurosci *26*, 520-522.

Rappert, A., Biber, K., Nolte, C., Lipp, M., Schubel, A., Lu, B., Gerard, N.P., Gerard, C., Boddeke, H.W., and Kettenmann, H. (2002). Secondary lymphoid tissue chemokine (CCL21) activates CXCR3 to trigger a Cl- current and chemotaxis in murine microglia. J Immunol *168*, 3221-3226.

Riedl, P., Moll, M., Klenk, H.D., and Maisner, A. (2002). Measles virus matrix protein is not cotransported with the viral glycoproteins but requires virus infection for efficient surface targeting. Virus Res *83*, 1-12.

Rietdorf, J., Ploubidou, A., Reckmann, I., Holmstrom, A., Frischknecht, F., Zettl, M., Zimmermann, T., and Way, M. (2001). Kinesin-dependent movement on microtubules precedes actin-based motility of vaccinia virus. Nat Cell Biol *3*, 992-1000.

Rima, B.K., Duffy, N., Mitchell, W.J., Summers, B.A., and Appel, M.J. (1991). Correlation between humoral immune responses and presence of virus in the CNS in dogs experimentally infected with canine distemper virus. Arch Virol *121*, 1-8.

Rima, B.K., and Duprex, W.P. (2006). Morbilliviruses and human disease. J Pathol *208*, 199-214.

Roelke-Parker, M.E., Munson, L., Packer, C., Kock, R., Cleaveland, S., Carpenter, M., O'Brien, S.J., Pospischil, A., Hofmann-Lehmann, R., Lutz, H., *et al.* (1996). A canine distemper virus epidemic in Serengeti lions (Panthera leo). Nature *379*, 441-445.

Rudd, P.A., Bastien-Hamel, L.E., and von Messling, V. (2010). Acute canine distemper encephalitis is associated with rapid neuronal loss and local immune activation. J Gen Virol *91*, 980-989.

Rudd, P.A., Cattaneo, R., and von Messling, V. (2006). Canine distemper virus uses both the anterograde and the hematogenous pathway for neuroinvasion. J Virol *80*, 9361-9370.

Runkler, N., Pohl, C., Schneider-Schaulies, S., Klenk, H.D., and Maisner, A. (2007). Measles virus nucleocapsid transport to the plasma membrane requires stable expression and surface accumulation of the viral matrix protein. Cell Microbiol *9*, 1203-1214.

Ryman, K.D., Klimstra, W.B., Nguyen, K.B., Biron, C.A., and Johnston, R.E. (2000). Alpha/beta interferon protects adult mice from fatal Sindbis virus infection and is an important determinant of cell and tissue tropism. J Virol *74*, 3366-3378.

Ryon, J.J., Moss, W.J., Monze, M., and Griffin, D.E. (2002). Functional and phenotypic changes in circulating lymphocytes from hospitalized zambian children with measles. Clin Diagn Lab Immunol *9*, 994-1003.

Sakaguchi, M., Yoshikawa, Y., Yamanouchi, K., Sata, T., Nagashima, K., and Takeda, K. (1986). Growth of measles virus in epithelial and lymphoid tissues of cynomolgus monkeys. Microbiol Immunol *30*, 1067-1073.

Sanchez-Lanier, M., Guerin, P., McLaren, L.C., and Bankhurst, A.D. (1988). Measles virus-induced suppression of lymphocyte proliferation. Cell Immunol *116*, 367-381.

Sanderson, C.M., Wu, H.H., and Nayak, D.P. (1994). Sendai virus M protein binds independently to either the F or the HN glycoprotein in vivo. J Virol *68*, 69-76.

Sato, C., Kuriyama, R., and Nishizawa, K. (1983). Microtubule-organizing centers abnormal in number, structure, and nucleating activity in x-irradiated mammalian cells. J Cell Biol *96*, 776-782.

Sato, M., Suemori, H., Hata, N., Asagiri, M., Ogasawara, K., Nakao, K., Nakaya, T., Katsuki, M., Noguchi, S., Tanaka, N., *et al.* (2000). Distinct and essential roles of transcription factors IRF-3 and IRF-7 in response to viruses for IFN-alpha/beta gene induction. Immunity *13*, 539-548.

Schlender, J., Schnorr, J.J., Spielhoffer, P., Cathomen, T., Cattaneo, R., Billeter, M.A., ter Meulen, V., and Schneider-Schaulies, S. (1996). Interaction of measles virus glycoproteins with the surface of uninfected peripheral blood lymphocytes induces immunosuppression in vitro. Proc Natl Acad Sci U S A *93*, 13194-13199.

Schmid, A., Spielhofer, P., Cattaneo, R., Baczko, K., ter Meulen, V., and Billeter, M.A. (1992). Subacute sclerosing panencephalitis is typically characterized by alterations in the fusion protein cytoplasmic domain of the persisting measles virus. Virology *188*, 910-915.

Schmitt, A.P., He, B., and Lamb, R.A. (1999). Involvement of the cytoplasmic domain of the hemagglutinin-neuraminidase protein in assembly of the paramyxovirus simian virus 5. J Virol *73*, 8703-8712.

Schneider-Schaulies, J., and Schneider-Schaulies, S. (2008). Receptor interactions, tropism, and mechanisms involved in morbillivirus-induced immunomodulation. Adv Virus Res *71*, 173-205.

Schneider-Schaulies, J., Schnorr, J.J., Brinckmann, U., Dunster, L.M., Baczko, K., Liebert, U.G., Schneider-Schaulies, S., and ter Meulen, V. (1995). Receptor usage and differential downregulation of CD46 by measles virus wild-type and vaccine strains. Proc Natl Acad Sci U S A *92*, 3943-3947.

Schneider-Schaulies, S., Schneider-Schaulies, J., Niewiesk, S., and Ter Meulen, V. (2002). Measles virus: immunomodulation and cell tropism as pathogenicity determinants. Med Microbiol Immunol *191*, 83-87.

Schneider-Schaulies, S., and ter Meulen, V. (2002). Modulation of immune functions by measles virus. Springer Semin Immunopathol *24*, 127-148.

Schnorr, J.J., Dunster, L.M., Nanan, R., Schneider-Schaulies, J., Schneider-Schaulies, S., and ter Meulen, V. (1995). Measles virus-induced down-regulation of CD46 is associated with enhanced sensitivity to complement-mediated lysis of infected cells. Eur J Immunol *25*, 976-984.

Schobesberger, M., Summerfield, A., Doherr, M.G., Zurbriggen, A., and Griot, C. (2005). Canine distemper virus-induced depletion of uninfected lymphocytes is associated with apoptosis. Vet Immunol Immunopathol *104*, 33-44.

Seifert, G., Schilling, K., and Steinhauser, C. (2006). Astrocyte dysfunction in neurological disorders: a molecular perspective. Nat Rev Neurosci *7*, 194-206.

Seki, F., Ono, N., Yamaguchi, R., and Yanagi, Y. (2003). Efficient isolation of wild strains of canine distemper virus in Vero cells expressing canine SLAM (CD150) and their adaptability to marmoset B95a cells. J Virol *77*, 9943-9950.

Sellin, C.I., Davoust, N., Guillaume, V., Baas, D., Belin, M.F., Buckland, R., Wild, T.F., and Horvat, B. (2006). High pathogenicity of wild-type measles virus infection in CD150 (SLAM) transgenic mice. J Virol *80*, 6420-6429.

Shaffer, J.A., Bellini, W.J., and Rota, P.A. (2003). The C protein of measles virus inhibits the type I interferon response. Virology *315*, 389-397.

Shapshak, P., Graves, M.C., and Imagawa, D.T. (1982). Polypeptides of canine distemper virus strains derived from dogs with chronic neurological diseases. Virology *122*, 158-170.

Sidorenko, S.P., and Clark, E.A. (2003). The dual-function CD150 receptor subfamily: the viral attraction. Nat Immunol *4*, 19-24.

Siegel, M.M., Walter, T.K., and Ablin, A.R. (1977). Measles pneumonia in childhood leukemia. Pediatrics *60*, 38-40.

Sieling, P.A., Abrams, J.S., Yamamura, M., Salgame, P., Bloom, B.R., Rea, T.H., and Modlin, R.L. (1993). Immunosuppressive roles for IL-10 and IL-4 in human infection. In vitro modulation of T cell responses in leprosy. J Immunol *150*, 5501-5510.

Sips, G.J., Chesik, D., Glazenburg, L., Wilschut, J., De Keyser, J., and Wilczak, N. (2007). Involvement of morbilliviruses in the pathogenesis of demyelinating disease. Rev Med Virol *17*, 223-244.

Smallwood, S., Ryan, K.W., and Moyer, S.A. (1994). Deletion analysis defines a carboxyl-proximal region of Sendai virus P protein that binds to the polymerase L protein. Virology *202*, 154-163.

Spehner, D., Kirn, A., and Drillien, R. (1991). Assembly of nucleocapsidlike structures in animal cells infected with a vaccinia virus recombinant encoding the measles virus nucleoprotein. J Virol *65*, 6296-6300.

Stallcup, K.C., Raine, C.S., and, B.N. (1983). Cytochalasin B inhibits the maturation of measles virus. Virology *124*, 59-74.

Steele, M.D., Giddens, W.E., Jr., Valerio, M., Sumi, S.M., and Stetzer, E.R. (1982). Spontaneous paramyxoviral encephalitis in nonhuman primates (Macaca mulatta and M. nemestrina). Vet Pathol *19*, 132-139.

Stephenson, J.R., Siddell, S.G., and Meulen, V.T. (1981). Persistent and lytic infections with SSPE virus: a comparison of the synthesis of virus-specific polypeptides. J Gen Virol *57*, 191-197.

Summers, B.A., and Appel, M.J. (1987). Demyelination in canine distemper encephalomyelitis: an ultrastructural analysis. J Neurocytol *16*, 871-881.

Summers, B.A., and Appel, M.J. (1994). Aspects of canine distemper virus and measles virus encephalomyelitis. Neuropathol Appl Neurobiol *20*, 525-534.

Summers, B.A., Greisen, H.A., and Appel, M.J. (1979). Early events in canine distemper demyelinating encephalomyelitis. Acta Neuropathol *46*, 1-10.

Summers, B.A., Greisen, H.A., and Appel, M.J. (1984). Canine distemper encephalomyelitis: variation with virus strain. J Comp Pathol *94*, 65-75.

Suryanarayana, K., Baczko, K., ter Meulen, V., and Wagner, R.R. (1994). Transcription inhibition and other properties of matrix proteins expressed by M genes cloned from measles viruses and diseased human brain tissue. J Virol *68*, 1532-1543.

Svitek, N., and von Messling, V. (2007). Early cytokine mRNA expression profiles predict Morbillivirus disease outcome in ferrets. Virology *362*, 404-410.

Tahara, M., Takeda, M., and Yanagi, Y. (2007). Altered interaction of the matrix protein with the cytoplasmic tail of hemagglutinin modulates measles virus growth by affecting virus assembly and cell-cell fusion. J Virol *81*, 6827-6836.

Takasu, T., Mgone, J.M., Mgone, C.S., Miki, K., Komase, K., Namae, H., Saito, Y., Kokubun, Y., Nishimura, T., Kawanishi, R., *et al.* (2003). A continuing high incidence of subacute sclerosing panencephalitis (SSPE) in the Eastern Highlands of Papua New Guinea. Epidemiol Infect *131*, 887-898.

Takeuchi, K., Kadota, S.I., Takeda, M., Miyajima, N., and Nagata, K. (2003). Measles virus V protein blocks interferon (IFN)-alpha/beta but not IFN-gamma signaling by inhibiting STAT1 and STAT2 phosphorylation. FEBS Lett *545*, 177-182.

Takimoto, T., and Portner, A. (2004). Molecular mechanism of paramyxovirus budding. Virus Res *106*, 133-145.

Tatsuo, H., Ono, N., Tanaka, K., and Yanagi, Y. (2000). SLAM (CDw150) is a cellular receptor for measles virus. Nature *406*, 893-897.

Tatsuo, H., Ono, N., and Yanagi, Y. (2001). Morbilliviruses use signaling lymphocyte activation molecules (CD150) as cellular receptors. J Virol *75*, 5842-5850.

Techangamsuwan, S., Haas, L., Rohn, K., Baumgartner, W., and Wewetzer, K. (2009). Distinct cell tropism of canine distemper virus strains to adult olfactory ensheathing cells and Schwann cells in vitro. Virus Res *144*, 195-201.

tenOever, B.R., Servant, M.J., Grandvaux, N., Lin, R., and Hiscott, J. (2002). Recognition of the measles virus nucleocapsid as a mechanism of IRF-3 activation. J Virol *76*, 3659-3669.

Thomas, S.M., Lamb, R.A., and Paterson, R.G. (1988). Two mRNAs that differ by two nontemplated nucleotides encode the amino coterminal proteins P and V of the paramyxovirus SV5. Cell *54*, 891-902.

Tipold, A., Moore, P., Zurbriggen, A., Burgener, I., Barben, G., and Vandevelde, M. (1999). Early T cell response in the central nervous system in canine distemper virus infection. Acta Neuropathol *97*, 45-56.

Tsai, S.C., Summers, B.A., and Appel, M.J. (1982). Interferon in cerebrospinal fluid. A marker for viral persistence of canine distemper encephalomyelitis. Arch Virol *72*, 257-265.

Vandevelde, M., Fankhauser, R., Kristensen, F., and Kristensen, B. (1981). Immunoglobulins in demyelinating lesions in canine distemper encephalitis. An immunohistological study. Acta Neuropathol *54*, 31-41.

Vandevelde, M., Higgins, R.J., Kristensen, B., Kristensen, F., Steck, A.J., and Kihm, U. (1982). Demyelination in experimental canine distemper virus infection: immunological, pathologic, and immunohistological studies. Acta Neuropathol *56*, 285-293.

Vandevelde, M., and Zurbriggen, A. (2005). Demyelination in canine distemper virus infection: a review. Acta Neuropathol *109*, 56-68.

Vandevelde, M., Zurbriggen, A., Higgins, R.J., and Palmer, D. (1985). Spread and distribution of viral antigen in nervous canine distemper. Acta Neuropathol *67*, 211-218.

Vandevelde, M., Zurbriggen, A., Steck, A., and Bichsel, P. (1986). Studies on the intrathecal humoral immune response in canine distemper encephalitis. J Neuroimmunol *11*, 41-51.

von Messling, V., Milosevic, D., and Cattaneo, R. (2004). Tropism illuminated: lymphocyte-based pathways blazed by lethal morbillivirus through the host immune system. Proc Natl Acad Sci U S A *101*, 14216-14221.

von Messling, V., Springfeld, C., Devaux, P., and Cattaneo, R. (2003). A ferret model of canine distemper virus virulence and immunosuppression. J Virol *77*, 12579-12591.

von Messling, V., Svitek, N., and Cattaneo, R. (2006). Receptor (SLAM [CD150]) recognition and the V protein sustain swift lymphocyte-based invasion of mucosal tissue and lymphatic organs by a morbillivirus. J Virol *80*, 6084-6092.

Wallin, R.P., Lundqvist, A., More, S.H., von Bonin, A., Kiessling, R., and Ljunggren, H.G. (2002). Heat-shock proteins as activators of the innate immune system. Trends Immunol *23*, 130-135.

Wang, Z., Trillo-Pazos, G., Kim, S.Y., Canki, M., Morgello, S., Sharer, L.R., Gelbard, H.A., Su, Z.Z., Kang, D.C., Brooks, A.I., *et al.* (2004). Effects of human immunodeficiency virus type 1 on astrocyte gene expression and function: potential role in neuropathogenesis. J Neurovirol *10 Suppl 1*, 25-32.

Wansley, E.K., and Parks, G.D. (2002). Naturally occurring substitutions in the P/V gene convert the noncytopathic paramyxovirus simian virus 5 into a virus that induces alpha/beta interferon synthesis and cell death. J Virol *76*, 10109-10121.

Watanabe, A., Yoneda, M., Ikeda, F., Terao-Muto, Y., Sato, H., and Kai, C. (2010). CD147/EMMPRIN Acts as a Functional Entry Receptor for Measles Virus on Epithelial Cells. J Virol.

Watanabe, M., Hirano, A., Stenglein, S., Nelson, J., Thomas, G., and Wong, T.C. (1995). Engineered serine protease inhibitor prevents furin-catalyzed activation of the fusion glycoprotein and production of infectious measles virus. J Virol *69*, 3206-3210.

Weidmann, A., Fischer, C., Ohgimoto, S., Ruth, C., ter Meulen, V., and Schneider-Schaulies, S. (2000a). Measles virus-induced immunosuppression in vitro is independent of complex glycosylation of viral glycoproteins and of hemifusion. J Virol *74*, 7548-7553.

Weidmann, A., Maisner, A., Garten, W., Seufert, M., ter Meulen, V., and Schneider-Schaulies, S. (2000b). Proteolytic cleavage of the fusion protein but not membrane fusion is required for measles virus-induced immunosuppression in vitro. J Virol *74*, 1985-1993.

Weingartl, H., Czub, S., Copps, J., Berhane, Y., Middleton, D., Marszal, P., Gren, J., Smith, G., Ganske, S., Manning, L., *et al.* (2005). Invasion of the central nervous system in a porcine host by nipah virus. J Virol *79*, 7528-7534.

Wewetzer, K., Kern, N., Ebel, C., Radtke, C., and Brandes, G. (2005). Phagocytosis of O4+ axonal fragments in vitro by p75- neonatal rat olfactory ensheathing cells. Glia *49*, 577-587.

Wisniewski, H., Raine, C.S., and Kay, W.J. (1972). Observations on viral demyelinating encephalomyelitis. Canine distemper. Lab Invest *26*, 589-599.

Wohlsein, P., Trautwein, G., Harder, T.C., Liess, B., and Barrett, T. (1993). Viral antigen distribution in organs of cattle experimentally infected with rinderpest virus. Vet Pathol *30*, 544-554.

Wong, T.C., Ayata, M., Hirano, A., Yoshikawa, Y., Tsuruoka, H., and Yamanouchi, K. (1989). Generalized and localized biased hypermutation affecting the matrix gene of a measles virus strain that causes subacute sclerosing panencephalitis. J Virol *63*, 5464-5468.

Woodley, S.K., Cloe, A.L., Waters, P., and Baum, M.J. (2004). Effects of vomeronasal organ removal on olfactory sex discrimination and odor preferences of female ferrets. Chem Senses *29*, 659-669.

Woolf, A., Gremillion-Smith, C., and Evans, R.H. (1986). Evidence of canine distemper virus infection in skunks negative for antibody against rabies virus. J Am Vet Med Assoc *189*, 1086-1088.

Wunschmann, A., Alldinger, S., Kremmer, E., and Baumgartner, W. (1999). Identification of CD4+ and CD8+ T cell subsets and B cells in the brain of dogs with spontaneous acute, subacute and chronic-demyelinating distemper encephalitis. Vet Immunol Immunopathol *67*, 101-116.

Wyde, P.R., Ambrose, M.W., Voss, T.G., Meyer, H.L., and Gilbert, B.E. (1992). Measles virus replication in lungs of hispid cotton rats after intranasal inoculation. Proc Soc Exp Biol Med *201*, 80-87.

Yamabe, T., Dhir, G., Cowan, E.P., Wolf, A.L., Bergey, G.K., Krumholz, A., Barry, E., Hoffman, P.M., and Dhib-Jalbut, S. (1994). Cytokine-gene expression in measles-infected adult human glial cells. J Neuroimmunol *49*, 171-179.

Yanagi, Y., Cubitt, B.A., and Oldstone, M.B. (1992). Measles virus inhibits mitogen-induced T cell proliferation but does not directly perturb the T cell activation process inside the cell. Virology *187*, 280-289.

Yanagi, Y., Takeda, M., Ohno, S., and Seki, F. (2006). Measles virus receptors and tropism. Jpn J Infect Dis *59*, 1-5.

Yin, H.S., Wen, X., Paterson, R.G., Lamb, R.A., and Jardetzky, T.S. (2006). Structure of the parainfluenza virus 5 F protein in its metastable, prefusion conformation. Nature *439*, 38-44.

Zhang, X., Glendening, C., Linke, H., Parks, C.L., Brooks, C., Udem, S.A., and Oglesbee, M. (2002). Identification and characterization of a regulatory domain on the carboxyl terminus of the measles virus nucleocapsid protein. J Virol *76*, 8737-8746.

Zurbriggen, A., Graber, H.U., and Vandevelde, M. (1995a). Selective spread and reduced virus release leads to canine distemper virus persistence in the nervous system. Vet Microbiol *44*, 281-288.

Zurbriggen, A., Graber, H.U., Wagner, A., and Vandevelde, M. (1995b). Canine distemper virus persistence in the nervous system is associated with noncytolytic selective virus spread. J Virol *69*, 1678-1686.

Zurbriggen, A., Schmid, I., Graber, H.U., and Vandevelde, M. (1998). Oligodendroglial pathology in canine distemper. Acta Neuropathol *95*, 71-77.

Zuri, I., and Halpern, M. (2005). Modification of odor investigation and discrimination in female opossums (Monodelphis domestica) following the ablation of the accessory olfactory bulbs. Behav Neurosci *119*, 612-621.

CHAPTER 4

RÉSUMÉ

CARACTÉRISATION DE LA NEUROINVASION DU VIRUS DE LA MALADIE DE CARRÉ EN UTILISANT LE FURET COMME MODÈLE EXPÉRIMENTAL

1. INTRODUCTION

1.1. Taxonomie

Les morbillivirus appartiennent à l'ordre des *Mononegavirales*, à la famille des *Paramyxoviridae* et à la sous-famille des *Paramyxovirinae*. Parmi les morbillivirus, on retrouve d'importants agents pathogènes humains et animaux tels que la rougeole et la maladie de Carré (*canine distemper virus*, CDV). Ce genre comprend également la peste bovine, la peste-des-petits-ruminants ainsi que les morbillivirus des phocidés et des cétacés. Les morbillivirus sont des virus à acide ribonucléique (ARN) monocaténaire, de polarité négative. Leur génome, d'une taille d'environ 16 000 nucléotides, est non segmenté et composé de six gènes (N : nucléoprotéine, P : phosphoprotéine, M : matrice, F : fusion, H : hémagglutinine et L : large; ARN polymérase ARN dépendante) qui sont traduits en huit protéines (N, P, V, C, M, F, H et L). Les produits des gènes N, P et L s'associent avec l'ARN génomique viral pour former la ribonucléocapside. Cette dernière a pour rôle de protéger le génome viral, et de former un complexe polymérasique permettant la réplication et la transcription du virus. Les produits des gènes F et H font partie de l'enveloppe virale. La glycoprotéine H permet l'attachement du virus à la cellule cible, et la glycoprotéine F intervient dans la fusion de l'enveloppe virale et de la membrane cellulaire. Le produit du gène M assure l'interface entre la nucléocapside et l'enveloppe virale. Les protéines V et C sont des protéines non essentielles dont leurs rôles demeurent encore méconnus. Toutefois, il a été démontré que V et C sont impliqués dans l'immunosuppression et dans l'assemblage viral (Devaux and Cattaneo, 2004; Kerdiles et al., 2006).

1.2 Récepteurs

À ce jour, deux récepteurs de la rougeole ont été identifiés soit le CD46 et le *signaling lymphocyte activation molecule* (SLAM ou CD150). C'est le CD46 qui fut le premier récepteur identifié (Dorig et al., 1993; Naniche et al., 1993). CD46 est une glycoprotéine transmembranaire de type-I, ubiquitaire, ayant une masse de 47-56 kilodaltons (kDa), dépendant des isoformes. À priori, cette molécule a été décrite comme étant un des éléments de la régulation du complément (Liszewski et al., 1991; Sidorenko

and Clark, 2003). Des études génétiques et biomoléculaires ont identifié plusieurs acides aminés du virus de la rougeole qui se lient au CD46. Plus particulièrement, l'acide aminé qui se trouve à la position 481 de la protéine H de la rougeole a été démontré comme étant le plus important (Lecouturier et al., 1996). Toutefois, des études subséquentes ont établi que seulement les souches vaccinales et les souches sauvages adaptées à la culture cellulaire utilisent ce récepteur. En 2000, un groupe de recherche a identifié le SLAM comme étant un récepteur de la rougeole (Tatsuo et al., 2000). SLAM est une glycoprotéine qui est exprimée à la surface de plusieurs cellules immunitaires telles que les thymocytes immatures, les cellules T et B activées, les cellules dendritiques matures et les macrophages. SLAM a été initialement identifié comme étant un récepteur des lymphocytes et il joue un rôle dans l'activation des cellules T (Cocks et al., 1995). Contrairement à CD46, jusqu'à présent, toutes les souches sauvages utilisent le SLAM comme récepteur. A posteriori, SLAM a aussi été identifié comme étant le récepteur du CDV et de la peste bovine (Tatsuo et al., 2001).

Malgré que la distribution tissulaire de SLAM explique le lymphotropisme des morbillivirus, ce n'est pas suffisant pour expliquer comment le virus peut infecter des tissus épithéliaux, endothéliaux et neuronaux (Herndon and Rubinstein, 1968; McChesney et al., 1997; Sakaguchi et al., 1986). Des études employant des souches recombinantes de la rougeole, exprimant la protéine fluorescente verte (GFP), ont démontré que l'entrée de ces virus dans les lignées cellulaires CHO *(Chinese Hamster Ovary)* ou EL*A* (lymphomes de souris) était indépendante de CD46 ou de SLAM soutenant ainsi l'existence d'au moins un autre récepteur supplémentaire (Hashimoto et al., 2002; Leonard et al., 2008). De plus, des conclusions similaires ont été tirées à propos des autres morbillivirus. Toutefois, ce n'est pas certain que ce récepteur serait le même pour tous les membres de ce genre (Bundza et al., 1988; Di Guardo et al., 2005; von Messling et al., 2004; Wohlsein et al., 1993).

1.3 Complications neurologiques

Les morbillivirus sont des agents pathogènes hautement contagieux qui se transmettent par aérosols (Appel, 1969). Le virus de la rougeole est l'espèce type du genre *Morbillivirus*. Annuellement, la rougeole infecte quarante millions de personnes provoquant huit cent mille décès. La plupart des cas de rougeole ont lieu dans les pays en voie de développement, où le taux de vaccination est faible et les soins médicaux sont inadéquats (Otten et al., 2005). Une infection par le virus de la rougeole, comme toute infection par les morbillivirus, suscite non seulement une immunosuppression de longue durée, mais aussi des infections pulmonaires et gastro-intestinales chez son hôte. L'apparition des taches de Koplik est pathognomonique d'une infection à la rougeole. Ceci signifie que l'apparition de ces taches est suffisante pour diagnostiquer la maladie. Elles sont propres à la rougeole, et surviennent généralement 1 à 2 jours avant les autres symptômes.

Contrairement à la rougeole, qui ne peut infecter que les hommes et quelques grands singes, le CDV possède un large spectre d'hôtes naturels. Il peut infecter tous les carnivores des familles *Canidae* (chien, loup, coyote), *Mustelidae* (furets, blaireaux, loutres), *Ursidae* (ours), *Mephitidae* (mouffettes), *Hyaenidae* (hyènes), *Ailuridae* (pandas rouges), *Pinnipedia* (phoques), *Procyonidae* (ratons laveurs), *Viverridae* (civettes, linsangs) et *Felidae* (lions, tigres, guépards) (Appel et al., 1994; Cattet et al., 2004; Qin et al., 2007; Roelke-Parker et al., 1996; von Messling et al., 2003; Woolf et al., 1986).

Une des plus graves conséquences d'une infection par les morbillivirus est l'apparition de troubles neurologiques. Cependant, la prédominance de ce type de complication varie selon les différents membres de ce genre. Les complications neurologiques les plus fréquentes sont associées au CDV où près de 30 % des chiens en phase aiguë de la maladie seront affectés. De plus, presque la totalité des carnivores sauvages infectés par le CDV manifestent des troubles neurologiques. Les encéphalopathies survenant à la suite d'une infection à la rougeole sont moins nombreuses, mais concernent néanmoins un patient sur mille. De plus, très souvent ces troubles neurologiques causent des répercussions physiques et économiques importantes

(Baumgartner et al., 1989; Rima and Duprex, 2005). Finalement, les séquelles neurologiques ne sont pas associées avec la peste bovine ni avec la peste-des-petits-ruminants.

Une étude récente suggère qu'il y a couramment une infection du système nerveux central (SNC) lors de la phase aiguë de la rougeole. Plus précisément, ces travaux ont démontré des anomalies au niveau des électroencéphalogrammes chez 50 % des patients (Nasr et al., 2000). Toutefois, la plupart de ces patients parviennent à éliminer le virus de la rougeole sans séquelles. Ce sont surtout les patients ayant des réponses immunitaires inadéquates ou les individus immunocompromis, qui souffrent de conséquences neurologiques majeures. Il existe trois différentes sortes d'encéphalopathies possibles suite à une infection par la rougeole. La première est l'encéphalite démyélinisante aiguë, la seconde l'encéphalite à corps d'inclusion et la dernière la panencéphalite sclérosante subaiguë.

L'encéphalite démyélinisante aiguë survient en moyenne de 5 à 6 jours après l'exanthème. Ce type de complication atteint en moyenne un cas sur mille et parmi ceux-ci, 10 à 20 % des patients vont succomber à la maladie (Miller, 1964). Les manifestations cliniques se caractérisent par l'apparition de signes neurologiques focaux tels qu'une faiblesse au niveau locomoteur ou la paraplégie. Les patients vont souvent témoigner une altération de l'état de conscience, de la fièvre, de la raideur au niveau du cou et même parfois des crises convulsives. Normalement, on ne retrouve que peu voire pas de virus dans le cerveau des patients, ce qui implique qu'une réponse immunitaire locale au niveau du SNC pourrait être la cause de ce trouble neurologique. L'encéphalite démyélinisante aiguë est associée avec une démyélinisation périveineuse des neurones ainsi qu'une perte de la protéine de base de la myéline (*myelin basic protein, MBP*).

L'encéphalite à corps d'inclusion est une complication rare de la rougeole et ne se produit que chez les patients qui sont immunocompromis ou qui souffrent d'immunodéficiences et la maladie peut être accompagnée par une pneumonie à cellules géantes. Cette dernière est due à la réplication du virus dans les cellules épithéliales du

système respiratoire (Kaplan et al., 1992; Mustafa et al., 1993). Le taux de mortalité est d'environ 75 % et tous les survivants vont montrer d'importantes séquelles neurologiques (Mustafa et al., 1993). Des études utilisant l'imagerie à résonance magnétique ont révélé que les résultats sont souvent normaux, et que le diagnostic requiert une biopsie (Mustafa et al., 1993). L'encéphalite à corps d'inclusion apparaît environ 4 mois après l'infection primaire et est caractérisée par une détérioration neurologique progressive accompagnée par des convulsions. L'encéphalite à corps d'inclusion cause une gliose avec la présence de corps d'inclusions intracytoplasmique chez les neurones et les cellules gliales. Très peu d'inflammation est détectée et dans la plupart des cas, le virus peut être facilement isolé du SNC des patients (Ohuchi et al., 1987). Présentement, les traitements sont uniquement palliatifs. De plus, il a été rapporté que ce type d'encélopathie peut également survenir après la vaccination. Toutefois, cela a été observé que chez les gens qui possédaient préalablement des anomalies au niveau de leur système immunitaire (Bitnun et al., 1999; Mawhinney et al., 1971). L'encéphalite à corps d'inclusion est caractérisée par une persistance virale au niveau du SNC. Toutefois, la façon dont le virus se rend au SNC et établit une telle persistance demeure inconnue.

La dernière complication reliée à la rougeole est la panencéphalite sclérosante subaiguë. C'est la plus rare des complications neurologiques associées à la rougeole. Sa prévalence est un cas sur un million. Toutefois, certaines données semblent indiquer que la fréquence est accrue selon la région géographique (Sips et al., 2007; Takasu et al., 2003). Généralement, les premiers signes d'infection apparaissent plusieurs années après l'infection aiguë (Connolly et al., 1967; Modlin et al., 1977). Un des facteurs contribuant à l'augmentation des risques de développer cette complication est le fait de contracter la maladie avant l'âge de 2 ans (Jabbour et al., 1972). Les premiers symptômes comprennent des troubles de personnalité et des modifications du comportement. Le second stade est caractérisé par des mouvements anormaux de l'axe qui sont responsables de chutes brèves et la manifestation de spasmes involontaires de la tête, voire de tout le corps. Ces mouvements anormaux se répètent périodiquement à des fréquences variables. Puis, les patients voient une dégradation motrice caractérisée par un syndrome pyramidal avec des dyskinésies ainsi qu'une hypertonie fréquente. On l'associe également à une démence

sévère. La phase terminale est marquée par un état végétatif, des troubles de déglutition et des difficultés respiratoires, menant inévitablement à la mort. À la suite d'une étude plus approfondie, on peut noter chez ces patients une démyélinisation et une infection importante des neurones. De plus, au stade tardif de l'infection, les oligodendocytes, les astrocytes et les cellules endothéliales sont infectés. Des analyses immunohistochimiques ont démontré une augmentation des niveaux de cellules exprimant les complexes majeurs d'histocompatibilité (CMH) de classe I et II. Ces cellules sont généralement des cellules de la microglie/macrophages, des astrocytes et parfois les neurones (Gendelman et al., 1984; Hofman et al., 1991).

On retrouve chez les patients atteints de la panencéphalite sclérosante subaiguë des réponses immunitaires humorales normales (Norrby and Kristensson, 1997), mais aussi des quantités très élevées d'anticorps neutralisants dans le liquide céphalo-rachidien ainsi que dans le sérum (Hall and Choppin, 1979). La plupart des anticorps présents sont dirigés contre les protéines structurales N, F et H tandis qu'un très petit nombre sont contre P et M. Des échantillons obtenus post-mortem ont démontré que les génomes viraux portent plusieurs mutations, principalement dans les protéines M, F et H, rendant ainsi le virus non fonctionnel (Ayata et al., 2007; Billeter et al., 1994). Cependant, les protéines impliquées dans la réplication virale restent inchangées. Parmi les modifications les plus fréquentes, on note des mutations ponctuelles, des hypermutations, des délétions, l'apparition de codons-stops hâtifs, des insertions et même de la distorsion ou le raccourcissement du domaine cytoplasmique de la protéine F (Cattaneo et al., 1986; Schmid et al., 1992; Wong et al., 1989). Ces types de changements pourraient expliquer pourquoi le virus maintient sa capacité de réplication, mais ne peut plus fusionner avec les cellules voisines ni de former des virions de façon efficace (Billeter et al., 1994; Cattaneo et al., 1989).

Il existe aussi trois différents types de complications neurologiques chez les chiens infectés par le CDV. Ces animaux peuvent développer une encéphalite aiguë, une polioencéphalite à corps d'inclusion ou une encéphalite avec une démyélinisation chronique ou subaiguë. Le CDV est responsable d'un éventail d'encéphalopathies chez le

chien dont l'encéphalite aiguë non inflammatoire, l'encéphalite aiguë associée avec une infiltration de lymphocyte et des manchons périvasculaires, la démyélinisation aiguë de la matière blanche, une encéphalite subaiguë ou chronique qui implique la dégénération et la nécrose de diverses populations cellulaires accompagnée de la démyélinisation et finalement, l'encéphalite du vieux chien ou « *old dog encephalitis* » (Axthelm and Krakowka, 1998). Des études antérieures ont montré que les neuropathologies observées sont liées à la souche de CDV (Summers et al., 1984 b). Chez les chiens, les souches Cornell A75/17 et Ohio strain R252 induisent une démyélinisation progressive, tandis qu'une infection par la souche Snyder Hill mène à une maladie aiguë causant des convulsions et une polioencéphalite (McCullough et al., 1974; Summers et al., 1979, 1984 b; Vandevelde and Zurbriggen, 2005). Le CDV s'introduit dans le SNC via l'infection des cellules mononucléaires qui peuvent traverser la barrière hématoencéphalique. Toutefois, il a aussi été démontré que le CDV pouvait être relâché dans le liquide céphalo-rachidien par les cellules épithéliales du plexus choroïde. À ce moment, le CDV peut fusionner avec les cellules épendymales des ventricules afin d'atteindre le SNC (Higgins et al., 1982a; Vandevelde and Zurbriggen, 2005).

Ce ne sont pas tous les chiens qui vont succomber à la maladie de Carré. En fait, le CDV cause une maladie très hétérogène chez les chiens, seulement 50 % vont montrer des signes cliniques de la maladie. Le taux de mortalité est dépendant de la capacité de l'animal à produire une réponse immunitaire efficace (Appel, 1969; Appel et al., 1982; Krakowka et al., 1975 b). À la suite des examens histologiques et l'analyse du liquide céphalo-rachidien provenant des chiens infectés, il est proposé que le CDV transiterait toujours par le SNC lors d'une infection. Cependant, si l'animal peut contrôler et éliminer l'infection, il subirait seulement des dommages minimaux. Toutefois, dans les cas où l'animal ne parvient pas à contrôler l'infection, ou sa réponse immunitaire est retardée, il subirait une encéphalopathie plus ou moins sévère (Summers and Appel, 1994).

L'encéphalite qui survient au cours de la phase aiguë, corrèle généralement avec la présence du virus dans le cerveau, et la progression de la maladie est facilement prédictible (Vandevelde and Zurbriggen, 2005). Initialement, les lésions dans la myéline

se développent pendant la période d'immunosuppression systémique et ne sont pas accompagnées d'une réponse inflammatoire (Vandevelde et al., 1982). Un des premiers signes de démyélinisation implique le ballonnement des feuillets de myéline, la vacuolation de la matière blanche et le gonflement des astrocytes. Afin d'expliquer ces observations, plusieurs études ont voulu établir une corrélation entre ces manifestations pathologiques et l'infection des oligodendrocytes. Néanmoins, les oligodendrocytes semblent réfractaires à une infection par le CDV et l'ARN messager viral est très peu détecté dans ce type cellulaire (Vandevelde and Zurbriggen, 2005). La démyélinisation semble plutôt corréler avec l'infection des cellules gliales présentes dans la matière blanche (Vandevelde et al., 1985; Zurbriggen et al., 1995 b). Cependant, le mécanisme régissant la démyélinisation au cours de la phase aiguë de l'infection demeure encore inconnu. Il est possible que les oligodendrocytes soient affectés par un effet « by-stander ». De surcroît, pendant la phase aiguë, il a été observé que l'expression des CMH de classe II est accrue dans la matière blanche. Cette augmentation est probablement due aux cellules de la microglie permettant d'expliquer les effets néfastes sur les feuillets de myéline puisque ces derniers peuvent être phagocytés par les cellules activées de la microglie (Alldinger et al., 1996).

La démyélinisation inflammatoire survient généralement lors de la phase chronique de la maladie. C'est à partir de la sixième ou septième semaine après l'infection, lorsque le système immunitaire commence à être rétabli, que les premiers signes apparaissent : des manchons périvasculaires et une infiltration des monocytes dans les lésions du cerveau. Cette infiltration va mener à des dommages supplémentaires causés par le système immunitaire (Vandevelde et al., 1981; Wisniewski et al., 1972). Une quantité accrue de cytokines pro-inflammatoires telles que les interleukine-6 (IL-6), IL-8, IL-12 et *tumor necrosis factor*-alpha est alors détectée tandis que les taux de cytokines anti-inflammatoires telles que IL-10 et *transforming growth factor*-beta sont à la baisse. IL-1, IL-2 et interferon-gamma ne sont pas détectés (Markus et al., 2002). Des études ont prouvé que des complexes immunitaires antiviraux contre le CDV ont la capacité de dégénérer des oligodendrocytes dans les cultures primaires. Ils ont aussi observé que la déplétion de macrophages dans ces mêmes cultures empêchait la perte

d'oligodendrocytes et par conséquent freinait la démyélinisation. Ces résultats suggèrent encore une fois que la démyélinisation pourrait résulter d'un effet « by-stander » causé par la toxicité cellulaire induite par la réponse immunitaire (Botteron et al., 1992; Griot-Wenk et al., 1991). Des anticorps contre la myéline et la MBP ont également été retrouvés dans le sérum et le liquide céphalo-rachidien des chiens infectés expérimentalement par le CDV (Botteron et al., 1992; Griot-Wenk et al., 1991). Par contre, l'importance de ces événements immunologiques n'a pas encore été déterminée (Summers et al., 1984a).

L'encéphalite du vieux chien est une condition rare qui se produit chez les chiens âgés qui ont été infectés par le CDV plusieurs années auparavant. Dans des cas plus rares, cette condition peut aussi survenir suite à une vaccination sans aucun signe d'infection préalable. Les signes cliniques qui caractérisent cette maladie sont l'ataxie, des tremblements et l'hyperkinésie. Cette maladie est aussi caractérisée par des signes neurologiques progressifs avec l'apparition de manchons périvasculaires et une encéphalite lymphoplasmacytaire. À des stades plus tardifs, les chiens peuvent aussi développer des crises tonico-cloniques (grand mal), des mouvements répétitifs, l'aveuglement ou même une paralysie importante avant de succomber à la maladie (Axthelm and Krakowka, 1998).

Les similarités entre l'encéphalite du vieux chien et la panencéphalite sclérosante subaiguë ont généré beaucoup d'intérêt. Premièrement, les deux types de maladies sont extrêmement rares et se manifestent des années après l'infection initiale. Les deux maladies sont accompagnées par une démyélinisation qui résulte d'une persistance virale au cerveau. Toutefois, une disparité existe entre ces deux formes d'encéphalopathies. Dû au grand nombre de mutations présentes dans les protéines structurales, les virus isolés des patients atteints de la panencéphalite sclérosante subaiguë ne se répliquent pas bien dans les lignées cellulaires normalement susceptibles à la rougeole tandis que les virus récupérés des chiens ayant l'encéphalite du vieux chien ne sont pas modifiés. De plus, ces animaux produisent des anticorps contre toutes les protéines virales ce qui n'est pas le cas chez les patients atteints de la panencéphalite sclérosante subaiguë.

Il existe plusieurs modèles animaux pour étudier la neurovirulence des morbillivirus. Ces modèles ont chacun leurs avantages et leurs inconvénients, mais aucun ne réussit à bien représenter la situation *in vivo*. Les souris transgéniques sont souvent les modèles de choix pour étudier la neurovirulence de la rougeole. Ces souris sont modifiées génétiquement pour exprimer soit CD46 ou SLAM. Jusqu'à présent, il existe 3 modèles de souris exprimant le CD46, les souris NSE (*neuron specific enolase*)— CD46, les souris YAC-CD46 (*yeast artificial chromosome*) et finalement une deuxième génération de souris YAC-CD46, croisées avec des souris déficientes pour le récepteur de l'interféron-α. Les plus grands défauts de ces systèmes sont que parfois le neurotropisme n'est pas identique à ce qu'on observe lors d'une infection naturelle. Aussi, des injections intracrâniennes sont parfois nécessaires pour démarrer une infection ou même l'utilisation de souriceaux est parfois requise afin de pouvoir observer des effets pathologiques. Il existe aussi 4 différents types de souris qui expriment le SLAM. Toutefois, jusqu'à maintenant seulement un type a été employé pour étudier la neurovirulence. Ce modèle utilise des souris ayant un fond génétique C57BL/6 exprimant le SLAM humain couplé au promoteur murin de l'hydroxyméthylglutaryl-coenzyme A réductase. Ce promoteur permet l'expression ubiquitaire de SLAM cependant, à des taux plus élevés dans le cerveau. Lorsque les souris sont infectées de façon intracrânienne, aucun virus ne peut être isolé. Par contre, l'ARN messager contre la protéine virale N est détectable jusqu'à 3 mois postinfection. Lorsque des souris allaitantes sont infectées, des particules infectieuses peuvent être isolées du cerveau et de la moelle épinière suggérant une réplication et une dissémination virales efficace (Sellin et al., 2006).

2. PROBLÉMATIQUE ET OBJECTIFS

Dû à l'absence d'un modèle animal adéquat, il est difficile de caractériser les événements menant à la neuroinvasion. Depuis quelques années, le furet (*Mustela putorius furo*), un hôte naturel du CDV, est utilisé pour étudier la pathogenèse du CDV. Lorsque ces animaux sont infectés avec le CDV, ils manifestent tous les signes cliniques typiques dont l'apparition de rougeurs, la présence d'une forte fièvre, de l'anorexie et une immunosuppression sévère. De plus, étant donné les similitudes entre le tropisme et la distribution tissulaire de tous les morbillivirus, les conclusions tirées du modèle furet peuvent être souvent appliquées aux autres morbillivirus.

Notre hypothèse de travail était que le modèle furet pourrait aussi servir à étudier la neurovirulence des morbillivirus. Dans le cadre de mes études doctorales, le premier but de mon projet était de caractériser la neuroinvasion des morbillivirus en utilisant le la souche A75/17 dans le modèle furet. En premier lieu, j'ai validé le furet comme modèle pour étudier la neurovirulence du CDV. Par la même occasion, j'ai confirmé le potentiel neurovirulent de la souche sauvage A75/17. De plus, j'ai caractérisé les événements qui mènent à l'encéphalite aiguë. En employant des techniques d'histologie et de la microscopie confocale, j'ai démontré que le CDV emprunte deux voies différentes pour infecter le SNC, les voies hématogène et olfactive. En plus, j'ai identifié les cellules du SNC qui sont ciblées par le CDV.

Mon deuxième objectif était de vérifier s'il y avait une réponse immunitaire locale dans le SNC lors d'une infection aiguë par le CDV et de la caractériser. Pour ce faire, nous avons généré un virus recombinant de la souche hautement neurovirulente: Snyder Hill. Par le biais de ce virus, nous avons aussi évalué l'influence de la route d'inoculation, la mort cellulaire et la réponse inflammatoire sur la pathogenèse observée.

À la suite des résultats du premier objectif, nous avons remarqué que le CDV semble suivre la voie olfactive pour atteindre le SNC. Cette observation suggère que le CDV à la capacité de se propager le long des neurones communicants. Pour mieux étudier

la dissémination transneuronale du CDV, j'ai mis au point un système *in vitro* qui permet de répondre à de telles questions. Pour accomplir ceci, j'ai d'abord développé un protocole qui permet d'isoler des neurones primaires provenant de foetus de furets. Ensuite, j'ai caractérisé la culture primaire et étudié la dissémination transneuronale.

3. RÉSULTATS ET ANALYSE

3.1 Article 1 : La maladie de Carré utilise les voies hématogène et olfactive pour la neuroinvasion.

Dans ce premier article, j'avais pour but de mieux caractériser les événements menant à l'encéphalite aiguë causée par le CDV. Pour ce faire, j'ai utilisé le modèle de furet qui a été préalablement établi comme étant un bon modèle pour étudier la pathogenèse des morbillivirus. Un des avantages du furet est que c'est un hôte naturel du CDV et contrairement aux chiens, le CDV cause une maladie homogène chez ces animaux (von Messling et al., 2003). Lors de cette étude, nous avons généré un virus recombinant de la souche neurovirulente A75/17 qui exprime la protéine fluorescente verte (eGFP), afin de faciliter la visualisation de l'infection. La souche A75/17 est une souche typique de CDV qui a été très bien caractérisé chez les chiens.

Notre premier résultat a montré que cette souche cause une maladie aiguë. Tous les animaux infectés ont développé des signes cliniques typiques d'infection par les morbillivirus à savoir une immunosuppression sévère, des rougeurs et une inhibition de la prolifération lymphocytaire suite à une stimulation à la phytohémagglutinine (PHA) (Heaney et al., 2005; Kauffman et al., 1982; Krakowka et al., 1975a; Krakowka et al., 1980). De plus, nous avons observé des signes neurologiques chez tous les animaux tels qu'un déplacement circulaire et des spasmes faciaux. Suivant l'euthanasie, nos observations macroscopiques ont révélé plusieurs foyers d'infection dans le tronc cérébral ainsi que dans les lobes frontaux et le bulbe olfactif. Cependant, les régions plus caudales telles que le cortex et le cervelet étaient négatives.

Afin de mieux comprendre la cinétique des événements régissant la neuroinvasion, nous avons poursuivi notre étude en inoculant par voie intranasale plusieurs groupes d'animaux qui ont été sacrifiés à différents intervalles de temps suivant l'infection. Nous avons constaté que l'intensité et l'étendue de l'infection sont accrues

proportionnellement au temps d'infection. De plus, nous avons déterminé que l'infection au SNC est un événement tardif qui se produit seulement après une infection des tissus lymphatiques et des tissus épithéliaux. Suite à cette série d'expériences, nous avons également vu que la première structure du SNC à exprimer la eGFP fut le bulbe olfactif. Des travaux antérieurs utilisant le CDV chez le chien et les échantillons de patients infectés par la rougeole, ont dénoté l'importance de la voie hématogène pour l'infection du SNC (Esolen et al., 1995; Summers et al., 1979). Toutefois, c'était la première fois que la voie olfactive semble jouer un rôle important. Pour mieux saisir l'importance de ces deux voies lors de l'infection du SNC par le CDV, nous avons fait des coupes histologiques au cryostat et nous avons regardé la localisation de la eGFP dans ces structures à différents temps postinfection. À partir de 7 jours postinfection, nous avons vu des cellules qui ressemblent à des lymphocytes dans le plexus choroïde et dans les capillaires. Après 14 jours d'infection, lorsque les animaux ont une virémie et que les cellules épithéliales sont infectées, des cellules du plexus choroïde exprimaient la eGFP de même que les nerfs olfactifs. Ceci suggère que peu importe la voie empruntée pour infecter le SNC, ce dernier doit subir un contact prolongé avec des cellules infectées avant que le virus puisse se propager dans les cellules du cerveau. Ensuite, nous avons identifié les cellules du SNC qui sont ciblées par le CDV. En utilisant des techniques d'immunohistochimie, nous avons déterminé que les cellules infectées dans le plexus choroïde étaient des lymphocytes. De plus, on a aussi noté que les cellules endothéliales des capillaires étaient infectées de même que les neurones et les cellules gliales.

Étant donné que nos premiers résultats semblaient indiquer que le bulbe olfactif pouvait être un point d'entrée important au SNC, nous avons essayé de suivre l'infection de la voie olfactive en utilisant des coupes histologiques. Pour accomplir ceci, nous avons utilisé différents réactifs tels que le 530/615 NeuroTrace Nissl et la phalloidine qui nous permettaient d'identifier respectivement des neurones olfactifs ainsi que les filaments d'actine. Nous avons démontré qu'à partir de jour 14 postinfections, la muqueuse olfactive ainsi que les neurones olfactifs étaient infectés par le CDV. Par la suite, nous avons pu suivre l'infection au niveau des nerfs olfactifs et ensuite aux glomérules olfactifs. À cet endroit, les nerfs olfactifs synapsent avec des cellules mitrales qui sont des

neurones de deuxième ordre (Zou et al., 2009). Des analyses histologiques ont révélé que les cellules mitrales étaient également infectées par le CDV. Ces résultats suggèrent que le CDV peut emprunter la voie olfactive pour atteindre le SNC des furets et cette dissémination pourrait se faire de façon antérograde.

Dans le cadre de cette étude, nous avons validé le modèle furet comme étant un bon modèle pour l'étude de la neuroinvasion. Une infection par le CDV chez les furets suit une cinétique d'infection très similaire à celle observée chez les chiens incluant l'infection des cellules lymphatiques, endothéliales et du plexus choroïde, ce qui correspondent à une dissémination virale par voie hématogène (Higgins et al., 1982 b; Summers et al., 1979). Toutefois, la moitié des chiens montent une réponse immunitaire adéquate permettant l'élimination du virus et une cessation des signes cliniques (Appel, 1969; Appel et al., 1982; Krakowka et al., 1975 b). Par contre, les furets infectés avec les souches sauvages ont toujours une réponse immunitaire déficiente et les animaux meurent de l'infection. Nous avons démontré que chez le furet immunosupprimé, l'infection par le CDV se propage dans le SNC de façon tardive. La propagation peut se faire par voie hématogène et par voie olfactive. Notre modèle reflète la dissémination virale observée chez les patients qui ont succombé d'une encéphalite aiguë causée par la rougeole. Nos observations concordent aussi avec celles faites chez d'autres paramyxovirus tels que la rubéole ou la maladie de Newcastle suggérant ainsi un mécanisme général pour la neuroinvasion par la voie hématogène des paramyxovirus (Saika et al., 2002; Wilczynski et al., 1977).

De plus, plusieurs virus sont connus pour utiliser la voie olfactive pour infecter le SNC. Entre autres, on retrouve le virus Sendai, la Piedad Michoacan et plus récemment le virus Nipah, qui est aussi un paramyxovirus (Allan et al., 1996; Mori et al., 1995; Weingartl et al., 2005). Dans la cavité nasale, la muqueuse olfactive est en proximité avec les neurones olfactifs ce qui peut faciliter la transmission virale entre ces deux types cellulaires. Lorsque les neurones olfactifs sont infectés, cela permet un accès direct au SNC. La capacité de se propager entre ces types cellulaires est un déterminant important pour la neuroinvasion. En somme, nous avons démontré que la voie olfactive devrait être

considérée comme étant une voie importante pour la neuroinvasion des morbillivirus et potentiellement pour les paramyxovirus en général.

3.2 Article 2 : L'encéphalite aiguë engendrée par la maladie de Carré est associée avec une perte neuronale importante et l'activation du système immunitaire local.

Dans cette deuxième publication, nous voulions investiguer la nature de la réponse immunitaire locale qui survienne après une infection par le CDV. Il est connu que le SNC n'est pas un endroit immunopriviliégé et que la présence virale peut engendrer une multitude de réponses variées telles qu'une augmentation des cytokines pro-inflammatoires, l'activation de la microglie et la sécrétion des interférons. Nous savons que la sévérité de la pathologie observée dans le SNC, suite à une infection virale, peut dépendre de plusieurs facteurs, dont la réponse immunitaire, la voie d'inoculation et la mort des cellules infectées. Au cours de cette étude, nous avions examiné l'importance de ces facteurs lors de la neuropathogénèse causée par le CDV.

Pour accomplir ces travaux, nous avons généré un virus recombinant de la souche Snyder Hill (SH) qui exprime aussi la eGFP comme unité transcriptionnelle supplémentaire. La souche SH est la plus reproductible des souches de CDV au niveau du déroulement de la maladie neuroinvasive. Cette souche a souvent été utilisée pour effectuer des études chez le chien et est bien caractérisée chez ce dernier. Chez le furet, il a été démontré que cette souche est mortelle et cause des signes neurologiques tels que les tremblements, les comportements répétitifs, la paralysie et même des convulsions (Stephensen *et al.*, 1997). Nous avons d'abord déterminé que l'ajout du eGFP n'a pas altéré la virulence de SH. Pour ce faire, nous avons infecté par la voie intranasale un groupe de quatre furets avec le virus parental et quatre autres furets avec le virus recombinant. Tous les animaux ont développé les mêmes signes cliniques généraux et les signes neurologiques qui incluent des nausées et des vomissements, des spasmes faciaux et de l'ataxie. Il est à noter que lors des examens post-mortem, l'expression du eGFP était décelée dans tous les cerveaux.

Ensuite, nous voulions vérifier les répercussions de la voie d'inoculation sur la neuroinvasion. Étant donné que chez le furet, la cavité nasale est en proximité avec le bulbe olfactif, nous voulions nous assurer que ce n'était pas la méthode d'inoculation qui favorisait la neuroinvasion. C'est pourquoi nous avons infecté deux groupes de six furets soit par voie intrapéritonéale ou par voie intranasale. Des groupes de deux animaux ont été sacrifiés à différents temps postinfection et nous avons comparé la dissémination virale ainsi que le déroulement général de la maladie. Tous les animaux ont manifesté les premiers signes cliniques comme les rougeurs et la fièvre autour du jour 6 postinfection. À partir du 7e jour, tous les animaux avaient une leucopénie sévère et leurs lymphocytes ne pouvaient plus répondre à une stimulation par le PHA. De plus, le taux de virémie était identique dans les deux groupes de furets donc, la méthode d'inoculation n'influence pas le déroulement de la maladie. Nous avons aussi examiné les cerveaux des furets provenant des divers groupes et nous avons vu que l'apparition macroscopique de la eGFP a lieu au même moment confirmant que la méthode d'inoculation ne change pas la cinétique de la neurovirulence.

Afin de mieux comprendre la cinétique d'infection et les conséquences de la présence de SH dans le cerveau des furets, nous avons sacrifié des groupes de 2 à 3 furets aux jours 7, 10 et 14 postinfection. Dès jour 7 post-infection, nous avons détecté la présence du virus dans le cervelet et dans le bulbe olfactif. Par la suite, le virus a été détecté dans le tronc cérébral, le plexus choroïde et l'hippocampe. Seulement une très petite quantité de virus fut détectée dans le cortex cérébral. Ce sont les cellules de Purkinje et les cellules granulaires qui ont été préférentiellement ciblées par le CDV. De plus, à l'aide d'analyse histologique, nous avons observé plusieurs changements morphologiques chez les neurones infectés comme la nécrose, l'atrophie et le ballonnement. On a voulu vérifier si ces changements neurologiques menaient à la mort neuronale. Pour réaliser ceci, nous avons quantifié sur les coupes histologiques la perte neuronale dans la région qui était la plus fortement infectée par SH soit le cervelet. L'accroissement graduel de l'infection entraîne une perte concomitante des cellules de Purkinje. En fait, aux termes de l'infection, cette région a subi une perte neuronale de

35 %. Des essais Tunel ont démontré que la mort des cellules de Purkinje induite par le virus était due à un mécanisme autre que l'apoptose.

La prochaine étape était de regarder quelles réponses immunitaires étaient enclenchées par la présence de SH dans le SNC. Étant donné que nous avons établi qu'il existait une perte neuronale suivant l'infection, nous avons évalué s'il y a activation des astrocytes et induction d'une gliose. La gliose astrocytaire est un développement exagéré des astrocytes du SNC et un marqueur de la neuroinflammation. Ce phénomène, de même que l'activation de la microglie, est l'un des premiers à se manifester lorsque la réponse immunitaire du SNC est activée. Par des techniques d'immunohistochimie, nous avons démontré que les régions hautement infectées par le SH, dont l'hippocampe, subissaient aussi une augmentation du nombre d'astrocytes au cours de l'infection. En utilisant un anticorps spécifique pour Mac-2, un marqueur d'activation de la microglie, nous avons observé qu'un nombre limité de ces cellules était présentes au début de l'infection, mais diminuait par la suite.

Finalement, nous avons utilisé des anticorps générés spécifiquement contre les cytokines de furets afin de déterminer si la réponse immunitaire locale consistait aussi en la production de cytokines pro-inflammatoires. L'activation de ces cytokines pourrait expliquer pourquoi dans certaines formes de la maladie, lorsque le système immunitaire de l'hôte parvient à contrôler l'infection, il peut y avoir des répercussions neurologiques à long terme comme la démyélinisation. Ces conséquences pourraient découlées d'une activation du système immunitaire lors de la phase aiguë d'infection. Dans notre modèle, nous avons observé la présence de l'interleukin-6 (IL-6), de *tumor necrosis factor*-alpha (TNF-α) et d'interféron bêta (IFN-β). C'est à des périodes précoces de l'infection que nous avons détectée l'apparition de IL-6. De plus, l'expression de cette cytokine diminue au cours de l'infection. Une raison serait que les cellules de la microglie peuvent être une source de production d'IL-6, expliquant leurs cinétiques similaires. Quant à la présence de l'IFN-β et le TNF-α, la production de ces cytokines semble être accrue au cours de l'infection. C'est à la fin de l'infection où le taux de TNF-α est maximal. La présence de cette cytokine pourrait avoir un effet sur la perte d'étanchéité de la barrière

hématoencéphalique observée à la fin de l'infection lorsque les furets succombent à la maladie et présentent le plus de signes neurologiques. En résumé, notre étude appuie les résultats trouvés chez les chiens qui ont montré que la leucoencéphalite démyélinisante implique un processus en deux-temps (Alldinger et al., 1996; Baumgartner et al., 1989; Summers and Appel, 1994). Premièrement, les dommages initiaux au SNC découlent directement de l'infection virale qui cause la mort cellulaire. Ensuite, la présence du virus déclenche une réponse immunitaire locale qui par la production de cytokines pro-inflammatoires peut continuer à contribuer à la pathogenèse. Bien entendu, dans notre modèle nos furets succombent à la maladie, mais on pourrait penser que s'ils y survivaient, ils subiraient des conséquences à long terme dû à l'activation du système immunitaire lors de la phase aiguë.

3.3 Article 3 : La maladie de Carré se propage de façon non directionnelle le long des neurones communicants.

La propagation virale dans les neurones ainsi que la dissémination dans le SNC jouent des rôles primordiaux dans la neuropathogénèse. Le CDV, bien qu'il ne soit pas considéré comme un virus neurotrope, cause souvent des complications neurologiques suivant une infection primaire. Dans notre première publication, nous avons démontré l'importance de la voie olfactive pour sa dissémination dans le SNC. Suivant ces travaux, nous avons également suggéré que le CDV peut se propager de façon antérograde le long des neurones olfactifs afin d'atteindre des régions plus profondes du SNC. Nous voulions valider, au cours de cette étude, un modèle *in vitro* qui nous permettrait d'étudier la façon par laquelle le CDV se propage entre les neurones communicants.

Pour pouvoir faire des parallèles entre nos observations *in vivo* et *in vitro*, nous avons décidé de mettre au point une culture primaire de neurones de furets. Depuis très longtemps, ces cultures ont été générées à partir d'animaux juvéniles ou embryonnaires afin d'étudier différents aspects de la neurologie incluant la neurovirologie. Nous avons généré des cultures à partir de foetus de furets âgés de 39 jours de gestation. Après une purification par gradient de Percoll, nous avons ensemencé les cellules sur des boîtes de

pétri préalablement enduites de laminine de souris et de poly-D-lysine. Nous avons vérifié la viabilité de la culture à l'aide d'un marquage au bromure d'éthidium et acridine orange. Suite à cette coloration, nous avons vu qu'à 3 et 7 jours post-ensemencement, plus de 87 % des cellules purifiées étaient vivantes. De plus, même après 28 jours de culture, une grande quantité de cellules demeurent viables. La prochaine étape consistait à identifier le ou les types cellulaires présents dans notre culture primaire. Afin d'accomplir ceci, nous avons marqué les cellules avec un colorant spécifique pour les neurones, le Nissl, ainsi qu'un anticorps spécifique des cellules gliales le GFAP. À 3 et 7 jours post-ensemencement, plus de 95 % de la population était des neurones. Après 14 jours, la proportion de cellules gliales était accrue dû à leur capacité proliférative, mais les neurones restaient toujours majoritaires.

Pour d'établir les meilleures conditions expérimentales, nous avons vérifié la capacité du CDV à infecter cette culture primaire. Les cultures ont été infectées à différentes multiplicités d'infection variant de 0.1 à 5 et à différents temps post-ensemencement avec la souche neurovirulente SH. Cette dernière a été modifiée afin d'exprimer la eGFP comme unité transcriptionnelle supplémentaire (voir chapitre 3.2). Nous avons constaté que l'infection des cultures neuronales est efficace à partir du moment où les cellules ensemencées commencent à former des prolongements soit 24 heures après leur mise en culture. De petits foyers d'infection ont été détectés à partir de 2 jours postinfection et continuaient de se multiplier jusqu'à 10 jours postinfection lorsque la majorité des cellules exprimaient la eGFP. Par la suite, des cinétiques d'infections ont été entamées afin de déterminer si les neurones peuvent soutenir une réplication adéquate du CDV. Nous avons comparé la réplication virale dans la culture primaire à celle dans une lignée cellulaire entièrement permissive au CDV soit les VerodogSLAM. Malgré le fait que la réplication virale est plus lente chez les neurones, les titres obtenus étaient similaires dans les deux types cellulaires.

Nos observations des cultures infectées semblent démontrer que la propagation virale nécessite un contact cellulaire. Lorsqu'on aperçoit les premiers foyers d'infection, nous notons que la propagation, c'est-à-dire l'expression du eGFP, se fait uniquement

entre des cellules qui se trouvent très proches les unes des autres. En fait, nous avons pris des photos d'une même région infectée à différents intervalles de temps et nous avons vu que les cellules infectées sont toujours soit en contact direct ou font partie d'un même regroupement de cellules neuronales.

Une fois la culture caractérisée, nous avons déterminé si le CDV peut se disséminer de façon antérograde ou rétrograde dans la culture. Afin d'accomplir ceci, nous avons utilisé un système modifié des chambres de Campenot. Ce système a été utilisé auparavant pour des études similaires chez les herpèsvirus et chez le virus du Nil Occidental (Ch'ng and Enquist, 2006; Samuel et al., 2007). Brièvement, ce système consiste à fixer avec du silicone un anneau de Teflon au fond d'un pétri dans lequel nous avons préalablement créé des rainures. L'anneau de Teflon forme deux chambres distinctes dans lesquelles nous pouvons ensemencer différents types cellulaires. L'ajout du méthylcellulose dans le milieu constitue une barrière supplémentaire pour éviter la propagation aléatoire des particules virales. Le contact entre les deux chambres adjacentes n'est possible qu'à travers les prolongements neuronaux qui ont crû le long des rainures.

Nous avons utilisé ce système afin de déterminer si le CDV peut se déplacer de façon rétrograde. Nous avons mis en culture des neurones primaires de furet d'un côté de l'anneau et lorsque les prolongements furent assez développés, nous avons ajouté des cellules VerodogSLAM de l'autre côté. Les cellules VerodogSLAM ont été infectées avec la souche SH à un m.o.i. de 0.1. Trois jours postinfection, l'expression du eGFP fut observée dans le compartiment contenant les neurones, montrant que le CDV peut se propager de façon rétrograde. L'expérience inverse a aussi été effectuée, c'est-à-dire qe nous avons d'abord infecté les neurones et lorsque leurs prolongements ont rejoint la chambre avoisinante, nous avons ajouté des cellules VerodogSLAM dans le compartiment vide. L'infection des cellules VerodogSLAM était visible 3 jours après l'infection des neurones, donc nous avons conclu que le CDV peut également se propager de façon antérograde.

Ce travail souligne l'importance de ces cultures primaires puisqu'elles reproduisent les observations faites *in vivo*. En général, les études qui examinent la neurovirulence des morbillivirus, et en particulier de la rougeole, utilisent des souris transgéniques comme source de neurones primaires (Lawrence et al., 1999; Manchester et al., 1999; Manchester and Rall, 2001). Or, ces souris ne sont pas naturellement susceptibles à une infection et même lorsqu'elles expriment un des récepteurs de la rougeole, elles ne reproduisent pas une maladie similaire à celle observée chez l'homme. Nous avons démontré que notre nouveau modèle *in vitro* miroite assez bien ce qu'on observe *in vivo*. Ce modèle est un outil intéressant pour approfondir nos connaissances quant au mécanisme régissant la dissémination transneuronale. Notre étude a aussi montré que le CDV ne se propage pas de façon directionnelle le long des neurones communicants. Cette observation pourrait avoir d'importantes conséquences quand à la neuroinvasion et à la pathogenèse observée dans le SNC suite à une infection des morbillivirus. Toutefois, des expériences supplémentaires sont requises afin de bien comprendre comment ce déplacement bidirectionnel contribue à la pathogenèse.

4. DISCUSSION ET CONCLUSION

La somme de ce travail a permis de valider le furet comme modèle pour étudier la neurovirulence. Les travaux que j'ai entrepris au cours de ma thèse ont également contribué aux connaissances générales des événements régissant l'encéphalite aiguë. De plus, grâce à mes travaux, nous savons plus à propos de la réponse immunitaire engendrée lors de la phase aiguë de l'infection ainsi que la façon dont le CDV se propage entre les neurones communicants.

Au cours de ma première publication, j'ai observé que la neurovirulence est un phénomène tardif qui se déroule seulement après l'infection des cellules immunitaires et épithéliales. Plus important encore, j'ai démontré que deux voies sont empruntées par le CDV afin d'atteindre le SNC soit la voie hématogène et la voie olfactive. J'ai utilisé des techniques d'immunohistochimie pour montrer que les neurones, les nerfs ainsi que le bulbe olfactif sont infectés à tour de rôle pour ensuite permettre au virus d'atteindre des régions plus internes du SNC. C'était la première que l'utilisation de la voie olfactive par un morbillivirus a été observée. Cependant en 2005, il a été rapporté que le virus Nipah, membre de la famille des *Pramyxoviridae*, pouvait se propager le long des nerfs crâniens, notamment le nerf olfactif, afin d'atteindre le SNC (Weingartl et al., 2005). C'est donc possible que la voie olfactive soit également importante pour la neuroinvasion pour plusieurs autres membres de cette famille.

Il serait intéressant de voir si le CDV possède la capacité de se propager le long d'autres nerfs crâniens tels le nerf vague. L'infection du nerf vague pourrait expliquer certains signes cliniques comme la nausée et des vomissements observés chez la majorité des furets infectés avec des souches de CDV hautement neurovirulentes. De plus, l'infection du nerf vague par les virus herpès simplex et influenza a déjà été démontrée (Gesser et al., 1994; Matsuda et al., 2004).

Les raisons pour lesquelles certains individus développent des infections persistantes suite à la rougeole ou à la maladie de Carré sont encore méconnues. Nous savons que l'équilibre qui existe entre le virus et le système immunitaire de l'hôte contribue à la variété des types de complications neurologiques qui peuvent surgir. Très peu est connu à propos de la réponse immunitaire qui se déroule lors de l'encéphalite aiguë. Selon la littérature, les lésions initiales seraient dues à la présence du virus (Krakowka et al., 1975a; Krakowka et al., 1980; Schobesberger et al., 1999; Zurbriggen et al., 1998). Toutefois, d'autres groupes de chercheurs ont démontré l'importance de la réponse immunitaire lors de ce stade par la détection de certaines cytokines et chimiokines (Alldinger et al., 1996; Tipold et al., 1999). Mes travaux ont démontré que dans notre modèle de furet, les premières étapes de l'infection consistent en une dissémination importante du CDV dans plusieurs régions du SNC telles que le bulbe olfactif, le cervelet, l'hippocampe et le tronc cérébral. Suite à cette infection, il y a une perte neuronale substantielle et une apparition de la gliose. De plus, nous avons décelé l'activation de la réponse immunitaire par le biais de l'activation des cellules microgliales et la production de l'IL-6, l'IFN-β et le TNF-α. Ceci confirme l'idée que le virus lui-même ainsi que le système immunitaire de l'hôte sont responsables pour la pathogenèse observée suivant une infection par les morbillivirus. Ceci peut aussi expliquer pourquoi certains individus développent des complications neurologiques après qu'ils se rétablissent d'une immunosuppression généralisée. Il serait intéressant de mieux caractériser la réponse immunitaire en utilisant des technologies de fines pointes comme la microdissection par laser suivie soit de techniques d'immunohistochimie ou d'une RT-PCR (*Reverse transcription polymerase chain reaction*) afin d'identifier quelles cellules produisent des cytokines ou chimiokines suite à une infection par le CDV. Il serait également intéressant de traiter nos furets infectés avec des anticorps neutralisants afin de les permettre de survivre à l'infection. Ceci pourrait nous permettre d'observer à plus long terme les effets de l'activation du système immunitaire lors de la phase aiguë de l'infection.

Au cours de la dernière partie de mon projet de thèse, j'ai voulu approfondir nos connaissances quant aux mécanismes qui sont impliqués dans la propagation transneuronale du CDV. Pour ce faire, j'ai mis au point un système *in vitro* à partir de cultures primaires de neurones de furets. Ce modèle s'est avéré très intéressant puisqu'il réplique plusieurs aspects observés *in vivo* incluant la permissivité des neurones à une infection par le CDV de même que la nécessité du contact cellulaire pour la dissémination virale.

Des observations similaires ont déjà été effectuées pour d'autres systèmes qui étudient la neurovirulence des morbillivirus (Ehrengruber et al., 2002; Lawrence et al., 2000; Zurbriggen et al., 1995a). Nous avons observé une très longue longévité de nos cellules infectées. Même après 18 jours d'infection, les cellules étaient toujours viables et ne semblaient pas souffrir de conséquences morphologiques dues à l'infection par le CDV. Une étude récente a démontré que *in vivo*, les cellules immunitaires infectées par CDV étaient résistantes à l'apoptose (Pillet and von Messling, 2009). Ces auteurs suggèrent que ce phénomène pourrait permettre au virus de s'échapper du système immunitaire. L'infection prolongée observée dans les neurones pourrait jouer un rôle similaire afin de permettre au virus suffisamment de temps pour se répandre dans le SNC avant d'être décelée par le système immunitaire.

Suite à mes travaux, nous savons que le CDV se déplace de manière non directionnelle dans les neurones. Ceci signifie qu'il peut voyager tant de façon antérograde que rétrograde. Malgré ces résultats, le mécanisme exact de transport neuronal demeure irrésolu. Il est probable que le CDV, tout comme d'autres virus, utilise le système des microtubules pour effectuer ses déplacements (Greber and Way, 2006; Jouvenet et al., 2004; Radtke et al., 2006; Rietdorf et al., 2001). Plusieurs expériences pourraient être entamées afin de vérifier cette hypothèse. On pourrait vérifier s'il y a colocalisation entre les microtubules et le CDV en utilisant un virus recombinant qui exprime la eGFP et un anticorps qui reconnait soit la tubuline soit une protéine associée au microtubule nommé MAP-1 (*microtubule associated protein-1*) (Sato et al., 1983). Une autre expérience serait de perturber la polymérisation des microtubules avec des

agents pharmacologiques comme le nocodazole ou la colchicine et d'observer par la suite leurs effets sur la dissémination transneuronale du CDV.

Finalement, les travaux accomplis au cours de mon doctorat nous ont permis de mieux caractériser les événements qui sont impliqués dans la neuroinvasion lors de la phase aiguë d'une infection par les morbillivirus. Ces connaissances pourraient contribuer au développement de nouvelles stratégies afin de limiter ou même prévenir entièrement les séquelles neurologiques causées par les morbillivirus.

5. RÉFÉRENCES

Allan, G.M., McNeilly, F., Walker, I., Linne, T., Moreno-Lopez, J., Hernandez, P., Kennedy, S., Carroll, B.P., Herron, B., Foster, J.C., *et al.* (1996). A sequential study of experimental porcine paramyxovirus (LPMV) infection of pigs: immunostaining of cryostat sections and virus isolation. J Vet Diagn Invest *8*, 405-413.

Alldinger, S., Wunschmann, A., Baumgartner, W., Voss, C., and Kremmer, E. (1996). Up-regulation of major histocompatibility complex class II antigen expression in the central nervous system of dogs with spontaneous canine distemper virus encephalitis. Acta Neuropathol *92*, 273-280.

Appel, M.J. (1969). Pathogenesis of canine distemper. Am J Vet Res *30*, 1167-1182.

Appel, M.J., Shek, W.R., and Summers, B.A. (1982). Lymphocyte-mediated immune cytotoxicity in dogs infected with virulent canine distemper virus. Infect Immun *37*, 592-600.

Appel, M.J., Yates, R.A., Foley, G.L., Bernstein, J.J., Santinelli, S., Spelman, L.H., Miller, L.D., Arp, L.H., Anderson, M., Barr, M., *et al.* (1994). Canine distemper epizootic in lions, tigers, and leopards in North America. J Vet Diagn Invest *6*, 277-288.

Axthelm, M.K., and Krakowka, S. (1998). Experimental old dog encephalitis (ODE) in a gnotobiotic dog. Vet Pathol *35*, 527-534.

Ayata, M., Shingai, M., Ning, X., Matsumoto, M., Seya, T., Otani, S., Seto, T., Ohgimoto, S., and Ogura, H. (2007). Effect of the alterations in the fusion protein of measles virus isolated from brains of patients with subacute sclerosing panencephalitis on syncytium formation. Virus Res *130*, 260-268.

Baumgartner, W., Orvell, C., and Reinacher, M. (1989). Naturally occurring canine distemper virus encephalitis: distribution and expression of viral polypeptides in nervous tissues. Acta Neuropathol *78*, 504-512.

Billeter, M.A., Cattaneo, R., Spielhofer, P., Kaelin, K., Huber, M., Schmid, A., Baczko, K., and ter Meulen, V. (1994). Generation and properties of measles virus mutations typically associated with subacute sclerosing panencephalitis. Ann N Y Acad Sci *724*, 367-377.

Bitnun, A., Shannon, P., Durward, A., Rota, P.A., Bellini, W.J., Graham, C., Wang, E., Ford-Jones, E.L., Cox, P., Becker, L., *et al.* (1999). Measles inclusion-body encephalitis caused by the vaccine strain of measles virus. Clin Infect Dis *29*, 855-861.

Botteron, C., Zurbriggen, A., Griot, C., and Vandevelde, M. (1992). Canine distemper virus-immune complexes induce bystander degeneration of oligodendrocytes. Acta Neuropathol *83*, 402-407.

Bundza, A., Afshar, A., Dukes, T.W., Myers, D.J., Dulac, G.C., and Becker, S.A. (1988). Experimental peste des petits ruminants (goat plague) in goats and sheep. Can J Vet Res *52*, 46-52.

Cattaneo, R., Schmid, A., Rebmann, G., Baczko, K., Ter Meulen, V., Bellini, W.J., Rozenblatt, S., and Billeter, M.A. (1986). Accumulated measles virus mutations in a case of subacute sclerosing panencephalitis: interrupted matrix protein reading frame and transcription alteration. Virology *154*, 97-107.

Cattaneo, R., Schmid, A., Spielhofer, P., Kaelin, K., Baczko, K., ter Meulen, V., Pardowitz, J., Flanagan, S., Rima, B.K., Udem, S.A., *et al.* (1989). Mutated and hypermutated genes of persistent measles viruses which caused lethal human brain diseases. Virology *173*, 415-425.

Cattet, M.R., Duignan, P.J., House, C.A., and Aubin, D.J. (2004). Antibodies to canine distemper and phocine distemper viruses in polar bears from the Canadian arctic. J Wildl Dis *40*, 338-342.

Ch'ng, T.H., and Enquist, L.W. (2006). An in vitro system to study trans-neuronal spread of pseudorabies virus infection. Vet Microbiol *113*, 193-197.

Cocks, B.G., Chang, C.C., Carballido, J.M., Yssel, H., de Vries, J.E., and Aversa, G. (1995). A novel receptor involved in T-cell activation. Nature *376*, 260-263.

Connolly, J.H., Allen, I.V., Hurwitz, L.J., and Millar, J.H. (1967). Measles-virus antibody and antigen in subacute sclerosing panencephalitis. Lancet *1*, 542-544.

Devaux, P., and Cattaneo, R. (2004). Measles virus phosphoprotein gene products: conformational flexibility of the P/V protein amino-terminal domain and C protein infectivity factor function. J Virol *78*, 11632-11640.

Di Guardo, G., Marruchella, G., Agrimi, U., and Kennedy, S. (2005). Morbillivirus infections in aquatic mammals: a brief overview. J Vet Med A Physiol Pathol Clin Med *52*, 88-93.

Dorig, R.E., Marcil, A., Chopra, A., and Richardson, C.D. (1993). The human CD46 molecule is a receptor for measles virus (Edmonston strain). Cell *75*, 295-305.

Ehrengruber, M.U., Ehler, E., Billeter, M.A., and Naim, H.Y. (2002). Measles virus spreads in rat hippocampal neurons by cell-to-cell contact and in a polarized fashion. J Virol *76*, 5720-5728.

Esolen, L.M., Takahashi, K., Johnson, R.T., Vaisberg, A., Moench, T.R., Wesselingh, S.L., and Griffin, D.E. (1995). Brain endothelial cell infection in children with acute fatal measles. J Clin Invest *96*, 2478-2481.

Gendelman, H.E., Wolinsky, J.S., Johnson, R.T., Pressman, N.J., Pezeshkpour, G.H., and Boisset, G.F. (1984). Measles encephalomyelitis: lack of evidence of viral invasion of the central nervous system and quantitative study of the nature of demyelination. Ann Neurol *15*, 353-360.

Gesser, R.M., Valyi-Nagy, T., Altschuler, S.M., and Fraser, N.W. (1994). Oral-oesophageal inoculation of mice with herpes simplex virus type 1 causes latent infection of the vagal sensory ganglia (nodose ganglia). J Gen Virol *75 (Pt 9)*, 2379-2386.

Greber, U.F., and Way, M. (2006). A superhighway to virus infection. Cell *124*, 741-754.

Griot-Wenk, M., Griot, C., Pfister, H., and Vandevelde, M. (1991). Antibody-dependent cellular cytotoxicity in antimyelin antibody-induced oligodendrocyte damage in vitro. J Neuroimmunol *33*, 145-155.

Hall, W.W., and Choppin, P.W. (1979). Evidence for lack of synthesis of the M polypeptide of measles virus in brain cells in subacute sclerosing panencephalitis. Virology *99*, 443-447.

Hashimoto, K., Ono, N., Tatsuo, H., Minagawa, H., Takeda, M., Takeuchi, K., and Yanagi, Y. (2002). SLAM (CD150)-independent measles virus entry as revealed by recombinant virus expressing green fluorescent protein. J Virol *76*, 6743-6749.

Heaney, J., Cosby, S.L., and Barrett, T. (2005). Inhibition of host peripheral blood mononuclear cell proliferation ex vivo by Rinderpest virus. J Gen Virol *86*, 3349-3355.

Herndon, R.M., and Rubinstein, L.J. (1968). Light and electron microscopy observations on the development of viral particles in the inclusions of Dawson's encephalitis (subacute sclerosing panencephalitis). Neurology *18*, 8-20.

Higgins, R.J., Krakowka, S.G., Metzler, A.E., and Koestner, A. (1982a). Experimental canine distemper encephalomyelitis in neonatal gnotobiotic dogs. A sequential ultrastructural study. Acta Neuropathol *57*, 287-295.

Higgins, R.J., Krakowka, S.G., Metzler, A.E., and Koestner, A. (1982 b). Primary demyelination in experimental canine distemper virus induced encephalomyelitis in gnotobiotic dogs. Sequential immunologic and morphologic findings. Acta Neuropathol *58*, 1-8.

Hofman, F.M., Hinton, D.R., Baemayr, J., Weil, M., and Merrill, J.E. (1991). Lymphokines and immunoregulatory molecules in subacute sclerosing panencephalitis. Clin Immunol Immunopathol *58*, 331-342.

Jabbour, J.T., Duenas, D.A., Sever, J.L., Krebs, H.M., and Horta-Barbosa, L. (1972). Epidemiology of subacute sclerosing panencephalitis (SSPE). A report of the SSPE registry. JAMA *220*, 959-962.

Jouvenet, N., Monaghan, P., Way, M., and Wileman, T. (2004). Transport of African swine fever virus from assembly sites to the plasma membrane is dependent on microtubules and conventional kinesin. J Virol *78*, 7990-8001.

Kaplan, L.J., Daum, R.S., Smaron, M., and McCarthy, C.A. (1992). Severe measles in immunocompromised patients. JAMA *267*, 1237-1241.

Kauffman, C.A., Bergman, A.G., and O'Connor, R.P. (1982). Distemper virus infection in ferrets : an animal model of measles-induced immunosuppression. Clin Exp Immunol *47*, 617-625.

Kerdiles, Y.M., Sellin, C.I., Druelle, J., and Horvat, B. (2006). Immunosuppression caused by measles virus: role of viral proteins. Rev Med Virol *16*, 49-63.

Krakowka, S., Cockerell, G., and Koestner, A. (1975a). Effects of canine distemper virus infection on lymphoid function in vitro and in vivo. Infect Immun *11*, 1069-1078.

Krakowka, S., Higgins, R.J., and Koestner, A. (1980). Canine distemper virus: review of structural and functional modulations in lymphoid tissues. Am J Vet Res *41*, 284-292.

Krakowka, S., Olsen, R., Confer, A., Koestner, A., and McCullough, B. (1975 b). Serologic response to canine distemper viral antigens in gnotobiotic dogs infected with canine distemper virus. J Infect Dis *132*, 384-392.

Lawrence, D.M., Patterson, C.E., Gales, T.L., D'Orazio, J.L., Vaughn, M.M., and Rall, G.F. (2000). Measles virus spread between neurons requires cell contact but not CD46 expression, syncytium formation, or extracellular virus production. J Virol *74*, 1908-1918.

Lawrence, D.M., Vaughn, M.M., Belman, A.R., Cole, J.S., and Rall, G.F. (1999). Immune response-mediated protection of adult but not neonatal mice from neuron-restricted measles virus infection and central nervous system disease. J Virol *73*, 1795-1801.

Lecouturier, V., Fayolle, J., Caballero, M., Carabana, J., Celma, M.L., Fernandez-Munoz, R., Wild, T.F., and Buckland, R. (1996). Identification of two amino acids in the hemagglutinin glycoprotein of measles virus (MV) that govern hemadsorption, HeLa cell fusion, and CD46 downregulation: phenotypic markers that differentiate vaccine and wild-type MV strains. J Virol *70*, 4200-4204.

Leonard, V.H., Sinn, P.L., Hodge, G., Miest, T., Devaux, P., Oezguen, N., Braun, W., McCray, P.B., Jr., McChesney, M.B., and Cattaneo, R. (2008). Measles virus blind to its epithelial cell receptor remains virulent in rhesus monkeys but cannot cross the airway epithelium and is not shed. J Clin Invest *118*, 2448-2458.

Liszewski, M.K., Post, T.W., and Atkinson, J.P. (1991). Membrane cofactor protein (MCP or CD46): newest member of the regulators of complement activation gene cluster. Annu Rev Immunol *9*, 431-455.

Manchester, M., Eto, D.S., and Oldstone, M.B. (1999). Characterization of the inflammatory response during acute measles encephalitis in NSE-CD46 transgenic mice. J Neuroimmunol *96*, 207-217.

Manchester, M., and Rall, G.F. (2001). Model Systems: transgenic mouse models for measles pathogenesis. Trends Microbiol *9*, 19-23.

Markus, S., Failing, K., and Baumgartner, W. (2002). Increased expression of pro-inflammatory cytokines and lack of up-regulation of anti-inflammatory cytokines in early distemper CNS lesions. J Neuroimmunol *125*, 30-41.

Matsuda, K., Park, C.H., Sunden, Y., Kimura, T., Ochiai, K., Kida, H., and Umemura, T. (2004). The vagus nerve is one route of transneural invasion for intranasally inoculated influenza a virus in mice. Vet Pathol *41*, 101-107.

Mawhinney, H., Allen, I.V., Beare, J.M., Bridges, J.M., Connolly, J.H., Haire, M., Nevin, N.C., Neill, D.W., and Hobbs, J.R. (1971). Dysgammaglobulinaemia complicated by disseminated measles. Br Med J *2*, 380-381.

McChesney, M.B., Miller, C.J., Rota, P.A., Zhu, Y.D., Antipa, L., Lerche, N.W., Ahmed, R., and Bellini, W.J. (1997). Experimental measles. I. Pathogenesis in the normal and the immunized host. Virology *233*, 74-84.

McCullough, B., Krakowka, S., and Koestner, A. (1974). Experimental canine distemper virus-induced demyelination. Lab Invest *31*, 216-222.

Miller, D.L. (1964). Frequency of Complications of Measles, 1963. Report on a National Inquiry by the Public Health Laboratory Service in Collaboration with the Society of Medical Officers of Health. Br Med J *2*, 75-78.

Modlin, J.F., Jabbour, J.T., Witte, J.J., and Halsey, N.A. (1977). Epidemiologic studies of measles, measles vaccine, and subacute sclerosing panencephalitis. Pediatrics *59*, 505-512.

Mori, I., Komatsu, T., Takeuchi, K., Nakakuki, K., Sudo, M., and Kimura, Y. (1995). Parainfluenza virus type 1 infects olfactory neurons and establishes long-term persistence in the nerve tissue. J Gen Virol *76 (Pt 5)*, 1251-1254.

Mustafa, M.M., Weitman, S.D., Winick, N.J., Bellini, W.J., Timmons, C.F., and Siegel, J.D. (1993). Subacute measles encephalitis in the young immunocompromised host: report of two cases diagnosed by polymerase chain reaction and treated with ribavirin and review of the literature. Clin Infect Dis *16*, 654-660.

Naniche, D., Varior-Krishnan, G., Cervoni, F., Wild, T.F., Rossi, B., Rabourdin-Combe, C., and Gerlier, D. (1993). Human membrane cofactor protein (CD46) acts as a cellular receptor for measles virus. J Virol *67*, 6025-6032.

Nasr, J.T., Andriola, M.R., and Coyle, P.K. (2000). ADEM: literature review and case report of acute psychosis presentation. Pediatr Neurol *22*, 8-18.

Norrby, E., and Kristensson, K. (1997). Measles virus in the brain. Brain Res Bull *44*, 213-220.

Ohuchi, M., Ohuchi, R., Mifune, K., Ishihara, T., and Ogawa, T. (1987). Characterization of the measles virus isolated from the brain of a patient with immunosuppressive measles encephalitis. J Infect Dis *156*, 436-441.

Otten, M., Kezaala, R., Fall, A., Masresha, B., Martin, R., Cairns, L., Eggers, R., Biellik, R., Grabowsky, M., Strebel, P., *et al.* (2005). Public-health impact of accelerated measles control in the WHO African Region 2000-03. Lancet *366*, 832-839.

Pillet, S., and von Messling, V. (2009). Canine distemper virus selectively inhibits apoptosis progression in infected immune cells. J Virol *83*, 6279-6287.

Qin, Q., Wei, F., Li, M., Dubovi, E.J., and Loeffler, I.K. (2007). Serosurvey of infectious disease agents of carnivores in captive red pandas (Ailurus fulgens) in China. J Zoo Wildl Med *38*, 42-50.

Radtke, K., Dohner, K., and Sodeik, B. (2006). Viral interactions with the cytoskeleton : a hitchhiker's guide to the cell. Cell Microbiol *8*, 387-400.

Rietdorf, J., Ploubidou, A., Reckmann, I., Holmstrom, A., Frischknecht, F., Zettl, M., Zimmermann, T., and Way, M. (2001). Kinesin-dependent movement on microtubules precedes actin-based motility of vaccinia virus. Nat Cell Biol *3*, 992-1000.

Rima, B.K., and Duprex, W.P. (2005). Molecular mechanisms of measles virus persistence. Virus Res *111*, 132-147.

Roelke-Parker, M.E., Munson, L., Packer, C., Kock, R., Cleaveland, S., Carpenter, M., O'Brien, S.J., Pospischil, A., Hofmann-Lehmann, R., Lutz, H., *et al.* (1996). A canine distemper virus epidemic in Serengeti lions (Panthera leo). Nature *379*, 441-445.

Saika, S., Kidokoro, M., Ohkawa, T., Aoki, A., and Suzuki, K. (2002). Pathogenicity of mumps virus in the marmoset. J Med Virol *66*, 115-122.

Sakaguchi, M., Yoshikawa, Y., Yamanouchi, K., Sata, T., Nagashima, K., and Takeda, K. (1986). Growth of measles virus in epithelial and lymphoid tissues of cynomolgus monkeys. Microbiol Immunol *30*, 1067-1073.

Samuel, M.A., Wang, H., Siddharthan, V., Morrey, J.D., and Diamond, M.S. (2007). Axonal transport mediates West Nile virus entry into the central nervous system and induces acute flaccid paralysis. Proc Natl Acad Sci U S A *104*, 17140-17145.

Sato, C., Kuriyama, R., and Nishizawa, K. (1983). Microtubule-organizing centers abnormal in number, structure, and nucleating activity in x-irradiated mammalian cells. J Cell Biol *96*, 776-782.

Schmid, A., Spielhofer, P., Cattaneo, R., Baczko, K., ter Meulen, V., and Billeter, M.A. (1992). Subacute sclerosing panencephalitis is typically characterized by alterations in the fusion protein cytoplasmic domain of the persisting measles virus. Virology *188*, 910-915.

Schobesberger, M., Zurbriggen, A., Summerfield, A., Vandevelde, M., and Griot, C. (1999). Oligodendroglial degeneration in distemper: apoptosis or necrosis? Acta Neuropathol *97*, 279-287.

Sellin, C.I., Davoust, N., Guillaume, V., Baas, D., Belin, M.F., Buckland, R., Wild, T.F., and Horvat, B. (2006). High pathogenicity of wild-type measles virus infection in CD150 (SLAM) transgenic mice. J Virol *80*, 6420-6429.

Sidorenko, S.P., and Clark, E.A. (2003). The dual-function CD150 receptor subfamily : the viral attraction. Nat Immunol *4*, 19-24.

Sips, G.J., Chesik, D., Glazenburg, L., Wilschut, J., De Keyser, J., and Wilczak, N. (2007). Involvement of morbilliviruses in the pathogenesis of demyelinating disease. Rev Med Virol *17*, 223-244.

Stephensen, C.B., Welter, J., Thaker, S.R., Taylor, J., Tartaglia, J., and Paoletti, E. (1997). Canine distemper virus (CDV) infection of ferrets as a model for testing Morbillivirus vaccine strategies : NYVAC- and ALVAC-based CDV recombinants protect against symptomatic infection. J Virol *71*, 1506-1513.

Summers, B.A., and Appel, M.J. (1994). Aspects of canine distemper virus and measles virus encephalomyelitis. Neuropathol Appl Neurobiol *20*, 525-534.

Summers, B.A., Greisen, H.A., and Appel, M.J. (1979). Early events in canine distemper demyelinating encephalomyelitis. Acta Neuropathol *46*, 1-10.

Summers, B.A., Greisen, H.A., and Appel, M.J. (1984a). Canine distemper and experimental allergic encephalomyelitis in the dog: comparative patterns of demyelination. J Comp Pathol *94*, 575-589.

Summers, B.A., Greisen, H.A., and Appel, M.J. (1984b). Canine distemper encephalomyelitis: variation with virus strain. J Comp Pathol *94*, 65-75.

Takasu, T., Mgone, J.M., Mgone, C.S., Miki, K., Komase, K., Namae, H., Saito, Y., Kokubun, Y., Nishimura, T., Kawanishi, R., *et al.* (2003). A continuing high incidence of subacute sclerosing panencephalitis (SSPE) in the Eastern Highlands of Papua New Guinea. Epidemiol Infect *131*, 887-898.

Tatsuo, H., Ono, N., Tanaka, K., and Yanagi, Y. (2000). SLAM (CDw150) is a cellular receptor for measles virus. Nature *406*, 893-897.

Tatsuo, H., Ono, N., and Yanagi, Y. (2001). Morbilliviruses use signaling lymphocyte activation molecules (CD150) as cellular receptors. J Virol *75*, 5842-5850.

Tipold, A., Moore, P., Zurbriggen, A., Burgener, I., Barben, G., and Vandevelde, M. (1999). Early T cell response in the central nervous system in canine distemper virus infection. Acta Neuropathol *97*, 45-56.

Vandevelde, M., Fankhauser, R., Kristensen, F., and Kristensen, B. (1981). Immunoglobulins in demyelinating lesions in canine distemper encephalitis. An immunohistological study. Acta Neuropathol *54*, 31-41.

Vandevelde, M., Higgins, R.J., Kristensen, B., Kristensen, F., Steck, A.J., and Kihm, U. (1982). Demyelination in experimental canine distemper virus infection: immunological, pathologic, and immunohistological studies. Acta Neuropathol *56*, 285-293.

Vandevelde, M., and Zurbriggen, A. (2005). Demyelination in canine distemper virus infection: a review. Acta Neuropathol *109*, 56-68.

Vandevelde, M., Zurbriggen, A., Higgins, R.J., and Palmer, D. (1985). Spread and distribution of viral antigen in nervous canine distemper. Acta Neuropathol *67*, 211-218.

von Messling, V., Milosevic, D., and Cattaneo, R. (2004). Tropism illuminated: lymphocyte-based pathways blazed by lethal morbillivirus through the host immune system. Proc Natl Acad Sci U S A *101*, 14216-14221.

von Messling, V., Springfeld, C., Devaux, P., and Cattaneo, R. (2003). A ferret model of canine distemper virus virulence and immunosuppression. J Virol *77*, 12579-12591.

Weingartl, H., Czub, S., Copps, J., Berhane, Y., Middleton, D., Marszal, P., Gren, J., Smith, G., Ganske, S., Manning, L., *et al.* (2005). Invasion of the central nervous system in a porcine host by nipah virus. J Virol *79*, 7528-7534.

Wilczynski, S.P., Cook, M.L., and Stevens, J.G. (1977). Newcastle disease as a model for paramyxovirus-induced neurologic syndromes. II. Detailed characterization of the encephalitis. Am J Pathol *89*, 649-666.

Wisniewski, H., Raine, C.S., and Kay, W.J. (1972). Observations on viral demyelinating encephalomyelitis. Canine distemper. Lab Invest *26*, 589-599.

Wohlsein, P., Trautwein, G., Harder, T.C., Liess, B., and Barrett, T. (1993). Viral antigen distribution in organs of cattle experimentally infected with rinderpest virus. Vet Pathol *30*, 544-554.

Wong, T.C., Ayata, M., Hirano, A., Yoshikawa, Y., Tsuruoka, H., and Yamanouchi, K. (1989). Generalized and localized biased hypermutation affecting the matrix gene of a measles virus strain that causes subacute sclerosing panencephalitis. J Virol *63*, 5464-5468.

Woolf, A., Gremillion-Smith, C., and Evans, R.H. (1986). Evidence of canine distemper virus infection in skunks negative for antibody against rabies virus. J Am Vet Med Assoc *189*, 1086-1088.

Zou, D.J., Chesler, A., and Firestein, S. (2009). How the olfactory bulb got its glomeruli: a just so story? Nat Rev Neurosci *10*, 611-618.

Zurbriggen, A., Graber, H.U., and Vandevelde, M. (1995a). Selective spread and reduced virus release leads to canine distemper virus persistence in the nervous system. Vet Microbiol *44*, 281-288.

Zurbriggen, A., Graber, H.U., Wagner, A., and Vandevelde, M. (1995b). Canine distemper virus persistence in the nervous system is associated with noncytolytic selective virus spread. J Virol *69*, 1678-1686.

Zurbriggen, A., Schmid, I., Graber, H.U., and Vandevelde, M. (1998). Oligodendroglial pathology in canine distemper. Acta Neuropathol *95*, 71-77.

Annex I: Summary of The Various CDV Strains Used

Virus Strain	Wild Type	Disease Duration	Tropism	Neurovirulence	Lethal in Ferrets
5804P	Yes	14 Days	Lymphoid and epithelial cells.	Ferrets do not display clinical signs of CNS involvement. Viral infection of the CNS is not detected during the disease.	Yes
A75/17	Yes	35 to 40 Days	Lymphoid cells, epithelial cells and brain tissue. Causes multifocal lesions in white and grey matter. Olfactory bulb is highly infected, brain stem, hippocampus, pia matter, parenchyma, ependyma, choroid plexus and endothelial cells are also infected in ferrets.	Ferrets show clinical signs of CNS infection at late stages of disease including ataxia, circling behavior and facial spasms. Virus is detected in all ferret brains.	Yes
Snyder Hill (SH)	Yes	14 Days	Lymphoid cells, epithelial cells and brain tissue, especially cerebellum. Brain stem, hippocampus, pia matter, ependyma, parenchyma, choroid plexus and endothelial cells are also infected in ferrets.	Causes acute neurological disease. Ferrets show signs of nausea and vomiting, ataxia, circling behavior and facial spasms. Virus is detected in all ferret brains.	Yes

Table 2. Description of the various CDV strains used in these studies. Table summarizing the different aspects of the CDV strains used during this work including disease duration, tropism, neurovirulence and lethality.

Annex II: List of Publications and Communications

Publications (Peer Reviewed)

1) **Rudd, P.A.,** Bastien, L.-É. and von Messling V. 2010. Acute Canine Distemper Encephalitis is Associated with Rapid Neuronal Loss and Local Immune Activation. J GenVirol. 91 (4): 980-989.

2) Svitek, N.†, **Rudd, P.A.**†, Obojes, K., Pillet, S. and von Messling, V. 2008. Severe Seasonal Influenza in Ferrets Correlates with Reduced Interferon and Increased IL-6 Induction. Virology, 376 (1): 53-9.
†- N.S. and P.A.R. contributed equally to this work.

3) Bonami, F., **Rudd, P.A.** and von Messling, V. 2007. The Canine Distemper Virus Attachment Protein Modulates Neuroinvasion. J Virol., 81 (21): 12066-70.

4) **Rudd, P.A.,** Cattaneo, R., and von Messling, V. 2006. Canine Distemper Virus Uses Both the Anterograde and the Hematogenous Pathway for Neuroinvasion. J Virol., 80 (19): 9361-9370.

Communications

Oral

1) Mechanisms of Canine Distemper Virus Neuroinvasion and Dissemination. **Penny A. Rudd**, Karola Obojes, François Bonami and Veronika von Messling. The 26th annual meeting of the American Society for Virology, Corvallis, Oregon. 2007.

2) Canine Distemper Virus Neuroinvasion is a Late Event. **Penny A. Rudd** and Veronika von Messling. The 25th annual meeting of the American Society for Virology, Madison, Wisconsin. 2006.

3) La Neuroinvasion du Système Nerveux Central (SNC) Causée par Certains Morbillivirus est un Événement Tardif de l'Infection. **Penny A. Rudd** et Veronika von Messling. Congrès INRS-Institut Armand-Frappier, St-Alexis-des-Monts, Québec, 2005.

Poster

1) Canine Distemper Virus Neuroinvasion is Independent of the Route of Inoculation. **Penny A. Rudd** and Veronika von Messling, The 27th annual meeting of the American Society for Virology, Ithaca, New York. 2008.

Contributed Communications

Oral

1) Immune Responses to Non-Lethal Human Influenza Strains in Ferrets. Veronika von Messling, **Penny A. Rudd**, Karola Obojes, Stéphane Pillet and Nicholas Svitek. The 26th annual meeting of the American Society for Virology, Corvallis,Oregon. 2007.

2) The Attachment Protein Plays a Major Role in Canine Distemper Neurovirulence. François Bonami, **Penny A. Rudd** and Veronika von Messling. The 25th annual meeting of the American Society for Virology, Madison, Wisconsin. 2006.

Poster

1) Cytokine Profiles in Epithelial and Immune Tissues of Ferrets Infected with Lethal or Attenuated CDV Strains. Louis-Etienne Bastien, **Penny Ann Rudd**, Nicholas Svitek, and Veronika von Messling. The 28th annual meeting of the American Society for Virology, Vancouver, British Colombia. 2009.

2) The Hemagglutinin Protein Plays an Important Role in Canine Distemper Virus Neurovirulence. **Penny A. Rudd**, François Bonami, Roberto Cattaneo and Veronika von Messling. The 13th International Conference of Negative Strand Virology. Salamanca, Spain. 2006.

Annex III: Other Significant Contributions

Publication no. 4

Journal of Virology, November 2007, p. 12066-12070, Vol. 81, No. 21

Disease Duration Determines Canine Distemper Virus Neurovirulence

François Bonami, Penny A. Rudd, and Veronika von Messling*
INRS-Institut Armand-Frappier, University of Quebec, Laval, Quebec, Canada

* Corresponding author.
Mailing address: INRS-Institut Armand-Frappier, University of Quebec,
531, Boul. des Prairies,
Laval, Quebec H7V 1B7,
Canada. Phone: (450) 687-5010. Fax: (450) 686-5305.
E-mail: veronika.vonmessling@iaf.inrs.ca

Specific Contributions:

Contribution ≅ 25%: For this publication, I performed all of the histological stainings and took pictures using the confocal microscope, thereby generating the fourth and final figure. Furthermore, I helped F. Bonami with all of the *in vivo* experiments including taking macroscopic photographs of the olfactory bulbs.

JOURNAL OF VIROLOGY, Nov. 2007, p. 12066–12070
0022-538X/07/$08.00+0 doi:10.1128/JVI.00818-07

Vol. 81, No. 21

Disease Duration Determines Canine Distemper Virus Neurovirulence▽

François Bonami, Penny A. Rudd, and Veronika von Messling*
INRS-Institut Armand-Frappier, University of Quebec, Laval, Quebec, Canada

Received 16 April 2007/Accepted 6 August 2007

The *Morbillivirus* hemagglutinin (H) protein mediates attachment to the target cell. To evaluate its contribution to canine distemper virus neurovirulence, we exchanged the H proteins of the wild-type strains 5804P and A75 and assessed the pathogenesis of the chimeric viruses in ferrets. Both strains are lethal to ferrets; however, 5804P causes a 2-week disease without neurological signs, whereas A75 is associated with a longer disease course and neurological involvement. We observed that both H proteins supported neuroinvasion and the subsequent development of clinical neurological signs if given enough time, demonstrating that disease duration is the main neurovirulence determinant.

Canine distemper virus (CDV), which infects a broad range of carnivores, is a close relative of the human pathogen measles virus (MV) (5). In its natural hosts, CDV reproduces all the signs of MV disease, including the characteristic rash, fever, respiratory and gastrointestinal involvement, and immunosuppression (16, 23). In addition, CDV displays one of the highest incidences of central nervous system (CNS) involvement within the *Morbillivirus* genus. During or after natural and experimental infections, about 30% of dogs exhibit neurological signs, but lesions are present in many more animals (17, 26). Ferrets are even more susceptible to CDV than dogs, and the lethality of wild-type strains reaches 100% (16, 23). When infected with a neurovirulent strain, most ferrets will develop neurological signs that increase with disease progression (4, 13).

The hemagglutinin (H) protein mediates viral particle attachment to the receptor on the target cell. With up to 10% variability among CDV strains, H is the least-conserved protein, and it determines in vitro tropism (9, 25). The role of the H protein in pathogenesis was initially investigated in rodent models of MV infection. The majority of mutations that accumulated during virus adaptation to growth in rodent brains map to the H protein (8), and introduction of these mutations into the parental strain replicated a neurovirulent phenotype (3, 15).

In ferrets, the wild-type strain 5804P leads to death within 2 weeks due to sepsis and multiorgan failure without neurological signs of disease (21). In contrast, the disease caused by the A75 strain usually lasts between 3 and 5 weeks, and most animals develop classical distemper-associated neurological signs, including chewing gum seizures and head pressing (13, 17). To evaluate the contribution of the H protein to these differences in neurological manifestation and disease duration, we exchanged the H genes in the two strains.

Chimeric viruses retain parental growth characteristics in vitro. The H proteins of the two strains (5804P and A75) are 2.8% divergent, consistent with the differences reported for unrelated strains (9, 19). The residues that vary are evenly distributed (Fig. 1A) and do not include amino acids interacting with the immune cell receptor SLAM (Fig. 1A, black bars) (20, 22). To assess the contribution of the H protein to the observed differences in pathogenesis, we produced two chimeric viruses: 5804P with the H gene of A75 (58/HA75) and A75 with the H gene of 5804P (A75/H58) (Fig. 1B). All viruses in this study express the enhanced green fluorescent protein (eGFP) protein from an additional transcription unit located between the H and polymerase genes. The viruses were recovered as described previously (25), and they displayed growth characteristics (Fig. 1C and D) and syncytium phenotypes (data not shown) similar to those of the parental strains in cell culture.

Disease duration determines the extent of CNS infection. The pathogenesis and neurovirulent potential of the chimeric viruses were assessed in ferrets, following protocols approved by the Institutional Animal Care and Use Committee of the INRS-Institut Armand Frappier. Intranasal inoculation with 10^5 50% tissue culture infectious doses ($TCID_{50}$) of the control parental viruses resulted in disease that was lethal within 2 weeks for virus strain 5804P and persisted for 3 to 6 weeks for virus strain A75 (Fig. 2A). Disease duration and clinical course correlated with the strain providing the genome backbone rather than the source of the H protein (Fig. 2A). One A75/H58-infected ferret experienced only a weak and short-lived viremia and survived the infection without developing any disease signs, which might have been due to residual maternal antibodies below detection levels. Immunological and virological parameters were assessed as described previously (24). The levels of cell-associated viremia and leukopenia caused by the different viruses were similar (Fig. 2B and C), but inhibition of lymphocyte proliferation upon phytohemagglutinin stimulation was less pronounced in A75-infected animals and significantly reduced in those inoculated with A75/H58 (Fig. 2D).

The A75 H protein facilitates neuroinvasion. We have shown that the olfactory bulb is the first site of macroscopically detectable infection in the CNS (13). We thus compared the extent of eGFP expression in the olfactory bulbs of animals infected with the parental and chimeric viruses. No eGFP expression was observed at 2 weeks in animals infected with

* Corresponding author. Mailing address: INRS-Institut Armand-Frappier, University of Quebec, 531, boul. des Prairies, Laval, Quebec H7V 1B7, Canada. Phone: (450) 687-5010. Fax: (450) 686-5305. E-mail: veronika.vonmessling@iaf.inrs.ca.
▽ Published ahead of print on 15 August 2007.

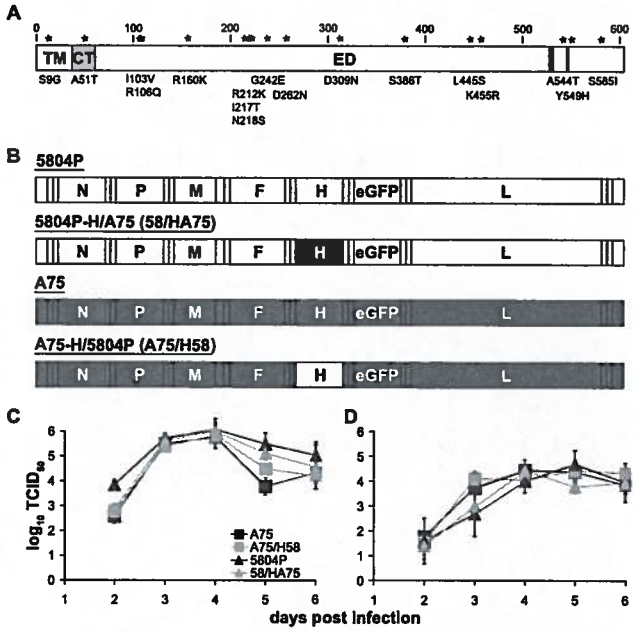

FIG. 1. Scheme and growth characteristics of the recombinant viruses produced. (A) Location of amino acids that vary between 5804P and A75 H proteins. The cytoplasmic tail (CT), transmembrane region (TM), and extracellular domain (ED) are represented by rectangles. SLAM-interacting residues (at positions 526 to 529 and 547 and 548) are represented by black bars. Amino acid numbers are indicated above the rectangles, and the locations of exchanged residues are marked by black stars. The A75 amino acid and its number within the protein, followed by the 5804P amino acid at that position, are noted below the rectangles. (B) Schemes of the parental and chimeric viruses. H genes were exchanged using the unique restriction sites BsrGI, located in the 3′ end of F gene, and AscI, positioned upstream of the eGFP start codon. A chimeric fragment combining the end of F and the FH untranslated region (UTR) from the recipient genome with the H open reading frame and the H-eGFP UTR from the donor strain by overlap extension PCR (6), and introduced into the recipient genome. Genetic material originating from 5804P is shown in white elongated boxes, while genetic material originating from A75 is represented by gray elongated boxes. Viral genes are represented by the letters N (nucleocapsid), P (phosphoprotein), M (matrix), F (fusion), and L (polymerase). The full names and abbreviated forms used throughout the article are indicated above the respective genome scheme. (C and D) Cell-associated virus (C) and free virus (D) production after infection of VerodogSLAMtag cells with a multiplicity of infection of 0.01. Virus titers were determined by 50% endpoint dilution at the indicated times after infection with a limit of virus detection at 1.7 50% $TCID_{50}$. Viruses in the A75 genomic context are represented by squares, while viruses in the 5804P genomic context are represented by triangles. Parental strains are shown in black, and recombinant viruses in gray. Values indicate the averages of at least three experiments, and error bars represent standard deviations.

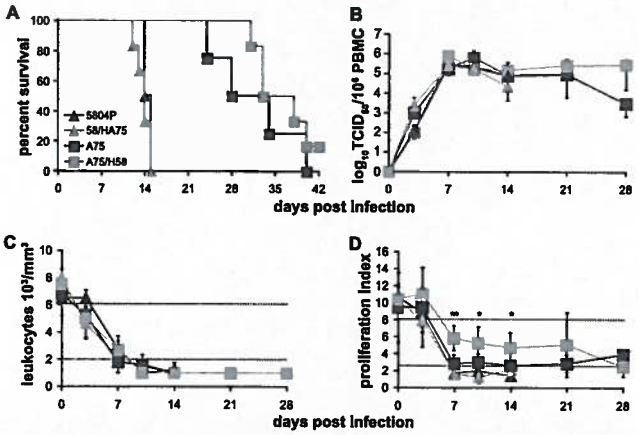

FIG. 2. Comparison of survival and immunological parameters of parental and chimeric viruses. (A) Survival curves of animals infected with parental strains 5804P and A75 (n = 4) and chimeric viruses 58/HA75 and A75/H58 (n = 6). Viruses in the A75 genomic context are represented by squares, while viruses in the 5804P genomic context are represented by triangles. Parental strains are shown in black, and recombinant viruses in gray. (B to D) Cell-associated CDV titer per million peripheral blood mononuclear cells (PBMC) (B), leukocyte number (C), and in vitro proliferation activity (D) of animals inoculated with the different viruses. Days after infection are plotted on the x axes, and the 50% $TCID_{50}$ per million PBMC, leukocyte number, or proliferation index is indicated on the y axis. Leukocyte numbers were determined directly from whole blood using the Unopette system (BD Biosciences). PBMC were isolated by Ficoll gradient centrifugation. Proliferation activity is expressed as a ratio of 5-bromo-2′-deoxyuridine incorporation of PBMC either stimulated with 100 μg/ml phytohemagglutinin or left untreated. The top dotted lines represent the threshold level for normal values, while the bottom dotted lines separate moderate and severe immunosuppression. Error bars indicate standard deviations. Two stars represent a P value of <0.005, one star indicates P values of <0.05. P values were calculated by comparing 5804P- and A75/H58-infected groups at the indicated time points with an unpaired, two-tailed Student t test.

5804P or viruses of A75 genomic origin (Fig. 3A). However, the presence of the A75 H protein resulted in clearly detectable eGFP expression in five out of the six animals infected (Fig. 3A, 58/HA75). No H-protein-mediated differences in infection levels were noted at the time of death for A75 viruses (Fig. 3B, compare top and bottom panels).

Histological analysis of sagittal olfactory bulb cryosections revealed few infected foci for virus strain 5804P (Fig. 3C), indicating that the macroscopically observed difference was quantitative rather than qualitative. A large number of infected olfactory glomeruli were detected in sections of 58/HA75-infected animals, confirming the macroscopically observed extent of infection (Fig. 3C). Consistent with our macroscopic results, the level of infection in olfactory bulbs from A75- and A75/H58-inoculated animals was similar (Fig. 3C, compare top and bottom right panels). In contrast, when comparing the infection in the choroid plexus, which is an important site of hematogenous neuroinvasion, we found similar amounts of infected cells in sections from animals sacrificed at similar time points (Fig. 3D, compare top and bottom panels).

We then compared the macroscopic distribution of eGFP expression throughout the brains of animals infected with A75 or A75/H58. The infection was predominantly concentrated in the olfactory bulb, the rostral region of the frontal lobe, and the brain stem, regardless of the H protein present (data not shown). Confocal microscopy analysis of cryosections stained with the respective cellular markers revealed that most of the infected cells in the macroscopically identified regions were either neurons (Fig. 4A and C) or glial cells (Fig. 4B and D), as described previously for A75 (13).

Despite their differences in clinical neurological presentation, all strains established a microscopically detectable infec-

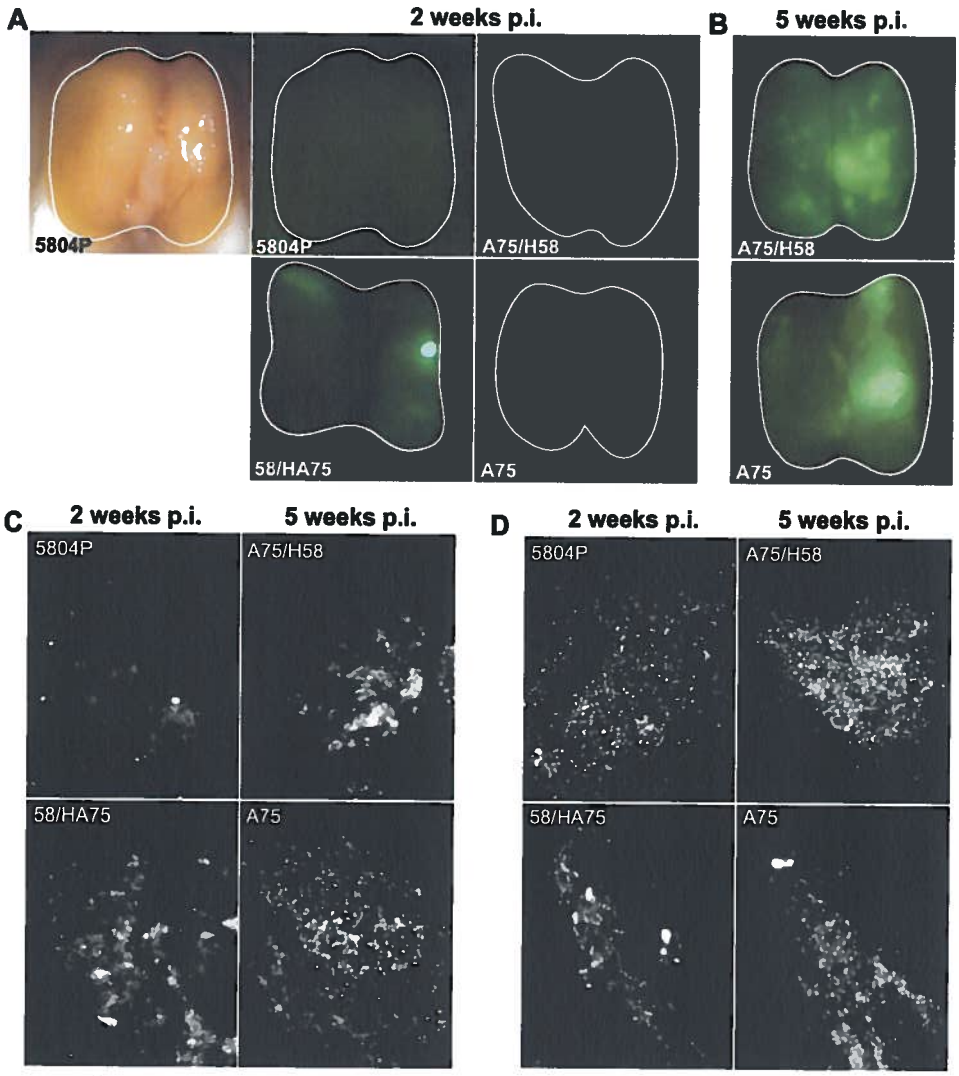

FIG. 3. Macroscopic and microscopic visualization of CNS infection. (A and B) Macroscopic imaging of the olfactory bulbs. The contours of the individual olfactory bulbs are outlined by a white line. Normal light photograph of the olfactory bulb originating from a 5804P-infected animal, and photographs of the same organ from animals infected with the parental and chimeric viruses after eGFP fluorescence excitation using the Macro-Illumination imaging system (Lightools, Encinitas, CA). The name of the respective virus is indicated on the picture. Pictures were taken at 2 weeks postinfection (p.i.) for all viruses (A) and at 5 weeks for A75 and A75/H58 (B). (C and D) Microscopic analysis of CNS infection. Ten- to 15-μm sagittal cryosections of paraformaldehyde-perfused and fixed brains were analyzed for eGFP expression at a magnification of ×200. Representative regions of olfactory bulbs (C) and choroid plexus (D) photographed at the time of death, 2 weeks after infection for 5804P and 58/HA75, and 5 weeks for A75 and A75/H58, are shown.

tion in the choroid plexus and the olfactory bulb and are thus neuroinvasive. Furthermore, introduction of the 5804P H protein into the A75 background resulted in disease duration and neurovirulence similar to those of the parental A75 strain, demonstrating that the 5804P H protein is able to mediate CNS invasion if given sufficient time. The lack of neurological signs in 5804P-infected animals might therefore be due to its rapid disease progression in other organs, rather than the virus' inability to infect CNS cells. The similar levels of cell-associated viremia and leukopenia indicate that it is a qualitative rather than quantitative difference determining disease duration. These findings, in combination with the observed variation in lymphocyte proliferation inhibition, point towards a difference in immunosuppression as the underlying cause. In vitro studies and experiments in rodent models have shown that contact between the H protein and immune cells is essential to induce proliferation inhibition (11, 14). Our chimeric viruses, in which H proteins were exchanged between two lethal strains, provide the first evidence that viral proteins other than H modulate the severity of this inhibition, thereby influencing disease duration and ultimately outcome.

The CDV H protein determines viral tropism and thus the potential target cells and tissues within the infected organism (3, 7, 20). We have observed the A75 H protein facilitates neuroinvasion in the 5804P genomic context without altering disease duration. This is consistent with the observation that the transfer of the H protein originating from a rodent brain-adapted MV strain into the vaccine virus conferred neuroin-

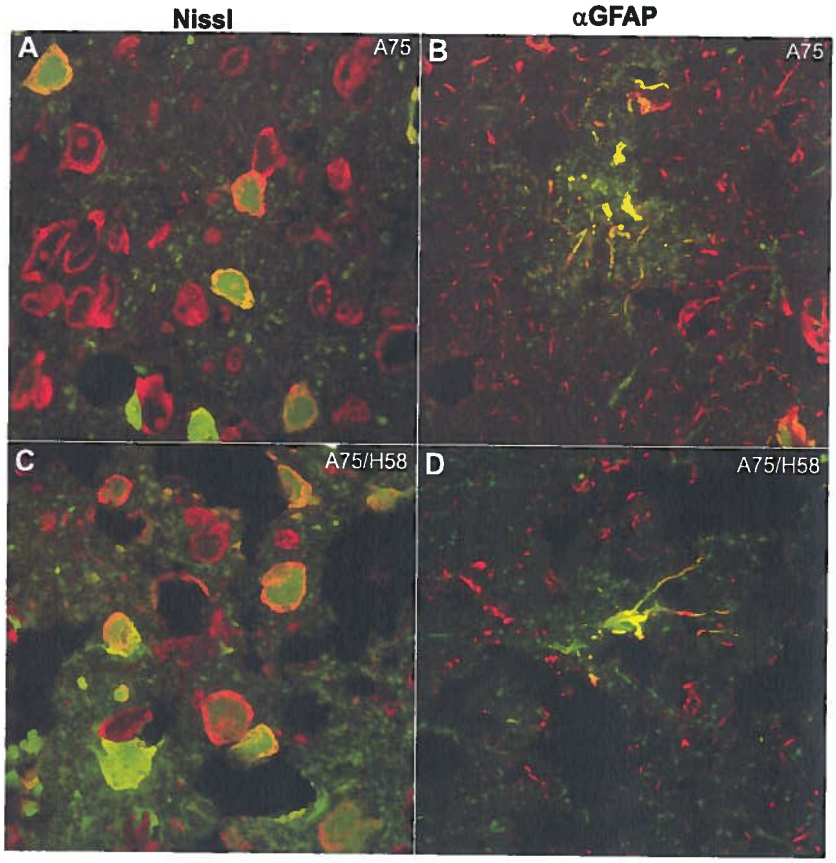

FIG. 4. Microscopic identification of target cells of viruses with A75 backbone. (A and C) Infected neurons; (B and D) glial cells. Infected cells are detected by eGFP expression, and neurons and glial cells are visualized with the 530/615 NeuroTrace Nissl stain (Nissl) and a rabbit anti-glial fibrillary acidic protein polyclonal antiserum (αGFAP), respectively, and an Alexa Fluor 568-labeled secondary antibody. Yellow staining and red and green staining of the same cell represent infected cells positive for the respective cellular marker. Shown are composite images of confocal microscopy analyses of cryosections at a magnification of ×1,000 of an A75-infected brain in the top panels and of an A75/H58-infected brain in the bottom panels.

vasive properties but failed to reproduce the extent of CNS dissemination seen with the parental strain (3, 15). Taken together, these findings indicate that H proteins from neurovirulent strains are more efficient at mediating neuron infection, probably due to an increased affinity for the yet to be identified receptor on these cells.

Ferrets infected with wild-type CDV are unable to mount an effective antiviral immune response (18) and thus provide us with a unique insight into the full spectrum of *Morbillivirus* disease. Inoculation with the highly virulent strain 5804P results in rapidly progressing disease characterized by the complete loss of immune system function, impaired mucosal membrane integrity, and death, similar to rinderpest virus in cattle (1, 2). The course of A75 represents an intermediate scenario where, despite widespread infection of immune and epithelial tissues, residual immune function seems to be maintained, resulting in prolonged survival and CNS invasion, consistent with the course of MV in severely immunodeficient individuals (10, 12). Finally, sublethal viruses, which mirror the course and signs of an uncomplicated MV infection in humans (5), do not cause CNS involvement, and the immune system is able to overcome its infection-induced suppression sufficiently to control and eliminate the virus (21). This dynamic interplay between the virus and the host's immune system, and the resulting differences in the duration of the infection observed in our CDV model, might also explain the variety of CNS diseases associated with MV.

We thank Roberto Cattaneo and Christoph Springfeld for helpful comments on the manuscript. We are also thankful to all laboratory members for continuing support and lively discussions.

This work was supported by CIHR operating funds (MOP-66989) and salary support to V.V.M. and an Armand-Frappier Foundation scholarship to P.R.

REFERENCES

1. **Banyard, A. C., M. D. Baron, and T. Barrett.** 2005. A role for virus promoters in determining the pathogenesis of *Rinderpest virus* in cattle. J. Gen. Virol. **86:**1083–1092.
2. **Brown, D. D., B. K. Rima, I. V. Allen, M. D. Baron, A. C. Banyard, T. Barrett, and W. P. Duprex.** 2005. Rational attenuation of a morbillivirus by modulating the activity of the RNA-dependent RNA polymerase. J. Virol. **79:** 14330–14338.
3. **Duprex, W. P., I. Duffy, S. McQuaid, L. Hamill, S. L. Cosby, M. A. Bitleter, J. Schneider-Schaulies, V. ter Meulen, and B. K. Rima.** 1999. The H gene of rodent brain-adapted measles virus confers neurovirulence to the Edmonston vaccine strain. J. Virol. **73:**6916–6922.
4. **Evermann, J. F., C. W. Leathers, J. R. Gorham, A. J. McKeirnan, and M. J. Appel.** 2001. Pathogenesis of two strains of lion (Panthera leo) morbillivirus in ferrets (Mustela putorius furo). Vet. Pathol. **38:**311–316.
5. **Griffin, D. E.** 2001. Measles virus. p. 1401–1441. *In* D. M. Knipe and P. M.

Howley (ed.), Fields virology, 4th ed., vol. 1. Lippincott Williams & Wilkins, Philadelphia, PA.
6. **Ho, S. N., H. D. Hunt, R. M. Horton, J. K. Pullen, and L. R. Pease.** 1989. Site-directed mutagenesis by overlap extension using the polymerase chain reaction. Gene 77:51–59.
7. **Johnston, I. C., V. ter Meulen, J. Schneider-Schaulies, and S. Schneider-Schaulies.** 1999. A recombinant measles vaccine virus expressing wild-type glycoproteins: consequences for viral spread and cell tropism. J. Virol. 73: 6903–6915.
8. **Liebert, U. G., S. G. Flanagan, S. Loffler, K. Baczko, V. ter Meulen, and B. K. Rima.** 1994. Antigenic determinants of measles virus hemagglutinin associated with neurovirulence. J. Virol. 68:1486–1493.
9. **Martella, V., F. Cirone, G. Elia, E. Lorusso, N. Decaro, M. Campolo, C. Desario, M. S. Lucente, A. L. Bellacicco, M. Blixenkrone-Moller, L. E. Carmichael, and C. Buonavoglia.** 2006. Heterogeneity within the hemagglutinin genes of canine distemper virus (CDV) strains detected in Italy. Vet. Microbiol. 116:301–309.
10. **McQuaid, S., S. L. Cosby, K. Koffi, M. Honde, J. Kirk, and S. B. Lucas.** 1998. Distribution of measles virus in the central nervous system of HIV-seropositive children. Acta Neuropathol. (Berlin) 96:637–642.
11. **Ohgimoto, S., K. Ohgimoto, S. Niewiesk, I. M. Klagge, J. Pfeuffer, I. C. Johnston, J. Schneider-Schaulies, A. Weidmann, V. ter Meulen, and S. Schneider-Schaulies.** 2001. The haemagglutinin protein is an important determinant of measles virus tropism for dendritic cells in vitro. J. Gen. Virol. 82:1835–1844.
12. **Plaza, J. A., and G. J. Nuovo.** 2005. Histologic and molecular correlates of fatal measles infection in children. Diagn. Mol. Pathol. 14:97–102.
13. **Rudd, P. A., R. Cattaneo, and V. von Messling.** 2006. Canine distemper virus uses both the anterograde and the hematogenous pathway for neuroinvasion. J. Virol. 80:9361–9370.
14. **Schlender, J., J. J. Schnorr, P. Spielhoffer, T. Cathomen, R. Cattaneo, M. A. Billeter, V. ter Meulen, and S. Schneider-Schaulies.** 1996. Interaction of measles virus glycoproteins with the surface of uninfected peripheral blood lymphocytes induces immunosuppression in vitro. Proc. Natl. Acad. Sci. USA 93:13194–13199.
15. **Schubert, S., K. Moller-Ehrlich, K. Singethan, S. Wiese, W. P. Duprex, B. K. Rima, S. Niewiesk, and J. Schneider-Schaulies.** 2006. A mouse model of persistent brain infection with recombinant *Measles virus*. J. Gen. Virol. 87:2011–2019.
16. **Stephensen, C. B., J. Welter, S. R. Thaker, J. Taylor, J. Tartaglia, and E. Paoletti.** 1997. Canine distemper virus (CDV) infection of ferrets as a model for testing *Morbillivirus* vaccine strategies: NYVAC- and ALVAC-based CDV recombinants protect against symptomatic infection. J. Virol. 71:1506–1513.
17. **Summers, B. A., H. A. Greisen, and M. J. Appel.** 1984. Canine distemper encephalomyelitis: variation with virus strain. J. Comp. Pathol. 94:65–75.
18. **Svitek, N., and V. von Messling.** 2007. Early cytokine mRNA profiles predict Morbillivirus disease outcome in ferrets. Virology 362:404–410.
19. **Takeda, M., T. Sakaguchi, Y. Li, F. Kobune, A. Kato, and Y. Nagai.** 1999. The genome nucleotide sequence of a contemporary wild strain of measles virus and its comparison with the classical Edmonston strain genome. Virology 256:340–350.
20. **Vongpunsawad, S., N. Oezgun, W. Braun, and R. Cattaneo.** 2004. Selectively receptor-blind measles viruses: identification of residues necessary for SLAM- or CD46-induced fusion and their localization on a new hemagglutinin structural model. J. Virol. 78:302–313.
21. **von Messling, V., D. Milosevic, and R. Cattaneo.** 2004. Tropism illuminated: lymphocyte-based pathways blazed by lethal morbillivirus through the host immune system. Proc. Natl. Acad. Sci. USA 101:14216–14221.
22. **von Messling, V., N. Oezguen, Q. Zheng, S. Vongpunsawad, W. Braun, and R. Cattaneo.** 2005. Nearby clusters of hemagglutinin residues sustain SLAM-dependent canine distemper virus entry in peripheral blood mononuclear cells. J. Virol. 79:5857–5862.
23. **von Messling, V., C. Springfeld, P. Devaux, and R. Cattaneo.** 2003. A ferret model of canine distemper virus virulence and immunosuppression. J. Virol. 77:12579–12591.
24. **von Messling, V., N. Svitek, and R. Cattaneo.** 2006. Receptor (SLAM [CD150]) recognition and the V protein sustain swift lymphocyte-based invasion of mucosal tissue and lymphatic organs by a morbillivirus. J. Virol. 80:6084–6092.
25. **von Messling, V., G. Zimmer, G. Herrler, L. Haas, and R. Cattaneo.** 2001. The hemagglutinin of canine distemper virus determines tropism and cytopathogenicity. J. Virol. 75:6418–6427.
26. **Winters, K. A., L. E. Mathes, S. Krakowka, and R. G. Olsen.** 1983. Immunoglobulin class response to canine distemper virus in gnotobiotic dogs. Vet. Immunol. Immunopathol. 5:209–215.

Publication no. 5

Virology, Volume 376, Issue 1, 20 June 2008, Pages 53-59
http://dx.doi.org/10.1016/j.virol.2008.02.035

Severe Seasonal Influenza in Ferrets Correlates with Reduced Interferon and Increased IL-6 Induction

Nicholas Svitek[1], [a], Penny A. Rudd[1], [a], Karola Obojes[a], Stéphane Pillet[a] and Veronika von Messling, [a*]

[a] INRS-Institut Armand-Frappier, University of Quebec, Laval, QC, Canada

* Corresponding author.
Mailing address: INRS-Institut Armand-Frappier, University of Quebec,
531, Boul. des Prairies,
Laval, Quebec, Canada H7V 1B7.
Fax: (450) 686-5305.
E-mail: veronika.vonmessling@iaf.inrs.ca

[1] N.S. and P.A.R. contributed equally to this work.

Specific Contributions:

Contribution ≅ 30%: For this publication, I performed all of the histological stainings and analysed the histopathological changes seen in figure 2. I also optimized the anti-influenza staining and produced figure 3. In addition, I participated in collecting nasal washes from the ferrets.